



Universidade do Minho
Escola de Engenharia

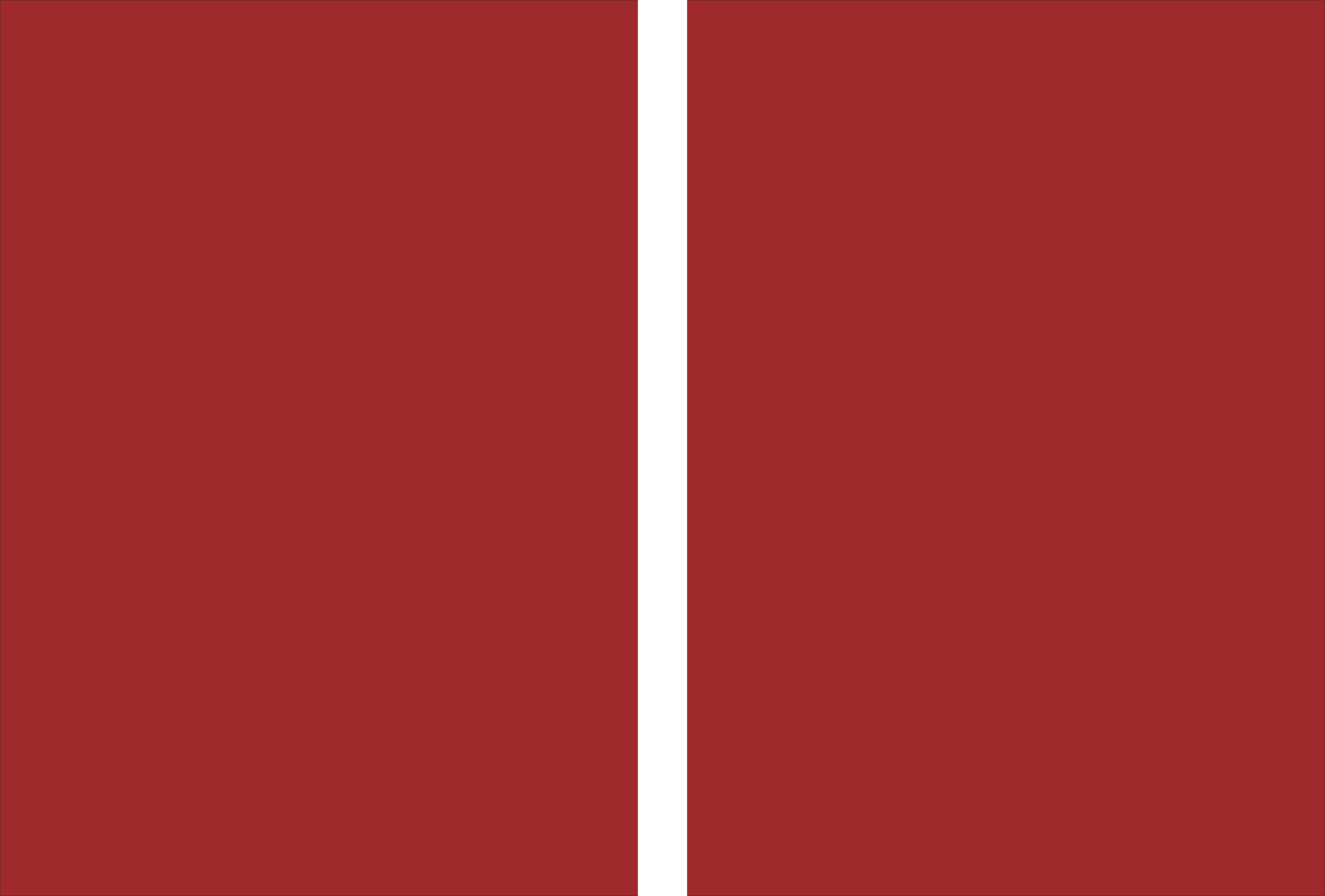
Bruno Daniel de Oliveira Fernandes

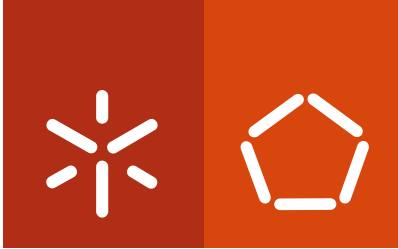
**Development and optimization of
microalgae cultivation systems - microalgal
composition, photobioreactor design and
characterization**

Bruno Daniel de Oliveira Fernandes
Development and optimization of microalgae cultivation systems –
microalgal composition, photobioreactor design and characterization

UMinho | 2013

May of 2013





Universidade do Minho

Escola de Engenharia

Bruno Daniel de Oliveira Fernandes

**Development and optimization of
microalgae cultivation systems - microalgal
composition, photobioreactor design and
characterization**

Doctoral Dissertation for PhD degree in Biological and
Chemical Engineering

Supervisors of the thesis:

**Professor António Augusto Martins de Oliveira
Soares Vicente**

Professor José António Couto Teixeira

May of 2013

DE ACORDO COM A LEGISLAÇÃO EM VIGOR, NÃO É PERMITIDA A REPRODUÇÃO DE QUALQUER PARTE DESTA TESE

Universidade do Minho, ___/___/_____

Assinatura: _____

“Science is facts; just as houses are made of stone, so is science made of facts; but a pile of stones is not a house, and a collection of facts is not necessarily science. “

Jules Henri Poincaré (1854-1912)

à minha Família

Acknowledgments

My first acknowledgment are to my two supervisors professors António Augusto Vicente and José António Teixeira, who believed in my scientific abilities and whom invited me to this project. I also thank to Fundação para a Ciência e Tecnologia that financially supported this study during 48 months through a PhD scholarship (SFRH/BD/44724/2008). I also have to acknowledge all my foreign supervisors: Tomas Brányik (Institute of Chemical Technology in Prague, Czech Republic) and Vilém Zachleder (Institute of Microbiology, Academy of Sciences of the Czech Republic, Trebon, Czech Republic) for their unique scientific support that was essential to me.

I also want to extend a special thanks to Giuliano Dragone, André Mota and António Ferreira for their valuable scientific support.

My second acknowledgments are to all my laboratory colleagues (from Portugal and Czech Republic), who had, during my PhD studying years, supported me. Also for solving a lot of my technical problems during the last years I sincerely thank to the engineering-technician Manuel Santos.

I also have to acknowledge my friends for their friendship and support. And last but not the least, I thank to Ana Cristina and my dearest family (grandparents, uncles, aunts and cousins). Especially to my parents (Daniel and Maria das Dores) and my brother Fábio. To you all, this thesis is in part, from you. Thank you all.

This thesis was financially supported by a PhD scholarship from Fundação para a Ciência e Tecnologia (Ref.: SFRH/BD/44724/2008), inserted in the Programa Potencial Humano Quadro de Referência Estratégico Nacional (POPH – QREN) - Tipologia 4.1 - Formação Avançada. The POPH-QREN is co-financed by Fundo Social Europeu (FSE) and by Ministério da Ciência, Tecnologia e Ensino Superior (MCTES).



Abstract

This work aimed at the development and optimization of systems and techniques for microalgae cultivation, in order to make the process economically and environmentally sustainable. Three different strategies were adopted: *i*) maximize productivity through the optimization of culture conditions, *ii*) maximize productivity and decrease costs by the use of agro-industrial waste as cultivation medium; *iii*) development of a new, low cost and highly productive microalgae cultivation system.

Carbon dioxide (CO₂) is the most widely used carbon source for photoautotrophic growth of microalgae. The rate of CO₂ fixation (R_{CO_2}) by *Chlorella vulgaris* was maximized by defining the values of CO₂ concentration in air feed and aeration rate. The results revealed that the maximum R_{CO_2} (2.22 g L⁻¹ d⁻¹) was obtained using 6.5% (v/v) CO₂ and 0.5 vvm. Although biomass concentration and mass productivity were affected by growth conditions, no differences were obtained in the biochemical composition of cells.

The optimization of specific productivity (starch and lipids for the production of bioethanol and biodiesel, respectively) was performed using strategies of nutrient limitation. Starch accumulation in *C. vulgaris* cells was evaluated under different initial concentrations of urea (nitrogen source) and FeNa-EDTA (iron source) in the medium. Based on the results, a two-stage process for obtaining culture cells with high concentrations of starch (> 40%) was proposed: a first stage of cultivation with initial urea and FeNa-EDTA concentrations of 1 and 0.08 g L⁻¹, respectively, which aims at maximizing biomass productivity, followed by a second stage of cultivation in the absence of these nutrients to induce starch accumulation.

The increase of lipid content in *Parachlorella kessleri* cells was induced using a culture medium dilution strategy. Photosynthetic carbon partitioning into starch and neutral lipid, as well as the influence of nutrient depletion and repletion on growth and pigment content in the green microalga *P. kessleri* were studied. The study revealed that *P. kessleri* used starch as a primary carbon and energy storage, but the stress caused by the decrease of nutrients concentration made the microalgae to shift the fixed carbon into reserve lipids as a secondary storage product. These findings indicate that nutritional limitation can be used in *P. kessleri* cultivation as a very effective and cheap

strategy to increase lipid productivity, for biofuel production.

Growth parameters and biochemical composition of the green microalga *C. vulgaris* cultivated under different mixotrophic conditions were determined and compared to those obtained from a photoautotrophic control culture. Supplementation of the inorganic culture medium with hydrolysed cheese whey powder solution, when compared photoautotrophic growth, led to a significant improvement in microalgal biomass production (from 0.10 ± 0.01 to 0.75 ± 0.01 g L d⁻¹) and an increase in carbohydrate utilization when compared with the culture enriched with a mixture of pure glucose and galactose (from 80.5 and 49.5% of glucose and galactose utilization, respectively, to an utilization of 100% of these carbohydrates), possibly due to the presence of growth promoting nutrients in cheese whey. Mixotrophic cultivation of *C. vulgaris* using the main dairy industry by-product could be considered a feasible alternative to reduce the costs of microalgal biomass production, since it does not require the addition of expensive carbohydrates to the culture medium.

A characterization of liquid and gas phases was performed, the mass transfer coefficient was determined, together with the light distribution profiles and flow patterns of three different photobioreactors (PBRs), namely bubble column (BC), split cylinder airlift photobioreactor (SCAPBR) 75 and SCAPBR 50. The effect of these parameters on biomass productivity was discussed. The developed SCAPBRs proved to be extremely suitable for microalgae cultivation. The design of photobioreactors (PBR), particularly the designed gas sparger, allowed meeting the needs of microalgae in terms of efficient mixing and good mass transfer coefficients (efficient supply and removal of CO₂ and O₂, respectively). SCAPBR 50 (at $U_{Gr} = 0.0044$ m s⁻¹) showed, among the tested PBRs, the highest value of biomass productivity (0.75 g L⁻¹ d⁻¹). This result has been attributed to a higher efficiency of light distribution inside the PBR and to a regular and defined flow pattern, which allows exposing cells to regular light-dark periods, as demonstrated in the present work.

Keywords: Microalgae; specific productivity; photoautotrophy; mixotrophy; SCAPBR; light regime; gas and liquid phase hydrodynamic characterization.

Resumo

A realização deste trabalho visou o desenvolvimento e optimização de sistemas e técnicas de cultivo de microalgas de forma a tornar o processo económica e ambientalmente sustentável. Três estratégias distintas foram adoptadas: *i)* maximização da produtividade recorrendo à optimização das condições de cultivo; *ii)* maximização da produtividade e diminuição de custos recorrendo à utilização de resíduos agroindustriais como meio de cultivo; *iii)* desenvolvimento de um novo sistema de cultivo de baixo custo e elevada produtividade.

O dióxido de carbono (CO_2) é a fonte de carbono mais utilizada no crescimento fotoautotrófico de microalgas. A taxa de fixação de CO_2 (R_{CO_2}) por parte da *Chlorella vulgaris*, foi optimizada através da definição dos valores de concentração de CO_2 e taxa de arejamento. Os resultados obtidos revelaram que a R_{CO_2} máxima ($2,22 \text{ g L}^{-1} \text{ d}^{-1}$) foi observada utilizando 6,5 % CO_2 e 0,5 vvm. Apesar da concentração de biomassa e produtividade mássica terem sido afectadas pelas condições de cultivo, não foram obtidas diferenças na composição bioquímica das células.

A optimização da produtividade específica (amido e lípidos destinados à produção de bioetanol e biodiesel, respectivamente) foi efectuada recorrendo a estratégias de limitação nutricional. A acumulação de amido em células de *C. vulgaris* foi avaliada sob diferentes concentrações iniciais de ureia (fonte de azoto) e FeNa-EDTA (fonte de ferro) no meio de cultivo. Com base nos resultados obtidos, foi proposto um processo de cultivo para a obtenção de células com elevadas concentrações de amido (> 40%), composto por duas fases: uma primeira fase de cultivo com concentrações iniciais de ureia e FeNa-EDTA de 1,1 e 0,08 g L^{-1} , respectivamente, que tem como objectivo maximizar a produtividade em biomassa; seguida por uma segunda etapa de cultivo sem a presença destes nutrientes, induzindo a acumulação de amido nas células.

O aumento do teor de lípidos em células *Parachlorella kessleri* foi induzida utilizando como estratégia a diluição do meio de cultura. A partição do carbono fotossintético em amido e lípidos neutros, bem como a influência da depleção e repleção de nutrientes no crescimento e teor de pigmentos na microalga *P. kessleri* foi estudada. O estudo revelou que a *P. kessleri* utiliza amido como fonte primária de armazenamento de carbono e energia, mas o stress causado pela diminuição da

concentração de nutrientes faz a microalga direccionar o seu metabolismo para a acumulação de lípidos, sendo estes reserva energética secundária. Estes resultados indicam que a limitação nutricional pode ser usada na *P. kessleri* cultivo como uma estratégia muito eficaz e barata para aumentar a produtividade de lípidos.

Foram determinados os parâmetros de crescimento e composição bioquímica da microalga *C. vulgaris*, cultivada em diferentes condições de mixotrofia, e comparados com os obtidos no cultivo padrão, efectuado em condições fotoautotróficas. A suplementação do meio de crescimento com soro de queijo hidrolisado levou a um aumento muito significativo da produtividade em termos de biomassa quando comparado com o crescimento fotoautotrófico (de $0,10 \pm 0,01$ para $0,75 \pm 0,01$ g L d⁻¹) e a um aumento da utilização dos hidratos de carbono presentes no meio quando comparado com uma cultura enriquecida apenas com glucose e galactose (de 80,5 e 49,5% de consumo de glucose e galactose, respectivamente, para 100% de utilização destes hidratos de carbono), possivelmente devido à presença de nutrientes do soro de queijo que promovem o crescimento. O cultivo mixotrófico de *C. vulgaris* recorrendo ao principal subproduto da indústria dos lacticínios, pode ser considerada como uma alternativa bastante promissora para a redução de custos da produção de microalgas.

A caracterização das fases líquida e gasosa, bem como a determinação do coeficiente de transferência de massa, a determinação do perfil de distribuição da luz e do padrão de fluxo foi efectuada em três fotobioreactores diferentes (BC, SCAPBR 75 e 50). Os SCAPBRs desenvolvidos revelaram-se extremamente adequados para o cultivo de microalgas. O design do SCAPBR, particularmente o sistema de arejamento desenvolvido, permitiu colmatar na totalidade as necessidades da microalga em termos de coeficientes de massa de mistura eficientes (fornecimento eficiente e remoção de CO₂ e O₂, respectivamente). SCAPBR 50 (com $U_{Gr} = 0,0044$ m s⁻¹) apresentou o valor mais elevado de produtividade ($0,75$ g L⁻¹ d⁻¹). Este resultado deveu-se a uma maior eficiência da distribuição de luz no interior da PBR e um padrão de fluxo regular e definido, o que permite expor as células a ciclos regulares de luz e sombra.

Palavras-chave: microalgas; produtividade específica; fotoautotrofia; mixotrofia; SCAPBR; regime de luz; caracterização hidrodinâmica da fase líquida e gasosa.

Table of Contents

CHAPTER1 Motivation and Outline.....	1
1.1 Thesis Motivation	3
1.2 Research Aims	4
1.3 Thesis Outline	4
1.4 References	5
CHAPTER 2 Microalgae cultivation and applications.....	7
2.1 Microalgae and their applications	9
2.1.1 Microalgae as a source of biofuel	14
2.1.2 Microalgae as a CO ₂ biological mitigation system	18
2.2 Cultivation systems, design considerations and downstream processes	20
2.2.1 Cultivation systems.....	20
2.2.2 Design considerations	27
2.2.3 Downstream processes.....	30
2.3 Cost/effectiveness considerations.....	36
2.3.1 Microalgae selection	36
2.3.2 Cultivation system location	38
2.3.3 Cultivation system selection	40
2.3.4 CO ₂ and nutrient supply	41
2.3.5 Induction of specific products' accumulation in microalgae ...	44
2.3.6 Biorefinery approach.....	45
2.3.7 Genetic manipulation	47
2.4 References	48
CHAPTER 3 Optimization of CO₂ concentration and flow rate and their influence in growth and biochemical composition of <i>Chlorella vulgaris</i>	57
3.1 Abstract	59
3.2 Introduction	59
3.3 Material and Methods	60
3.3.1 Microorganism and culture conditions	60
3.3.2 Determination of microalgal cell concentration.....	61
3.3.3 Determination of biomass productivity and specific growth rate	62

3.3.4	Determination of CO ₂ fixation rate.....	62
3.3.5	Biochemical characterization of microalgal cells	62
3.3.6	Experimental design and optimization by response surface methodology.....	63
3.4	Results and discussion	64
3.4.1	Effect of CO ₂ concentration and aeration rate on microalgal growth	64
3.4.2	Optimization of CO ₂ biofixation rate.....	66
3.4.3	Influence of CO ₂ concentration and aeration rate on the biochemical composition of <i>C. vulgaris</i>	70
3.5	Conclusions	71
3.6	References.....	71
CHAPTER 4 Strategies for increasing energy-rich materials' concentration in microalgae		73
4.1 Nutrient limitation as a strategy for increasing starch accumulation in microalgae		75
4.1.1	Abstract	75
4.1.2	Introduction.....	75
4.1.3	Material and Methods	76
4.1.4	Results and discussion	79
4.1.5	Conclusions	85
4.1.6	References	85
4.2 Study of relationship between accumulation of starch and lipids in the microalga <i>Parachlorella kessleri</i> induced by nutrient depletion and their repletion		89
4.2.1	Abstract	89
4.2.2	Introduction.....	90
4.2.3	Material and Methods	92
4.2.4	Results and discussion	95
4.2.5	Conclusions	107
4.2.6	References	107
CHAPTER 5 Mixotrophic cultivation of <i>Chlorella vulgaris</i> using industrial dairy waste as organic carbon source		111
5.1	Abstract.....	113

5.2	Introduction	113
5.3	Material and Methods	115
5.3.1	Microalgal strain and inoculum preparation	115
5.3.2	Media and culture conditions	115
5.3.3	Determination of microalgal cell concentration	116
5.3.4	Determination of carbohydrate concentration in culture media 116	
5.3.5	Determination of microalgal starch	116
5.3.6	Measurement of lipid and protein content in microalgae	116
5.3.7	Measurement of chlorophylls and total carotenoids concentration	117
5.3.8	Determination of specific growth rate	117
5.3.9	Determination of productivity of biomass, starch, lipids and proteins	117
5.4	Results and discussion	118
5.4.1	Growth parameters of microalgae cultivated under photoautotrophic and mixotrophic conditions	118
5.4.2	Consumption of glucose and galactose by <i>C. vulgaris</i>	120
5.4.3	Influence of nutritional modes on biochemical composition of <i>C. vulgaris</i>	121
5.5	Conclusions	124
5.6	References	124
CHAPTER 6 Selection of cultivation system type and geometry.		129
6.1	Abstract	131
6.2	Cultivation system selection	132
6.2.1	Open pond <i>versus</i> photobioreactor	132
6.2.2	Horizontal <i>versus</i> vertical PBRs	133
6.2.3	Bubble column <i>versus</i> airlift PBRs	135
6.2.4	Airlift PBR type selection	137
6.3	Geometry selection based on light regime characterization	139
6.3.1	Abstract	139
6.3.2	Introduction	139
6.3.3	Material and methods	141
6.3.4	Results and discussion	142
6.3.5	Conclusions	148

6.4	Split Cylinder Airlift Photobioreactor (SCAPBR) description	149
6.5	References.....	152
CHAPTER 7 Characterization and performance evaluation of SCAPBR as microalgae cultivation system.....		
157		
7.1	Abstract.....	159
7.2	Introduction.....	159
7.3	Material and methods.....	161
7.3.1	Description of tested photobioreactors.....	161
7.3.2	Hydrodynamic and mass transfer characterization of PBRs ...	162
7.3.3	Evaluation of PBRs biomass productivity	165
7.3.4	Determination of cells' light history	166
7.4	Results and Discussion.....	167
7.4.1	Liquid phase characterization	167
7.4.2	Gas phase characterization	171
7.4.3	Mass transfer of CO ₂	176
7.4.4	Biomass productivity	178
7.4.5	Determination of cells' light history	181
7.5	Conclusions.....	189
7.6	References.....	189
CHAPTER 8 General conclusions and suggestions for future work		
195		
8.1	General conclusions.....	197
8.2	Suggestions for future work.....	198

List of Publications

This thesis is based on the following original publications:

Book chapter

Dragone G., **Fernandes B.**, Vicente A., Teixeira J.A., 2010. *Third generation biofuels from microalgae*. In: Vilas AM, editor. Current research, technology and education topics in applied microbiology and microbial biotechnology. Badajoz: Formatex Research Center; pag. 1355–66.

Papers in peer reviewed journals

Fernandes B., Dragone G., Teixeira J., Vicente A., 2010. *Light regime characterization in an airlift photobioreactor for production of microalgae with high starch content*. Applied Biochemistry Biotechnology 161:218–26.

Dragone G., **Fernandes B. D.**, Abreu A. P., Vicente A. A., Teixeira J. A., 2011. *Nutrient limitation as a strategy for increasing starch accumulation in microalgae*. Applied Energy 88 (10): 3331-3335.

Fernandes, B., Dragone, G., Abreu, Ana P., Geada, P., Teixeira, J., Vicente, A., 2012. *Starch determination in Chlorella vulgaris - a comparison between acid and enzymatic methods*. Journal of Applied Phycology 24 (5): 1203 – 1208.

Abreu, A.P., **Fernandes, B.**, Vicente, A.A., Teixeira, J., Dragone, G., 2012. *Mixotrophic cultivation of Chlorella vulgaris using industrial dairy waste as organic carbon source*. Bioresource Technology 118: 61-66.

Ruiz H. A., Rodríguez-Jasso R. M., **Fernandes B. D.**, Vicente A. A., Teixeira J. T., 2013. *Hydrothermal processing, as an alternative for upgrading agriculture residues and marine biomass according to the biorefinery concept: a review*. Renewable & Sustainable Energy Reviews 21: 35-51.

Mariana Anjos, **Bruno D. Fernandes**, Giuliano Dragone, António A. Vicente, José A. Teixeira. *Optimization of CO₂ bio-mitigation by Chlorella vulgaris*. Bioresource Technology 139: 149-154.

Bruno Fernandes, José Teixeira, Giuliano Dragone, António A. Vicente, Kawano S., Katerina Bišová, Milada Vítová, Vilém Zachleder. *Relationship between starch and*

lipid accumulation in the microalga Parachlorella kessleri, induced by nutrient depletion and replenishment. Submitted to Bioresource Technology.

Bruno D. Fernandes, André Mota, António Ferreira, Giuliano Dragone, José A. Teixeira, António A. Vicente. *Characterization of a low cost split cylinder airlift for efficient microalgae production. – Submitted to Chemical Engineering Journal.*

Bruno D. Fernandes, André Mota, João L. Oliveira, Giuliano Dragone, José A. Teixeira, António A. Vicente. *Influence of light distribution profile and microalgae cells flow pattern on biomass productivity for different column photobioreactors – Submitted to Bioresource Technology.*

List of Figures

- Figure 2.1** Some of the microalgae strains currently mass cultivated. 1 - *Spirulina* (*Arthrospira platensis*); 2 - *Dunaliella salina*; 3 - *Chlorella vulgaris*; 4 - *Haematococcus pluvialis* (adapted from Benemann, 2008). 11
- Figure 2.2** Conversion processes for biofuel production from microalgal biomass (modified from Wang et al., 2008). 14
- Figure 2.3** Integrated process for biodiesel and bioethanol production from microalgae. 17
- Figure 2.4** Different types of microalgae cultivation systems. A - Raceway pond (<http://www.makebiofuel.co.uk/biofuel-from-algae>); B - Tubular photobioreactor (<http://www.sardi.sa.gov.au/aquaculture/aquaculture/AlgaeAndBiofuelsFacility>); C - Flat photobioreactor (<http://www.oilgae.com/blog/2011/04/intel-demonstrates-pilot-model-for-algae-based-carbon-capture.html>); D - Column photobioreactor (Zhu et al., 2013). 22
- Figure 2.5** Solvent extraction of lipids (<http://www.oilgae.com>). 34
- Figure 2.6** An integrated biorefining scheme for algal biomass utilization (Chen et al., 2009). 46
- Figure 3.1** Response surface of R_{CO_2} by *C. vulgaris* P12 as a function of CO_2 concentration in air and aeration rate. 69
- Figure 3.2** Contents of starch, proteins and lipids of *C. vulgaris* cultivated in bubble column photobioreactors under different CO_2 concentrations (2% (a), 6% (b), 10% (c) and 6.5% (d)) and aeration rates. 70
- Figure 4.1** Response surface of starch accumulation in *C. vulgaris* as a function of initial urea concentration and initial FeNa-EDTA concentration. 83
- Figure 4.2** Cell growth of *C. vulgaris* with different urea concentrations (a) 0 g L^{-1} , (b) 1.1 g L^{-1} and (c) 2.2 g L^{-1} . Initial FeNa-EDTA concentration: (■) 0 g L^{-1} , (◇) 0.04 g L^{-1} and (○) 0.08 g L^{-1} 84
- Figure 4.3** Laboratory photobioreactor used for the experiments. A: Cultures at the beginning of experiment; B: Cultures after 7.5 days of the growth. C: Cultures were transferred into complete mineral medium and diluted to have the same initial biomass concentrations. D: Recovery from starvation in complete mineral medium. Cuvettes in Figure 1A and 1B - 1: complete mineral medium; 0.2: 5-fold diluted medium; 0.1: 10-fold diluted medium. Cuvettes in Figure 1C and 1D - 1: complete mineral medium with cells from previous complete mineral medium; 0.2: complete mineral medium with cells cultivated in 5-fold diluted medium; 0.1: complete mineral medium with cells cultivated in 10-fold diluted medium. 96
- Figure 4.4** Changes in chlorophyll content in cultures of *Parachlorella kessleri* cultivated in medium 0.2 (Figure 2 A) and medium 0.1 (Figure 2 B) and then replaced in medium 1 (complete mineral medium). The chlorophyll content is expressed in mg L^{-1} (●) and in pg cell^{-1} (Δ). 97
- Figure 4.5** Changes in dry weight (DW) (●), mean cell volume (V) (○) and cell number (No) (Δ) in cultures of *Parachlorella kessleri*. Cultures were grown either in complete mineral medium (medium 1) (A); 5-fold diluted medium (medium 0.2) (B) and; 10-fold diluted medium (medium 0.1) (C). After 9 days

- (B) or 7.5 days (C) cells were transferred into complete mineral medium (medium 1)..... 99
- Figure 4.6** Changes in relative starch (Δ), total lipid (\circ) and, reserve (or neutral) lipid (\bullet) content in cultures of *Parachlorella kessleri*. Cultures were grown either in complete mineral medium (medium 1) (A) or 5-fold (medium 0.2) (B) or 10-fold (medium 0.1) (C) diluted medium. After 9 days (B) or 7.5 days (C) cells were transferred into complete mineral medium (medium 1)..... 102
- Figure 4.7** Fluorescence (A-C) and light microscopy (D) photomicro-graphs of the cell population of the microalga of *Parachlorella kessleri* initially grown in medium 0.1. Lipid bodies were stained using Nile Red (yellow). A: Cells grown for 7.5 days in 10-fold diluted mineral medium, B: 1 day after transfer the cells into complete mineral medium, degradation of lipid bodies started. The cells grew more or less synchronously to a large size. C, D: 2 days after transfer into complete mineral medium. The large cells with several small oil bodies (C) started to divide (D). Scale bar = 10 μm 106
- Figure 5.1** Lipid content and lipid productivity of *C. vulgaris* under different nutritional conditions. 121
- Figure 5.2** Comparison of starch content and starch productivity of *C. vulgaris* grown under photoautotrophic and mixotrophic conditions. 122
- Figure 5.3** Effect of nutritional mode on protein content and protein productivity of *C. vulgaris*. 123
- Figure 6.1** Schematic representation of sequential decisions made to select the most appropriate cultivation system for microalgae mass production (^{LR} – literature review; ^{EW} – experimental work)..... 131
- Figure 6.2** Schematic diagrams of: bubble column PBR (A); internal-loop (draft-tube) airlift PBR (B); split cylinder airlift PBR (C); external-loop airlift PBR (D) (adapted from Wang *et al.*, 2012). 134
- Figure 6.3** Top view of a PBR: *a* PBR_C, *a'* PBR_P, and *b* lateral view of a PBR section with an optical fibre attached; the position of the measuring points is indicated by circles. All dimensions are in mm. 141
- Figure 6.4** Cross-sectional distribution of light intensity within the airlift downcomer filled with algal cell suspension as a function of the light penetration distance (*Pd*) and radial coordinate (*r*), where *r* = 0 corresponds to the axis of the reactor, where: *a* PBR_C with 0.95 kg m⁻³; *a'* PBR_C with 2.67 kg m⁻³; *b* PBR_P with 0.95 kg m⁻³ and; *b'* PBR_P with 2.76 kg m⁻³. 143
- Figure 6.5** Relative light intensity distribution (in percent) in the two airlift downcomer geometries (closed symbols circular geometry and open symbols planar geometry) filled with algal cell suspension ($\blacklozenge, \blacklozenge$ 0.35 kg m⁻³, \blacksquare, \square 0.50 kg m⁻³ and; $\blacktriangle, \triangle$ 0.95 kg m⁻³) as a function of the light penetration distance (*Pd*). These data points correspond to measurements made for *r* = 0 mm. 144
- Figure 6.6** Volume fraction of the PBR (referred to the total culture volume) where the *RLI* is higher than 10% of the reference intensity (70 $\mu\text{E m}^{-2} \text{s}^{-1}$); \bullet PBR_C, \blacktriangle PBR_P 146
- Figure 6.7** Relative light intensity spectra for different light penetration distances within the PBR_C (cell concentration=0.95 kg m⁻³); *a* 5 mm, *b* 10 mm, *c* 15 mm, *d* 20 mm, *e* 25 mm, *f* 30 mm, and *g* 35 mm. 147

Figure 6.8 Relative light intensity spectra for different cell concentrations within PBR _C (light penetration distance=5 mm); a 0.18 kg m ⁻³ , b 0.50 kg m ⁻³ , c 0.95 kg m ⁻³ , and d 1.99 kg m ⁻³	148
Figure 6.9 The geometry of SCAPBR and air sparger (frontal and top view). Sparger (a); baffle (b); heat exchanger inlet and outlet (c).	149
Figure 6.10 Schematic representation of top view (A) and front view (B) of SCAPBRs baffle, acting as heat exchanger and light guide. Cold water inlet (a); warm water outlet (b).	150
Figure 6.11 Schematic representation of the aeration system used in the tested PBRs. Mass flow controller (a); gas mixing chamber (b); air filter (c); pressure chamber (d); needle sparger (e).	152
Figure 7.1 The geometry of photobioreactors and air spargers (frontal and top view). Sparger (a); baffle (b); heat exchanger inlet and outlet (c).	161
Figure 7.2 Liquid velocity for SCAPBR 50 (▲) and SCAPBR 75 (■), at different values of U_{Gr}	168
Figure 7.3 Mixing time for SCAPBR 50 (▲), SCAPBR 75 (■) and BC (●), at different values of U_{Gr}	169
Figure 7.4 Circulation time for SCAPBR 50 (▲) and SCAPBR 75 (■), at different values of U_{Gr}	170
Figure 7.5 Riser gas holdup for SCAPBR 50 (▲), SCAPBR 75 (■) and BC (●), at different values of U_{Gr}	172
Figure 7.6 Bubble Sauter mean diameter (d_{32}) for SCAPBR 50 (▲), SCAPBR 75 (■) and BC (●), at different values of U_{Gr}	173
Figure 7.7 Bubbles elongation for SCAPBR 50 (▲), SCAPBR 75 (■) and BC (●), at different values of U_{Gr}	174
Figure 7.8 Bubbles mean complexity degree (B_{CD}) for SCAPBR 50 (▲), SCAPBR 75 (■) and BC (●), at different values of U_{Gr}	175
Figure 7.10 Gas velocity _{Riser} for SCAPBR 50 (▲), SCAPBR 75 (■) and BC (●), at different values of U_{Gr}	176
Figure 7.10 K_La for SCAPBR 50 (▲), SCAPBR 75 (■) and BC (●), at different values of U_{Gr}	177
Figure 7.11 Biomass productivity for SCAPBR 50 (▲), SCAPBR 75 (■) and BC (●), at three different values of U_{Gr}	179
Figure 7.12 Light intensity ($L.I.$) profiles inside the PBRs (SCAPBR 50, SCAPBR 75 and BC) at different <i>C. vulgaris</i> cell concentrations (0.25, 0.50 and, 1.0 g L ⁻¹).	182
Figure 7.13 Particle tracking inside the three different PBRs at three different values of U_{Gr} (riser is on the left side and downcomer on the right side of each individual SCAPBR image).	185
Figure 7.14 Particle tracking inside the two different SCAPBRs at three different U_{Gr} (riser is on the foreground and the downcomer on the background of each individual SCAPBR image).	187

List of Tables

Table 2.1 Main microalgae groups based on their colours (Alam et al., 2012)	9
Table 2.2 Biomass composition of microalgae expressed on a dry matter basis (modified from Um (2009); Sydney et al., (2010))	12
Table 2.3 Products synthesized by microalgae (adapted from Spolaore et al., 2006)	13
Table 2.4 Advantages and limitations of various microalgae culture systems	26
Table 3.1 Experimental range and levels of the independent process variables according to the 2 ² full-factorial central composite design	61
Table 3.2 Growth parameters of <i>C. vulgaris</i> cultivated under different CO ₂ concentrations and aeration rates at 30 °C	65
Table 3.3 Elemental composition of <i>C. vulgaris</i> cells	67
Table 3.4 Experimental matrix and results of R _{CO₂} (g L ⁻¹ d ⁻¹) with coded levels of CO ₂ concentration (X_1) and aeration rate (X_2) according to the 2 ² full-factorial central composite design	67
Table 3.5 Effect estimates, standard errors and t-test for R _{CO₂} by <i>C. vulgaris</i> according to the 2 ² full-factorial central composite design	68
Table 4.1 Levels and range of the independent variables (initial concentration of nitrogen and iron sources) based on full CCD for two factors	78
Table 4.2 Experimental matrix and results of microalgal starch accumulation (%) with coded levels of initial urea concentration (X_1) and initial FeNa-EDTA concentration (X_2) according to the 2 ² full-factorial CCD	79
Table 4.3 Starch content of green microalgal species cultivated under photoautotrophic conditions	80
Table 4.4 Effect estimates, standard errors and t-test for starch accumulation in <i>C. vulgaris</i> according to the 2 ² full-factorial central composite design	81
Table 4.5 Evolution of total lipid content in cells kept in sedimentation vessel, for 22 days	106
Table 5.1 Different cultivation conditions of <i>C. vulgaris</i> and respective carbon sources	115
Table 5.2 Growth parameters of <i>C. vulgaris</i> cultivated under photoautotrophic and mixotrophic conditions at 30 °C	119
Table 5.3 Consumption of glucose and galactose by <i>C. vulgaris</i> cultivated under mixotrophic conditions at 30 °C	120
Table 5.4 Total pigment (chlorophylls + carotenoids) content of <i>C. vulgaris</i> cultivated under photoautotrophic and mixotrophic conditions at 30 °C	124

Table 6.1 Coefficients from Equation 2 for the circular and planar geometries and for different microalgae cell concentrations, with the respective value of R^2 .	145
Table 7.1 $K_L a$ values obtained in different cultivation systems (adapted from Ugwu <i>et al.</i> , 2003)	177
Table 7.2 Continuously illuminated PBRs surface area	183
Table 7.3 Particle mean circulation time inside SCAPBRs	188

Nomenclature

Symbol	Description	Unit
B_{CD}	Bubble complexity degree	%
C_C	Carbon content	% (w/w)
d_{32}	Sauter mean diameter	mm
DW	Dry weight	g L^{-1}
F_{max}	Maximum Feret diameter	mm
F_{min}	Minimum Feret diameter	mm
$L.I.$	Light intensity	$\mu\text{E m}^{-2} \text{s}^{-1}$
No	Cell number	cell ml^{-1}
Pd	Penetration distance	mm
P_{max}	Maximum biomass productivity	$\text{g L}^{-1} \text{d}^{-1}$
$PPFD$	Photosynthetic photon flux density	$\mu\text{E m}^{-2} \text{s}^{-1}$
R_{CO_2}	CO_2 biofixation rate	$\text{g L}^{-1} \text{d}^{-1}$
RLI	Relative light intensity	%
U_{Gr}	Superficial gas velocity	m s^{-1}
V	Cell volume	μm^3
X	Biomass concentration	g L^{-1}
X_{max}	Final biomass concentration	g L^{-1}
ε	Gas holdup	%
μ_{max}	Specific growth rate	d^{-1}

Abbreviations

AA	Arachidonic acid
BC	Bubble column
BOD	Biochemical oxygen demand
CCD	Central composite design
COD	Chemical oxygen demand
CW	Cheese whey
DHA	Docosahexaenoic acid
DIC	Dissolved inorganic carbon
DW	Dry weight
EPA	Eicosapentaenoic acid
GRAS	Generally recognized as safe
hCW	Hydrolysed cheese whey
HPLC	High-performance liquid chromatography
nhCW	Non-hydrolysed cheese whey
OGM	Original growth medium
PAR	Photosynthetically active radiation
PBR	Photobioreactor
PUFA	Polyunsaturated fatty acid
PVC	Polyvinyl chloride
SCAPBR	Split cylinder airlift photobioreactor
TAG	Triacylglyceride

CHAPTER 1

Motivation and Outline

1.1 Thesis Motivation	3
1.2 Research Aims	4
1.3 Thesis Outline	4
1.4 References	5

1.1 Thesis Motivation

The driving force for the development of microalgae-related technology is the fact that these microorganisms are one of the most promising feedstocks for biofuel production since they are able to convert solar energy to chemical energy via carbon dioxide (CO₂) fixation (Ahmad *et al.* 2011). These photosynthetic microorganisms accumulate significant quantities of lipids and carbohydrates over short periods of time that can be subsequently processed into biodiesel and bioethanol, respectively. Microalgae can also produce a wide range of other different valuable compounds, and currently they are being exploited industrially as a source of long-chain polyunsaturated fatty acids (PUFAs), polysaccharides, vitamins (*e.g.* tocopherols), pigments (carotenoids, phycobiliproteins), and aquaculture feed for rotifers. Despite all these options, much of the interest in microalgae cultivation is due to its great potential as feedstock for biofuel production.

Comparing with other energy crops, microalgae have several advantages such as: *i*) faster growth, higher photosynthetic efficiency and biomass production; *ii*) they need less water; *iii*) possibility of being cultivated in seawater or brackish water on non-arable land, while not competing for resources with conventional agriculture; *iv*) possibility of combining microalgae biomass production with direct bio-fixation of waste CO₂ (1 kg of dry algal biomass requiring about 1.8 kg of CO₂); *v*) nutrients for microalgae cultivation (especially nitrogen and phosphorus) can be obtained from wastewaters; *vi*) no need for herbicides or pesticides during microalgae cultivation; *vii*) the residual algal biomass after oil extraction may be used as feed or fertilizer, or fermented to produce ethanol or methane (Liu *et al.*, 2008; Rodolfi *et al.*, 2009; Fernandes *et al.*, 2010; Huang *et al.*, 2010; Amaro *et al.*, 2010; Dragone *et al.*, 2011). Another important fact is that the microalgal biomass composition can be influenced via different cultivation conditions, in order to achieve better outputs *e.g.* reserve materials (starch, oil) (Fernandes *et al.*, 2010).

In spite of the huge interest in microalgae cultivation, the economic aspects of the process are still to be satisfactorily solved, thus requiring the reduction of costs associated with microalgae mass production. Assuming that the best microalgal specie for the process is identified and selected, the next quest remaining is an optimal design

of the microalgae cultivation system and the selection of cultivation techniques that lead to a productivity increase.

1.2 Research Aims

The main objective of this thesis was the development and optimization of a cultivation system and techniques that would overcome the existing technology, for an economical and environmental sustainable microalgae mass production. In order to attain this main goal some, more concrete, objectives were established:

- Optimization of CO₂ supply conditions in order to maximize its biofixation rate by microalgal cells;
- Optimization of culture medium composition in order to increase the cultivation system productivity;
- Development of low cost strategies in order to achieve high specific productivities (*e.g.* starch and lipid productivities);
- Implementation of techniques to allow the utilization of agro-industrial wastes as cheap culture medium for microalgae cultivation;
- Design, test and characterize a PBR that overcome the limitations of the existing cultivation systems, namely in terms of efficient light utilization, mass transfer and temperature control.

All these objectives should be accomplished taking in mind the need to use materials and technologies with reasonable investments and maintenances costs.

1.3 Thesis Outline

Based on these objectives, this thesis was organized in eight chapters. Chapter 2 provides a literature review about microalgae production. Chapters 3 to 7 contain the main experimental results and each one is divided in: Abstract, Introduction, Material and Methods, Results and Discussion and Conclusions. Chapter 8 presents the overall conclusions and future perspectives.

Chapter 2 provides an overview of state of the art on microalgae applications, existing cultivation systems and its main design concerns and finally, cost/effectiveness

considerations that are important in order to achieve a sustainable process for microalgae mass production.

In Chapter 3 CO₂ supply conditions, namely CO₂ concentration and aeration rate, are optimized in order to obtain a maximum CO₂ biofixation rate, and thus a maximum biomass productivity;

In Chapter 4 two different strategies are explored in order to maximize biomass and, specially, starch and lipid productivities. These strategies are nutrient depletion and nutrient limitation.

In Chapter 5 the utilization of a dairy industry waste (cheese whey) is tested as an inexpensive carbon source for mixotrophic growth of microalgae, as a cheap and more productive alternative to typical photoautotrophic growth.

In Chapter 6 the selection and design process of a new cultivation system for the production of microalgae is presented. The proposed cultivation system is a Split Cylinder Airlift Photobioreactor (SCAPBR). Photobioreactor geometry selection is made based on studies using optical fibre technology.

In Chapter 7, three different photobioreactors (SCAPBR 75, SCAPBR 50 and a bubble column) are characterized and tested. A full description in terms of gas and liquid phase characterization, mass transfer, light distribution and flow patterns inside the photobioreactors is performed.

Finally, Chapter 8 presents the overall conclusions, recommendations and suggestions for future work.

1.4 References

- Ahmad A. L., Yasin N. H. M. , Derek C. J. C. , Lim J. K., 2011. Microalgae as a sustainable energy source for biodiesel production: a review. *Renew. Sust. Energ. Rev.* 15: 584-593.
- Amaro H. M., Guedes A. C., Malcata F. X., 2011. Advances and perspectives in using microalgae to produce biodiesel. *Appl. Energy* 88 (10): 3402-3410.
- Dragone G., Fernandes B. D., Abreu A. P., Vicente A. A., Teixeira J. A., 2011. Nutrient limitation as a strategy for increasing starch accumulation in microalgae. *Applied Energy* 88 (10): 3331-3335.
- Fernandes B., Dragone G., Teixeira J., Vicente A., 2010. Light regime characterization in an airlift photobioreactor for production of microalgae with high starch content. *Appl. Biochem. Biotechnol.* 161: 218-26.

- Fernandes B., Dragone G., Abreu Ana P., Geada P., Teixeira J., Vicente A., 2012. Starch determination in *Chlorella vulgaris*—a comparison between acid and enzymatic methods. *Journal of Applied Phycology* 24 (5): 1203–1208.
- Huang G., Chen F., Wei D., Zhang X., Chen G., 2010. Biodiesel production by microalgal biotechnology. *Appl Energy* 87: 38–46.
- Liu Z.Y., Wang G.C., Zhou B.C., 2008. Effect of iron on growth and lipid accumulation in *Chlorella vulgaris*. *Bioresour Technol* 99: 4717–22.
- Rodolfi L., Zittelli G.C., Bassi N., Padovani G., Biondi N., Bonini G., 2009. Microalgae for oil: strain selection, induction of lipid synthesis and outdoor mass cultivation in a low-cost photobioreactor. *Biotechnol Bioeng* 102: 100–12.

CHAPTER 2

Microalgae cultivation and applications

2.1 Microalgae and its applications	9
2.2 Cultivation systems, design considerations and downstream processes	20
2.3 Cost/effectiveness considerations	36
2.4 References	48

Most of the information presented in this Chapter was adapted from:

Dragone G., **Fernandes B.**, Vicente A., Teixeira J.A., 2010. *Third generation biofuels from microalgae*. In: Vilas AM, editor. Current research, technology and education topics in applied microbiology and microbial biotechnology. Badajoz: Formatex Research Center; p. 1355–66.

Ruiz H. A., Rodríguez-Jasso R. M., **Fernandes B. D.**, Vicente A. A., Teixeira J. T., 2013. *Hydrothermal processing, as an alternative for upgrading agriculture residues and marine biomass according to the biorefinery concept: a review*. *Renewable & Sustainable Energy Reviews* 21: 35-51.

2.1 Microalgae and their applications

Microalgae are recognised as one of the oldest forms of life. They are thallophytes (plants lacking roots, stems, and leaves) that have chlorophyll *a* as their primary photosynthetic pigment and lack a sterile covering of cells around the reproductive cells (Brennan and Owende, 2010). Although the mechanism of photosynthesis in microalgae is similar to that of higher plants, they are generally more efficient converters of solar energy because of their simple cellular structure. In addition, because the cells grow in aqueous suspension, they have more efficient access to water, CO₂, and other nutrients (Chisti, 2007).

Traditionally microalgae have been classified according to their colour and this characteristic continues to be of a certain importance. Some major groups of microalgae are shown in Table 2.1.

Table 2.1 Main microalgae groups based on their colours (Alam *et al.*, 2012)

Colour	Group
Yellow-green algae	<i>Xanthophyceae</i>
Red algae	<i>Rhodophyceae</i>
Golden algae	<i>Chrysophyceae</i>
Green algae	<i>Chlorophyceae</i>
Brown algae	<i>Phaeophyceae</i>
Cyanobacteria	<i>Cyanophyceae</i>

The current systems of microalgae classification are based on the following main criteria: kinds of pigments, chemical nature of storage products and cell wall constituents. Additional criteria take into consideration the following cytological and morphological characters: occurrence of flagellate cells, structure of the flagella, scheme and path of nuclear and cell division, presence of an envelope of endoplasmic reticulum around the chloroplast, and possible connection between the endoplasmic reticulum and the nuclear membrane (Tomaselli, 2004). There are two basic types of microalgae cells, prokaryotic and eukaryotic. Prokaryotic cells lack membrane-bounded organelles (plastids, mitochondria, nuclei, Golgi bodies, and flagella) and occur in the cyanobacteria. The remainder of the microalgae are eukaryotic and have organelles (Lee, 2008). Microalgae can be either autotrophic or heterotrophic. If they are

autotrophic, they use inorganic compounds as a carbon source. Autotrophs can be photoautotrophic, using light as a source of energy, or chemoautotrophic, oxidizing inorganic compounds for energy. If they are heterotrophic, microalgae use organic compounds for growth. Heterotrophs can be photoheterotrophs, using light as a source of energy, or chemoheterotrophs, oxidizing organic compounds for energy. Some photosynthetic microalgae are mixotrophic, combining heterotrophy and autotrophy by photosynthesis (Lee, 2008).

For autotrophic microalgae, photosynthesis is a key component of their survival, whereby they convert solar radiation and CO₂ absorbed by chloroplasts into adenosine triphosphate (ATP) and O₂, the usable energy currency at cellular level, which is then used in respiration to produce energy to support growth (Brennan and Owende, 2010).

Microalgae are able to fix CO₂ efficiently from different sources, including the atmosphere, industrial exhaust gases, and soluble carbonate salts. Fixation of CO₂ from atmosphere is probably the most basic method to sink carbon, and relies on the mass transfer from the air to the microalgae in their aquatic growth environments during photosynthesis. Industrial exhaust gases such as flue gas contain up to 15% CO₂, providing a CO₂-rich source for microalgal cultivation and a potentially more efficient route for CO₂ bio-fixation.

Microalgae are present in all existing earth ecosystems living in a wide range of environmental conditions. It is estimated that more than 50,000 species exist, but only a limited number, of around 30,000, have been studied and analysed (Richmond, 2004_a) and a very limited number is mass cultured for commercial purposes (Figure 2.1). One of the world's largest microalgae collections is the freshwater microalgae collection of University of Coimbra (Portugal) having more than 4,000 strains and 1,000 species (Mata *et al.*, 2010). Microalgal biomass contains three main components: proteins, carbohydrates, and lipids. The biomass composition of various microalgae in terms of those main components is shown in Table 2.2.

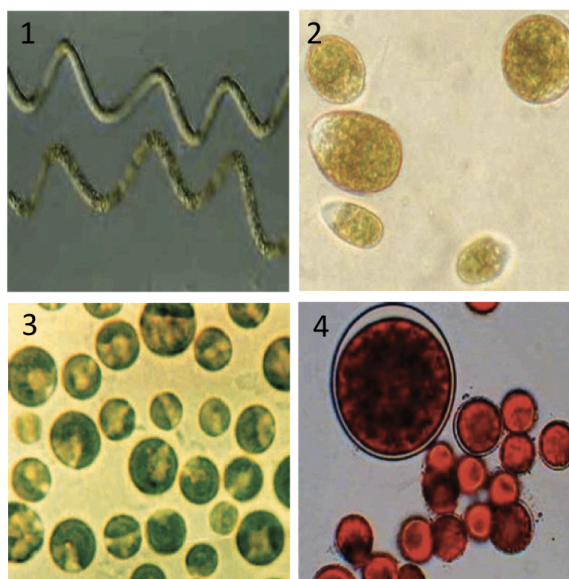


Figure 2.1 Some of the microalgae strains currently mass cultivated. 1 - *Spirulina* (*Arthrospira platensis*); 2 - *Dunaliella salina*; 3 - *Chlorella vulgaris*; 4 - *Haematococcus pluvialis* (adapted from Benemann, 2008).

Microalgae have a wide range of potential applications ranging from direct use of biomass (*e.g.* aquaculture feed) or indirect use for the production of high-value compounds (*e.g.* vitamins and pigments) and for environmental applications (*e.g.* biofuel production and CO₂ mitigation). Biomolecules expressed by microalgae are generally regarded as safe (GRAS) for human consumption; consequently nutritional and medical applications are especially suitable for these microorganisms (Rosenberg *et al.*, 2008). Beside other uses, microalgae are exploited industrially as a source of long-chain polyunsaturated fatty acids (PUFAs), polysaccharides, vitamins (*e.g.* tocopherols), β -carotene and pigments (carotenoids, phycobiliproteins) (Abalde *et al.*, 1991; Molina Grima *et al.*, 1994; Chini Zittelli *et al.*, 1999; Arad and Richmond, 2004). Also, microalgae cultivation has been carried out throughout the world as essential aquaculture feed (constituting both a source of energy as well as the essential vitamins and PUFAs (Sandnes *et al.*, 2006) for rotifers, and as very important live food for larvae of marine fish, filter-feeding invertebrates. In 1999, the production of microalgae for aquaculture was 1,000 ton: 62% for molluscs, 22% for shrimps and 16% for fish (Muller, 2000). More recently, microalgae have been used for wastewater treatment, CO₂ mitigation, or as a feedstock for biofuel production (Brennan and Owende, 2010).

As it can be seen in Table 2.3 some of the most successful commercial utilization of

microalgae has been established in low-volume, high-value derivatives such as nutritional supplements, antioxidants, cosmetics, natural dyes, and polyunsaturated fatty acids (PUFA) (Spolaore *et al.*, 2006).

Table 2.2 Biomass composition of microalgae expressed on a dry matter basis (modified from Um (2009); Sydney *et al.*, (2010))

Strain	Protein (%)	Carbohydrates (%)	Lipid (%)
<i>Anabaena cylindrica</i>	43–56	25–30	4–7
<i>Botryococcus braunii</i>	40	2	33
<i>Chlamydomonas reinhardtii</i>	48	17	21
<i>Chlorella pyrenoidosa</i>	57	26	2
<i>Chlorella vulgaris</i>	41–58	12–17	10–22
<i>Dunaliella bioculata</i>	49	4	8
<i>Dunaliella salina</i>	57	32	6
<i>Dunaliella tertiolecta</i>	29	14	11
<i>Euglena gracilis</i>	39–61	14–18	14–20
<i>Porphyridium cruentum</i>	28–39	40–57	9–14
<i>Prymnesium parvum</i>	28–45	25–33	22–39
<i>Scenedesmus dimorphus</i>	8–18	21–52	16–40
<i>Scenedesmus obliquus</i>	50–56	10–17	12–14
<i>Scenedesmus quadricauda</i>	47	–	1.9
<i>Spirogyra</i> sp.	6–20	33–64	11–21
<i>Spirulina maxima</i>	60–71	13–16	6–7
<i>Spirulina platensis</i>	42–63	8–14	4–11
<i>Synechococcus</i> sp.	63	15	11
<i>Tetraselmis maculata</i>	52	15	3

The worldwide annual production of algal biomass is estimated to be 8,000 – 10,000 ton year⁻¹ (Brennan and Owende, 2010) with an average market value of about 330 USD kg⁻¹ (Pulz and Gross, 2004). Commercial production of microalgae is primarily intended to direct use of biomass as aquaculture feed (approximately one-fifth of produced biomass) or indirect use for the production of speciality chemicals and high-value compounds (Muller-Fuega, 2004). Presently, the development of pharmaceutical compounds and biofuels is a priority of the industry (Rosenberg *et al.*, 2008).

In this work the emphasis is going to be given to microalgae cultivation for biofuel

production (biodiesel and bioethanol) and CO₂ mitigation. Thus, all studies performed in this work will take into account the composition of microalgae in terms of energy-rich materials and continuous CO₂ utilization.

Table 2.3 Products synthesized by microalgae (adapted from Spolaore *et al.*, 2006)

Product	Microalgae	Price (USD)	Producer
- β - carotene	<i>Dunaliella</i>	300 – 3000 /kg	- AquaCarotene (USA) - Cognis Nutrition & Health (Australia) - Cyanotech (USA) - Nikken Sohonsa Corporation (Japan) - Tianjin Lantai Biotechnology (China) - Parry Pharmaceuticals (India)
- Astaxanthin	<i>Haematococcus</i>	10,000 /kg	- AlgaTechnologies (Israel) - Bioreal (Hawaii, USA) - Cyanotech (Hawaii, USA) - Mera Pharmaceuticals (Hawaii, USA) - Parry Pharmaceuticals (India)
- Whole-cell dietary supplements	<i>Spirulina</i> <i>Chlorella</i> <i>Chlamydomonas</i>	50 /kg	- BlueBiotech International GmbH (Germany) - Cyanotech (USA) - Earthrise Nutritionals (USA) - Phycotransgenics (USA)
- Whole-cell aquaculture feed	<i>Tetraselmis</i> <i>Nannochloropsis</i> <i>Isochrysis</i> <i>Nitzschia</i>	70 /L	- Aquatic Eco-Systems (USA) - BlueBiotech International GmbH (Germany) - Coastal BioMarine (USA) - Reed Mariculture (USA)
- Polyunsaturated fatty acids	<i>Cryptocodinium</i> <i>Schizochytrium</i>	60 /g	- BlueBiotech International GmbH (Germany) - Spectra Stable Isotopes (USA) - Martek Biosciences (USA)
- Heavy isotope labeled metabolites	N/A	1000 – 20,000 /g	- Spectra Stable Isotopes (USA)
- Phycoerythrin (fluorescent label)	Red Algae Cyanobacteria	15 /mg	- BlueBiotech International GmbH (Germany) - Cyanotech (USA)
- Anticancer drugs	N/A	N/A	- PharmaMar (Spain)
- Pharmaceutical proteins	<i>Chlamydomonas</i>	N/A	- Rincon Pharmaceuticals (USA)
- Biofuels	<i>Botryococcus</i> <i>Chlamydomonas</i> <i>Chlorella</i> <i>Dunaliella</i> <i>Neochloris</i>	N/A	- Cellana (USA) - GreenFuel Technologies (USA) - LiveFuels, Inc. (USA) - PetroAlgae (USA) - Sapphire Energy (USA) - Solazyme, Inc. (USA) - Solix Biofuels (USA)

2.1.1 Microalgae as a source of biofuel

Biofuel production from renewable sources is widely considered to be one of the most sustainable alternatives to petroleum-sourced fuels and a viable means for environmental and economic sustainability. Microalgae are currently being promoted as an ideal third generation biofuel feedstock because of their rapid growth rate, CO₂ fixation ability and high production capacity of lipids; they also do not compete with food or feed crops, and can be produced on non-arable land. Microalgae have broad bioenergy potential as they can be used to produce liquid transportation and heating fuels, such as biodiesel and bioethanol (Figure 2.2). Therefore, third generation biofuels derived from microalgae are considered to be a viable alternative energy resource that is devoid of the major drawbacks associated with first and second generation biofuels (Chisti, 2007; Li *et al.*, 2008; Nigam and Singh, 2010).

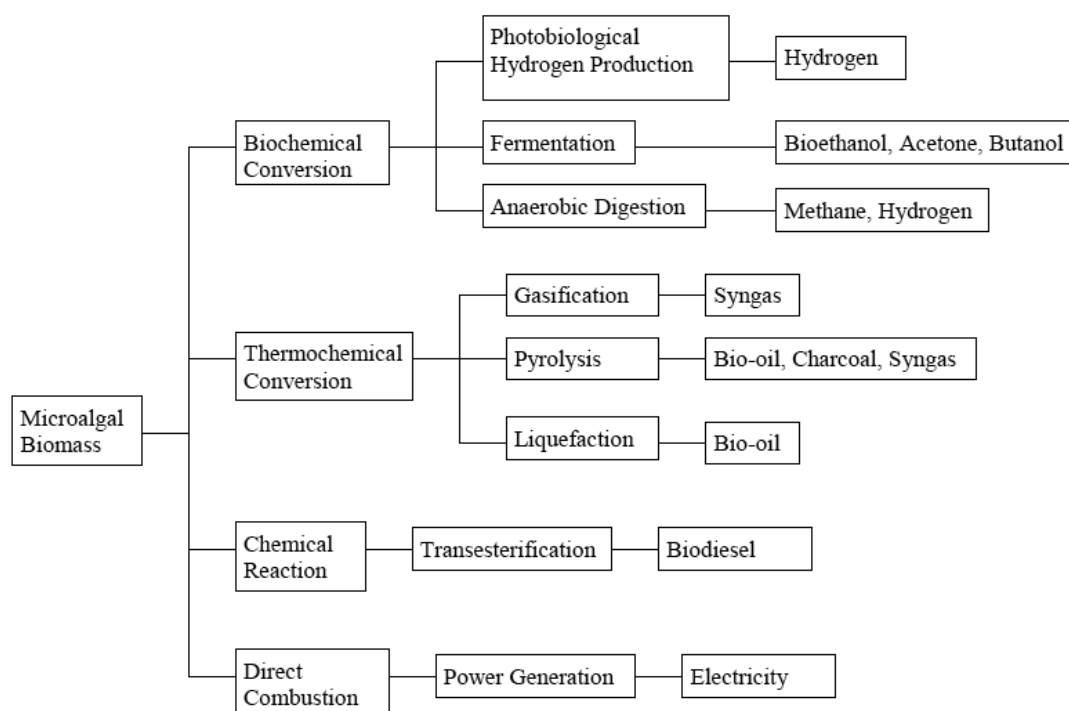


Figure 2.2 Conversion processes for biofuel production from microalgal biomass (modified from Wang *et al.*, 2008).

Microalgae are able to produce 15 – 300 times more oil for biodiesel production than traditional crops on an area basis. Furthermore compared with conventional crop plants, which are usually harvested once or twice a year, microalgae have a very short harvesting cycle ($\approx 1 - 10$ days depending on the process), allowing multiple or

continuous harvests with significantly increased yields (Schenk *et al.*, 2008).

There are several ways to convert microalgal biomass to energy sources, which can be classified into biochemical conversion, chemical reaction, direct combustion, and thermochemical conversion (Figure 2.2).

The idea of using microalgae as a source of biofuel is not new, but it is now being taken seriously because of the rising price of petroleum and, more significantly, the emerging concern about global warming that is associated with burning of fossil fuels (Chisti, 2007). The utilization of microalgae for biofuels production offers the following advantages over higher plants (Um and Kim, 2009; Brennan and Owende, 2010; Mata *et al.*, 2010):

1. microalgae synthesize and accumulate large quantities of neutral lipids (20 – 50% dry weight of biomass) and grow at high rates;
2. microalgae are capable of all year round production, therefore, oil yield per area of microalgae cultures could greatly exceed the yield of best oilseed crops;
3. microalgae need less water than terrestrial crops therefore reducing the load on freshwater sources;
4. microalgae cultivation does not require herbicides or pesticides application;
5. microalgae can sequester CO₂ from flue gases emitted from fossil fuel-fired power plants and other sources, thereby reducing emissions of a major greenhouse gas (1 kg of dry algal biomass utilise about 1.83 kg of CO₂);
6. wastewater bioremediation by removal of NH₄⁺, NO₃⁻, PO₄³⁻ from a variety of wastewater sources (*e.g.* agricultural run-off, concentrated animal feed operations, and industrial and municipal wastewaters);
7. combined with their ability to grow under harsher conditions and their reduced needs for nutrients, microalgae can be cultivated in saline/brackish water/coastal seawater on non-arable land;
8. microalgae cultivation do not compete for resources with conventional agriculture.

9. depending on the microalgae species other compounds may also be extracted, with valuable applications in different industrial sectors, including a large range of fine chemicals and bulk products, such as polyunsaturated fatty acids, natural dyes, polysaccharides, pigments, antioxidants, high-value bioactive compounds, and proteins.

Recent studies have shown that microalgal biomass is one of the most promising sources of renewable biodiesel that is capable of meeting the global demand for transport fuels. Biodiesel production by microalgae will not compromise production of food, fodder and other products derived from crops (Chisti, 2007). Much of the on-going research work is focused on a small number of fast-growing microalgal species which have been found to accumulate substantial quantities of lipids, though under specific conditions. Within the green algae, typical species include *Chlamydomonas reinhardtii*, *Dunaliella salina*, and various *Chlorella* species, as well as *Botryococcus braunii*, which although slow growing can accumulate large quantities of lipids (Scott *et al.*, 2010).

While many microalgae strains naturally have high lipid content, it is possible to increase that concentration by optimising growth-determining factors such as the control of nitrogen level, light intensity, temperature, salinity, CO₂ concentration and harvesting procedure. However, increasing lipid accumulation could not result in increased lipid productivity as biomass productivity and lipid accumulation are not necessarily correlated. Lipid accumulation refers to increased concentration of lipids within the microalgae cells without consideration of the overall biomass production. Lipid productivity takes into account both the lipid concentration within cells and the biomass produced by these cells and is therefore a more useful indicator of the potential costs of liquid biofuel production (Brennan and Owende, 2010).

An integrated production of biofuels from microalgae (Figure 2.3) includes a microalgal cultivation step, followed by the separation of the cells from the growth medium and subsequent lipid extraction for biodiesel production through transesterification. Following oil extraction, amylolytic enzymes are used to promote starch hydrolysis and formation of fermentable sugars. These sugars can be fermented and distilled into bioethanol using conventional ethanol distillation technology.

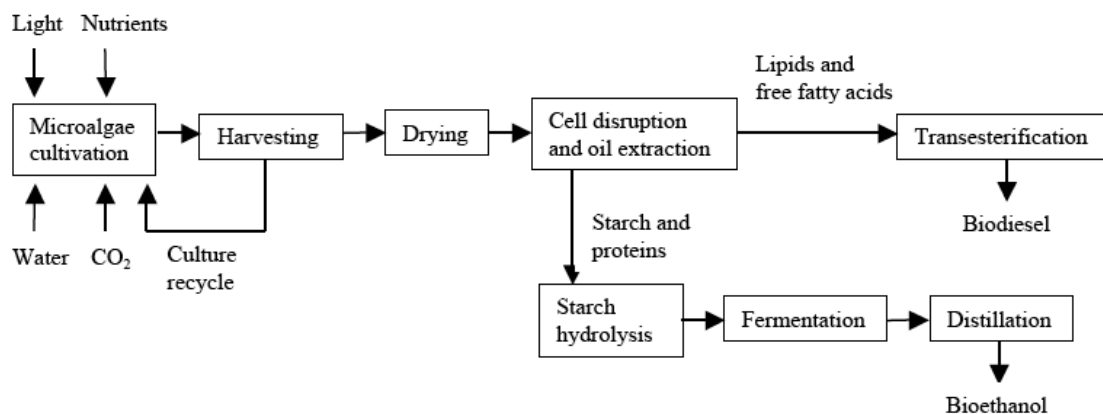


Figure 2.3 Integrated process for biodiesel and bioethanol production from microalgae.

2.1.1.1 Biodiesel production

After the extraction processes, the resulting microalgal oil can be converted into biodiesel through a process called transesterification. The transesterification reaction consists of transforming triglycerides into fatty acid alkyl esters, in the presence of an alcohol, such as methanol or ethanol, and a catalyst, such as an alkali or acid, with glycerol as a by-product (Vasudevan and Briggs, 2008).

For user acceptance, microalgal biodiesel needs to comply with existing standards, such as ASTM Biodiesel Standard D 6751 (United States) or Standard EN 14214 (European Union). Microalgal oil contains a high degree of polyunsaturated fatty acids (with four or more double bonds) when compared to vegetable oils, which makes it susceptible to oxidation in storage and therefore reduces its acceptability for use in biodiesel. However, the extent of unsaturation of microalgal oil and its content of fatty acids with more than four double bonds can be reduced easily by partial catalytic hydrogenation of the oil, the same technology that is commonly used in making margarine from vegetable oils (Chisti, 2007). Nevertheless, microalgal biodiesel has similar physical and chemical properties to petroleum diesel, first generation biodiesel from oil crops and compares favourably with the international standard EN14214 (Brennan and Owende, 2010).

2.1.1.2 Bioethanol production

The current interests in producing bioethanol are focusing on microalgae as a feedstock for fermentation process. Microalgae provide carbohydrates (in the form of glucose, starch and other polysaccharides) and proteins that can be used as carbon sources for fermentation by bacteria, yeast or fungi (Harun *et al.*, 2010_a). For instance, *Chlorella vulgaris* has been considered as a potential raw material for bioethanol production because it can accumulate high levels of starch (Hirano *et al.*, 1997). *Chlorococum* sp. was also used as a substrate for bioethanol production under different fermentation conditions. Results showed a maximum bioethanol concentration of 3.83 g L⁻¹ obtained from 10 g L⁻¹ of lipid-extracted microalgae debris (Harun *et al.*, 2010_b). Production of bioethanol by using microalgae can also be performed via self-fermentation. Previous studies reported that dark fermentation in the marine green algae *Chlorococum littorale* was able to produce 450 μmol ethanol g⁻¹ at 30 °C (Ueno *et al.*, 1998).

Even though limited reports on microalgal fermentation are available, a number of advantages were detected in order to produce bioethanol from microalgae. Fermentation process requires less consumption of energy and simplified process compared to biodiesel production system. Besides, CO₂ produced as by-product from fermentation process can be recycled as carbon sources to microalgae in cultivation process thus reducing the greenhouse gases emissions. However, the production of bioethanol from microalgae is still under investigation and this technology has not yet been commercialized (Harun *et al.*, 2010_a).

2.1.2 Microalgae as a CO₂ biological mitigation system

The increasing concentration of anthropogenic CO₂ in the atmosphere appears to be the major cause of global warming, which may have catastrophic consequences for the environment and the climate (Chiu *et al.*, 2009). The amount of CO₂ in the atmosphere was 390.9 ppm in 2011, increasing on average 2 ppm per year for the past 10 years and reaching 140% of the pre-industrial level (280 ppm) (WMO, 2012). In order to reduce its atmospheric concentration, different abiotic (physical) methods have been evaluated, including injection into geological formations/deep oceans or utilization of absorbent

materials (Kumar *et al.*, 2010). These methods, however, require significant space of storage associated with elevated costs of monitoring, operation, and maintenance, raising serious concerns about potential CO₂ leakage over time (Bilanovic *et al.*, 2009).

On the other hand, biological mitigation of atmospheric CO₂ has been deemed as a sustainable approach to physical methods (Kumar *et al.*, 2011). Biofixation of CO₂ can be performed either by plants or photosynthetic microorganisms. Nevertheless, the process of CO₂ sequestration by plants can be viewed as an inadequate strategy of mitigation, since its contribution to CO₂ capture has been estimated to only 3 – 6% of fossil fuel emissions, mainly because of slow growth rates of terrestrial vegetation (Wang *et al.*, 2008). Alternatively, microalgae have received renewed attention in recent years due to their faster growth rates and higher photosynthetic efficiency than terrestrial plants (Chiu *et al.*, 2009; Dragone *et al.*, 2011). These photosynthetic microorganisms can efficiently convert CO₂ from a point source into O₂ and biomass (Tang *et al.*, 2011).

Phototrophic microalgal growth requires a continuous supply of CO₂ as a carbon source, and the CO₂ supply also contributes to control the pH of the culture. Chemical analysis has shown that algal biomass consists of 40% to 50% carbon, which indicates that approximately 1.5 to 2.0 kg of CO₂ is required to produce 1.0 kg of microalgal biomass (Sobczuk *et al.*, 2000). For these reasons, cultivation of microalgae can be exploited as an additional step in flue gas treatment, aiming the reduction of CO₂ levels in the exhaust flue gas. Previous studies have demonstrated that microalgae can be successfully employed for the treatment of simulated flue gases (Lee *et al.*, 2000) or flue gases emitted from municipal waste incinerators (Douskova *et al.*, 2009), coal-fired power plants (McGinn *et al.*, 2011), industrial heater using kerosene as fuel (Chae *et al.*, 2006) and gas boiler (Doucha *et al.*, 2005).

2.2 Cultivation systems, design considerations and downstream processes

2.2.1 Cultivation systems

After selecting the microalgae strain to obtain the product of interest, it becomes necessary to develop a whole range of bioprocesses that make viable its commercialization. Thus, the design and optimization of adequate bioreactors to cultivate these microorganisms is a major step in the strategy that aims at transforming scientific findings into a marketable product. Despite of many possible applications, only a few species of microalgae are cultured commercially because of poorly developed microalgal bioreactor technology.

From a commercial point of view, a microalgae culture system must have as many of the following characteristics as possible: high area productivity; high volumetric productivity; inexpensiveness (both in terms of investment and maintenance costs); easiness of control of the culture parameters (temperature, pH, O₂, turbulence); and reliability (Olaizola, 2003). Cultivation systems of different designs attempt to achieve these characteristics differently (Figure 2.4). Although the term “photobioreactor” (PBR) has been applied to open ponds and channels, applied phycologists have generally distinguished between open-air systems and PBRs (devices that allow monoseptic culture). Thus in this thesis the term PBR is used only for closed systems.

2.2.1.1 *Open-air systems*

Open-air systems were extensively studied in the past few years (Chaumont, 1993; Borowitzka, 1999; Tredici 2004), but these algae cultivation systems have been used since the 1950s. The classical open-air cultivation systems comprise lakes and natural ponds, circular ponds, raceway ponds and inclined systems. Open-air systems are the most widespread growth systems, and all very large commercial systems used today are of this type. The reasons for this relate to economic and operational issues, since these systems are easier and less expensive to build, operate more durably and have a larger production capacity than most closed systems; further, they can utilize sunlight and the

nutrients can be provided through runoff water from nearby land areas or by channelling the water from sewage/water treatment plants (Carlsson *et al.*, 2007) making it the cheapest method of large-scale algal biomass production.

Although these systems are the most widely used at industrial level, open-air systems still present significant technical challenges. Open ponds are susceptible to weather conditions, not allowing control of water temperature, evaporation and lighting, which make these systems dependent on the prevailing regional climate conditions (daily and annual temperature range, annual rainfall and rainfall pattern, number of sunny days, and degree of cloud cover). Furthermore, contamination by predators and other fast growing heterotrophs have restricted the commercial production of algae in open culture systems to fast growing, naturally occurring or extremophilic species. Consequently, this strictly limits the species of algae that can be grown in such systems. As a result, only *Dunaliella* (adaptable to very high salinity), *Spirulina* (adaptable to high alkalinity) and *Chlorella* (adaptable to nutrient-rich media) have been successfully grown in commercial open pond systems (Carlsson *et al.*, 2007).

Natural and artificial ponds are only viable when a series of conditions are met. The existence of favourable climatic conditions and sufficient nutrients in order to the microalgae grow is profusely unavoidable and it also requires that the water presents selective characteristics (*e.g.* high salinity, high pH, high nutrients concentration) to ensure the existence of a monoculture. Successful examples of this type of cultivation are the *Arthrospira* production in Lake Kossorom (soda lake at the irregular northeast fringe of Lake Chad) where the Kanembu people harvest about 40 t year⁻¹ of *Arthrospira* (*Spirulina*), to use it as food (Abdulqader *et al.*, 2000) and in Myanmar, where four old volcanic craters, full of alkaline water are used as cultivation system for the production of around 30 t year⁻¹ of *Arthrospira* that are sold on the local market (Thein, 1993). The Australian producer of *D. salina* (extremely halophilic and highly light-tolerant green alga) Betatene Ltd, uses very large ponds (up to 250 ha with an average depth of 0.2 to 0.3 m) at the extremely halophilic waters of Hutt-Lagoon, Western Australia which are unmixed other than by wind and convection.

The inclined system (cascade system) is the only open-air system which achieves high sustainable cell densities (up to 10 g L⁻¹). This system is very well suited for algae

such as *Chlorella* and *Scenedesmus*, which can tolerate repeated pumping (Šetlík *et al.*, 1970). In inclined systems turbulence is created by gravity, the culture suspension flowing from the top to the bottom of a sloping surface, thus achieving highly turbulent flow and allowing the adoption of very thin culture layers (< 2 cm), facilitating higher cell concentrations and a higher surface-to-volume ratio (s/v) compared to raceway ponds.

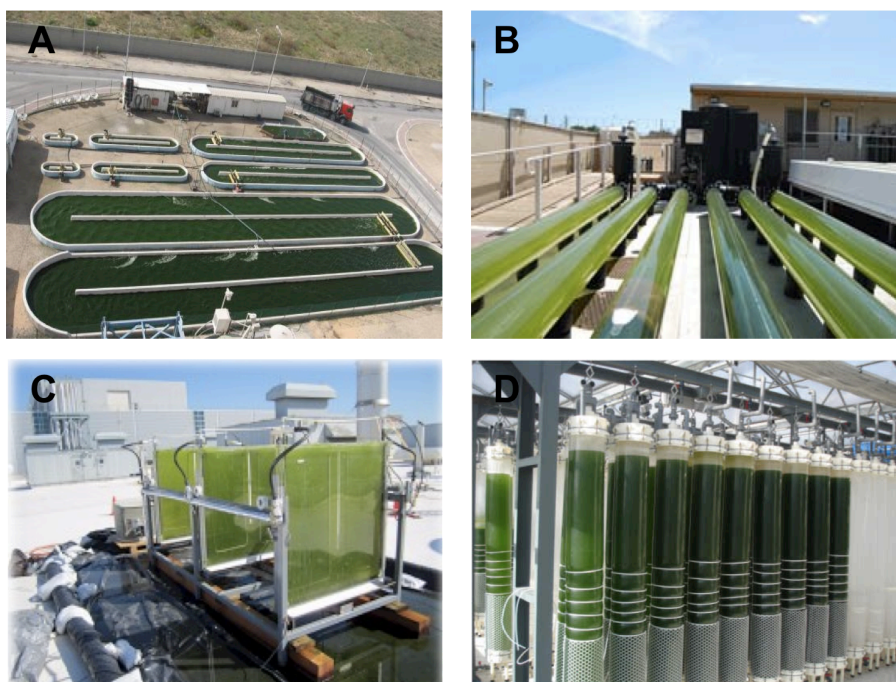


Figure 2.4 Different types of microalgae cultivation systems. A - Raceway pond (<http://www.makebiofuel.co.uk/biofuel-from-algae>); B - Tubular photobioreactor (<http://www.sardi.sa.gov.au/aquaculture/aquaculture/AlgaeAndBiofuelsFacility>); C - Flat photobioreactor (<http://www.oilgae.com/blog/2011/04/intel-demonstrates-pilot-model-for-algae-based-carbon-capture.html>); D - Column photobioreactor (Zhu *et al.*, 2013).

Circular ponds with a centrally pivoted rotating agitator are widely used in Indonesia, Japan and Taiwan for the production of *Chlorella*. Depth is about 0.3 m. The design of these systems, however, limits pond size to about 10,000 m², because mixing by the rotating arm is no longer possible in larger ponds. Circular ponds are not favoured in commercial plants since they require expensive concrete construction and high energy input for mixing (Borowitzka, 2005). Raceway ponds (Figure 2.4 A) are the most commonly used artificial system.

They are typically made of a closed loop, oval shaped recirculation channels, generally between 0.2 and 0.5 m deep, with mixing and circulation required to stabilize algae growth and productivity (Table 2.4). In a continuous production cycle, microalgae broth and nutrients are introduced in front of the paddlewheel and circulated through the loop to the harvest extraction point. The paddlewheel is in continuous operation to prevent sedimentation. At water depths of 0.15 - 0.20 m, biomass concentrations of up to 1 g L^{-1} and productivities of $10 - 25 \text{ g m}^{-2} \text{ day}$, are possible (Pulz, 2001). The largest raceway-based biomass production facility located in Calipatria, CA (USA) occupies an area of $440,000 \text{ m}^2$ to grow *Spirulina* (Spolaore *et al.*, 2006).

2.2.1.2 Photobioreactors

Photobioreactors (PBRs) are characterized by the regulation and control of nearly all the biotechnologically important parameters as well as by a reduced contamination risk, no CO_2 losses, reproducible cultivation conditions, controllable hydrodynamics and temperature, and flexible technical design (Pulz, 2001). These systems receive sunlight either directly through the transparent container walls or via light fibres or tubes that channel it from sunlight collectors. Despite the relative success of open systems, recent advances in microalgal mass culture require closed systems, as many of the new algae and algal high-value products for use in the pharmaceutical and cosmetics industry must be grown free of pollution and potential contaminants such as heavy metals and microorganisms.

Many different designs have been developed, but the main categories include: (1) tubular (*e.g.* helical, manifold, serpentine, and α -shaped); (2) flat (*e.g.* alveolar panels and glass plates); and (3) column (*e.g.* bubble columns and airlift). A great amount of developmental work has been carried out in order to optimize different PBR systems for microalgae cultivation (Chaumont, 1993; Janssen *et al.*, 2003; Tredici, 2004; Carvalho *et al.*, 2006).

Tubular photobioreactors

Tubular PBRs can be horizontal/serpentine- (Molina *et al.*, 2001), near horizontal- (Tredici and Zittelli, 1998), vertical- (Pirt *et al.*, 1983), inclined- (Lee and Low, 1991) and conical-shaped (Watanabe and Saiki, 1997). Microalgae are circulated through the

tubes by a pump, or preferably with airlift technology. Generally these PBR systems are relatively cheap, have a large illumination surface area and have fairly good biomass productivities (Figure 2.4 B). Disadvantages include fouling, some degree of wall growth, dissolved O₂ and CO₂ gradients along the tubes, and pH gradients that lead to frequent re-carbonation of the cultures, which would consequently increase the cost of algal production (Table 2.4).

The largest closed PBRs are tubular, like the 25 m³ plant at Mera Pharmaceuticals, Hawaii, and the 700 m³ plant in Klötze, Germany. A maximum productivity of 25 g m⁻² day⁻¹ (*Spirulina*) has been achieved in a 10 m³ serpentine bioreactor with intermitted culture circulation (Torzillo *et al.*, 1986). Further improvements were obtained by constructing a two-plane tubular photobioreactor with mean daylight productivities of about 30 g m⁻² day (Torzillo *et al.*, 1993). Helical tubular PBRs are a suitable alternative to straight tubular PBRs. The most frequently used layout is the Biocoil, currently traded by Biotechna (Melbourne, Australia). This reactor is composed of a set of polyethylene tubes (3.0 cm of inner diameter) coiled in an open circular framework, coupled with a gas exchange tower and a heat exchange system; a centrifugal pump drives the culture broth through the long tube to the gas exchange tower (Carvalho *et al.*, 2006). A 300 L α-shaped tubular PBR has been used for the cultivation of *Chlorella pyrenoidosa* (Lee *et al.*, 1995). That system comprises of an airlift pump to promote an ascending/descending trajectory, with several CO₂ injection points along its path.

Flat photobioreactors

Some of the earliest forms of closed systems are flat PBRs which have received much research attention due to the large surface area exposed to illumination and high densities (> 80 g L⁻¹) of photoautotrophic cells observed (Brennan and Owende, 2010). In these PBR a thin layer of very dense culture is mixed or flown across a flat transparent panel, which allows radiation absorbance in the first few millimetres thickness (Figure 2.4 C). Flat PBRs are suitable for mass cultures of microalgae due to the low accumulation of dissolved oxygen and the high photosynthetic efficiency achieved when compared to tubular designs (Brennan and Owende, 2010).

Usually, the panels are illuminated mainly on one side by direct sunlight and have the added advantage that they can be positioned vertically or inclined at an optimum

angle facing the sun permitting a better efficiency in terms of energy absorbed from incident sunlight. Packed flat panels mixed by air bubbling can potentially achieve very high overall ground-areal productivities through lamination of solar light. Limitations include difficulty in controlling culture temperature, some degree of wall growth, scale-up requires many compartments and support materials, and possibility of hydrodynamic stress to some algal strains (Table 2.4).

Column photobioreactors

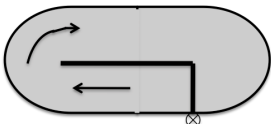
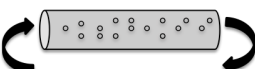
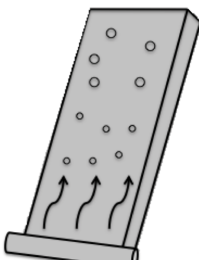
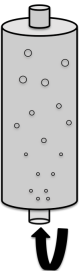
Column PBRs are occasionally stirred tank reactors (Sobczuk *et al.*, 2006), but more often bubble columns (Zittelli *et al.*, 2006), or airlifts (Krichnavaruk *et al.*, 2007). The columns are placed vertically, aerated from the bottom, and illuminated through transparent walls or internally (Figure 2.4 D). Column bioreactors offer the most efficient mixing, the highest volumetric gas transfer rates, and the best controllable growth conditions. They are low-cost, compact and easy to operate. Their performance (*i.e.* final biomass concentration and specific growth rate) compares favourably with the values typically reported for tubular PBRs.

Vertical bubble columns and airlift cylinders can attain substantially increased radial movement of fluid that is necessary for improved light–dark cycling. These reactor designs have a low surface/volume, but substantially greater gas hold-ups than horizontal reactors and a much more chaotic gas–liquid flow. Consequently, cultures suffer less from photo-inhibition and photo-oxidation, and experience a more adequate light–dark cycle.

2.2.1.3 Photobioreactors versus open-air systems

Table 2.4 shows a comparison between PBR (tubular, flat and column) and open systems for several culture conditions and growth parameters. Selection of a suitable production system clearly depends on the purpose of the production facility, microalgae strain and product of interest. In conclusion, PBR and open ponds should not be viewed as competing technologies.

Table 2.4 Advantages and limitations of various microalgae culture systems

Culture Systems	Advantages	Limitations
Open systems 	<ul style="list-style-type: none"> - Relatively economical - Easy to clean up - Easy maintenance - Utilization of non-agricultural land - Low energy inputs 	<ul style="list-style-type: none"> - Little control of culture conditions - Poor mixing, light and CO₂ utilization - Difficult to grow algal cultures for long periods - Poor productivity - Limited to few strains - Cultures are easily contaminated
Tubular PBR 	<ul style="list-style-type: none"> - Relatively cheap - Large illumination surface area - Suitable for outdoor cultures - Good biomass productivities 	<ul style="list-style-type: none"> - Gradients of pH, dissolved oxygen and CO₂ along the tubes - Fouling - Some degree of wall growth - Requires large land space - Photoinhibition
Flat PBR 	<ul style="list-style-type: none"> - Relatively cheap - Easy to clean up - Large illumination surface area - Suitable for outdoor cultures - Low power consumption - Good biomass productivities - Good light path - Readily tempered - Low oxygen build-up Shortest oxygen path 	<ul style="list-style-type: none"> - Difficult to scale-up - Difficult temperature control - Some degree of wall growth - Hydrodynamic stress to some algal strains - Low photosynthetic efficiency
Column PBR 	<ul style="list-style-type: none"> - Low energy consumption - Readily tempered - High mass transfer - Good mixing - Best exposure to light-dark cycles - Low shear stress - High potentials for scalability - Easy to sterilize - Reduced photoinhibition - Reduced photo-oxidation - High photosynthetic efficiency 	<ul style="list-style-type: none"> - Small illumination surface area - Sophisticated construction materials - Shear stress to algal cultures - Decrease of illumination surface area upon scale-up - Expensive compared to open ponds - Support costs - Scalability

2.2.2 Design considerations

Despite various configurations, several essential issues need addressing when building a PBR: effective and efficient provision of light; supply of CO₂ while minimizing desorption; efficient mixing and circulation of the culture; scalable PBR technology and the material used in the construction of the PBR.

2.2.2.1 Light

Light as the energy source for photoautotrophic life is the principal limiting factor in photobiotechnology. The light regimen inside the PBR is influenced by incident light intensity, reactor design and dimension, cell density, pigmentation of the cells, mixing pattern, etc. In outdoor PBRs the light regimen is also influenced by geographical location, time of the day, and weather conditions. Due to the light gradient inside the reactor and depending on the mixing properties, microalgae are subjected to light-dark cycles where the light period is characterized by a light gradient. These light-dark cycles will determine productivity and biomass yield on light energy (Fernandes *et al.*, 2010).

Only a fraction of the electromagnetic spectrum of sunlight in the wavelength range 400 – 700 nm (also known as the photosynthetic active radiation or, PAR) is used in photosynthesis, where 8 light photons of mid-wavelength PAR (*i.e.*, 550 nm or green light) has the minimum energy requirement to form CH₂O. A single ‘green’ photon of light (*i.e.*, 550 nm) has 20% more energy than one red photon (*i.e.*, 680 nm) and 15.5% less energy than a blue photon (*i.e.*, 470 nm) (Das *et al.*, 2011). Thus, information about quantitative (photosynthetic photon flux density) and qualitative (spectral intensity distribution) aspects of light patterns in different points of a PBR is vital. This information can be obtained by using optical fibre technology (Fernandes *et al.*, 2010).

In highly dense cultures, while the region close to PBR surface are subject, in certain periods of the day, to light intensities that are greater than the saturation value of microalgae species, causing photoinhibition of cells (Wu and Merchuk, 2002) more inner regions remain in the dark due to optical absorption and self-shading of the cells causing photolimitation. In this region, the light intensity is too weak to maintain positive growth of the cells (Degen *et al.*, 2001). It is known that microalgae

productivity can be enhanced if cells are made to repeatedly cycle between the well-lit exterior and the dimly lit interior of the PBR, experiencing periodical light/dark cycles (Lee and Pirt, 1981; Merchuk et al., 1998; Wu and Merchuk, 2001).

2.2.2.2 *CO₂ supply*

The supply of CO₂ to microalgal mass culture systems is one of the principal difficulties that must be solved (Benemann *et al.*, 1987). The principal point of all considerations relating to the CO₂ budget is that, on one hand, CO₂ must not reach the upper concentration that produces inhibition and, on the other hand, must never fall below the minimum concentration that limits growth. These maximum (inhibition) and minimum (limitation) concentrations varies from one species to another and are not yet adequately known, ranging from 2.3×10^{-2} M to 2.3×10^{-4} M. Gas injection as little bubbles into a column of a downcoming culture in which the culture velocity is adjusted to that of the rising CO₂ bubbles may increase the efficiency of absorption of CO₂ and thus the utilisation efficiency can be increased up to 70% (Molina, 1999). In a dual sparging bubble column PBR, the CO₂ transfer rate was increased 5 times compared to a similar reactor where the CO₂ was blended into the aeration air (Eriksen *et al.*, 1998), while another study showed that, in the same PBR configuration, CO₂ transfer efficiencies were 100% at certain conditions (Poulsen and Iversen, 1999). These results highlight the need to develop an adequate aeration system in order to increase the efficiency of CO₂ supply and, consequently the microalgae cultivation systems productivity.

2.2.2.3 *Mixing*

The level of mixing in a PBR strongly contributes to the growth of microalgae. Mixing is necessary to prevent cells from settling, to avoid thermal stratification, to distribute nutrients and break down diffusion gradients at the cell surface, to remove photosynthetically generated O₂ and to ensure that cells experience alternating periods of light and darkness of adequate length (Tredici, 2004). Mixing is the simplest and most immediate strategy to attempt distributing radiation evenly to all cells in the culture, as well as accelerating growth by reducing diffusion barriers around the cells (Richmond, 2004_a).

The fluid dynamics of the culture medium and the type of mixing influence average irradiance and the light regimen to which cells are exposed, which in turn determine productivity. Fluctuations in light intensity faster than 1 s^{-1} enhance specific growth rates and productivities of microalgal cultures. In outdoor cultures exposed to photosynthetic photon flux densities above $1,000 \mu\text{E m}^{-2} \text{ s}^{-1}$ light exposure times should be as short as 10 ms to maintain high photosynthetic efficiency (Janssen *et al.*, 2001). In addition, dissolved O_2 builds up in cultures in which mixing is inadequate, inhibiting photosynthesis. The positive effect that optimal mixing exerts on the output-rate of biomass is accentuated with the increase of cell density and light limitation. Inadequate mixing resulting in high O_2 tensions and in laminar – instead of turbulent – flows resulting in cell precipitation and wall growth, which is one of the main reasons for industrial failures of microalgae cultivation (Richmond, 2004_a).

The choice of the mixing device and the intensity of mixing should be dictated by the characteristics of the organism to be cultivated.

2.2.2.4 *Scale-up strategies and construction issues*

Tubular PBRs and raceway ponds are suitable for large-scale production (Chisti, 2007). However the scalability of vertical airlift PBR and bubble columns was considered also an advantage of these systems (Miron *et al.*, 1999). Scale-up of closed systems is only possible by increasing the number of units in a production scheme. This method can become expensive, since each unit requires a variety of devices that control the wide range of growth factors (*e.g.* pH, temperature, aeration, CO_2 supply, nutrients supply). In addition, maintaining a monoculture in all of the units becomes challenging as the number of units to monitor grows (Janssen *et al.*, 2001). Other than scale-up by multiplication of identical modules, the only way to increase volume is by increasing length or/and diameter or/and the light path of the PBR; however, this strategy is limited by the existence of changes in the performance of the PBR. Commercial-scale closed PBR have not been widely reported in scientific literature.

The type of material used is of fundamental importance for a suitable PBR construction. Materials such as plastic or glass sheets, collapsible or rigid tubes should have high transparency, high mechanical strength, high durability, chemical stability,

low cost, must lack toxicity and be easy to clean (Tredici, 2004). The ease of cleaning and loss of the plastics transparency exposed outdoors are operational issues to consider. The construction materials to build a microalgae cultivation system can vary from simple sand or clay, to brick or cement, and to expensive plastics like polyvinyl chloride (PVC), glass fibre or polyurethane (Mata *et al.*, 2010).

Advantages and drawbacks of the most common materials used for building PBR have been reported in the literature (Tredici, 1999).

2.2.3 Downstream processes

Downstream processes represent an economic limitation to the production of low cost commodities (fuels, feeds and foods) and also to higher value products. The downstream processes used are highly specific and strongly depend on the desired products. This section deals with the main techniques for harvesting/dewatering, drying, cell disruption and metabolites extraction from microalgae cells.

2.2.3.1 Harvesting and dewatering processes

Given the relatively low biomass concentration obtainable in microalgal cultivation systems due to the limit of light penetration (typically in the range of 1 - 5 g L⁻¹) and the small size of microalgal cells (typically in the range of 2 - 20 µm in diameter), costs and energy consumption for biomass harvesting are a significant concern that needs to be addressed properly (Li *et al.*, 2008). In this sense, harvesting of microalgal cultures is a major bottleneck towards the industrial-scale processing of microalgae for biofuel production. The cost of biomass recovery from the broth can make up to 20 – 30% of the total cost of producing the biomass (Molina *et al.*, 2003). Microalgal biomass harvesting can be achieved in several physical, chemical or biological ways: flocculation, centrifugation, filtration, ultrafiltration, air-flotation, autoflotation, etc. Generally, microalgae harvesting is a two-stage process, involving:

1) Bulk harvesting: aimed at separation of biomass from the bulk suspension. The concentration factors for this operation are generally 100 – 800 times to reach 2 – 7%

total solid matter. This will depend on the initial biomass concentration and technologies employed, including flocculation, flotation or gravity sedimentation;

2) Thickening: the aim is to concentrate the slurry through techniques such as centrifugation, filtration and ultrasonic aggregation; hence, it is generally a more energy intensive step than bulk harvesting.

Flocculation

Flocculation can be used as an initial dewatering step in the bulk harvesting process that will significantly enhance the ease of further processing. This stage is intended to aggregate microalgal cells from the broth in order to increase the effective *particle size* (Harun *et al.*, 2010_a). Since microalgae cells carry a negative charge that prevents them from self-aggregation in suspension, addition of chemicals known as flocculants neutralises or reduces the negative surface charge. These chemicals coagulate the algae without affecting the composition and toxicity of the product (Molina *et al.*, 2003). Multivalent metal salts like ferric chloride (FeCl₃), aluminium sulphate (Al₂(SO₄)₃) and ferric sulphate (Fe₂(SO₄)₃) are commonly used (Brennan and Owende, 2010).

Flotation

Some strains naturally float at the surface of the water as the microalgal lipid content increase. Although flotation has been mentioned as a potential harvesting method, there is very limited evidence of its technical or economic viability (Brennan and Owende, 2010).

Centrifugation

Centrifugation involves the application of centripetal acceleration to separate the microalgal growth medium into regions of greater and less densities. Once separated, the microalgae can be removed from the culture by simply draining the excess medium (Harun *et al.*, 2010_a). Centrifugal recovery is a rapid method of recovering microalgal cells, especially for producing extended shelf-life concentrates for aquaculture hatcheries and nurseries (Molina *et al.*, 2003). However, high gravitational and shear forces during the centrifugation process can damage cell structure. Additionally, it is not cost effective due to high power consumption especially when considering large volumes (Harun *et al.*, 2010_a).

Filtration

Filtration is the method of harvesting that has proved to be the most competitive compared to other harvesting options. There are many different forms of filtration, such as dead end filtration, microfiltration, ultra filtration, pressure filtration, vacuum filtration and tangential flow filtration. Generally, filtration involves running the broth with microalgae through filters on which the microalgae accumulate and allow the medium to pass through the filter. The broth continually runs through the microfilters until the filter contains a thick algae paste. Although filtration methods appear to be an attractive dewatering option, they are associated with extensive running costs and hidden pre-concentration requirements (Harun *et al.*, 2010_a).

2.2.3.2 Drying processes

Harvested microalgae contain 80 – 90% water (Ruiz *et al.*, 2013). Removal of most of the water is necessary for long-term storage of the microalgae feedstock and is required for many downstream processes such as metabolite extraction (Chen *et al.*, 2009). The most common methods for microalgae dehydration include spray-drying, drum-drying, freeze-drying and sun-drying (Richmond, 2004). These methods increase microalgae and the final product shelf-life, particularly if the moisture level is kept below 7% (Chen *et al.*, 2009). Because of the high-water content of microalgal biomass some methods are not very effective for microalgal powder production (*e.g.* sun-drying), while others are not economically feasible for low value products, such as biofuel or protein (*e.g.* spray-drying) (Mata *et al.*, 2010). For example, the conventional approach to produce biodiesel requires harvesting of microalgae and subsequent drying of the harvested biomass paste, and then solvent extraction of triglycerides from dried biomass, all these steps representing up to 90% of the energy needed to synthesize biodiesel from microalgae (Lardon *et al.*, 2009).

2.2.3.3 Cell disruption

The next step is microalgae cells disruption for release of the metabolites of interest. Several methods can be used depending on the microalgae wall and on the nature of the product to be obtained (Mata *et al.*, 2010). Most cell disruption methods applicable to

microalgae have been adapted from applications to intracellular non-photosynthetic bioproducts. Cell disruption methods that have been used successfully include the application of mechanical action as glass and ceramic beads, ultrasonication, high-pressure homogenisers, autoclaving or the application of non-mechanical action as the addition of hydrochloric acid, sodium hydroxide, alkaline lysis and enzyme reactions (Mendes-Pinto, 2001; Mata *et al.*, 2010).

Haematococcus cells are typically disrupted using high-pressure homogenisers. Disruption greatly enhances the bioavailability of and the assimilation of the pigments when cells are used for fish feed. Agitation of microalgal biomass in presence of glass and ceramic beads (*ca.* 0.5 mm of diameter) in bead mills has been used to disrupt cells of *Scenedesmus obliquus*, *S. platensis* and *Monodus subterraneus*. *Haematococcus pluvialis* cells that had been autoclaved or mechanically disrupted in a high pressure homogenizer, yielded three times as much astaxanthin as biomass treated with chemical or enzymatic methods (Grima *et al.*, 2003).

2.2.3.4 Extraction of microalgae metabolites

Extracting the oil and converting the oil from microalgae to biodiesel are the primary driving force for algae to fuels technology development (Chen *et al.*, 2009) however, as stated previously, microalgae have a number of other metabolites of great commercial interest that also need to be extracted. Microalgae metabolites such as essential fatty acids, β -carotene and astaxanthin can be extracted from the cells using solvent extraction. Hexane, ethanol, chloroform and diethyl ether can extract fatty acids such as eicosapentaenoic acid (EPA), docosohexaenoic acid (DHA) and arachidonic acid (AA) from various microalgae (Grima *et al.*, 2003). Several authors (Robles Medina *et al.*, 1995; Giménez Giménez *et al.*, 1998; Belarbi *et al.*, 2000) have described fatty acid extraction from microalgae.

The extraction of phycobiliproteins from *P. cruentum* (Bermejo Román *et al.*, 2001, 2002) and lutein from *C. vulgaris* (Li *et al.*, 2001) using aqueous buffers has also been reported. When the objective is to obtain metabolites with high added value, crude extracts are generally filtered and purified by various chromatographic methods to obtain the metabolite of interest. Astaxanthin, polyunsaturated fatty acids and other

compounds can be recovered using supercritical fluid chromatography (Grima *et al.*, 2003). Some other chromatographic methods that have been used for recovering pure fatty acids (or equivalent esters) have included reverse phase chromatography, silica gel adsorption chromatography and argentated silica gel chromatography (Robles Medina *et al.*, 1995; Giménez Giménez *et al.*, 1998; Belarbi *et al.*, 2000). Proteins are usually purified using ion exchange chromatography Bermejo Román *et al.*, 2002).

Several techniques have been assessed for lipid extraction, which usually requires < 10% water, including the use of supercritical CO₂ or organic solvents (Kumar *et al.*, 2010). Numerous methods for extraction of lipids from microalgae have been applied; but most common methods are expeller/oil press, liquid–liquid extraction (solvent extraction), supercritical fluid extraction and ultrasound techniques (Harun *et al.*, 2010; Dragone *et al.*, 2010_a). Expeller/oil pressing is a mechanical method for extracting oil from raw materials such as nuts and seeds. Pressing uses high pressure to squeeze and break cells. In order for this process to be effective, algae must first need to be dried. Although this method can recover 75% of oil and no special skills are required, it was reported less effective due to comparatively longer extraction time (Harun *et al.*, 2010_a). Solvent extraction proved to be successful in order to extract lipids from microalgae. In this approach, organic solvents, such as benzene, cyclo-hexane, hexane, acetone, chloroform are added to algae paste. Solvents destroy algal cell wall, and extract oil from aqueous medium (Figure 2.5) because of its higher solubility in organic solvents than in water (Dragone *et al.*, 2010).



Figure 2.5 Solvent extraction of lipids (<http://www.oilgae.com>).

Solvent extract can then be subjected to distillation process to separate oil from solvent. Latter can be reclaimed for further use. Hexane is reported to be the most efficient solvent in extraction based on its highest extraction capability and low cost

(Harun *et al.*, 2010_a). Supercritical extraction makes use of high pressures and temperatures to rupture the cells. This particular method of extraction has proved to be extremely time-efficient and is commonly employed (Harun *et al.*, 2010_a). Another promising method to be used in extraction of microalgae is the application of ultrasounds. This method exposes algae to a high intensity ultrasonic wave, which creates tiny cavitation bubbles around cells. Collapse of bubbles emits shockwaves, shattering the cell wall and releasing the desired compounds into solution.

Although extraction of oil from microalgae using ultrasound is already in extensive use at laboratory scale, sufficient information on feasibility or cost for a commercial-scale operation is unavailable. This approach seems to have a high potential, but more research is needed (Harun *et al.*, 2010_a, Dragone *et al.*, 2010).

Hydrothermal liquefaction

High content of water often exists in microalgae after harvesting which requires a great deal of energy to remove moisture in the algal cells in the period of pre-treatment. Hydrothermal liquefaction has been developed to produce bio-fuel directly without the need of drying, disruption or extraction processes. The hydrothermal processing is an alternative technology that significantly improves the overall thermal efficiency of the process (Patil *et al.*, 2008), as the energy consumption required by hydrothermal processing is very low compared to other processes (Shuping *et al.*, 2010; Ruiz *et al.*, 2013). Hydrothermal liquefaction is a process in which biomass is converted in hot compressed water to a liquid bio-crude. Processing temperatures range from 200 to 350 °C with pressures of around 15 – 20 MPa. At these conditions complex molecules are broken down and repolymerise to oily compounds (Peterson *et al.*, 2008). Hydrothermal processing offers the advantage that lipids can be extracted while wet and upgraded to produce a crude oil-like product. Another major advantage is that the conventional lipid extraction methods only produce oil from the lipid fraction while hydrothermal processing can produce oil also from the carbohydrate and protein fraction (Ruiz *et al.*, 2013). Basically, this process converts the whole cell into bio-crude.

2.3 Cost/effectiveness considerations

Sustainability is a key principle in natural resource management, and it involves operational efficiency, minimization of environmental impact and socio-economic considerations, all of which are interdependent (Brennan and Owende, 2010). Despite the enormous interest in using microalgae in the energy or commodities markets, companies will not be available to make large investments unless the risk-return ratio is acceptable (Singh and Gu, 2010). For current cultivation systems, overall processing costs are around 5 € kg⁻¹. A conservative conceptual model to assess economics anticipates cost reductions to as low as 0.68 € kg⁻¹ within a decade, which would then make microalgae a fully competitive alternative for biofuel production (Malcata, 2011).

In order to reduce the microalgae production cost several issues should be considered:

- Microalgae strain selection;
- Cultivation system localization;
- Photobioreactor construction, operation and maintenance costs;
- Nutrients and CO₂ supply costs;
- High concentration of the product of interest;
- Biorefinery-based production strategy;
- Improving capabilities of microalgae through genetic engineering

Despite the increasing interest in microalgae for the production of biofuels or high added-value compounds, the commercial achievements on microalgal biotechnology are still modest. However, it is expectable that, within the next 10 – 15 years the microalgae production will reach an economical sustainable level. This expectation is based mainly in recent advances in PBR engineering, systems biology, material science, genetic engineering, and biorefining (Wijffels and Barbosa, 2010).

2.3.1 Microalgae selection

Microalgae species and strains vary greatly in terms of growth rate, productivity,

nutrient and light requirement, ability to accumulate different desirable compounds and ability to adapt to adverse conditions. Therefore, usually, the first step in mass cultivation of microalgae is to find or engineer right species and strains for specific purposes and cultivation systems (Chen *et al.*, 2009).

There are many screening programs around the world studying microalgae species in different locations for suitable strains. However, most of the research work is focused on a small number of fast-growing microalgal species which have been found to accumulate substantial quantities of lipids. Typical species include *Chlamydomonas reinhardtii*, *Dunaliella salina*, and various *Chlorella* species, as well as *Botryococcus braunii*. Other important algal groups include *Phaeodactylum tricornutum*, *Thalassiosira pseudonana*, *Nannochloropsis* and *Isochrysis spp* (Scott *et al.*, 2010).

According to Chen *et al.* (2009) there are three main categories that should be taken into account in microalgae selection:

i) Growth physiology – evaluated based on maximum specific growth rate, maximum cell density, tolerance to environmental variables (temperature, pH, salinity, oxygen levels, CO₂ levels). It is also desirable the capability of heterotrophic or mixotrophic growth and growing to high cell density.

ii) Metabolite production – assessed for both the unit concentration as well as the total yield of the metabolites useful for commercialization. The ability of an algal species to secrete metabolites in liquid or volatile forms is another feature of potential significance for harvest.

iii) Robustness - high culture consistency, reasonable resilience, high community stability, and low susceptibility to external predators.

Additionally, the selected microalgae should be susceptible to optimization of its performance through genetic manipulation and able to be used in a biorefinery concept.

For this study the selected microalgae was the freshwater *Chlorella vulgaris* P12 provided by the Algal Laboratory (CCALA), Institute of Botany, Academy of Sciences of the Czech Republic. *C. vulgaris* is a single celled, spherical non-motile green microalgae with 2.0 – 10.0 µm in diameter. The cells are devoid of flagella, stigma and

contractile vacuoles, but contain a centrally located nucleus. *Chlorella* occurs in both fresh and marine water. Some call *C. vulgaris* ubiquitous since it occurs in various different habitats. *C. vulgaris* is of immense economic importance ranging from human food to applications in space travel and biofuels production (Phukan *et al.*, 2011).

C. vulgaris was chosen due to its fast growth (doubling time of 19 h), robustness, easier cultivation (Lv *et al.*, 2010), tolerance to high levels of CO₂, as well as other compounds such as sulphur dioxides, nitrogen oxides, and volatile organic compounds (VOCs) (Keffer and Kleinheinz, 2002). *C. vulgaris* does not secrete any autoinhibitory or harmful factors at high-cell concentrations which would inhibit or retard growth. It is also known that it is able to grow mixotrophically and heterotrophically, and it is also possible to induce the accumulation of high concentrations of energy-rich materials.

2.3.2 Cultivation system location

The choice of the location where the cultivation system will be constructed is a major consideration to reduce the relation cost/effectiveness. Choosing the appropriate location can mean higher system productivity and lower construction and operation costs, for example. This can be achieved if the cultivation system is built in a location where climatic conditions are ideal for the selected microalgae (optimizing the growth and reducing the temperature control costs), or/and a location with CO₂ and nutrients sources with residual cost (*e.g.* CO₂ emitting industries that produce wastewaters with nitrogen and phosphorus).

According to Mata *et al.* (2010) the site selection has to be performed considering several criteria:

- (i) water supply/ demand, its salinity and chemistry;
- (ii) land topography, geology, and ownership;
- (iii) climatic conditions, temperature, insulation, evaporation, precipitation;
- (iv) easy access to nutrients and carbon supply sources.

The decisions made in terms of location will always be determined by the microalgae species selected, the product of interest (*e.g.* human consumption or production of

biofuels), type of cultivation (*e.g.* photoautotrophic or mixotrophic growth). The selected microalgae will determine the type of water used (fresh, marine, or even waste water); existence of special nutritional requirements (*e.g.* mixotrophy); growth temperature range; resistance to contamination; if the microalgae is extremophile or not.

One of the most interesting possibilities is to combine the microalgae growth with a pollution control strategy of other industry, for example for the removal of CO₂ from flue gas emissions or the removal of nitrogen and phosphorus from a wastewater effluent (Mata *et al.*, 2010). Power plants and wastewater treatment plants are very attractive locations for microalgae cultivation systems construction. Power plants are inexpensive CO₂ sources, with availability of heat that can be used in downstream processes (*e.g.* drying) and (usually) with availability of large quantities of water. Wastewater treatment plants have large amounts of nutrient-rich water and usually produce CO₂ that can be used in microalgae production.

Geographical areas with high irradiances along the year and moderate temperatures are optimal for microalgae cultivation. Because of the average amount of sunlight hours per day (10 – 12 h), and the mean solar irradiance ranging from 400 $\mu\text{E m}^{-2} \text{s}^{-1}$ (winter time) to 1,800 $\mu\text{E m}^{-2} \text{s}^{-1}$ (summer time), southern Spain (García-González *et al.*, 2003) and southern Portugal are considered especially suitable for outdoor cultivation of microalgae.

Most of microalgae commercial cultivation is done in developed countries. In most of these regions there are seasonal variations in temperatures and solar light energy throughout the year. Due to these constrains, it is difficult to carry out outdoor mass cultivation of microalgae all year round in such regions (Ugwu *et al.*, 2008). However, in most tropical developing countries, outdoor cultures of microalgae can be maintained for relatively long period of time in a year because there is neither winter nor cold seasons in those regions. Thus, according to Ugwu *et al.* (2008) tropical developing countries might be potential cultivation sites for commercial production of microalgal products.

2.3.3 Cultivation system selection

As previously demonstrated there are a wide variety of microalgae cultivation systems. Design and construction of any microalgae culture system should consider the type of strain, the target product, geographical location, as well as the overall cost of production. Large-scale microalgae culture systems should have large volume and occupy less land space, they must have transparent surfaces, high illumination surfaces, high mass transfer rates and should as well be able to give high biomass yields (Ugwu *et al.*, 2008).

Efficient and cost effective microalgae culture systems can be characterized as having high areal and volumetric productivities. These high productivities can be achieved by optimal light regime (*i.e.* a state in which all the parameters affecting the average light exposure of each cell are optimized) and high mass transfer rates. To ensure the economic viability of microalgae cultivation systems, it is necessary to achieve high volumetric and/or areal productivities, associated with a reduced annual investment and simple/cheap PBR operation and maintenance procedures. There are practical points in this context that must be addressed during the development and design of a cost effective microalgae cultivation system (Richmond, 2004_b):

- i)* Is the microalgae culture system illuminated through all surfaces, providing a high area:volume ratio, allowing a rational and efficient utilization of the incident radiation?
- ii)* The microalgae culture system allows maintaining continuous monocultures with little risk of contamination or deterioration? The detection and control of bio-fouling formation is quick, reducing the chances of contamination?
- iii)* CO₂ is supplied efficiently with high mass transfer rates?
- iv)* There are mechanisms to prevent that O₂ concentration reaches levels that cause stress to the cells?
- v)* The cooling system is suitable for local climatic conditions?
- vi)* The mixing system is efficient and does not cause significant cell

stress?

vii) The cost per PBR volume unit is reasonable in terms of depreciation and maintenance costs?

2.3.4 CO₂ and nutrient supply

Many elements have to be provided for the growth of microalgae, such as carbon (C), oxygen (O), hydrogen (H), nitrogen (N), potassium (K), calcium (Ca), magnesium (Mg), iron (Fe), sulphur (S), phosphorous (P), and trace elements. While, C, O and H are obtained from water and air, N, P and K have to be absorbed from the culture medium (Zhu *et al.*, 2013). Production of biofuels and other bio-products from microalgae can be more environmentally sustainable, cost-effective and profitable, if combined with bioremediation processes such as wastewater and flue gas treatments. Microalgae cultivation using wastewater and flue gases as source of nutrients has proven to be a very feasible strategy (Mata *et al.*, 2010).

2.3.4.1 CO₂ supply

The most common sources of CO₂ for microalgae cultivation include: (i) atmospheric CO₂; (ii) CO₂ from industrial exhaust gases (*e.g.* flue gas and flaring gas); and (iii) CO₂ chemically fixed in the form of soluble carbonates (*e.g.* NaHCO₃ and Na₂CO₃) (Kumar *et al.*, 2010). CO₂ can be supplied to microalgae cultures by previous separation from flue gases or by directly injecting the flue gases into the culture. Several technologies are available to separate CO₂ from flue gases as chemical absorption, cryogenic fractionation, membrane separation, and adsorption using molecular sieves (Herzog *et al.*, 1997). The cost of CO₂ supply has to be considered when evaluating the economics of microalgae production. A review by Carvalho *et al.* (2006) suggested that if it is not possible to find a cheap source of CO₂, the CO₂ supply to the cells must be done in a discontinuous way. Direct bubbling of flue gases, without CO₂ separation, is the only source capable of supplying the CO₂ required for the mass production of microalgae in an affordable way.

In order to obtain a cost efficient microalgae culture system, with regard to the CO₂

supply, it is necessary to consider two very important aspects:

i) Cheap and continuous source of CO₂ - microalgae culture system should be built near facilities that emit CO₂, such as power plants, wastewater treatment plants, cement industries or industries with fermentation processes (e.g. breweries). Virtually, any industry that produces large amounts of CO₂ is a good candidate to have a microalgae cultivation system. Previous studies have demonstrated that microalgae can be successfully employed for the treatment of simulated flue gases (Lee *et al.*, 2000) or flue gases emitted from municipal waste incinerators (Douskova *et al.*, 2009), coal-fired power plants (McGinn *et al.*, 2011), industrial heater using kerosene as fuel (Chae *et al.*, 2006) and gas boiler (Doucha *et al.*, 2005). Flue gas is a desirable source of CO₂ because it reduces greenhouse gas emissions as well as the cost of microalgae production. Flue gas from typical coal-fired power plants contain up to 13% CO₂ (Haiduc *et al.*, 2009), whereas waste gases from combustion processes, however, typically contain >15% (v/v) CO₂ (Kumar *et al.*, 2010).

ii) Optimal CO₂ supply conditions - The aeration rate and CO₂ concentration in the gas stream must be optimized to maximize the productivity in terms of biomass and/or products of interest. This optimization allows a rational management of resources, particularly energetic, and allows that the largest possible amount of CO₂ is converted into biomass, with a minimum CO₂ release to the atmosphere. One approach to raising microalgae productivity is to increase the concentration of CO₂, however, an excess of CO₂ can also be detrimental to photosynthesis and cell growth. Lee and Tay (1991) found that microalgae cells exposed to high CO₂ concentrations experienced declining growth rates. According to Chen *et al.* (2009) careful regulation of CO₂ input could maximize CO₂ utilization and minimize undesirable CO₂ inhibition.

2.3.4.2 Nutrient supply

Among many challenges faced in the commercial cultivation of microalgae, low-cost water and nutrients availability is crucial. Culturing of microalgae at industrial scale for biofuels production requires substantial amount of nutrients, typically nitrogen and

phosphorus. These nutrients are normally from inorganic fertilizers.

With the expansion of the commercial microalgae growing industry, competition with the agricultural sector for inorganic fertilisers is expected to increase, this could result in the fact that inorganic fertilisers may be an economically unviable source of nutrients for micro-algal production systems (Fenton and hUallacháin, 2012). The use of chemical fertilizers has the advantage of reducing contamination in culturing medium and thus promotes water reutilization to re-culture microalgae. However, a recent life-cycle assessment study has pointed out that 50% of the overall energy use and green house gases emission were associated with utilization of chemical fertilizers (Clarens *et al.*, 2010). Thus, in a long run, using chemical fertilizers to culture microalgae for biofuel production is definitely not sustainable. Thus, it is necessary to find alternatives to the use of fertilizers in microalgae mass cultivation.

Currently, large amount of waste produced from the intensive livestock and food industries worldwide annually creates more greenhouse gas emission and causes more environmental problems. Thereby, some of these effluents could be an alternative nutrient source for mass microalgae production since contains nutrients such as N and P which are suitable for growing microalgae or even organic carbon sources that could be used for mixotrophic growth of microalgae. The use of algae for nutrient removal from municipal wastewater has been extensively investigated and in general this nutrient stream provides a good microalgal growth medium. Other waste streams promise to also provide most of the nutrients for abundant microalgal growth (Cabanelas *et al.* 2013, Cho *et al.* 2013).

Additionally, heterotrophic and mixotrophic microalgae are known to grow much faster with higher cellular oil content suitable as biofuels feedstock as compared to photoautotrophic cells (García *et al.*, 2000; Miao and Wu, 2004). However, they require organic carbon sources like glucose or acetate for growth, which are responsible for 80% of the medium costs (Li *et al.*, 2007). In order to reduce microalgal production costs, it is imperative to find cheap organic substrates that meet the nutritional requirements of microalgae. Wastes produced from the intensive livestock and food industries are promising candidates as organic carbon sources for mixotrophic and heterotrophic cultivation of microalgae.

From the environmental and economic point of view, utilization of municipal or

industrial wastewaters is a very attractive strategy since waste stream is used to generate alternative renewable biofuels to mitigate the current energy crisis.

2.3.5 Induction of specific products' accumulation in microalgae

The economic feasibility of microalgae mass cultivation is dependent on the high biomass productivity but also on high productivities in terms of product of interest. To make microalgae biofuels cost competitive as a liquid fuel, microalgae should be capable of high lipid or starch productivities in order to produce biodiesel or bioethanol, at low cost. Several studies have demonstrated that it is possible to modify the growth and secondary metabolism of microalgae, namely the accumulation of energy-rich materials (lipids and starch) (Behrens and Kyle, 1996; Hsieh and Wu, 2009).

Previous studies reported that accumulation of lipids and starch in some microalgae could be induced by various strategies such as nitrogen deprivation (Illman *et al.*, 2000), silicon deficiency (Lynn *et al.*, 2000), phosphate limitation (Reitan *et al.*, 1994), high salinity (Rao *et al.*, 2007) or increasing the temperature to sub-lethal levels (Douskova *et al.*, 2008). Although these strategies may increase up to 10 times the amount of lipid or starch in the cells (Dragone *et al.*, 2011), they cause a decrease in biomass productivity. It is therefore necessary to find a balance between energy-rich materials' accumulation and biomass productivity, which will result in increased product productivity.

One alternative to overcome this limitation and find a balance between metabolite accumulation and biomass growth, is to use a strategy of microalgae cultivation in two stages. In the first stage biomass is cultivated under optimal conditions for microalgal growth and during the second stage of cultivation the conditions are changed in order to slow down or stop the cytoplasmic proteosynthesis, (photosynthesis and metabolism of chloroplasts should remain unaffected). During this period of limited proteosynthesis and cell growth the algae transform the energy of light and CO₂ into reserve materials resulting in an increase of intracellular starch or oil content (Douskova *et al.*, 2008).

2.3.6 Biorefinery approach

An integrated biorefinery is capable of producing multiple product streams and thus multiple income streams from a single biomass feedstock, therefore being more economically viable than single product-based production schemes (Chen *et al.*, 2009). Like a petroleum refinery, a biorefinery uses several components of the biomass raw material to produce useable products and, because several components of the biomass are used, the overall cost of producing any given product is lowered.

The primary driving force for microalgae cultivation technology development is the potential to reduce emerging environmental and economic problems, such as the greenhouse effect, industrial water pollution and fuel crisis. However, as has been demonstrated above, microalgae biomass also has other valuable components and uses. Microalgae product portfolio stretches from straightforward biomass production for food and animal feed to valuable products extracted from microalgal biomass, including carbohydrates, long chain fatty acids, pigments and proteins. For most of these applications, the production process is moderately economically viable and the market is developing (Harun *et al.*, 2010_{a,b}).

Different approaches can be made to the biorefinery concept, depending on the selected microalgae, and therefore their metabolites as well as the main product of interest. For example, if the products of interest are the lipids (for biodiesel production), after lipid extraction some of the residual biomass may be used to produce methane by anaerobic digestion, to generate the electrical power necessary for running the microalgal biomass production facility. The residual biomass from biodiesel production processes can also be used as animal feed or feedstock for bioethanol production. A microalgal biorefinery can simultaneously produce biodiesel, animal feed, biogas, bioethanol and electrical power (Figure 2.6). Extraction of other high-value products may be feasible, depending on the specific microalgae used, but this is probably the simplest approach to the microalgae biorefinery concept.

According to Vanthoor-Koopmans *et al.* (2012), when the whole potential of microalgae ingredients is exploited, the market value will be higher than production costs and therefore focus should be put on maximal exploitation of microalgal metabolites. However, the application of this concept of biorefinery is neither simple

nor straightforward. The main bottleneck of the biorefinery approach is to separate the different fractions without damaging one or more of the product fractions. There is a need for mild, inexpensive and low energy consumption separation techniques to overcome these bottlenecks, and they should also be applicable for a variety of end products of sufficient quality at large quantities (Vanthoor-Koopmans *et al.*, 2012).

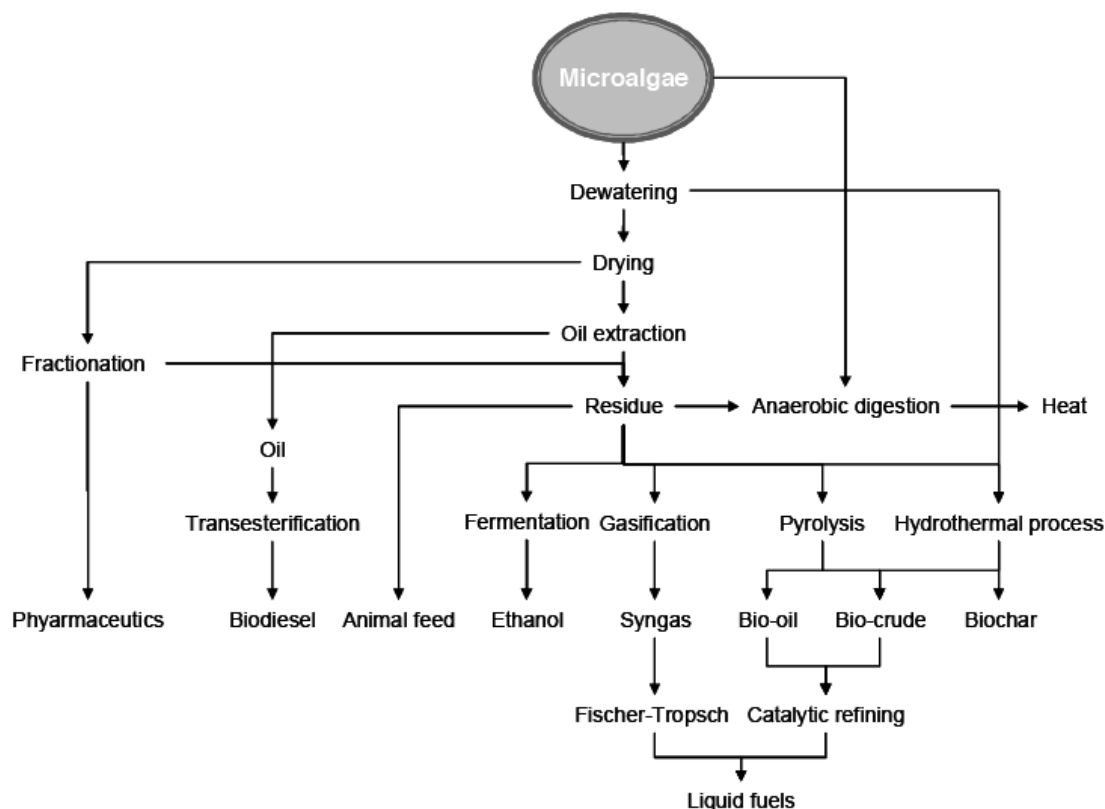


Figure 2.6 An integrated biorefining scheme for algal biomass utilization (Chen *et al.*, 2009).

The conventional techniques for cell disruption and metabolite extraction, like *e.g.* the use of chemicals or very high pressure, are very effective technologies but they are not mild and mainly focused on one product. Some of the biorefinery techniques appropriate for mild processing are enzymes, pulsed electric field, supersonic flow fluid processing, ultrasound (for cell disruption) and ionic liquids or surfactants (for metabolite separation and extraction). These techniques are relatively new and should therefore be studied thoroughly before commercial use is possible (Vanthoor-Koopmans *et al.*, 2012).

2.3.6.1 *Microalgal metabolites and their applications*

Microalgae oils and proteins have the potential to replace and add to the current oil and protein markets. Globally the demand is rising due to the rising population. Therefore it is necessary to find sustainable sources of lipids and proteins (Vanthoor-Koopmans *et al.*, 2012). Lipids extracted from the microalgal biomass could be also used as a potential feedstock for biodiesel production. In addition, some long chain fatty acids (such as DHA and EPA) are important health food supplements. The microalgae-based carbohydrates consist mainly of cellulose and starch without lignin; thus they can be ready carbon sources to replace traditional crop carbohydrates in the fermentation industry. Phycobiliproteins are water-soluble proteins that capture light energy, which is then passed on to chlorophylls during photosynthesis. Phycobiliproteins are promising fluorescent labelling reagents that can be employed in flow cytometry, fluorescence immunoassay, fluorescence microscopy, immuno-histochemistry and other biomedical research purposes (Matamala *et al.*, 2007; Waggoner, 2006). The global market was estimated to be approximately US\$50 million in 1997, with prices varying from US \$3 mg⁻¹ to US \$25 mg⁻¹ (Milledge, 2011; Yen *et al.*, 2012). The three major classes of photosynthetic pigments that appear in microalgae are chlorophylls, carotenoids and phycobilins. Pigments as chlorophyll can be used as anti-inflammatory and wound healing additive to pharmaceuticals, carotenoids reduce the risk of cancer, and astaxanthin is a powerful antioxidant (Christaki *et al.*, 2011). These higher valuable products make microalgae even more attractive as food and feed additives (Vanthoor-Koopmans *et al.*, 2012).

2.3.7 **Genetic manipulation**

Genetic manipulation techniques have been developed for some species (*e.g.* *Chlamydomonas reinhardtii*, *Volvox carteri*, and the diatom *Phaeodactylum tricorutum*), and are increasingly being applied to optimize biofuel production in several microalgal systems (Beer *et al.*, 2009). Although genetic manipulation remains limited to a few selected algal laboratory models the expanding interest in algal biofuels will likely lead to the development of techniques in other organisms and the establishment of new model systems (Beer *et al.*, 2009).

Many researchers are seeking to overcome the production and harvesting challenges through genetic and metabolic engineering of microalgae. Using nutrient deprivation or other stresses to induce a natural lipid trigger is not always beneficial because productivity and lipid accumulation are often inversely related. According to Hu *et al.* (2008), an increased understanding of the control mechanisms behind lipid production is needed to enable genetic manipulation for simultaneous rapid growth and high lipid content (Christenson and Sims, 2011).

Thus, it is reasonable to conclude that genetic and metabolic engineering are likely to have a great impact on improving the economics of mass production of microalgal (Roessler *et al.*, 1994; Dunahay *et al.*, 1996). According to Chisti (2007) molecular level engineering can be used to potentially:

1. increase photosynthetic efficiency to enable increased biomass yield on light;
2. enhance biomass growth rate;
3. increase oil, starch or other products content in biomass;
4. improve temperature tolerance to reduce the expense of cooling;
5. eliminate the light saturation phenomenon so that growth continues to increase in response to increasing light level;
6. reduce susceptibility to photooxidation that damages cells.

Stability of engineered strains and methods for achieving stable production in industrial microbial processes are known to be important issues (Zhang *et al.*, 1996), but have been barely examined for microalgae. In combination with increasingly refined genetic manipulation tools, the ability of scientists to engineer algae for the accumulation of specific metabolites is entering a new era (Beer *et al.*, 2009)

2.4 References

- Abalde J., Fabregas J., Herrero C., 1991. β -Carotene, Vitamin C, Vitamin E content of the marine microalga *Dunaliella tertiolecta* cultured with different nitrogen source. *Biores. Technol.* 38: 121–125.
- Abdulqader G., Barsanti L., Tredici M. R., 2000. Harvest of *Arthrospira platensis* from Lake Kossorom (Chad) and its household usage among the Kanembu. *Journal of Applied Phycology* 12: 493-498.
- Alam F., Date A., Rasjidin R., Mobin S, Moria H., Baqui A., 2012. Biofuel from Algae - Is It a Viable

- Alternative? *Procedia Engineering*, 49: 221-227.
- Arad S., Richmond A., 2004. Industrial production of microalgal cell-mass and secondary products—species of high potential: *Porphyridium* sp. In: Richmond, A. (Ed.), *Handbook of Microalgal Culture: Biotechnology and Applied Phycology*. Blackwell Science Ltd., UK, pp. 289–298.
- Beer L. L., Boyd E. S., Peters J. W., Posewitz M. C., 2009. Engineering algae for biohydrogen and biofuel production. *Curr Opin Biotech.*, 20: 264–71
- Behrens P.W., Kyle D. J., 1996. Microalgae as a source of fatty acids. *J Food Lipids* 3: 259–72.
- Belarbi H., Molina E., Chisti Y., 2000. A process for high and scaleable recovery of high purity eicosapentaenoic acid esters from microalgae and fish oil. *Enzyme Microb Technol* 26: 516–29.
- Benemann J. R., Tillett D.M., Weissman J.C., 1987. Microalgae biotechnology. *Trends in Biotechnology* 5: 47-53.
- Benemann, 2008. Opportunities and challenges in algae biofuels production. Position paper, *Algae World*, Singapore.
- Bermejo Román R., Talavera E. M., Alvarez-Pez J.M., 2001. Chromatographic purification and characterization of b-phycoerythrin from *Porphyridium cruentum*. Semipreparative HPLC separation and characterization of its subunits. *J Chromatogr A* 917: 135–45.
- Bilanovic D., Andargatchew A., Kroeger T., Shelef G., 2009. Freshwater and marine microalgae sequestering of CO₂ at different C and N concentrations – Response surface methodology analysis. *Energy Convers Manage* 50: 262-267.
- Borowitzka M. A., 1999. Commercial production of microalgae: ponds, tanks, tubes and fermenters. *Journal of Biotechnology* 70: 313-321.
- Borowitzka M. A., 2005. Culturing microalgae in outdoor ponds In: Andersen RA, eds. *Algal Culturing Techniques*. Burlington, MA: Elsevier Academic Press 205-218.
- Brennan L., Owende P., 2010. Biofuels from microalgae--A review of technologies for production, processing, and extractions of biofuels and co-products. *Renewable and Sustainable Energy Reviews* 14: 557-577.
- Cabanelas I.T.D., González J.R., Arbib Z., Chinalia F.A., Pérez C.G., Rogalla F., Nascimento I.A., José Perales Vargas-Machuca P., 2013. Comparing the use of different domestic wastewaters for coupling microalgal production and nutrient removal. *Bioresource Technology* DOI: <http://dx.doi.org/10.1016/j.biortech.2012.12.152>
- Carlsson A.S., van Beilen J. B., Möller R., Clayton D., 2007. *Micro- and Macro-Algae: Utility for Industrial Applications* 1st ed. Newbury: CPL Press.
- Carvalho A. P., Meireles L. A., Malcata F. X., 2006. Microalgal reactors: A review of enclosed system designs and performances. *Biotechnology Progress* 22: 1490-1506.
- Chae S. R., Hwang E. J., Shin H. S., 2006. Single cell protein production of *Euglena gracilis* and carbon dioxide fixation in an innovative photo-bioreactor. *Bioresour. Technol.* 97: 322-329.
- Chaumont D., 1993. Biotechnology of algal biomass production: a review of systems for outdoor mass culture. *Journal of Applied Phycology*. 5: 593-604.
- Chen P., M. Min, Y. Chen, L. Wang, Y. Li, Q. Chen, C. Wang, Y. Wan, X. Wang, Y. Cheng, S. Deng, K.

- Hennessy, X. Lin, Y. Liu, Y. Wang, B. Martinez, R. Ruan, 2009. Review of biological and engineering aspects of algae to fuel approach. *International Journal of Agricultural and Biological Engineering* 2(4): 1-30.
- Chini Zittelli, G., Lavista, F., Bastianini, A., Rodolfi, L., Vincenzini, M., Tredici, M.R., 1999. Production of eicosapentaenoic acid (EPA) by *Nannochloropsis* sp. Cultures in outdoor tubular photobioreactors. *J. Biotechnol.* 70, 299–312.
- Chisti Y., 2007. Biodiesel from microalgae. *Biotechnology Advances* 25: 294-306.
- Chiu, S. Y., Kao, C. Y., Tsai, M. T., Ong, S. C., Chen, C. H., Lin, C. S., 2009. Lipid accumulation and CO₂ utilization of *Nannochloropsis oculata* in response to CO₂ aeration. *Bioresour. Technol.* 100: 833-838.
- Cho S., Lee N., Park S., Yu J., Luong T.T., Oh Y.-K., Lee T., 2013, Microalgae cultivation for bioenergy production using wastewaters from a municipal WWTP as nutritional sources. *Bioresour Technol* DOI: <http://dx.doi.org/10.1016/j.biortech.2012.12.176>
- Christaki E., Florou-Paneri P., Bonos E., 2011. Microalgae: a novel ingredient in nutrition. *Int. J. Food Sci. Nutr.*, 62(8): 794-799.
- Christenson L., Sims R., 2011. Production and harvesting of microalgae for wastewater treatment, biofuels, and bioproducts. *Biotechnol Adv* 29(6): 686–702.
- Clarens A.F., Resurreccion E.P., White M.A., Colosi L.M., 2010. Environmental life cycle comparison of algae to other bioenergy feedstocks. *Environ. Sci. Technol.* 44:1813–9.
- Das P., Lei W., Aziz S. S., Obbard J. P., 2011. Enhanced algae growth in both phototrophic and mixotrophic culture under blue light, *Bioresource technology* 102: 3883-7.
- Degen J.; Uebele A.; Retze A.; Schmid-Staiger U.; Trosch W., 2001. A novel airlift photobioreactor with baffles for improved light utilization through the flashing light effect. *J. Biotechnol.* 92: 89-94.
- Doucha J., Straka F., Lívanský K., 2005. Utilization of flue gas for cultivation of microalgae (*Chlorella* sp.) in an outdoor open thin-layer photobioreactor. *J. Appl. Phycol.* 17: 403-412.
- Douskova, I., Doucha, J., Machat, J., Novak, P., Umysova, D., Vitova, M., Zachleder, V., 2008. Microalgae as a means for converting flue gas CO₂ into biomass with a high content of starch, *Bioenergy: Challenges and Opportunities. International Conference and Exhibition on Bioenergy, April 6th – 9th 2008, Universidade do Minho, Guimaraes, Portugal.*
- Douskova I., Doucha J., Livansky K., Machat J., Novak P., Umysova D., Zachleder V., Vitova M., 2009. Simultaneous flue gas bioremediation and reduction of microalgal biomass production costs. *Appl. Microbiol. Biotechnol.* 82: 179-185.
- Dragone G., Fernandes B. D., Abreu A.P., Vicente A. A., Teixeira J. A., 2011. Nutrient limitation as a strategy for increasing starch accumulation in microalgae. *Appl Energy* 88: 3331-3335.
- Dunahay T.G., Jarvis E.E., Dais S.S., Roessler P.G., 1996. Manipulation of microalgal lipid production using genetic engineering. *Appl. Biochem. Biotechnol.* 57–58: 223–31.
- Eriksen N., Poulsen B., Lønsmann Iversen J., 1998. Dual sparging laboratory-scale photobioreactor for continuous production of microalgae. *Journal of Applied Phycology* 10: 377-382.
- Fenton O., Ó hUallacháin D., 2012. Agricultural nutrient surpluses as potential input sources to grow

- third generation biomass (microalgae): A review, *Algal Research* 1(1): 49-56
- Fernandes B., Dragone G., Teixeira J., Vicente A., 2010. Light regime characterization in an airlift photobioreactor for production of microalgae with high starch content. *Applied Biochemistry and Biotechnology* 161: 218-226.
- García M. C. C., Sevilla J. M. F., Fernández F. G. A., Grima E. M., Camacho F. G., 2000. Mixotrophic growth of *Phaeodactylum tricornutum* on glycerol: growth rate and fatty acid profile, *Journal of Applied Phycology* 12: 239–248.
- García-González M., Moreno J., Cañavate J. P., Anguis V., Prieto A., Manzano C., Florencio F.J., Guerrero M.G., 2003. Conditions for open-air outdoor culture of *Dunaliella salina* in southern Spain. *J. Appl. Phycol.* 15: 177–184.
- Giménez Giménez A., Ibáñez M. J., Robles A., Molina E., Garcia S., Esteban L., 1998. Downstream processing and purification of eicosapentaenoic (20:5n-3) and arachidonic acids (20:4n-6) from the microalga *Porphyridium cruentum*. *Bioseparation* 7: 89– 99.
- Grima M. E., Belarbi E. H., Fernandez F. G. A., Medina A. R., Chisti Y., 2003. Recovery of microalgal biomass and metabolites: process options and economics. *Biotechnology Advances* 20(7-8): 491–515.
- Haiduc, A. G., Brandenberger M., Suquet S., Vogel F., Bernier-Latmani R., Ludwig C., 2009. SunCHEM: an integrated process for the hydrothermal production of methane from microalgae and CO₂ mitigation. *J. Appl. Phycol.* 21: 529– 541.
- Harun R., Singh M., Forde G. M., Danquah M. K., 2010_a. Bioprocess engineering of microalgae to produce a variety of consumer products. *Renewable and Sustainable Energy Reviews* 14: 1037-1047.
- Harun R., Danquah M. K., Forde G. M., 2010_b. Microalgal biomass as a fermentation feedstock for bioethanol production. *Journal of Chemical Technology & Biotechnology* 85: 199-203.
- Herzog H, Drake E, Adams E., 1997. CO₂ capture, reuse and storage technologies for mitigating global climate change. A White Paper. Department of Energy. Energy Laboratory. Massachusetts Institute of Technology. US.
- Hirano A., Ueda R., Hirayama S., Ogushi Y., 1997. CO₂ fixation and ethanol production with microalgal photosynthesis and intracellular anaerobic fermentation. *Energy*. 22:137-142.
- Hsieh C. H., Wu W. T., 2009. Cultivation of microalgae for oil production with a cultivation strategy of urea limitation. *Bioresour. Technol.* 100: 3921–6.
- <http://www.makebiofuel.co.uk/biofuel-from-algae> (07/03/2013)
- <http://www.oilgae.com> (07/03/2013)
- <http://www.oilgae.com/blog/2011/04/intel-demonstrates-pilot-model-for-algae-based-carbon-capture.html> (07/03/2013)
- <http://www.sardi.sa.gov.au/aquaculture/aquaculture/AlgaeAndBiofuelsFacility> (07/03/2013)
- Hu Q., Sommerfeld M., Jarvis E., Ghirardi M., Posewitz M., Seibert M., 2008. Microalgal triacylglycerols as feedstocks for biofuel production: perspectives and advances. *Plant J.*, 54: 621–39.
- Illman A.M., Scragg A.H., Shales S.W., 2000. Increase in *Chlorella* strains calorific values when grown in low nitrogen medium. *Enzyme Microb. Tech.* 27: 631–635.
- Janssen M., Slenders P., Tramper J., Mur L.R., Wijffels R., 2001. Photosynthetic efficiency of *Dunaliella*

- tertiolecta under short light/dark cycles. *Enzyme and Microbial Technology* 29: 298-305.
- Janssen M., Tramper J., Mur L. R., Wijffels R. H., 2003. Enclosed outdoor photobioreactors: Light regime, photosynthetic efficiency, scale-up, and future prospects. *Biotechnology and Bioengineering* 81: 193-210.
- Keffer J. E., Kleinheinz G. T., 2002. Use of *Chlorella vulgaris* for CO₂ mitigation in a photobioreactor. *Journal of Industrial Microbiology & Biotechnology* 29: 275-280.
- Krichnavaruk S., Powtongsook S., Pavasant P., 2007. Enhanced productivity of *Chaetoceros calcitrans* in airlift photobioreactors. *Bioresource Technology* 98: 2123-2130.
- Kumar A., Ergas S., Yuan X., Sahu A., Zhang Q., Dewulf J., Malcata F.X., van Langenhove H., 2010. Enhanced CO₂ fixation and biofuel production via microalgae: recent developments and future directions. *Trends Biotechnol* 28: 371-380.
- Kumar K., Dasgupta C. N., Nayak B., Lindblad P., Das D., 2011. Development of suitable photobioreactors for CO₂ sequestration addressing global warming using green algae and cyanobacteria. *Bioresour Technol* 102: 4945-4953.
- Lardon L., Sialve B, Steyer J. P., 2009. Bernard O. Life-Cycle Assessment of Biodiesel Production from Microalgae. *Environ. Sci. Technol.* 43: 6475-81.
- Lee, J.H., Lee, J.S., Shin, C.S., Park, S.C., Kim, S.W., 2000. Effects of NO and SO₂ on growth of highly-CO₂-tolerant microalgae. *J Microbiol. Biotechn.* 10, 338-343.
- Lee R. E., 2008. *Phycology*. 4th ed. Cambridge. Cambridge University Press.
- Lee Y. K., Low C. S., 1991. Effect of photobioreactor inclination on the biomass productivity of an outdoor algal culture. *Biotechnology and Bioengineering* 38: 995-1000.
- Lee Y. K., Tay H. S., 1991. High CO₂ partial pressure depresses productivity and bioenergetic growth yield of *Chlorella pyrenoidosa* culture. *J. Appl. Phycol.* 3: 95-101.
- Lee Y. K., Ding S.Y., Low C. S., Chang Y. C., Forday W., Chew P. C., 1995. Design and performance of an α -type tubular photobioreactor for mass cultivation of microalgae. *Journal of Applied Phycology* 7: 47-51.
- Li H. B., Chen F., Zhang T. Y., Yang F. Q., Xu G. Q., 2001. Preparative isolation and purification of lutein from the microalga *Chlorella vulgaris* by high-speed counter-current chromatography. *J Chromatogr A* 905: 151-5.
- Li X., Xu H., Wu Q., 2007. Large-scale biodiesel production from microalga *Chlorella protothecoides* through heterotrophic cultivation in bioreactors, *Biotechnology and Bioengineering* 98: 764-771
- Li Y., Horsman M., Wu N., Lan C. Q., Dubois-Calero N., 2008. Biofuels from microalgae. *Biotechnology Progress* 24: 815-820.
- Lv J. M., Cheng L. H., Xu X. H., Zhang L., Chen H. L., 2010. Enhanced lipid production of *Chlorella vulgaris* by adjustment of cultivation conditions. *Bioresource Technology*, 101(17): 6797-6804.
- Lynn S.G., Kilham S.S., Kreeger D.A., Interlandi S.J., 2000. Effect of nutrient availability on the biochemical and elemental stoichiometry in freshwater diatom *Stephanodiscus minutulus* acillariophyceae. *J. Phycol.*, 510-522.
- Malcata F. Xavier, 2011. Microalgae and biofuels: A promising partnership?. *Trends in Biotechnology* 29

- (11): 542-549.
- Mata T. M., Martins A. A., Caetano N. S., 2010. Microalgae for biodiesel production and other applications: A review. *Renewable and Sustainable Energy Reviews* 14: 217-232.
- Matamala A.R., Almonacid D.E., Figueroa M.F., Martinez-Oyanedel J., Bunster M.C., 2007. A semiempirical approach to the intra-phycoyanin and inter-phycoyanin fluorescence resonance energy-transfer pathways in phycobilisomes. *J. Computational Chem.*, 28: 1200-1207.
- McGinn P., Dickinson K., Bhatti S., Frigon J.-C., Guiot S., O'Leary S. B., 2011. Integration of microalgae cultivation with industrial waste remediation for biofuel and bioenergy production: opportunities and limitations. *Photosynth Res.* 109: 231-247.
- Mendes-Pinto M. M., Raposo M. F. J., Bowen J., Young A. J., Morais R., 2001. Evaluation of different cell disruption processes on encysted cells of *Haematococcus pluvialis*: effects on astaxanthin recovery and implications for bio-availability. *Journal of Applied Phycology* 13: 19-24.
- Merchuk J.C., Ronen M., Giris S., Arad (Malis) S., 1998. Light/dark cycles in the growth of the red microalga *Porphyridium* sp. *Biotechnology and Bioengineering* 59: 705-713.
- Miao X., Wu Q., 2004. High yield bio-oil production from fast pyrolysis by metabolic controlling of *Chlorella protothecoides*, *Journal of Biotechnology* 110: 85-93.
- Milledge J. J. 2011. Commercial application of microalgae other than as biofuels: a brief review. *Rev. Environment. Sci. Biotechnol.*, 10: 31-41.
- Mirón A., Contreras Gómez A, García Camacho F, Molina Grima E, Chisti Y., 1999. Comparative evaluation of compact photobioreactors for large-scale monoculture of microalgae. *Journal of Biotechnology* 70: 249-270.
- Molina Grima E., Garcia Camacho F., Sanchez Perez J. A., Urda Cardona J., Acien Fernandez F. G., Fernandez Servilla, J. M., 1994. Outdoor chemostat culture of *Phaeodactylum tricornutum* UTEX 640 in a tubular bioreactor for the production of eicosapentaenoic acid. *Biotechnol. Appl. Biochem.* 20: 279-290.
- Molina Grima E., 1999. Microalgae, mass culture methods. In: Flickinger MC, Drew SW, eds. *Encyclopedia of Bioprocess Technology: Fermentation, Biocatalysis, and Bioseparation*. New York, NY: John Wiley & Sons 1753-1769.
- Molina Grima E., Fernández J., Acien F. G, Chisti Y., 2001. Tubular photobioreactor design for algal cultures. *Journal of Biotechnology* 92: 113-131.
- Molina Grima E., Belarbi E.H., Acien Fernández F.G., Robles Medina A., Chisti Y., 2003. Recovery of microalgal biomass and metabolites: process options and economics. *Biotechnology Advances* 20: 491-515.
- Muller F.A., 2000. The role of microalgae in aquaculture: situation and trends, *J. Appl. Phycol.*, 12: 527-34.
- Muller-Feuga A., 2004. Microalgae for aquaculture: the current global situation and future trends. In *Handbook of Microalgal Culture*. Edited by Richmond A. Blackwell Science 352-364.
- Nigam P. S, Singh A., 2010. Production of liquid biofuels from renewable resources. *Progress in Energy and Combustion Science* 37(1): 52-68.

- Olaizola M., 2003. Commercial development of microalgal biotechnology: from the test tube to the marketplace. *Biomolecular Engineering* 20: 459-466.
- Patil V., Tran K. Q., Gislerød H.R., 2008. Towards Sustainable Production of Biofuels from Microalgae. *Int. J. Mol. Sci.* 9: 1188-95.
- Peterson A. A., Vogel F., Lachance R. P., Froling M., Antal Jr. M. J., Tester J. W., 2008. Thermochemical biofuel production in hydrothermal media: a review of sub- and supercritical water technologies, *Energy & Environmental Science* 1 (1): 32–65.
- Phukan M.M., Chutia R.S., Konwar B.K., Kataki Microalgae R., 2011. *Chlorella* as a potential bio-energy feedstock. *Appl Energy*, 88: 3307–3312.
- Pirt S. J., Lee Y. K., Walach M. R., Pirt M. W., Balyuzi H. H. M., Bazin M. J., 1983. A tubular bioreactor for photosynthetic production of biomass from carbon dioxide: Design and performance. *Journal of Chemical Technology and Biotechnology* 33: 35-58.
- Poulsen B.R., Iversen J. J. L., 1999. Membrane sparger in bubble column, airlift, and combined membrane-ring sparger bioreactors. *Biotechnology and Bioengineering* 64: 452-458.
- Pulz O., 2001. Photobioreactors: production systems for phototrophic microorganisms. *Applied Microbiology and Biotechnology* 57: 287-293.
- Pulz O., Gross W., 2004. Valuable products from biotechnology of microalgae. *Appl Microbiol Biotechnol* 65: 635-648.
- Rao A. R., Dayananda C., Sarada R., Shamala T. R., Ravishankar G.A., 2007. Effect of salinity on growth of green alga *Botryococcus braunii* and its constituents. *Bioresour. Technol.*, 98: 560-564.
- Reitan K.I., Rainuzzo J.R., Olsen Y., 1994. Effect of nutrient limitation on fatty acid and lipid content of marine microalgae. *J. Phycol.* 30: 972–979.
- Richmond A., 2004_a. *Handbook of Microalgal Culture: Biotechnology and Applied Phycology*. Oxford: Blackwell Science.
- Richmond, A., 2004_b. Principles for attaining maximal microalgal productivity in photobioreactors: an overview. *Hydrobiologia* 512: 33-37.
- Robles M. A., Giménez Giménez A., Garcia C. F., Sánchez P. J. A., Molina G. E, Contreras G. A., 1995. Concentration and purification of stearidonic, eicosapentaenoic, and docosahexaenoic acids from cod liver oil and the marine microalga *Isochrysis galbana*. *J Am Oil Chem Soc* 72: 575– 83.
- Roessler P.G., Brown L.M., Dunahay T.G., Heacox D.A., Jarvis E.E., Schneider J.C., 1994. Genetic-engineering approaches for enhanced production of biodiesel fuel from microalgae. *ACS Symp. Ser.* 566: 255–70.
- Rosenberg J. N., Oyler G. A., Wilkinson L., Betenbaugh M. J., 2008. A green light for engineered algae: redirecting metabolism to fuel a biotechnology revolution. *Current Opinion in Biotechnology* 19(5): 430–6.
- Ruiz H. A., Rodríguez-Jasso R. M., Fernandes B. D., Vicente A. A., Teixeira J. T., 2013. Hydrothermal processing, as an alternative for upgrading agriculture residues and marine biomass according to the biorefinery concept: a review. *Renewable & Sustainable Energy Reviews* 21: 35-51.
- Sandnes, J. M., Ringstad, T., Wenner, D., Heyerdahl, P. H., Kallqvist, T., Gislerød, H. R., 2006. Real-

- time monitoring and automatic density control of large-scale microalgal cultures using near infrared (NIR) optical density sensors. *J. Biotechnol.* 122: 209-215.
- Schenk P., Thomas-Hall S., Stephens E., Marx U., Mussgnug J., Posten C., Kruse O., Hankamer B., 2008. Second generation biofuels: high-efficiency microalgae for biodiesel production. *BioEnergy Research.* 1: 20-43.
- Scott S. A., Davey M. P., Dennis J. S., Horst I., Howe C. J., Lea-Smith D. J., Smith A. G., 2010. Biodiesel from algae: challenges and prospects. *Current Opinion in Biotechnology* 21(3): 277-286.
- Šetlík I, Šust V, Málek I., 1970. Dual purpose open circulation units for large scale culture of algae in temperate zones. I. Basic design considerations and scheme of a pilot plant *Algological Studies* 1: 111-164.
- Shuping Z., Yulong W., Mingde Y., Kaleem I., Chun L., Tong J., 2010. Production and characterization of bio-oil from hydrothermal liquefaction of microalgae *Dunaliella tertiolecta* cake. *Energy* 35: 5406-11.
- Singh J. and Gu, S., 2010. Commercialization potential of microalgae for biofuels production. *Renew Sustainable Energy Rev.* 14: 2596–2610.
- Sobczuk T. M., Camacho F. G., Rubio F. C., Fernández F. G. A., Molina E. M., 2000. Carbon dioxide uptake efficiency by outdoor microalgal cultures in tubular airlift photobioreactors. *Biotechnology and Bioengineering* 67: 465-475.
- Sobczuk T, Camacho F, Grima E, Chisti Y., 2006. Effects of agitation on the microalgae *Phaeodactylum tricornutum* and *Porphyridium cruentum*. *Bioprocess and Biosystems Engineering* 28: 243-250.
- Spolaore P., Joannis-Cassan C., Duran E., Isambert A., 2006. Commercial applications of microalgae. *J Biosci Bioeng* 101: 87-96.
- Sydney E. B., Sturm W., de Carvalho J. C., Thomaz-Soccol V., Larroche C., Pandey A., Soccol C. R., 2010. Potential carbon dioxide fixation by industrially important microalgae. *Bioresource Technology* 101: 5892-5896.
- Tang D., Han W., Li P., Miao X., Zhong J., 2011. CO₂ biofixation and fatty acid composition of *Scenedesmus obliquus* and *Chlorella pyrenoidosa* in response to different CO₂ levels. *Bioresour Technol* 102: 3071-3076.
- Thein M., 1993. Production of *Spirulina* in Myanmar (Burma). *Bulletin de l'Institut Océanographique* 12: 175-178.
- Tomaselli L., 2004. The microalgal cell. In: Richmond A, eds. *Handbook of Microalgal Culture: Biotechnology and Applied Phycology*. Oxford: Blackwell Publishing 3-19.
- Torzillo G., Pushparaj B., Bocci F., Balloni W., Materassi R., Florenzano G., 1986. Production of *Spirulina* biomass in closed photobioreactors. *Biomass* 11: 61-74.
- Torzillo G., Carlozzi P., Pushparaj B., Montaini E., Materassi R., 1993. A two-plane tubular photobioreactor for outdoor culture of *Spirulina*. *Biotechnology and Bioengineering* 42: 891-898.
- Tredici M. R., Zittelli G. C., 1998. Efficiency of sunlight utilization: Tubular versus flat photobioreactors. *Biotechnology and Bioengineering* 57: 187-197.
- Tredici M. R., 1999. Bioreactors, photo. In: Flickinger MC, Drew SW, eds. *Encyclopedia of Bioprocess*

- Technology: Fermentation, Biocatalysis, and Bioseparation. New York, NY: John Wiley & Sons 395-419.
- Tredici M.R., 2004. Mass production of microalgae: photobioreactors. In: Richmond A, eds. Handbook of Microalgal Culture: Biotechnology and Applied Phycology. Oxford: Blackwell Science 178-214.
- Ueno Y., Kurano N., Miyachi S., 1998. Ethanol production by dark fermentation in the marine green alga, *Chlorococcum littorale*. *Journal of Fermentation and Bioengineering* 86: 38-43.
- Ugwu C.U., Aoyagi H., Uchiyama H., 2008. Photobioreactors for mass cultivation of algae. *Bioresource Technology* 99(10): 4021–4028.
- Um B. H., Kim Y. S., 2009. Review: A chance for Korea to advance algal-biodiesel technology. *Journal of Industrial and Engineering Chemistry* 15: 1-7.
- Vanthoor-Koopmans M., Wijffels R.H., Barbosa M.J., Eppink M.H.M., 2012. Biorefinery of microalgae for food and fuel, *Bioresource Technology*, doi: <http://dx.doi.org/10.1016/j.biortech.2012.10.135>
- Vasudevan P., Briggs M., 2008. Biodiesel production—current state of the art and challenges. *Journal of Industrial Microbiology and Biotechnology* 35: 421-430.
- Waggoner A. 2006. Fluorescent labels for proteomics and genomics. *Curr Opin Chem Biol*, 10: 62-66.
- Wang B., Li Y., Wu N., Lan C., 2008. CO₂ bio-mitigation using microalgae. *Applied Microbiology and Biotechnology* 79: 707-718.
- Watanabe Y., Saiki H., 1997. Development of a photobioreactor incorporating *Chlorella* sp. for removal of CO₂ in stack gas. *Energy Conversion and Management* 38: S499-S503.
- Wijffels R. H., Barbosa M. J., 2010. An outlook on microalgal biofuels. *Science* 329: 796–799.
- WMO, 2012. The state of greenhouse gases in the atmosphere based on global observations through 2011, World Meteorological Organization. *Annual Greenhouse Gas Bulletin*, pp. 1-4.
- Wu X., Merchuk J.C., 2001. A model integrating 3uid dynamics in the photosynthesis and photoinhibition process. *Chemical Engineering Science* 56, 3527–3538.
- Wu X., Merchuk J. C., 2002. Simulation of algae growth in a bench scale bubble column reactor. *Biotechnol. Bioeng.* 80: 156-168.
- Yen H-W., Hu I-C., Chen C-Y., Ho S-H., Lee D-J., Chang, J-S., 2012. Microalgae-based biorefinery – From biofuels to natural products, *Bioresource Technology*, doi: <http://dx.doi.org/10.1016/j.biortech.2012.10.099>
- Zhang Z, Moo-Young M, Chisti Y., 1996. Plasmid stability in recombinant *Saccharomyces cerevisiae*. *Biotechnol Adv* 14: 401–35.
- Zhu J., Zong J., Zong B., 2013. Factors in mass cultivation of microalgae for biodiesel. *Chinese Journal of Catalysis*, 34: 80-100.
- Zittelli G., Rodolfi L., Biondi N., Tredici M.R., 2006. Productivity and photosynthetic efficiency of outdoor cultures of *Tetraselmis suecica* in annular columns. *Aquaculture* 261: 932-943.

CHAPTER 3

Optimization of CO₂ concentration and flow rate and their influence in growth and biochemical composition of *Chlorella vulgaris*

3.1 Abstract	59
3.2 Introduction	59
3.3 Material and Methods	60
3.4 Results and discussion	64
3.5 Conclusions	71
3.6 References	71

The results presented in this chapter were adapted from:

- Fernandes, B.**, Dragone, G., Abreu, Ana P., Geada, P., Teixeira, J., Vicente, A., 2012. *Starch determination in Chlorella vulgaris – a comparison between acid and enzymatic methods. Journal of Applied Phycology* 24 (5):1203 – 1208.
- Mariana Anjos, **Bruno D. Fernandes**, Giuliano Dragone, António A. Vicente, José A. Teixeira. *Optimization of CO₂ bio-mitigation by Chlorella vulgaris*. *Bioresource Technology* 139: 149-15.

3.1 Abstract

The main objective of the work presented in this chapter was to optimize the rate of CO₂ fixation (R_{CO_2}) by the green microalga *Chlorella vulgaris* P12 cultivated photoautotrophically under different CO₂ volumetric concentrations (ranging from 2% to 10%) and aeration rates (ranging from 0.1 vvm to 0.7 vvm). Results showed that the maximum R_{CO_2} (2.22 g L⁻¹ d⁻¹) was obtained by using 6.5% CO₂ and 0.5 vvm after 7 days of cultivation at 30 °C. Although final biomass concentration and maximum biomass productivity of microalgae were affected by the different cultivation conditions, no significant differences were obtained in the biochemical composition of microalgal cells for the evaluated levels of aeration and CO₂. The present study demonstrated that optimization of microalgal cultivation conditions can be considered a useful strategy for maximizing CO₂ bio-mitigation by *C. vulgaris*.

Keywords: aeration rate; biological mitigation; carbon dioxide sequestration; microalgae; photobioreactors

3.2 Introduction

The increasing concentration of anthropogenic CO₂ in the atmosphere appears to be the major cause of global warming, which may have catastrophic consequences for the environment and the climate (Chiu *et al.*, 2009). The amount of CO₂ in the atmosphere was 390.9 ppm in 2011, increasing on average 2 ppm per year for the past 10 years and reaching 140% of the pre-industrial level (280 ppm) (WMO, 2012). In order to reduce its atmospheric concentration, different abiotic (physical) methods have been evaluated, including injection into geological formations/deep oceans or utilization of absorbent materials (Kumar *et al.*, 2010). These methods, however, require significant space of storage associated with elevated costs of monitoring, operation, and maintenance, raising serious concerns about potential CO₂ leakage over time (Bilanovic *et al.*, 2009).

On the other hand, biological mitigation of atmospheric CO₂ has been deemed as a sustainable approach to physical methods (Kumar *et al.*, 2011). Biofixation of CO₂ can be performed either by plants or photosynthetic microorganisms. Nevertheless, the process of CO₂ sequestration by plants can be viewed as an inadequate strategy of mitigation, since its contribution to CO₂ capture has been estimated to only 3 – 6% of

fossil fuel emissions, mainly because of slow growth rates of terrestrial vegetation (Wang *et al.*, 2008). Alternatively, microalgae have received renewed attention in recent years due to their faster growth rates and higher photosynthetic efficiency than terrestrial plants (Chiu *et al.*, 2009; Dragone *et al.*, 2011). These photosynthetic microorganisms can efficiently convert CO₂ from a point source into O₂ and biomass (Tang *et al.*, 2011).

Cultivation of microalgae can be exploited as an additional step in flue gas treatment, aiming the reduction of CO₂ levels in the exhaust flue gas. Previous studies have demonstrated that microalgae can be successfully employed for the treatment of simulated flue gases (Lee *et al.*, 2000) or flue gases emitted from municipal waste incinerators (Douskova *et al.*, 2009), coal-fired power plants (McGinn *et al.*, 2011), industrial heater using kerosene as fuel (Chae *et al.*, 2006) and gas boiler (Doucha *et al.*, 2005).

Gas aeration in photobioreactors serves not only as a supply of CO₂ for cell growth, but also as a means of pH control, as well as for other important purposes such as provision of internal mixing to avoid nutrient concentration gradients, promotion of exposure of all cells to light (especially in high density cultures) to minimize self-shading and phototoxicity, and stripping of accumulated dissolved oxygen to reduce its toxicity to microalgae (Kumar *et al.*, 2010). Therefore, aeration rate and CO₂ concentration can be considered as key parameters to improve the performance of microalgal photobioreactors.

The aim of this study was to maximize the CO₂ fixation by the green microalga *Chlorella vulgaris* cultivated under different concentrations of CO₂ and aeration rates. The effect of each culture condition on growth parameters and biochemical composition of microalgal cells was also evaluated.

3.3 Material and Methods

3.3.1 Microorganism and culture conditions

The freshwater *C. vulgaris* (strain P12) was used for cultivation under photoautotrophic conditions. All experiments were carried out at 30 °C in 110 mL glass

bubble columns photobioreactors containing 90 mL of medium, during 7 days. Agitation during cultivation of microalgae was provided by bubbling CO₂-enriched air through a needle (inner diameter of 0.8 mm) at the bottom of the photobioreactors. Different values of initial CO₂ concentration and aeration rates were used in the experiments (Table 3.1).

Table 3.1 Experimental range and levels of the independent process variables according to the 2² full-factorial central composite design

Independent variable	Symbol	Range and levels		
		-1	0	+1
CO ₂ concentration (%)	X_1	2	6	10
Aeration rate (vvm)	X_2	0.1	0.4	0.7

Illumination was provided by four fluorescent lamps (Sylvania Standard F18 W) on one side of the photobioreactors, at an irradiance level of 70 $\mu\text{E m}^{-2} \text{s}^{-1}$ measured by a LI-250 Light Meter with a LI-190 quantum sensor (LI-COR, USA).

The growth medium based on the elementary composition of algal biomass had the following initial composition (mg L^{-1}): 1,100 (NH₂)₂CO, 237 KH₂PO₄, 204 MgSO₄·7H₂O, 40 C₁₀H₁₂O₈N₂NaFe, 88 CaCl₂, 0.83 H₃BO₃, 0.95 CuSO₄·5H₂O, 3.3 MnCl₂·4H₂O, 0.17 (NH₄)₆Mo₇O₂₄·4H₂O, 2.7 ZnSO₄·7H₂O, 0.6 CoSO₄·7H₂O, 0.014 (NH₄)VO₃ in distilled water; the initial pH was adjusted to 7.0 by 0.1 M NaOH.

The initial algal concentration was the same for all the cultivation conditions: 2.0 x 10⁷ cells mL⁻¹.

3.3.2 Determination of microalgal cell concentration

Microalgal concentration in photobioreactors was measured by using an improved Neubauer hemocytometer. Biomass was also determined by cell dry weight after centrifugation of the sample at 8,750 g (Hettich D-78532, Germany) during 15 min, washing with distilled H₂O and drying at 105 °C until constant weight.

3.3.3 Determination of biomass productivity and specific growth rate

Maximum biomass productivity (P_{max} , $\text{g L}^{-1} \text{d}^{-1}$) was calculated from Eq. 3.1, where X_t was the biomass concentration (g L^{-1}) at the end of the cultivation period (t_x) and X_0 the initial biomass concentration (g L^{-1}) at t_0 (day).

$$P_{max} = \frac{(X_t - X_0)}{(t_x - t_0)} \quad \text{Eq. 3.1}$$

Specific growth rate (μ_{max} , day^{-1}) was calculated from Eq. 3.2 according to Abreu *et al.* (2012).

$$\mu_{max} = (\ln N_2 - \ln N_1) / (t_2 - t_1) \quad \text{Eq. 3.2}$$

where N_1 and N_2 were the concentration of cells at the beginning (t_1) and at the end (t_2) of the exponential growth phase, respectively.

3.3.4 Determination of CO₂ fixation rate

Carbon dioxide biofixation rate, R_{CO_2} ($\text{g L}^{-1} \text{d}^{-1}$), was calculated from Eq. 3.3, as described by Tang *et al.* (2011).

$$R_{CO_2} = C_C P_{max} (M_{CO_2} / M_C) \quad \text{Eq. 3.3}$$

where C_C was the carbon content of microalgal cells (% w/w), measured by using a LECO CHNS-932 Elemental Analyser (USA), P_{max} was the maximum biomass productivity ($\text{g L}^{-1} \text{d}^{-1}$), M_{CO_2} was the molar mass of CO₂ (g mol^{-1}) and M_C was the molar mass of carbon (g mol^{-1}).

3.3.5 Biochemical characterization of microalgal cells

The concentration of microalgal starch was assayed by the hydrolysis of starch to glucose with amyolytic enzymes (α -amylase and amyloglucosidase) according to the procedure provided by Megazyme (Wicklow, Ireland) and accepted by AOAC (Official Method 996.11) and AACC (Method 76.13). Lyophilized microalgae biomass was disintegrated with a mortar and pestle, re-suspended in aqueous ethanol and incubated in a water bath at 80 – 85 °C for 5 min, to extract the pigments. Thermostable α -

amylase (3000 U mL⁻¹) in MOPS buffer (50 mM, pH 7.0) including 5 mM CaCl₂, was added to each sample. The samples were maintained at 100 °C during 6 min, followed by heating at 50 °C. Amyloglucosidase (3,300 U mL⁻¹) in sodium acetate buffer was then added to each sample. Samples were subsequently maintained at 50 °C for 30 min, and then centrifuged (10 min) at 3,000 rpm. Glucose in the supernatant was assessed by glucose oxidase method. Total starch content was determined by multiplying the percentage of microalgal starch with the corresponding biomass concentration (Fernandes *et al.*, 2012).

Total lipids were determined by the classic Folch *et al.* (1957) chloroform-based lipid extraction protocol. Total lipids were extracted from lyophilized biomass in CHCl₃-MeOH (2:1, v/v). Freeze-dried biomass was suspended in CHCl₃-MeOH (2:1, v/v) solution, extracted for 90 min, being the extract collected by centrifugation at 2,000 g (Hettich D-78532, Hettich, Germany) for 10 min. The pellet was resuspended and re-extracted in CHCl₃-MeOH solution twice. The collected extract was evaporated at 40 °C, dried at 70 °C for 2 h, and subsequently weighed after cooling to room temperature. Lipid content of microalgae was calculated by dividing the extraction residue weight by the freeze-dried cells weight.

The protein content of microalgal cells was quantified according to the method of Lowry *et al.* (1951). After a predigestion in 0.5 M NaOH at 80 °C for 30 min, protein content in microalgae cells was quantified at 750 nm using Folin-Ciocalteu reagent. Bovine serum albumin was used as standard protein solution.

3.3.6 Experimental design and optimization by response surface methodology

The influence of initial CO₂ concentration and aeration rate (independent variables) on CO₂ biofixation rate (dependent variable) by *C. vulgaris* was assessed through a 2² full-factorial central composite design (CCD). For statistical analysis, the independent variables were coded according to Eq. 3.4, where each independent variable is represented by x_i (coded value), X_i (real value), X_0 (real value at the centre point), and ΔX_i (step change value). The range and the levels of the variables are given in Table 3.1.

$$x_i = \frac{(X_i - X_0)}{\Delta X_i} \quad \text{Eq. 3.4}$$

The experimental results were fitted with a second-order polynomial equation by multiple regression analysis. The quadratic mode for predicting the optimal point was expressed according to Eq. 3.5, where \hat{y} represents the response variable, b_0 is the interception coefficient, b_i , b_{ii} and b_{ij} are the regression coefficients, n is the number of studied variables, and X_i and X_j represent the independent variables. Where possible, the model was simplified by elimination of statistically insignificant terms.

$$\hat{y}_i = b_0 + \sum_{i=1}^n b_i X_i + \sum_{i=1}^n b_{ii} X_i^2 + \sum_{i=1}^{n-1} \sum_{j=i+1}^n b_{ij} X_i X_j \quad \text{Eq. 3.5}$$

The quality of the fitted polynomial model was expressed by the coefficient of determination R^2 , and its statistical significance was checked by the F-test. The significance of the regression coefficients was tested by t-value. Results were analyzed by the Experimental Design Module of the Statistica 8.0 software (Statsoft, USA). The model permitted evaluation of the effects of linear, quadratic and interactive terms of the independent variables on the chosen dependent variables.

Data were compared using one-way ANOVA followed by a Tukey's multiple comparison tests with 95% confidence level.

3.4 Results and discussion

3.4.1 Effect of CO₂ concentration and aeration rate on microalgal growth

Final biomass concentration (X_{max}) and maximum biomass productivity (P_{max}) of *C. vulgaris* cultivated under different aeration rates and CO₂ concentration in the air stream are shown in Table 3.2.

C. vulgaris was able to grow under all the evaluated levels of aeration and CO₂; however X_{max} and P_{max} were significantly influenced by the cultivation conditions. Regardless the CO₂ level in air, higher values of X_{max} and P_{max} were obtained under the aeration rate of 0.4 vvm when compared with those values obtained at 0.1 vvm.

Table 3.2 Growth parameters of *C. vulgaris* cultivated under different CO₂ concentrations and aeration rates at 30 °C

Cultivation condition		Growth parameters	
CO ₂ concentration (%)	Aeration rate (vvm)	X_{max}^a (g L ⁻¹)	P_{max}^b (g L ⁻¹ d ⁻¹)
2	0.1	5.5 ± 1.7	0.7 ± 0.2
	0.4	6.9 ± 1.2	0.9 ± 0.2
	0.7	8.3 ± 2.8	1.1 ± 0.4
6	0.1	6.8 ± 0.5	0.9 ± 0.0
	0.4	10.0 ± 0.5	1.3 ± 0.0
	0.7	8.9 ± 0.8	1.2 ± 0.1
10	0.1	6.0 ± 1.9	0.8 ± 0.3
	0.4	8.6 ± 2.4	1.2 ± 0.3
	0.7	8.5 ± 0.1	1.2 ± 0.0

^a Final biomass concentration^b Maximum biomass productivity

These results are in good agreement with a previous study, which reported that cell concentration and biomass productivity of *Chlorella sp.* AG10002 rose when aeration rate is increased from 0.1 to 0.4 vvm (Ryu *et al.*, 2009). According to Fan *et al.* (2007), the gas-liquid mass transfer coefficient is strengthened by increasing the feed gas flow rate. Moreover, the higher turbulent motion of liquid intensifies the movement of cells at the region adjacent to the photobioreactor wall, leading to an enhanced use of light by microalgae.

On the other hand, X_{max} and P_{max} decreased as the aeration rate was increased from 0.4 to 0.7 vvm at 6 and 10% CO₂ concentrations. It has been suggested that high aeration air flux reduces the gas bubble retention time, releasing the gas mixture to the outside of the photobioreactor before an efficient mixing occurred (Fan *et al.*, 2007); as a consequence, the majority of the supplied CO₂ might have not been efficiently used by microalgal cells. Additionally, high mixing rates can cause shear damage to microalgae (Kumar *et al.*, 2010).

The final biomass concentration and maximum biomass productivity of *C. vulgaris* were also significantly influenced by the percentage of CO₂ in the air stream. It can be observed in Table 3.2 that X_{max} and P_{max} increased nearly 45% when CO₂ concentration

was raised from 2% to 6% at 0.4 vvm. This result is compatible with previous research observations. For example, Ryu *et al.* (2009) showed that maximum cell concentration and biomass productivity of *Chlorella* increased from 1.78 to 2.02 g L⁻¹ and from 0.295 to 0.335 g L⁻¹ d⁻¹, respectively, by elevating the CO₂ level in air from 2% to 5%.

It is worth mentioning that the dissolved inorganic carbon in the culture medium exists in the forms of CO₂, H₂CO₃, HCO₃⁻ and CO₃²⁻, usually in an equilibrium, and represents the carbon source for microalgae growth (Tang *et al.*, 2011). Therefore, the stimulatory effect of CO₂ (up to 6%) on growth parameters of *C. vulgaris* could be related to the increased availability of carbon as a result of the higher DIC concentration. Beyond that, CO₂ abundance influences several key enzymes in carbon metabolism, such as carbonic anhydrase and Rubisco. Thus, elevated CO₂ concentration can enhance the carboxylating activity and repress the oxygenating activity of Rubisco, resulting in increased photosynthesis (Yang and Gao, 2003).

However, high CO₂ concentration can also result in low pH. Decrease of pH will cause the decrease of the activity of carbonic extracellular anhydrase and inhibit cell growth (Tang *et al.*, 2011). The lower values of X_{max} and P_{max} obtained under 10% CO₂ concentration in air in comparison with those found at 6% CO₂ level validate such hypothesis.

Among the different cultivation conditions tested, the highest values of final biomass concentration (10.0 ± 0.5 g L⁻¹), maximum biomass productivity (1.3 ± 0.0 g L⁻¹ d⁻¹) and maximum specific growth rate (0.95 ± 0.04 d⁻¹) of *C. vulgaris* P12 were all obtained at 6% CO₂ and 0.4 vvm.

3.4.2 Optimization of CO₂ biofixation rate

In order to calculate the carbon dioxide biofixation rate (R_{CO_2}), the elemental composition of *C. vulgaris* cultivated under different growth conditions was determined. No statistically significant differences were found in terms of carbon, hydrogen and nitrogen content of cells cultivated under different CO₂ concentrations and aeration rates (data not shown). This result ratifies previous findings of Tang *et al.* (2011), where the carbon content of *C. pyrenoidosa* SJTU-2 was nearly 50%, without

greatly changes under CO₂ concentrations between 0.03% and 50%. In our study, the carbon content of *C. vulgaris* was $45.6 \pm 0.5\%$ in average (Table 3.3).

Table 3.3 Elemental composition of *C. vulgaris* cells

Element	Content (wt. %)
C	45.6 ± 0.5
H	6.9 ± 0.1
N	2.7 ± 0.2

C = carbon; H = hydrogen; N = nitrogen

Regarding the rate of CO₂ fixation by *C. vulgaris*, R_{CO_2} was calculated according to Eq. 3.3, and the results are shown in Table 3.4.

Table 3.4 Experimental matrix and results of R_{CO_2} (g L⁻¹ d⁻¹) with coded levels of CO₂ concentration (X_1) and aeration rate (X_2) according to the 2² full-factorial central composite design

Runs	Independent variables		R_{CO_2} (g L ⁻¹ d ⁻¹)	
	X_1	X_2	Experimental	Predicted
1	-1	-1	1.15	1.10
2	-1	+1	1.87	1.79
3	+1	-1	1.35	1.55
4	+1	+1	1.92	2.10
5	-1	0	1.50	1.69
6	+1	0	1.93	2.07
7	0	-1	1.54	1.64
8	0	+1	2.08	2.26
9	0	0	2.10	2.20
10	0	0	2.07	2.20
11	0	0	2.18	2.20
12	0	0	2.29	2.20

It can be noted that R_{CO_2} varied under the different cultivation conditions. The highest values of R_{CO_2} were obtained when *C. vulgaris* was cultivated at 6% CO₂ concentration and 0.4 vvm.

Due to the differences observed among values, a statistical analysis was carried out aiming at identifying which independent variable had significant influence on R_{CO_2} . The statistical significance of CO₂ concentration and aeration rate on the response variable (R_{CO_2}) is given in Table 3.5.

Table 3.5 Effect estimates, standard errors and t-test for R_{CO_2} by *C. vulgaris* according to the 2^2 full-factorial central composite design

Variables and interactions	Estimated effects	Standard errors	t_{value}	p
X_1	0.227	0.101	2.237	0.067
X_1^2	-0.683	0.152	-4.491	0.004 ^a
X_2	0.610	0.101	6.021	0.001 ^a
X_2^2	-0.493	0.152	-3.241	0.018 ^a
X_1X_2	-0.075	0.124	-0.604	0.568

X_1 = CO₂ concentration; X_2 = aeration rate

^a Significant influence at 95% confidence level

According to this analysis, the linear term of aeration rate as well as the quadratic terms of CO₂ concentration and aeration rate showed significant influence on R_{CO_2} at 95% confidence level.

After identification of the terms affecting R_{CO_2} , the experimental values were fitted to a second-order equation (Eq. 3.6) obtained by multiple regression analysis. The coefficients of the proposed equation are given below:

$$R_{CO_2} = 0.27 + 0.30 C - 0.02 C^2 + 3.39 A - 2.74 A^2 - 0.03 C A \quad (R^2 = 0.94) \quad \text{Eq. 3.6}$$

where C represents the CO₂ concentration in air and A represents the aeration rate.

The quality of the quadratic fit was represented by the coefficient of determination R^2 . As can be noted, the model explains more than 90% of the dependent variable's variability ($R^2 > 0.90$). The high R^2 means that the quadratic model is able to represent values in the experimental region in an accurate manner. The values predicted by the model are displayed in Table 3.4 along with the observed values. Comparison of these data indicates that there is a good agreement between the experimental and predicted values for the proposed range. Therefore, the experimental factorial design and regression analysis were effective to identify the optimal conditions for maximum biofixation of CO₂ by microalgae under the different levels of CO₂ in air and aeration rates.

The relation between independent variables and R_{CO_2} can be best visualized by examining the surface plot presented in Figure 3.1.

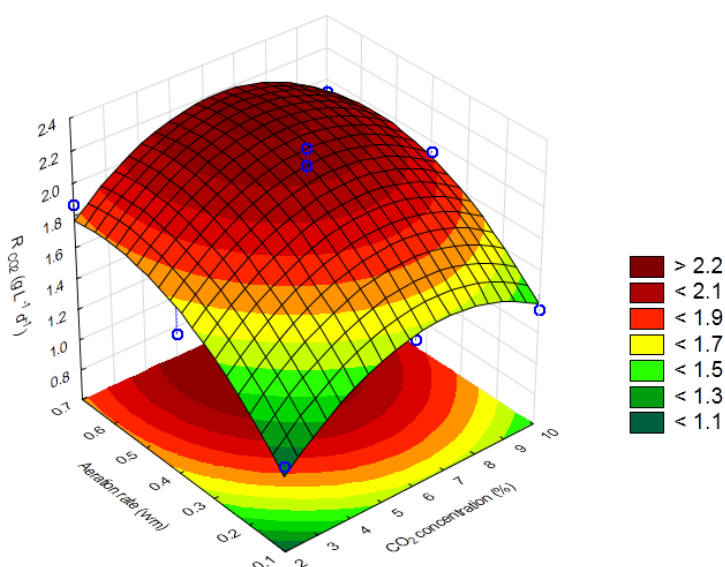


Figure 3.1 Response surface of R_{CO_2} by *C. vulgaris* P12 as a function of CO₂ concentration in air and aeration rate.

Figure 3.1 clearly shows that R_{CO_2} rate was not linearly increased when the process variables were increased, but there was an optimum point after which the use of higher CO₂ concentration and aeration rate did not improve R_{CO_2} . This is in agreement with the analysis presented in Table 3.5, which showed significant effect of the quadratic terms of both variables on R_{CO_2} . An estimate of the critical point revealed that 6.5% CO₂ and 0.5 vvm were the conditions able to maximize R_{CO_2} . Under these conditions the model predicts a rate of CO₂ fixation by *C. vulgaris* of 2.29 g L⁻¹ d⁻¹. Assays for validation of this model were then performed under the established operating conditions and the obtained values of R_{CO_2} , X_{max} and P_{max} were 2.22 g L⁻¹ d⁻¹, 9.97 ± 0.05 g L⁻¹ and 1.33 ± 0.02 g L⁻¹ d⁻¹, respectively.

The results achieved in our study compare favourably with others reported in the literature. For example, the R_{CO_2} by *C. vulgaris* LEB-104 cultivated under 5% CO₂ concentration was 0.25 g L⁻¹ d⁻¹ (Sydney *et al.*, 2010). A maximum R_{CO_2} of 0.87 g L⁻¹ d⁻¹ was obtained for *Chlorella* sp. UK001 using a gaseous mixture (CO₂:O₂:N₂ = 10:3:87 (v/v)) at a constant flow rate of 0.05 vvm (Hirata *et al.*, 1996).

3.4.3 Influence of CO₂ concentration and aeration rate on the biochemical composition of *C. vulgaris*

The content of starch, proteins and lipids of microalgae cultivated under different CO₂ concentration in air and aeration rates were determined and depicted in Figure 3.2. Despite differences in values of growth parameters and CO₂ fixation rates presented above, no statistically significant differences were observed in the biochemical composition of microalgal cells cultivated under different growth conditions. Such behaviour could be explained by mild conditions in terms of CO₂ concentration and aeration rates used in our study.

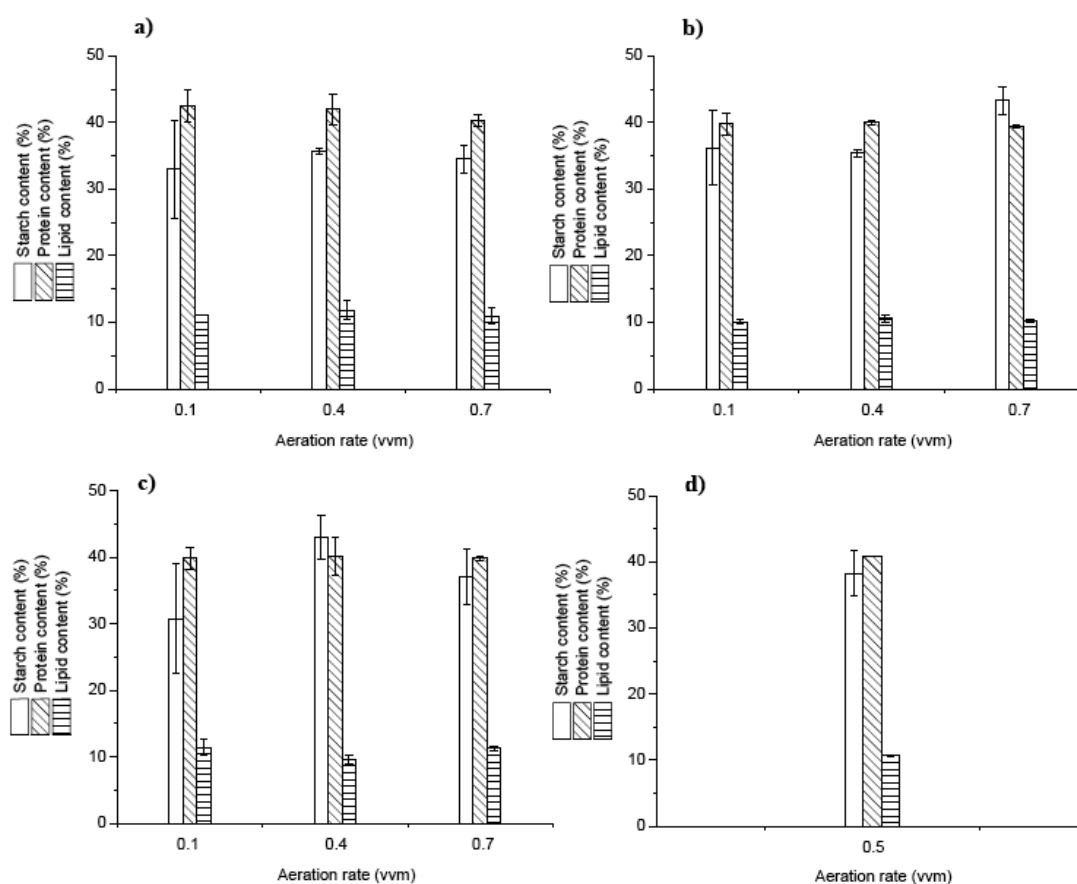


Figure 3.2 Contents of starch, proteins and lipids of *C. vulgaris* cultivated in bubble column photobioreactors under different CO₂ concentrations (2% (a), 6% (b), 10% (c) and 6.5% (d)) and aeration rates.

It is known that only extreme/stressful cultivation conditions tend to promote changes in the accumulation of starch or lipids in *C. vulgaris* P12 cells (Dragone *et al.*, 2011). The conditions used in this study were far to be stressful to the cells, as

demonstrated by the growth parameters presented in Table 3.2.

C. vulgaris P12 was able to accumulate about 37% starch, 41% proteins and 11% lipids under the evaluated cultivated conditions.

3.5 Conclusions

The present study revealed that growth parameters and CO₂ uptake by *C. vulgaris* P12 were significantly affected by CO₂ concentration in air stream (ranging from 2% to 10%) and aeration rate (ranging from 0.1 vvm to 0.7 vvm). The highest rate of CO₂ fixation by microalgae (2.22 g L⁻¹ d⁻¹) was obtained under 6.5% CO₂ and 0.5 vvm. This study constitutes an important step in the development of strategies to mitigate CO₂ in an environmentally sustainable manner by using a biological approach.

3.6 References

- Abreu A.P., Fernandes B., Vicente A.A., Teixeira J., Dragone G., 2012. Mixotrophic cultivation of *Chlorella vulgaris* using industrial dairy waste as organic carbon source. *Bioresour Technol* 118: 61-66.
- Bilanovic D., Andargatchew A., Kroeger T., Shelef G., 2009. Freshwater and marine microalgae sequestering of CO₂ at different C and N concentrations – Response surface methodology analysis. *Energy Convers Manage* 50: 262-267.
- Chae S.R., Hwang E.J., Shin H.S., 2006. Single cell protein production of *Euglena gracilis* and carbon dioxide fixation in an innovative photo-bioreactor. *Bioresour Technol* 97: 322-329.
- Chiu S.-Y., Kao C.-Y., Tsai M.-T., Ong S.-C., Chen C.-H., Lin C.-S., 2009. Lipid accumulation and CO₂ utilization of *Nannochloropsis oculata* in response to CO₂ aeration. *Bioresour Technol* 100: 833-838.
- Doucha J., Straka F., Livanský K., 2005. Utilization of flue gas for cultivation of microalgae (*Chlorella* sp.) in an outdoor open thin-layer photobioreactor. *J Appl Phycol* 17: 403-412.
- Douskova I., Doucha J., Livansky K., Machat J., Novak P., Umysova D., Zachleder V., Vitova M., 2009. Simultaneous flue gas bioremediation and reduction of microalgal biomass production costs. *Appl Microbiol Biotechnol* 82: 179-185.
- Dragone G., Fernandes B.D., Abreu A.P., Vicente A.A., Teixeira J.A., 2011. Nutrient limitation as a strategy for increasing starch accumulation in microalgae. *Appl Energy* 88: 3331-3335.
- Fan L.H., Zhang Y.T., Cheng L.H., Zhang L., Tang D.S., Chen H.L., 2007. Optimization of carbon dioxide fixation by *Chlorella vulgaris* cultivated in a membrane-photobioreactor. *Chem Eng Technol* 30: 1094-1099.
- Fernandes B., Dragone G., Abreu A.P., Geada P., Teixeira J., Vicente A., 2012. Starch determination in *Chlorella vulgaris*—a comparison between acid and enzymatic methods. *J Appl Phycol* 24: 1203-1208.

- Fernandes B., Dragone G., Teixeira J., Vicente A., 2010. Light regime characterization in an airlift photobioreactor for production of microalgae with high starch content. *Appl Biochem Biotechnol* 161: 218-226.
- Folch, J., Lees, M., Sloane Stanley, G.H., 1957. A simple method for the isolation and purification of total lipides from animal tissues. *Journal of Biological Chemistry*, 226(1): 497-509.
- Hirata S., Hayashitani M., Taya M., Tone S., 1996. Carbon dioxide fixation in batch culture of *Chlorella* sp. using a photobioreactor with a sunlight-collection device. *J Ferment Bioeng* 81: 470-472.
- Kumar A., Ergas S., Yuan X., Sahu A., Zhang Q., Dewulf J., Malcata F.X., van Langenhove, H., 2010. Enhanced CO₂ fixation and biofuel production via microalgae: recent developments and future directions. *Trends Biotechnol* 28: 371-380.
- Kumar K., Dasgupta C.N., Nayak B., Lindblad P., Das, D., 2011. Development of suitable photobioreactors for CO₂ sequestration addressing global warming using green algae and cyanobacteria. *Bioresour Technol* 102: 4945-4953.
- Lee J.H., Lee J.S., Shin C.S., Park S.C., Kim S.W., 2000. Effects of NO and SO₂ on growth of highly-CO₂-tolerant microalgae. *J Microbiol Biotechnol* 10: 338-343.
- Lowry, O.H., Rosebrough, N.J., Farr, A.L., Randall, R.J., 1951. Protein measurement with the Folin phenol reagent. *Journal of Biological Chemistry*, 193(1): 265-275.
- McGinn P., Dickinson K., Bhatti S., Frigon J.-C., Guiot S., O'Leary S.B., 2011. Integration of microalgae cultivation with industrial waste remediation for biofuel and bioenergy production: opportunities and limitations. *Photosynth Res* 109: 231-247.
- Milledge J.J., 2011. Commercial application of microalgae other than as biofuels: a brief review. *Rev Environ Sci Biotechnol* 10: 31-41.
- Ryu H.J., Oh K.K., Kim Y.S., 2009. Optimization of the influential factors for the improvement of CO₂ utilization efficiency and CO₂ mass transfer rate. *J Ind Eng Chem* 15: 471-475.
- Sydney E.B., Sturm W., de Carvalho J.C., Thomaz-Soccol V., Larroche C., Pandey A., Soccol C.R., 2010. Potential carbon dioxide fixation by industrially important microalgae. *Bioresour Technol* 101: 5892-5896.
- Tang D., Han W., Li P., Miao X., Zhong J., 2011. CO₂ biofixation and fatty acid composition of *Scenedesmus obliquus* and *Chlorella pyrenoidosa* in response to different CO₂ levels. *Bioresour Technol* 102: 3071-3076.
- Wang B., Li Y., Wu N., Lan C., 2008. CO₂ bio-mitigation using microalgae. *Appl Microbiol Biotechnol* 79: 707-718.
- WMO, 2012. The state of greenhouse gases in the atmosphere based on global observations through 2011, World Meteorological Organization. *Annual Greenhouse Gas Bulletin*, pp. 1-4.
- Yang Y., Gao K., 2003. Effects of CO₂ concentrations on the freshwater microalgae, *Chlamydomonas reinhardtii*, *Chlorella pyrenoidosa* and *Scenedesmus obliquus* (Chlorophyta). *J Appl Phycol* 15: 379-389.

CHAPTER 4

Strategies for increasing energy-rich materials' concentration in microalgae

4.1 Nutrient limitation as a strategy for increasing starch accumulation in microalgae

4.1.1 Abstract	75
4.1.2 Introduction	75
4.1.3 Material and Methods	76
4.1.4 Results and discussion	79
4.1.5 Conclusions	85
4.1.6 References	85

4.2 Unravelling the mechanism of accumulation of energy-rich reserves in the microalga *Parachlorella kessleri*

4.2.1 Abstract	89
4.2.2 Introduction	90
4.2.3 Material and Methods	92
4.2.4 Results and discussion	95
4.2.5 Conclusions	106
4.2.6 References	106

The results presented in this chapter were adapted from:

Dragone G., **Fernandes B. D.**, Abreu A. P., Vicente A. A., Teixeira J. A., 2011. *Nutrient limitation as a strategy for increasing starch accumulation in microalgae.* Applied Energy 88 (10): 3331-3335.

Bruno Fernandes, José Teixeira, Giuliano Dragone, António A. Vicente, Kawano S., Katerina Bišová, Milada Vítová, Vilém Zachleder. *Relationship between starch and lipid accumulation in the microalga Parachlorella kessleri, induced by nutrient depletion and replenishment.* Submitted to Bioresource Technology.

4.1 Nutrient limitation as a strategy for increasing starch accumulation in microalgae

4.1.1 Abstract

Increasing microalgal starch content by nutrient limitation has been regarded as an affordable approach for the production of third generation bioethanol. This work evaluated starch accumulation in *Chlorella vulgaris* P12 under different initial concentrations of nitrogen (0 – 2.2 g of urea L⁻¹) and iron (0 – 0.08 g of FeNa-EDTA L⁻¹) sources, using a central composite design (CCD) for two factors. The obtained model: starch content (%) = 8.220 - 16.133 X_I + 13.850 X_I^2 , relating starch accumulation in microalgae with the coded level for initial urea concentration in the growth medium (X_I), presented a good agreement between predicted and experimental values ($R^2 = 0.94$). Since accumulation of starch occurred at nitrogen depletion conditions under which the cell growth was much slower than that observed during nitrogen supplemented cultivations, a two-stage cultivation process for high starch accumulation (> 40%) and cell growth of *C. vulgaris* was proposed: a first cultivation stage using nitrogen- and iron-supplemented medium (initial urea and FeNa-EDTA concentrations of 1.1 and 0.08 g L⁻¹, respectively), followed by a second cultivation stage in a nitrogen- and iron-free medium. The high starch content obtained suggests *C. vulgaris* P12 as a very promising feedstock for bioethanol production.

Keywords: Bioethanol; biofuel; *Chlorella vulgaris*; starch; nutrient limitation.

4.1.2 Introduction

The microalga *Chlorella vulgaris* has been recognized as a potential feedstock for bioethanol production due to its capacity to accumulate high levels starch (up to 60% dry weight) (Brányiková *et al.*, 2011). Several studies have demonstrated that alteration in nutrient concentrations can modify the growth and secondary metabolism of microalgae (Behrens, 1996; Hsieh and Wu, 2009). Furthermore, microalgae growth depends not only on an adequate supply of essential macronutrient elements (carbon,

nitrogen, phosphorus, silicon) and major ions (Mg^{2+} , Ca^{2+} , Cl^- , and SO_4^{2-}) but also on a number of micronutrient metals such as iron, manganese, zinc, cobalt, copper, and molybdenum (Sunda *et al.*, 2005). Iron is needed for the growth of all phytoplankton. It serves essential metabolic functions in photosynthetic electron transport, respiratory electron transport, nitrate and nitrite reduction, sulphate reduction, dinitrogen (N_2) fixation, and detoxification of reactive oxygen species (*e.g.*, superoxide radicals and hydrogen peroxide) (Sunda and Huntsman, 1997). Although numerous reports have shown that cell composition of microalgae can be affected by a single chemical or physical factor, the effectiveness of such treatment is usually poor, and the change is slow (Hu, 2004). In fermentation processes, where several variables have to be simultaneously contemplated, it is necessary that the optimization method take their interactions in consideration (Dragone *et al.*, 2003). The statistical optimization technique through factorial design and response surface analysis satisfies this requirement. The use of factorial design is advantageous as it allows obtaining maximum information of the process by performing a reduced number of experiments (Dragone *et al.*, 2004). In this sense, central composite design (CCD), a useful methodology that is employed for sequential experimentation, provides reasonable amount of information for testing the goodness of fit from a fewer number of assays, therefore reducing the overall cost associated with the analysis (Sharma *et al.*, 2009). CCDs are $2k$ factorial treatment designs with $2k$ additional treatment combinations called axial points and n_0 replications at the centre of design. The property of rotatability developed for CCD requires the variance of estimated values to be constant at points equally distant from the centre of design (Djoudi *et al.*, 2007). Thus, our study evaluated the effect of initial concentrations of nitrogen and iron sources on starch accumulation in *C. vulgaris* using a central composite design (CCD) for two factors. Starch productivity and cell growth were also considered for optimization of the culture medium.

4.1.3 Material and Methods

4.1.3.1 Microorganism and culture conditions

Chlorella vulgaris (P12) obtained from the Culture Collection of Algal Laboratory

(CCALA, Czech Republic), was used for cultivation. All culture experiments were performed at 30 °C in 50 mL glass bubble column photobioreactors containing 40 mL of medium. The carbon source and agitation during cultivation of microalgae were supplied by bubbling CO₂-enriched air (2% v/v CO₂) through a tube (inner diameter, 2 mm) that ended near the bottom of the column, at an aeration rate of 0.833 vvm (volume of gases per volume of culture suspension per minute). Illumination was provided by four fluorescent lamps (Sylvania Standard F18 W) on one side of the photobioreactor, at an irradiance level of 70 μE m⁻² s⁻¹. The original growth medium (OGM) based on chemical components present in the microalgal biomass (Douskova *et al.*, 2009) had the following composition (mM): 18.32 (NH₂)₂CO, 1.74 KH₂PO₄, 0.83 MgSO₄·7H₂O, 0.79 CaCl₂, 0.11 FeNa-C₁₀H₁₂O₈N₂, 0.017 MnCl₂·4H₂O, 0.013 H₃BO₃, 0.009 ZnSO₄·7H₂O, 0.004 CuSO₄·5H₂O, 0.002 CoSO₄·7H₂O, 0.0001 (NH₄)₆Mo₇O₂₄·4H₂O and 0.0001 (NH₄)VO₃ in distilled water. Prior to the main experiments, microalgae were cultivated in the OGM to the late-exponential growth phase, then centrifuged at 6,000 rpm for 15 min, washed in distilled H₂O and re-suspended in culture medium with a nutrient composition defined by the experimental design. The starting algal density was the same in all experiments of the central composite design: 2 x 10⁷ cells mL⁻¹.

4.1.3.2 Biomass concentration

Microalgae and culture medium were withdrawn from the photobioreactors throughout the assay. Microalgal density was measured microscopically using an improved Neubauer hemocytometer. The growth rate of microalgae was complementarily measured by cell dry weight. Microalgae were harvested by centrifugation at 6,000 rpm during 15 min, washed with distilled H₂O, and dried at 105 °C until constant weight (24 h).

4.1.3.3 Starch determination

The concentration of microalgal starch at the beginning of the stationary growth phase was assayed by the hydrolysis of starch to glucose with amylolytic enzymes (α-amylase and amyloglucosidase) according to the procedure described previously in section 3.3.5. The productivity of starch was calculated by Eq. 4.1:

$$P_{Starch} (g L^{-1} day^{-1}) = \frac{(C_{Starch}(\%) \times W (g L^{-1}))}{T (day)} \quad \text{Eq. 4.1}$$

,where P_{Starch} is the starch productivity, C_{Starch} is the mass percentage of microalgal starch, W is the dry weight of microalgae, and T is the time of cultivation.

4.1.3.4 Statistical analysis of the design of experiments (DoE)

The influence of the initial concentration of nitrogen and iron sources (independent variables) on starch content (dependent variable) in *C. vulgaris* was assessed through a full central composite design (CCD) for two factors. The coding used for these variables is shown in Eq. (4.2).

$$v_i = \frac{(V_i - V_0)}{\Delta V_i} \quad \text{Eq. 4.2}$$

where v_i is the coded variable, V_i is the real value, V_0 is the real value at the central point and ΔV_i the step change value. Table 4.1 presents the range of real and coded values of the independent variables used in this study. The experimental results were fitted with a second-order polynomial equation by multiple regression analysis.

Table 4.1 Levels and range of the independent variables (initial concentration of nitrogen and iron sources) based on full CCD for two factors

Independent variable	Symbol	Range (g L ⁻¹) and levels		
		-1	0	+1
Initial nitrogen source (urea) concentration	X_1	0	1.1	2.2
Initial iron source (FeNa-EDTA) concentration	X_2	0	0.04	0.08

The quadratic mode for predicting the optimal point was expressed according to Eq. 4.3, where \hat{y}_i represents the response variable, b_0 is the interception coefficient, b_i , b_{ii} and b_{ij} are the regression coefficients, n is the number of studied variables, and X_i and X_j represent the independent variables. Where possible, the model was simplified by elimination of statistically insignificant terms.

$$\hat{y}_i = b_0 + \sum_{i=1}^n b_i X_i + \sum_{i=1}^n b_{ii} X_i^2 + \sum_{i=1}^{n-1} \sum_{j=i+1}^n b_{ij} X_i X_j \quad \text{Eq. 4.3}$$

The quality of the fitted polynomial model was expressed by the coefficient of determination R^2 , and its statistical significance was checked by the F-test. The

significance of the regression coefficients was tested by t-value. The statistical analysis of the results was carried out with the Experimental Design Module of the software Statistica 8.0 (Statsoft, USA). The model permitted evaluation of the effects of linear, quadratic and interactive terms of the independent variables on the chosen dependent variables.

4.1.4 Results and discussion

4.1.4.1 Starch accumulation in *C. vulgaris* P12

The experimental results obtained by the cultivation of *C. vulgaris* under different nutritional conditions based on the CCD for two factors, are shown in Table 4.2. It can be noted that *C. vulgaris* was able to accumulate starch under all the evaluated conditions; however, the amount of starch produced strongly varied according to the levels employed for the independent variables. The highest starch contents (41.0%, 40.5% and 39.8%) were obtained under nitrogen-deprived conditions (initial urea concentration = 0 g L⁻¹) and initial FeNa-EDTA concentrations of 0.04, 0 and 0.08 g L⁻¹, respectively (Runs 5, 1 and 2).

Table 4.2 Experimental matrix and results of microalgal starch accumulation (%) with coded levels of initial urea concentration (X_1) and initial FeNa-EDTA concentration (X_2) according to the 2² full-factorial CCD

Runs	Independent variables		Starch content (%)	
	X_1	X_2	Experimental	Predicted
1	-1	-1	40.5	38.2
2	-1	+1	39.8	38.2
3	+1	-1	9.9	5.9
4	+1	+1	3.2	5.9
5	-1	0	41.0	38.2
6	+1	0	11.5	5.9
7	0	-1	23.0	8.2
8	0	+1	8.4	8.2
9	0	0	4.8	8.2
10	0	0	5.6	8.2
11	0	0	5.9	8.2

The results obtained in our study were remarkable when compared with previously reported data, some of which are summarized in Table 4.3. As shown in this table, the microalgal starch content obtained in this study (41.0%) was the highest in comparison with those values reported in the literature resulting from the photoautotrophic cultivation of other *C. vulgaris* species.

This content of starch in *C. vulgaris* P12 was almost the double of the starch yield found in *Chlorella* sp. TISTR 8485 and *Chlorella* sp. TISTR 8593 (Rodjaroen *et al.*, 2007). It is worth mentioning that higher starch accumulations than those attained in our work were already reported by Hirano *et al.* (1997) and Choi *et al.* (2010) during the cultivation of *Chlamydomonas reinhardtii* species. However, the higher light intensity used for those experiments in comparison with that employed in our study could explain such differences (Table 4.3).

Table 4.3 Starch content of green microalgal species cultivated under photoautotrophic conditions

Species	Starch (%)	Illuminance (lx)	Irradiance ($\mu\text{mol m}^{-2} \text{s}^{-1}$)	References
<i>Chlorella</i> sp. TISTR 8485	21	-	60	Rodjaroen <i>et al.</i> , 2007
<i>Chlorella</i> sp. TISTR 8485	27	-	60	Rodjaroen <i>et al.</i> , 2007
<i>Chlorella</i> sp. TISTR 8593	22	-	60	Rodjaroen <i>et al.</i> , 2007
<i>Chlorococcum</i> sp. TISTR 8583	26	-	60	Rodjaroen <i>et al.</i> , 2007
<i>Chlorococcum</i> sp. TISTR 8973	17	-	60	Rodjaroen <i>et al.</i> , 2007
<i>Scenedesmus</i> sp. TISTR 8579	20	-	60	Rodjaroen <i>et al.</i> , 2007
<i>Scenedesmus</i> sp. TISTR 8982	13	-	60	Rodjaroen <i>et al.</i> , 2007
<i>S. acuminatus</i> TISTR 8457	7	-	60	Rodjaroen <i>et al.</i> , 2007
<i>S. acutiformis</i> TISTR 8495	16	-	60	Rodjaroen <i>et al.</i> , 2007
<i>S. acutus</i> TISTR 8447	19	-	60	Rodjaroen <i>et al.</i> , 2007
<i>S. arcuatus</i> TISTR 8587	13	-	60	Rodjaroen <i>et al.</i> , 2007
<i>S. armatus</i> TISTR 8591	15	-	60	Rodjaroen <i>et al.</i> , 2007
<i>S. obliquus</i> TISTR 8522	24	-	60	Rodjaroen <i>et al.</i> , 2007
<i>S. obliquus</i> TISTR 8546	23	-	60	Rodjaroen <i>et al.</i> , 2007
<i>Nannochlorum</i> sp. Tit-1	25	-	-	Hon-nami <i>et al.</i> , 1998
<i>Chlamydomonas</i> sp. YA-SH-1	30 - 39	-	-	Hon-nami <i>et al.</i> , 1998
<i>C. vulgaris</i> IAM C-534	37	15,000	-	Hirano <i>et al.</i> , 1997
<i>Chlamydomonas reinhardtii</i> UTEX2247	45	15,000	-	Hirano <i>et al.</i> , 1997
<i>Chlamydomonas reinhardtii</i> UTEX 90	44	-	450	Choi <i>et al.</i> , 2010
<i>C. vulgaris</i> P12	41	-	70	(This study)

^a Illuminance: the total luminous flux incident on a surface, per unit area.

^b Irradiance: the power per unit area of electromagnetic radiation at a surface.

High light intensities tend to enhance the production of polysaccharides in microalgae. Friedman *et al.* (1991) demonstrated that 0.6- and 3- fold increases in polysaccharide content were obtained in cultures of *Porphyridium sp.* and *Porphyridium aeruginum*, respectively, when the growth light intensity was raised from 75 to 300 $\mu\text{E m}^{-2} \text{s}^{-1}$. Tredici *et al.* (1991) reported that carbohydrate synthesis in *Spirulina platensis* grown outdoors was significantly higher on sunny days than on cloudy days. Due to the large differences observed in the amount of starch produced by *C. vulgaris* strain P12, a statistical analysis was carried out aiming at identifying which independent variable had significant influence on starch accumulation.

The statistical significance of the initial nitrogen and iron sources on the response variable (starch content) is given in Table 4.4.

According to this analysis, the initial urea concentration was the only variable with significant influence on starch content at 95% confidence level. Such effect was negative, indicating that starch content was enhanced by decreasing the initial concentration of nitrogen source. This result ratifies previous findings of Behrens *et al.* (1989), where starch accumulation in *C. vulgaris* increased under nitrogen-starvation conditions. The possible reason could be that under nitrogen deficiency/limitations the available nitrogen is utilized for synthesis of enzymes and essential cell structures. Any carbon dioxide subsequently fixed is therefore converted into carbohydrate or lipid rather than protein (Richardson *et al.*, 1969; Zittelli *et al.*, 2009).

Table 4.4 Effect estimates, standard errors and t-test for starch accumulation in *C. vulgaris* according to the 2² full-factorial central composite design

Variables and interactions	Estimated effects	Standard errors	t _{value}	p
X ₁	-32.267	4.559	-7.078	0.001*
X ₁ ²	27.700	7.016	3.948	0.011*
X ₂	-7.327	4.559	-1.607	0.169
X ₂ ²	6.660	7.016	0.949	0.386
X ₁ X ₂	-3.015	5.583	-0.540	0.612

X₁ = coded values of initial urea concentration; X₂ = coded values of initial FeNa-EDTA concentration

* Significant influence at 95% confidence level

The initial iron source concentration did not present a statistically significant effect on starch content, implying that chelated Fe(III) did not affect the starch accumulation

in *C. vulgaris*. Interaction effects among the studied variables were also not significant at 95% confidence level. After identification of the variable affecting the starch accumulation, the experimental values were fitted to a second-order equation (Eq. 4.4) obtained by multiple regression analysis. The coefficients of the proposed equation are given below:

$$\text{Starch content (\%)} = 8.220 - 16.133 X_1 + 13.850 X_1^2 \quad (R^2 = 0.94) \quad \text{Eq. 4.4}$$

where X_1 represents the coded level for initial urea concentration. The quality of the quadratic fit, simplified by elimination of statistically insignificant terms, was represented by the coefficient of determination R^2 . As can be noted, the model explains at least 90% of the dependent variable's variability ($R^2 > 0.90$). The high R^2 means that the quadratic model is able to represent values in the experimental region in an accurate manner. The values predicted by the model are displayed in Table 4.2 along with the observed values. Comparison of these data indicates that there is a good agreement between the predicted and experimental values for the proposed range. Therefore, the central composite design and regression analysis were effective in identifying the optimal conditions for maximum accumulation of microalgal starch for the different nutritional conditions. The relation between independent variables and starch content in *C. vulgaris* can be best visualized by examining the surface plot presented in Figure 4.1. Figure 4.1 clearly shows that decreasing initial urea concentration resulted in higher starch accumulation, with maxima values ($\geq 40\%$) being achieved under the minimum urea concentration (0 mg L^{-1}). These results implicate that the optimization using a response surface methodology based on the CCD can save the time and effort by the estimation of the variables that significantly influenced the starch accumulation in *C. vulgaris*.

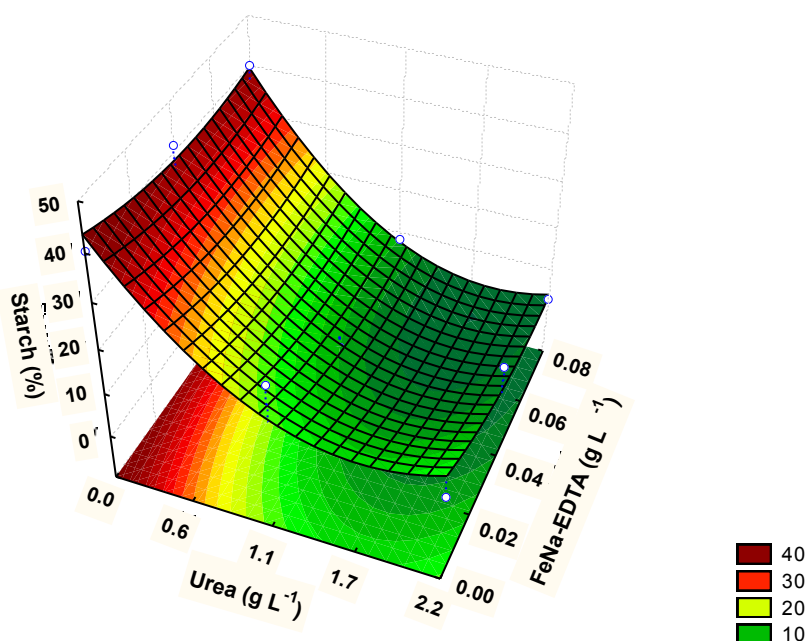


Figure 4.1 Response surface of starch accumulation in *C. vulgaris* as a function of initial urea concentration and initial FeNa-EDTA concentration.

4.1.4.2 Microalgal cell growth

To explore the influence of the initial nitrogen source concentration and initial chelated Fe(III) concentration on microalgal cell growth, the conditions of the experimental design which yielded higher starch content in microalgae (values of starch content >8.4%), were considered. The time-course profiles of cell growth obtained with different initial urea concentrations are depicted in Figure 4.2.

As shown in Figure 4.2 *a* and *b*, the cell growth of *C. vulgaris* improved significantly when urea concentration increased from 0 to 1.1 g L⁻¹ (0 – 18 mM, respectively). This result is compatible with previous research observations. For example, Hsieh and Wu (2009) reported that higher initial urea concentration (from 0.025 to 0.200 g L⁻¹) of the nutrient medium resulted in an increased biomass yield of *Chlorella sp.* However, cell growth did not show significant differences when urea concentration further increased from 1.1 to 2.2 g L⁻¹ (18 – 37 mM, respectively) (Figure 4.2 *b* and *c*).

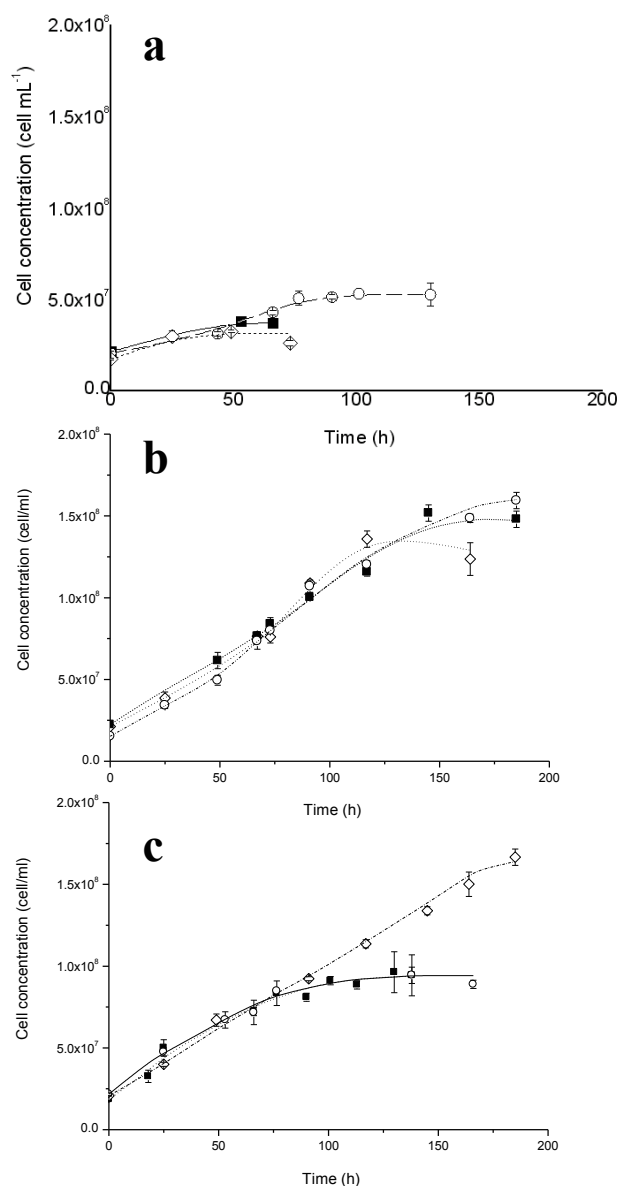


Figure 4.2 Cell growth of *C. vulgaris* with different urea concentrations (a) 0 g L⁻¹, (b) 1.1 g L⁻¹ and (c) 2.2 g L⁻¹. Initial FeNa-EDTA concentration: (■) 0 g L⁻¹, (◇) 0.04 g L⁻¹ and (○) 0.08 g L⁻¹.

Cell concentration reached the highest value at 1.1 and 2.2 g L⁻¹ initial urea concentration, which was 1.6 x 10⁸ cell mL⁻¹ when initial FeNa-EDTA concentrations were 0.08 and 0.04 g L⁻¹, respectively. Although final cell concentration rose from 3.7 x 10⁷ to 5.3 x 10⁷ cell mL⁻¹ when the concentration of FeNa-EDTA increased in the range 0 – 0.08 g L⁻¹ (0 – 190 μM) under nitrogen-deprived conditions (initial urea concentration = 0 g L⁻¹), there was no significant difference among them according to a Tukey's test ($p < 0.05$) (Figure 4.2 a). On the other hand, growth of microalgae was positively influenced as the initial concentration of the iron source was raised from 0 to

0.04 g L⁻¹, maintaining the initial urea concentration at the highest level (2.2 g L⁻¹) (Figure 4.2 c). The results described above suggest that the optimum concentration of urea required for the growth of microalgae was 1.1 g L⁻¹, while the lowest concentrations of nitrogen and iron sources led to the highest starch productivity (0.199 g L⁻¹ day⁻¹). These data imply that a two-stage cultivation process would likely be optimal for a high starch yield from *C. vulgaris* strain P12: a first cultivation stage using a N- and Fe-supplemented medium (initial urea and FeNa-EDTA concentrations of 1.1 and 0.08 g L⁻¹, respectively) to attain a maximum growth rate and concentration of biomass, followed by a second stage that involves cell cultivation in a N and Fe-free medium for a few days.

4.1.5 Conclusions

In this work, starch content of freshwater microalga *C. vulgaris* strain P12 reached up to 41.0% of dry cell weight, which was 8-fold higher than the control (central points of the experimental design). This result was achieved simply by altering the initial concentrations of urea and FeNa-EDTA in the culture medium. Since accumulation of starch occurred at nitrogen depletion conditions under which the cell growth was much slower than that observed during nitrogen supplemented cultivations, compromising between increasing starch content and cell growth will be necessary in order to attain high values of both biomass concentration and starch productivity.

4.1.6 References

- Behrens P., Bingham S., Hoeksema S., Cohoon D., Cox J., 1989. Studies on the incorporation of CO₂ into starch by *Chlorella vulgaris*. *J Appl Phycol* 1: 123–30.
- Behrens P.W., Kyle D.J., 1996. Microalgae as a source of fatty acids. *J Food Lipids* 3: 259–72.
- Brányiková I., Marsalková B., Doucha J., Brányik T., Bišová K., Zachleder V., Vítová M., 2011. Microalgae-novel highly efficient starch producers. *Biotechnol. Bioeng.*, 108: 766-776.
- Choi S. P., Nguyen M. T., Sim S. J., 2010. Enzymatic pretreatment of *Chlamydomonas reinhardtii* biomass for ethanol production. *Bioresour Technol* 101: 5330–6.
- Djoudi W., Aissani-Benissad F., Bourouina-Bacha S., 2007. Optimization of copper cementation process by iron using central composite design experiments. *Chem Eng J* 133: 1–6.
- Douskova I., Doucha J., Livansky K., Machat J., Novak P., Umysova D., 2009. Simultaneous flue gas

- bioremediation and reduction of microalgal biomass production costs. *Appl Microbiol Biotechnol* 82: 179–85.
- Dragone G., Fernandes B., Vicente A., Teixeira J.A., 2010. Third generation biofuels from microalgae. In: Vilas AM, editor. *Current research, technology and education topics in applied microbiology and microbial biotechnology*. Badajoz: Formatex Research Center; p. 1355–66.
- Dragone G., Silva D.P., e Silva J.B., 2004. Factors influencing ethanol production rates at high-gravity brewing. *Lebensm-Wiss u-Technol* 37: 797–802.
- Dragone G., Silva D.P., e Silva J.B., de Almeida Lima U., 2003. Improvement of the ethanol productivity in a high gravity brewing at pilot plant scale. *Biotechnol Lett* 25: 1171–4.
- Fernandes B., Dragone G., Teixeira J., Vicente A., 2010. Light regime characterization in an airlift photobioreactor for production of microalgae with high starch content. *Appl Biochem Biotechnol* 161: 218–26.
- Friedman O., Dubinsky Z., Arad S., 1991. Effect of light intensity on growth and polysaccharide production in red and blue-green rhodophyta unicells. *Bioresour Technol* 38: 105–10.
- Hirano A., Ueda R., Hirayama S., Ogushi Y., 1997. CO₂ fixation and ethanol production with microalgal photosynthesis and intracellular anaerobic fermentation. *Energy* 22:137–42.
- Hon-nami K., Kunito S., 1998. Microalgae cultivation in a tubular bioreactor and utilization of their cells. *Chin J Oceanol Limnol* 16: 75–83.
- Hsieh C-H, Wu W-T., 2009. Cultivation of microalgae for oil production with a cultivation strategy of urea limitation. *Bioresour Technol* 100: 3921–6.
- Hu Q., 2004. Environmental effects on cell composition. In: Richmond A, editor. *Handbook of microalgal culture: biotechnology and applied phycology*. Oxford: Wiley-Blackwell; p. 83–93.
- Richardson B., Orcutt D.M., Schwertner H.A., Martinez Cara L., Wickline Hazel E., 1969. Effects of nitrogen limitation on the growth and composition of unicellular algae in continuous culture. *Appl Microbiol* 18: 245–50.
- Rodjaroen S., Juntawong N., Mahakhant A., Miyamoto K., 2007. High biomass production and starch accumulation in native green algal strains and cyanobacterial strains of Thailand. *Kasetsart J (Nat Sci)* 41: 570–5.
- Rodolfi L., Zittelli G.C., Bassi N., Padovani G., Biondi N., Bonini G., 2009. Microalgae for oil: strain selection, induction of lipid synthesis and outdoor mass cultivation in a low-cost photobioreactor. *Biotechnol Bioeng* 102: 100–12.
- Sharma S., Malik A., Satya S., 2009. Application of response surface methodology (RSM) for optimization of nutrient supplementation for Cr (VI) removal by *Aspergillus lentulus* AML05. *J Hazard Mater* 164: 1198–204.
- Sunda W.G., Huntsman S.A., 1997. Interrelated influence of iron, light and cell size on marine phytoplankton growth. *Nature* 390: 389–92.
- Sunda W.G., Price N.M., Morel F.M.M., 2005. Trace metal ion buffers and their use in culture studies. In: Andersen RA, editor. *Algal culturing techniques*. Amsterdam: Elsevier; p. 35–63.
- Tredici M.R., Carlozzi P., Chini Zittelli G., Materassi R., 1991. A vertical alveolar panel (VAP) for

outdoor mass cultivation of microalgae and cyanobacteria. *Bioresour Technol* 38: 153–9.

4.2 Study of relationship between accumulation of starch and lipids in the microalga *Parachlorella kessleri* induced by nutrient depletion and their repletion

4.2.1 Abstract

Photosynthetic carbon partitioning into starch and neutral lipids, as well as the influence of nutrient depletion and repletion on growth and pigment content in the green microalga *Parachlorella kessleri* were studied. The study revealed that *P. kessleri* used starch as primary carbon and energy storage source, but the stress caused by the decrease of nutrients concentration makes the microalgae to shift the fixed carbon into reserve lipids as a secondary storage product. The depletion of minerals in diluted media inhibited both cellular division and growth, and very low content of chlorophylls and starch were found at the end of cultivations. On the other hand, the reserve lipids content was very high, approaching 30% of DW under given experimental conditions. All these parameters changed markedly after the transfer of cells from depleted into repleted mineral medium. Particularly, a tremendous decrease of lipid reserves from about 30% to 0% of DW was observed. The large lipid bodies decreased, fragmented into numerous small ones and finally disappeared. The cells recovered growth shortly after repleting medium and grew synchronously into large mother cells with high concentration of chlorophyll.

These findings indicate that a high content of lipid and starch reserves accumulated during starvation can serve as a sole source of energy and carbon for all recovering growth and reproductive processes. Additionally, these findings indicate that nutritional limitations can be used in *P. kessleri* cultivation as a very effective and cheap strategy to increase lipid productivity, for biofuel production.

Keywords: *Parachlorella kessleri*; *energy-rich reserves*; *nutrient depletion*; *nutrient repletion*

4.2.2 Introduction

During the photosynthetic process, microalgae accumulate significant quantities of lipids and carbohydrates over short periods of time that can be subsequently processed into biofuels, namely biodiesel and bioethanol (Fernandes *et al.*, 2012). Several studies have demonstrated that it is possible to control cell metabolism to produce high contents of energy-rich compounds, either starch (Brányiková *et al.*, 2011; Dragone, 2011) and/or lipids (Deng *et al.*, 2009; Chen *et al.*, 2011; Lee, 2011). Although the mechanisms of induction of lipid accumulation can be different from starch, there are several common approaches to induce both starch and lipid overproduction (Brányiková *et al.*, 2011; Li *et al.*, 2013). Lipid content could be increased by nitrogen or phosphate limitation (Liang *et al.*, 2009; Hsie *et al.*, 2009, Rodolfi *et al.*, 2009, Mutlu, *et al.*, 2011) high salt concentration (Takagi *et al.*, 2006), high iron concentration (Liu *et al.*, 2008) and the utilization of heterotrophic and mixotrophic culture conditions (Heredia-Arroyo *et al.*, 2010; Shen *et al.*, 2010).

Regarding starch, its accumulation can be induced by nitrogen depletion (Dragone *et al.*, 2011), sulphur depletion and high light intensity (Brányiková *et al.*, 2011), or high CO₂ concentration (Izumo *et al.*, 2007).

It was also shown that the algal strains appropriate for overproduction of starch are not usually suitable for overproduction of lipids and *vice versa* (Brányiková *et al.*, 2011; Li *et al.*, 2010).

The microalga *Parachlorella kessleri*, strain CCALA 255 is characterized by a high growth rate, tolerance to high temperature (40 °C), resistance to shear stress, low adhesion to bioreactor surfaces and low tendency to form aggregates. These are positive characteristics for its use in large-scale production bioreactors with potential for biofuel production (Li *et al.*, 2013). Under optimal conditions, is characterized by storage energy in the form of starch rather than lipids (Přibyl *et al.*, 2012; Li *et al.*, 2013). If untreated, the cultures propagated rapidly, producing large amounts of biomass in a relatively short time. The cells contained negligible lipid reserves (1 – 10 % of DW) but it is possible to induce hyperproduction of storage lipids in *P. kessleri* biomass by different methods (Přibyl *et al.*, 2012; Li *et al.*, 2013).

Under favourable growth conditions, algae synthesize fatty acids principally for esterification into glycerol-based polar lipids, the major constituents of intracellular membranes. However, under unfavourable environmental or stress conditions many algae alter their lipid biosynthetic pathways for the formation and accumulation of neutral lipids, mainly in the form of triacylglycerol (TAG) (Li *et al.*, 2011; Breuer *et al.*, 2012). These reserve neutral lipids (specially TAGs) are the preferred lipid class for most applications, mainly biodiesel production, since they can be readily converted to biodiesel through the existing oil refining processes (Hu *et al.*, 2008).

It is known that alteration in nutrient concentrations can modify both growth and secondary metabolism of microalgae (Behrens, 1996; Hsieh, 2009). Furthermore, microalgae growth depends not only on an adequate supply of essential macronutrient elements (carbon, nitrogen, phosphorus, silicon) and major ions (Mg^{2+} , Ca^{2+} , Cl^- , and SO_2^{-4}) but also on a number of micronutrient metals such as iron, manganese, zinc, cobalt, copper, and molybdenum (Sunda, 2005; Dragone, 2011). Thus, and since the reduction of nutrients is a simple and cheap method to increase lipid content in *P. kessleri* cells, we used in this work medium dilution (5 and 10 times) as a method to increase lipids content in *P. kessleri* cells.

However, the regulatory mechanism that controls the accumulation of starch and lipids in response to changes in growth conditions and the possible interaction between the two pathways, namely the interrelationship between storage and consumption of starch and lipids, remains unclear (Rawsthorne, 2002; Weselake *et al.*, 2009; Li *et al.*, 2010). According to Siaut *et al.* (2011) improving microalgal strain performances requires a good understanding of the mechanisms and regulations of carbon fixation, carbon allocation between biosynthetic pathways and induction by adverse growth conditions. Therefore, the aim of this work is to reveal the photosynthetic carbon partitioning into starch and neutral lipids, *i.e.* the temporal relationship between accumulation/consumption of starch and lipids, in *P. kessleri* cells, as a response to nutrient depletion and subsequent repletion. The profile of variation of starch and lipids concentration will be compared to the concentration of pigments and cell growth parameters in order to elucidate how photosynthetic carbon partitioning into starch and lipids is altered by different growth conditions, which are known to induce neutral lipids production.

4.2.3 Material and Methods

4.2.3.1 Strains and growth conditions

The green microalga *Parachlorella kessleri* (Krienitz *et al.*, 2004), strain CCALA 255, was provided by the Culture Collection of Autotrophic Organisms (CCALA) in Třeboň, Czech Republic (<http://www.butbn.cas.cz/ccala/index.php>). In the collection, the strain has been maintained on agar slants under irradiance of about $23 \mu\text{E m}^{-2} \text{s}^{-1}$, 12/12 h (light/dark) regime and at a temperature of 12 – 15 °C.

The cultures for experiments were prepared by transfer of algal inoculum from agar slant into liquid mineral medium and pre-cultured in laboratory photobioreactors (see section 4.2.3.2) at 30 °C in continuous light ($1,200 \mu\text{E m}^{-2} \text{s}^{-1}$) in order to obtain a sufficient concentration of cell for the experiments. A quantum/radiometer/photometer (LI-COR, Inc., U.S.A.) was used to measure light intensity.

The resulting cultures (“starting inocula”) were transferred into fresh complete mineral medium (medium 1) or 5-fold (medium 0.2) or 10-fold (medium 0.1) diluted medium in order to obtain an initial cell concentration of 0.2 g mL^{-1} . The control growth medium based on chemical components present in the microalgal biomass (Douskova *et al.*, 2009) had the following composition (mM): 18.32 $(\text{NH}_2)_2\text{CO}$, 1.74 KH_2PO_4 , 0.83 $\text{MgSO}_4 \cdot 7\text{H}_2\text{O}$, 0.79 CaCl_2 , 0.11 $\text{FeNa-C}_{10}\text{H}_{12}\text{O}_8\text{N}_2$, 0.017 $\text{MnCl}_2 \cdot 4\text{H}_2\text{O}$, 0.013 H_3BO_3 , 0.009 $\text{ZnSO}_4 \cdot 7\text{H}_2\text{O}$, 0.004 $\text{CuSO}_4 \cdot 5\text{H}_2\text{O}$, 0.002 $\text{CoSO}_4 \cdot 7\text{H}_2\text{O}$, 0.0001 $(\text{NH}_4)_6\text{Mo}_7\text{O}_{24} \cdot 4\text{H}_2\text{O}$ and 0.0001 $(\text{NH}_4)\text{VO}_3$ in distilled water. All culture experiments were performed at 30 °C.

4.2.3.2 Laboratory photobioreactor

The cultures were grown in 2.5 L glass plate cuvettes containing 2.0 L of suspension. Continuous irradiance of $1,200 \mu\text{E m}^{-2} \text{s}^{-1}$ on the photobioreactor surface was provided by a panel of light tubes Osram L 36W/830 Lumilux (Osram, Germany); a temperature of $30 \pm 0.5 \text{ °C}$ was maintained using a thermostatic water bath (Figure 4.3 A). Cultures were aerated vigorously with air enriched with 2% CO_2 (v/v) from a pressure can. Distilled water was daily added to the cultures to replenish that lost by evaporation.

4.2.3.3 *Biomass determination*

For dry weight determination, biomass was separated from the medium by centrifugation of 2 mL of the cell suspension in pre-weighed microtubes at 3,000 g for 5 min (Janetzki T23, Janetzki Maschinenbau, Germany); the sediment was dried at 105 °C for 12 h and weighed on an analytical balance (Sartorius 1601 MPB, Sartorius, Germany). Cell volume and concentration were measured using a Beckman Coulter Multisizer III (Coulter Corporation, Miami, FL) by diluting 10 - 50 µL of fixed (0.2 % glutaraldehyde) cell suspension into 10 mL of 0.9 % NaCl (w/v) electrolyte solution.

4.2.3.4 *Transfer to control medium*

After reaching the maximum concentration of total lipids in the cells, the original mineral medium (initially with 20 or 10% of the control nutrient concentration) was removed from the cell suspension by centrifugation and the cells were re-suspended in control complete mineral medium (medium 1).

4.2.3.5 *Starch quantification*

Starch content was quantified according to Brányiková *et al.*, (2011). Briefly, 10 mL of cell suspension was withdrawn and cells were recovered after centrifugation. The cell pellet was mixed with an equal volume of glass beads (0.1 mm of diameter) and 0.25 mL of distilled water and cells were disrupted by vortexing for 5 min (Vortex Genie 2, Scientific Industries, Inc., Bohemia, NY). Pigments in the cells were extracted using 80% ethanol pre-warmed at 50 °C and cell pellet containing starch was suspended in 0.15 mL of distilled water after centrifugation. For starch hydrolysis, the cell suspension was kept in a water bath at 100 °C for 15 min and then mixed with 0.25 mL of 60% perchloric acid after cooling down. After stirring the suspension for 15 min, the suspension was mixed with 0.6 mL of distilled water and centrifuged. Subsequently, 0.4 mL of the supernatant was mixed well with 2 mL of anthrone solution (0.2 g of anthrone in 100 mL of 75% H₂SO₄). The mixture was kept in a water bath at 100 °C for 8 min. It was cooled to room temperature and the absorbance at 625 nm was measured using a spectrophotometer (Shimadzu UV-1800 S, Shimadzu, Japan). Calibration was carried out simultaneously using glucose as the standard. The experiments were

repeated three times.

4.2.3.6 Lipid quantification

Visualization of lipids using Nile Red fluorescence

Intracellular lipid droplets were stained using the neutral lipid specific dye, Nile Red (9-diethylamino-5H-benzo(a)phenoxazine-5-one), following the protocol described earlier (Eltgroth *et al.*, 2005) with slight modifications. Briefly, 1 mL of the cell suspension was fixed with glutaraldehyde at a final concentration of 0.25% (v/v) and stained with 4 μ L of Nile Red (Sigma, N3013) stock solution (0.5 mg mL⁻¹ of acetone) that was stored in the dark at 48 °C. Samples were observed after 10 min using an epifluorescence OLYMPUS BX 51 microscope equipped with the filter combination U-MNU2 (360–370 nm excitation and > 420 nm emission). Photomicrographs were taken with a digital camera OLYMPUS DP72 and processed using Adobe Photoshop 7.

Nile Red fluorescence determination of lipids

The algal suspension was fixed with glutaraldehyde to a final concentration of 0.25% (v/v) and loaded into wells (100 μ L per well) of a 96-well plate. 4 μ L of Nile Red solution were added to wells, fluorescence intensity was measured using a 96-well plate luminometer (Tecan infinite 200, Switzerland) with the following filters: excitation 485 nm (bandwidth 20 nm), emission 595 nm (bandwidth 10 nm). Glyceryl trioleate (Sigma, T7140) was used as lipid standard to obtain a calibration curve.

Gravimetric lipid determination

Algal cultures were harvested by centrifugation at 5,000 rpm for 5 min. Cell pellets were stored frozen at -20 °C. Before analysis pellets were dried at 50 °C for at least 3 days. Lipids were extracted with 100 mL chloroform in a Soxhlet extractor from approximately 0.03 g dry cells. The dry biomass was grounded to powder and then put in the thimble of the Soxhlet extractor for extraction with reflux at 100 °C for 4 h. At the end of extraction, the extractant was distilled at 60 °C to evaporate chloroform, followed by drying the residue at 40 °C for 1 h and weighing after cooling to room temperature. Lipid content was calculated by dividing the residue weight by the dry weight before extraction.

4.2.3.7 Determination of pigments content

The algal suspension (10 mL) was centrifuged at 4,000 g for 3 min and the sediment was collected. Phosphate buffer, 7.7 pH (1 mL), a pinch of MgCO_3 , and Zircon beads (500 μL , size 0.7) were added to the sediment, which was then disintegrated by vortexing (Vortex Genie 2, Scientific Industries, Inc., Bohemia, NY) for 10 min. Acetone (4 mL, 100%) was added, mixed well and centrifuged at 4,000 g (Janetzki T23, Janetzki Maschinenbau, Germany) for 3 min. The supernatant was drained into a calibrated test tube using an exhaustor/air pump, closed with a stopper and left standing in a dark-block. Another 4 mL of acetone (80%) were added to the sediment, mixed well and centrifuged at 4,000 g for 3 min. Using an exhaustor/air pump, the supernatant was drained off to the same calibrated test tube used in the preceding step and topped up with 80% acetone up to 10 mL. Absorbances at 750, 664, 647, 470, 450 nm were measured in a 1 cm path length cuvette using a spectrophotometer (Shimadzu UV-1800 S, Shimadzu, Japan). Calculation of chlorophyll content was based on absorbances at different wavelengths and was carried out according to equations published previously (MacKinney, 1941).

4.2.4 Results and discussion

Cultures of the microalgae *Parachlorella kessleri* were grown in complete (medium 1), five-fold (medium 0.2) and ten-fold (medium 0.1) diluted mineral medium. The microalgae cells were, after depleting medium, transferred into complete mineral medium.

During two independent experiments the following parameters were monitored: chlorophyll (a+b) (pg cell^{-1} and mg L^{-1}), cell number (per mL), mean cell volume (μm^3), dry weight (g L^{-1}); relative starch content (% of dry weight (*DW*)); relative total lipid content (% of *DW*) and reserve (or neutral) lipids content (% of *DW*).

4.2.4.1 Effect of depleting and repleting of mineral medium on chlorophyll content

The green colour of microalgal suspension seen at the beginning of the experiments (Figure 4.3 A) had a yellowish appearance after 7.5 days of growth in 10-fold diluted

medium (medium 0.1) and 1 day later also in 5-fold diluted medium (medium 0.2) (Figure 4.3 B, cuvettes 0.2 and 0.1), while culture in complete medium became dark-green during continuous growth and chlorophyll synthesis (Figure 4.3 B, cuvette 1). These colour changes, from dark green to yellow-green, observed in the photobioreactors in which the nutrient concentration was 5 and 10 times lower than in the control medium, are in agreement with results obtained in previous studies with nutrient limitation (Richardson *et al.*, 1969; Rodolfi *et al.*, 2009; Siaut *et al.*, 2011).

When the cells, cultivated in the media 0.2 and 0.1, were transferred to complete medium (medium 1), it was possible to observe that the yellowish colour of cultures (Figure 1B), which occurred as an effect of depleting media, changed into a green colour within 24 h (Figure 4.3 D).

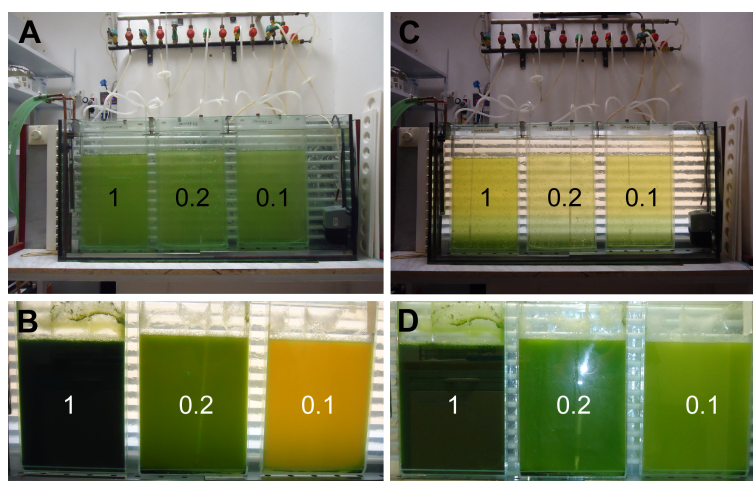


Figure 4.3 Laboratory photobioreactor used for the experiments. **A:** Cultures at the beginning of experiment; **B:** Cultures after 7.5 days of the growth. **C:** Cultures were transferred into complete mineral medium and diluted to have the same initial biomass concentrations. **D:** Recovery from starvation in complete mineral medium. **Cuvettes in Figure 1A and 1B - 1:** complete mineral medium; **0.2:** 5-fold diluted medium; **0.1:** 10-fold diluted medium. **Cuvettes in Figure 1C and 1D - 1:** complete mineral medium with cells from previous complete mineral medium; **0.2:** complete mineral medium with cells cultivated in 5-fold diluted medium; **0.1:** complete mineral medium with cells cultivated in 10-fold diluted medium

The determination of chlorophyll content (Figure 4.4) confirms the visual observations made in Figure 4.3. In microalgae cells cultivated in medium 0.2 (Figure 4.4 A) chlorophyll content increased during the first 0.5 day to approximately 3.6 pg cell^{-1} , whereas cells cultivated in medium 0.1 (Figure 4.4 B) reached in the same time

period 0.8 pg of chlorophyll per cell. The low initial concentration of chlorophyll in both situations is probably due to the conditions under which the inoculum was cultivated: high light intensity ($1,200 \mu\text{E m}^{-2} \text{s}^{-1}$) and batch cultivation (which leads to the continuous decrease of nutrient concentration in the medium). In both situations chlorophyll concentration continuously decreased to a very low value (about 0.2 pg cell^{-1}), during the period of cultivation. This low value was attained after about 7 days (Figure 4.4 A) in medium 0.2 (5-fold diluted medium) and after 5 days (Figure 4.4 B) in medium 0.1 (10-fold diluted medium).

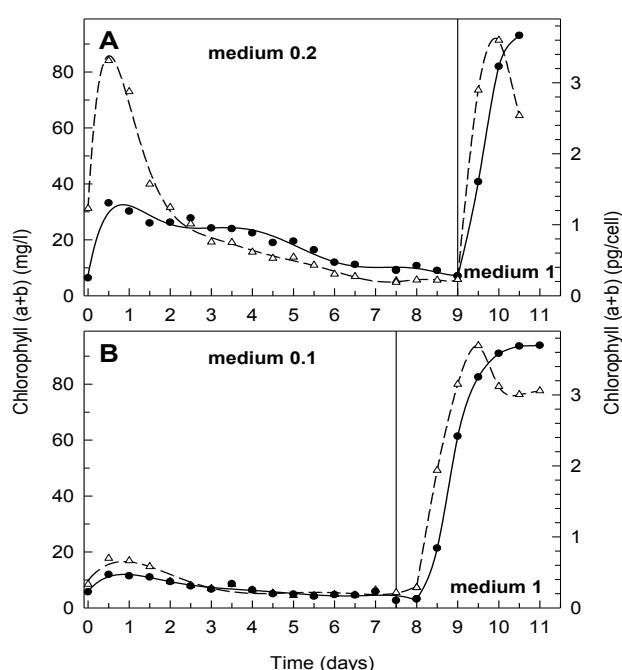


Figure 4.4 Changes in chlorophyll content in cultures of *Parachlorella kessleri* cultivated in medium 0.2 (Figure 2 A) and medium 0.1 (Figure 2 B) and then replaced in medium 1 (complete mineral medium).

The chlorophyll content is expressed in mg L^{-1} (●) and in pg cell^{-1} (△).

The fact that in the medium 0.2 a higher chlorophyll concentration was achieved in the first 0.5 day is probably explained by the higher initial nutrient concentration (two-fold concentrated) compared with medium 0.1. This difference in nutrient concentration of the medium is also the reason why cells cultivated in medium 0.1 reached the minimum chlorophyll concentration (0.2 pg cell^{-1}) two days before the cells cultivated in medium 0.2.

This decrease in pigment content, known as chlorosis, was also reported in several

previous studies as a result of nutrient limitation or depletion (mainly nitrogen limitation), and high light intensity in different microalgae species, such as *Neochloris oleoabundans* or *Cryptomonas maculate* (Rhiel *et al.*, 1985; Falkowski and LaRoche, 1991; Turpin, 1991; Mandalam and Palsson, 1998; Klok *et al.*, 2013). Rodolfi *et al.* (2009) refer that under nitrogen deprivation, at suitable irradiances, photosynthesis continues, although at a reduced rate, which explains the reduction in photosynthetic machinery. Also low magnesium concentration can contribute to these results since it is known that microalgae cells need magnesium to synthesize chlorophyll (Mandalam and Palsson, 1998). Bogorad (1962) reported that microalgae cells loose chlorophyll when grown in magnesium deficient cultures. Since, in this study, we use 5 and 10 fold diluted medium it is very probable that the decrease in chlorophyll content was due to low nutrient concentration, mainly nitrogen and magnesium. Ledford and Niyogi (2005), justify the decrease in pigment concentration with the nutrient shortage that disturbs the anabolic processes in the cells that need these nutrients. Subsequently, the energy demand for anabolism will decrease, as the need for energy supply through photosynthesis. This, ultimately, will lead to over-reduction of the photosynthetic machinery.

The transfer of depleted microalgae cells into complete medium (medium 1) (Figure 4.4 A and B) caused very fast synthesis of chlorophylls from values about 0.3 pg cell^{-1} to more than ten-fold higher content (3.6 pg cell^{-1}) within 1 day in both situations. These findings are matching those reported by Siaut *et al.* (2011) in nitrogen-deprived strains of *Chlamydomonas reinhardtii*.

4.2.4.2 Effect of depleting and repleting of mineral medium on cell number, cell size, and dry weight

Data shown in Figure 4.5A represent a typical synchronized microalgal growth, taking place under favourable growth conditions. Observing the dry weight (*DW*) and cell number (*No*) curve we can conclude that, during the first 6.5 days there was no limitation to cell growth. After this period, it is possible to check stagnation in *DW* and decrease in *No*. Regarding the mean cell volume (*V*) and its relationship with *DW* and *No*, it is possible to observe that cells are growing synchronously to the size of mother cells and then divided into daughter cells, which can be concluded by the sharp increase

of V in 3 different moments. These increases in V occur in periods in which N_0 is stable, while when N_0 increases a decrease in V is observed. This is because large-volume mother cells are divided into daughter cells. The results observed in Figure 4.5A are in agreement with the results presented by Mandalam and Palsson (1998), using *C. vulgaris*.

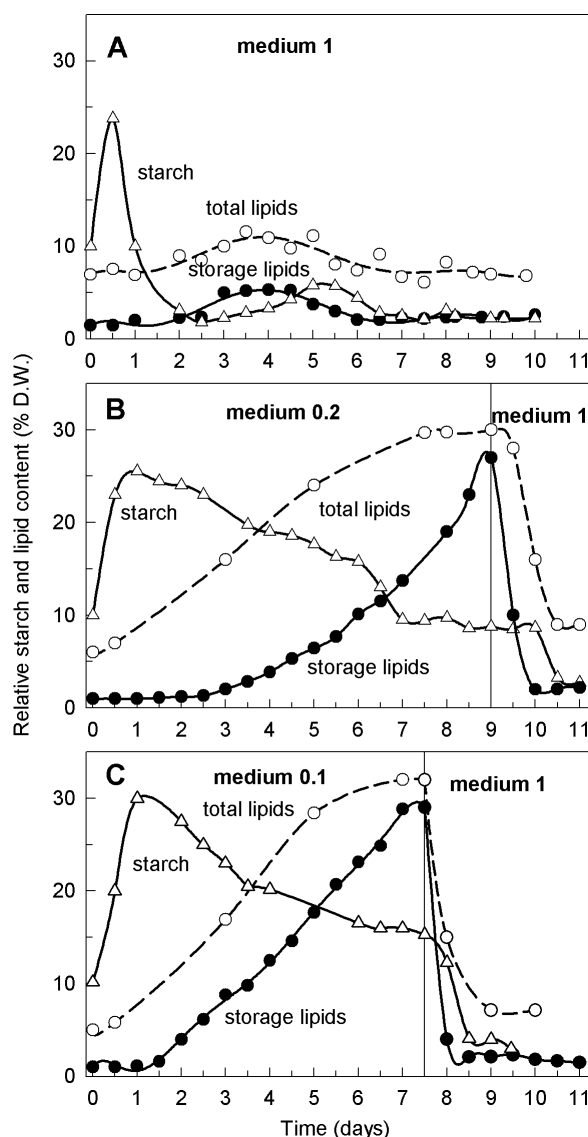


Figure 4.5 Changes in dry weight (DW) (\bullet), mean cell volume (V) (\circ) and cell number (N_0) (Δ) in cultures of *Parachlorella kessleri*. Cultures were grown either in complete mineral medium (medium 1) (A); 5-fold diluted medium (medium 0.2) (B) and; 10-fold diluted medium (medium 0.1) (C). After 9 days (B) or 7.5 days (C) cells were transferred into complete mineral medium (medium 1).

A relatively high growth rate illustrated by increases in both N_0 and DW occurred during the first 4 and 2 days in both 5-fold (medium 0.2) (Figure 4.5 B) and 10-fold

(medium 0.1) (Figure 4.5 C) diluted cultures. Thereafter, no or very low increase of N_0 indicated blockage of cellular division. Several authors report that growth continues very slowly for some time in a medium which is depleted or with deficient concentrations of nutrients, namely nitrogen or sulphur, and then the cell division is blocked after a short period in these conditions (Hase, 1962; Richardson *et al.*, 1969; Mandalam and Palsson, 1998). No remarkable changes in V curve (Figure 4.5 B and C) indicated that the cultures were asynchronous during this part of the experiment.

The transfer of *P. kessleri* cells cultivated in diluted medium into complete medium (medium 1) remarkably affected all measured growth parameters (Figure 4.5 B and C). Rapid increase of DW within 0.5 days was followed in the subsequent 0.5 days by an increase of cell number. The sharp increase of V concomitantly with DW and its decrease when cell division started indicated that cells started growing synchronously to the size of mother cells and then divided in to daughter cells.

4.2.4.3 *Effect of depleting and repleting of mineral medium on starch and lipids content*

In order to monitor the photosynthetic carbon flow into different storage compounds, starch, total lipid and reserve lipids content of *P. kessleri* were measured under the culture conditions previously described. To distinguish between total lipid cellular content and those accumulated as reserves in lipid droplets, gravimetric methods using Soxhlet apparatus were used for determination of total lipid content while fluorometric measurement of lipid droplets stained by Nile Red was applied for determination of neutral or reserve lipids.

In the control, *P. kessleri* cells grown in complete mineral medium (medium 1) accumulated basal amounts of starch (2 - 5% of DW), total lipids (6 - 10% of DW) and reserve lipids (2 - 5% of DW) (Figure 4.6 A). Lipid content has not changed significantly over the 10 days of cultivation, however, starch had a very significant increase in the first 0.5 days. This increase in starch concentration is concomitant with a sharp increase in the mean cell volume (V), and stagnation of cell number (N_0) shown in Figure 4.5 A. Changes in the parameters N_0 , V , DW (Figure 4.5 A), and the content of storage materials (Figure 4.6 A), indicate that cells were synchronized and, in an

initial phase (first 0.5 days), there was no cell multiplication and cells accumulated large amounts of starch (25% of *DW*), which resulted in a large increase in cell volume. Between 0.5 and day 1 cells began to multiply, which resulted in a large decrease in cell volume and starch content. These findings are in agreement with the variations in starch content in *C. vulgaris* verified by Brányiková *et al.* (2011), where relative starch content reached a maximum just prior to the first cell division (first 10 h), and when the cell division started the relative starch content decreased. Since the nutrients concentration in the medium were enough to prevent cell stress, from 1.5 days there were no major changes in the concentrations of storage materials (Figure 4.6 A).

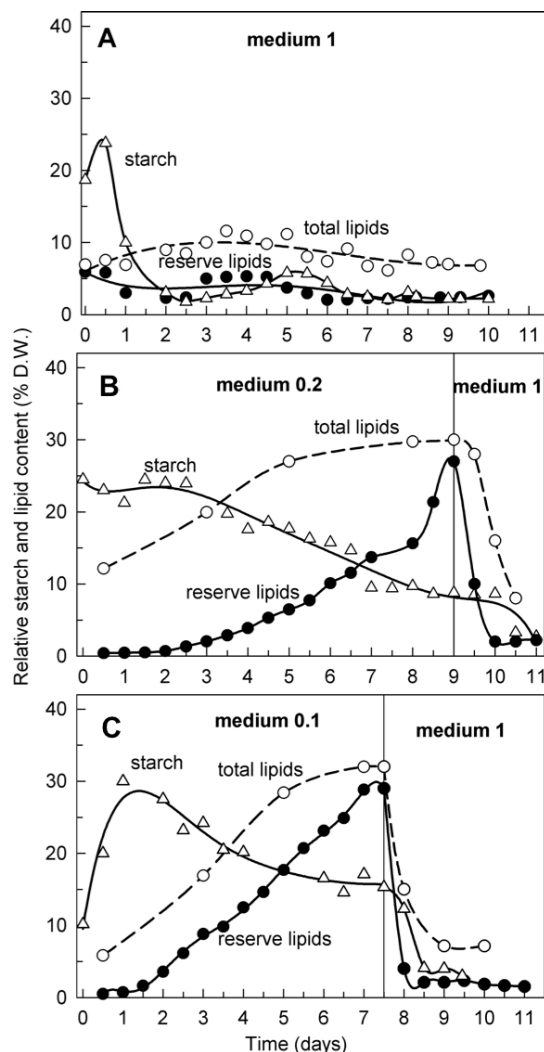


Figure 4.6 Changes in relative starch (Δ), total lipid (\circ) and, reserve (or neutral) lipid (\bullet) content in cultures of *Parachlorella kessleri*. Cultures were grown either in complete mineral medium (medium 1) (A) or 5-fold (medium 0.2) (B) or 10-fold (medium 0.1) (C) diluted medium. After 9 days (B) or 7.5 days (C) cells were transferred into complete mineral medium (medium 1).

Figure 4.6 B shows that in cells grown in 5-fold diluted medium (medium 0.2) there is a quite different pattern in starch and lipids content variation compared to that observed in cells grown in medium 1 (Figure 4.6 A). In cells cultivated in medium 0.2 starch content remained relatively constant until day 3. As noted in Figure 4.5 C, microalgae cells were not synchronized, which may explain the lack of peaks in starch content, unlike observed in Figure 4.6 A. While in cells cultured in medium 1, starch content begins to decrease after the first cell division, the cells cultured in medium 0.2 maintain very high levels of starch (25% of *DW*) which remains practically constant until day 3, even after cell division has started. Likewise, the reserve lipids content

remains constant at very low levels until day 3. From day 3 onwards the concentration of reserve lipids increases continuously up to day 9, while starch content follows the opposite path until day 7, remaining almost constant until day 9 (Figure 4.6 B).

The high starch content at an initial stage, which decreases over time with a concomitant increase in the content of reserve lipids, is in agreement with the results and explanations of several authors regarding photosynthetic carbon flow into these two storage compounds. Mizuno *et al.* (2013) observed, under sulphur-deficient conditions, a sequential accumulation of starch and lipid in *Chlorella* and *Parachlorella* species. Li *et al.* (2011) cultivated *Pseudochlorococcum* under nitrogen limited conditions, reporting that this microalgae used starch as a primary storage product for the photosynthetically assimilated carbon while little or no neutral (or reserve) lipids were found in *Pseudochlorococcum* cells. These authors also report that, after nitrogen depletion, starch content decreased while neutral lipids rapidly increased. These results suggest that *Pseudochlorococcum* (in Li *et al.* (2011) study) and *Parachlorella kessleri* (in this study) used starch as a primary carbon and energy storage product. Li *et al.* (2011) found that as nitrogen was depleted for an extended period of time, cells shift carbon partitioning into neutral lipid as a secondary storage product. Roessler (1990) explains this shift between the primary carbon storage product (starch) to a secondary storage product (reserve lipids), by the fact that these reserve lipids are composed primarily of saturated and monounsaturated fatty acids that can be efficiently packed in the cells and generate more energy than starch upon oxidation, thus constituting the best reserve for rebuilding the cell after stress conditions.

In our study, *P. kessleri* cells shift from starch to lipids after 3 days of cultivation (Figure 4.6 B), which may mean that the concentration of nutrients (particularly nitrogen) in the third day was already at levels that induce a change in carbon partitioning mechanism. Li *et al.* (2011) also mentioned that partial inhibition of starch synthesis and degradation enzymes resulted in a decrease of neutral lipids content, indicating that conversion of starch into neutral lipids may contribute to overall neutral lipids accumulation.

Although the hypothesis that starch is converted into reserve lipids is in agreement with the results shown in Figure 4.6 B, this hypothesis seems not to be the only

explanation for the large increase in reserve lipids content under conditions of nutritional limitation and/or depletion. In Figure 4.6 B it is possible to detect a large increase in reserve lipids content between days 7 and 9, however, in these days the starch content remains practically constant, which suggests that reserve lipids are not only produced at the expense of starch. However, it is known that there are several pathways for TAGs (major reserve lipids) synthesis by microalgae and the relative contribution of individual pathways to overall TAGs formation depends on environmental and culture conditions. Alternative pathways that convert membrane lipids to TAGs have been demonstrated in plants and yeast, but these have not yet been found in microalgae (Dahlqvist *et al.*, 2000; Arabolaza *et al.*, 2008; Zhu *et al.*, 2013). Additionally, cells cultivated in medium 0.2 revealed a large increase in reserve lipids content between days 8 and 9, becoming the larger fraction of lipids present in *P. kessleri* cells, i.e. the total lipids content stabilized and the reserve lipids content continued to increase until it becomes a very considerable fraction of all lipids present in the cells. Rodolfi *et al.* (2009) reveal that there are also indications that cellular lipids accumulation during stress conditions may derive from newly fixed carbon. The capacity for *de novo* lipid synthesis seems a characteristic of some oleaginous microalgae which, when grown under stress conditions, channel the excess of carbon and energy into storage lipids (mainly TAGs).

The results presented in Figure 4.6 B suggest that reserve lipids accumulation can be due to a combination of the three previously proposed pathways: *i.e.* part of reserve lipids are obtained from starch conversion, while the other part is obtained from conversion of membrane lipids or *de novo* lipid synthesis.

After placing the cells in complete medium (medium 1) a sharp decline in the levels of lipids (in days) and starch (two days) content was observed. The values of starch and lipid content tend to the final values observed in Figure 4.6 A, where the cells were grown in complete medium. This large decrease in reserve compounds coincides with a large increase observed in *No*, *DW* and *V* (Figure 4.5 B) and an increase in chlorophyll concentration (Figure 4.4 B). These results indicate that after cultivation in a depleted medium, *P. kessleri* cells are able to recover their characteristics if they are placed in a complete mineral medium.

The variation of starch and lipids content in *P. kessleri* cells cultivated in 10-fold diluted medium (medium 0.1) (Figure 4.6 C) exhibit very similar behaviour to the one seen in Figure 4.6 B. However, the time scale in which the variations take place is quite different. In this case the decrease of starch and an increase of reserve lipids content started on day 1.5, *i.e.* 1.5 days earlier than in the medium 0.2. This result indicates that, since the initial nutrient concentration in medium 0.1 is 2 times lower, the nutrient limitation is felt earlier than in medium 0.2.

The decrease in starch content and the increase in reserve lipids content are much sharper than the one observed in medium 0.2 cultivation. After day 1.5 the starch content decreases steadily until day 6 and lipid content increases continuously during the 7.5 days of cultivation. The final contents of starch and lipids are quite similar to those seen in medium 0.2. Although, using medium 0.1 it is possible to obtain the same amount of reserve lipids content (about 30% of *DW*) in fewer days, the biomass obtained with medium 0.2 cultivation (about 6 g L⁻¹) compared with that obtained with medium 0.1 (3.5 g L⁻¹) leads to a higher lipid productivity (0.20 against 0.14 g of reserve lipids L⁻¹ d⁻¹) of cells cultivated on medium 0.2.

Similarly to medium 0.2 (Figure 4.6 B), in medium 0.1 starch content remains constant in the period of greatest increase in reserve lipids content, and wherein the amount of total lipids is constant. When the amount of total lipids becomes constant, the lipids accumulated in lipid bodies as reserve continues to increase and becomes the major lipid constituent of cells (Figure 4.7 A). After placing the cells in medium 1 (Figure 4.6 C), the evolution of analysed parameters was very similar to that shown in Figure 4.6 B.

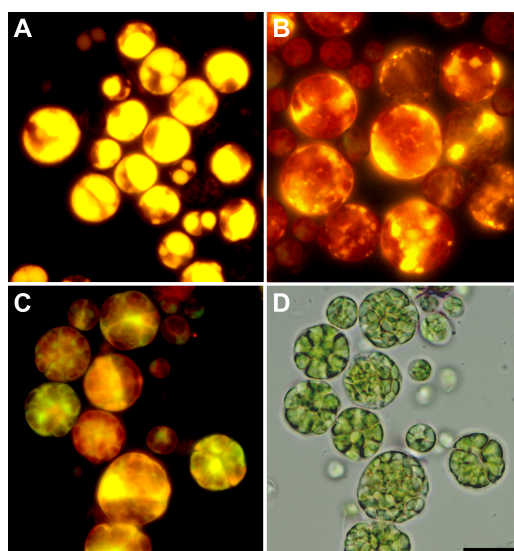


Figure 4.7 Fluorescence (A-C) and light microscopy (D) photomicro-graphs of the cell population of the microalga of *Parachlorella kessleri* initially grown in medium 0.1. Lipid bodies were stained using Nile Red (yellow). A: Cells grown for 7.5 days in 10-fold diluted mineral medium, B: 1 day after transfer the cells into complete mineral medium, degradation of lipid bodies started. The cells grew more or less synchronously to a large size. C, D: 2 days after transfer into complete mineral medium. The large cells with several small oil bodies (C) started to divide (D). Scale bar = 10 μm .

Cells recovered growth shortly after repleting medium (Fig. 4.5 B and C) and grew synchronously into large mother cells (Figure 4.7 B). Thereafter, they divided synchronously and the large lipid bodies decreased, fragmented into numerous small ones and finally disappeared (Figure 4.7 B and C).

As described by Přebyl *et al.*, (2013) the recovery of growth and cell division in complete medium can occur even in dark conditions. This finding indicates that a high content of lipid and starch reserves accumulated during starvation can serve as an exclusive source of energy and carbon for all recovering growth and reproductive processes.

The time during which cells retain their lipid content is a very important economic parameter in microalgae large-scale production. If the cells are capable of maintaining their lipid content for long periods of time, this allows cells storage thus reducing processing costs. In order to test this hypothesis, cells cultivated in 10-fold diluted medium (medium 0.2) were placed in a transparent vessel and allowed to sediment for 22 days. The results of the total lipid content are shown in Table 4.5.

Table 4.5 Evolution of total lipid content in cells kept in sedimentation vessel, for 22 days

N° of days	Total lipid content (% DW)
1	32.1 \pm 0.8
8	31.1 \pm 2.0
15	30.4 \pm 2.1
22	32.0 \pm 1.6

The results demonstrate that it is possible to store cells until 22 days without a

decrease in lipid content, which may reveal a very interesting element for the economic viability of the process.

4.2.5 Conclusions

Parachlorella kessleri cells use starch as a primary carbon and energy storage source under the first days of cultivation, but the stress caused by the decrease of nutrients concentration lead microalgae to shift the fixed carbon into reserve lipids as a secondary storage product. The cells recovered growth shortly after repleting medium and grew synchronously into large mother cells with high concentration of chlorophyll. These findings indicate that a high content of lipid and starch reserves accumulated during starvation can serve as a sole source of energy and carbon for all recovering growth and reproductive processes. Additionally, these findings indicate that nutritional limitation can be used in *P. kessleri* cultivation as a very effective strategy to increase lipid productivity for biofuel production.

4.2.6 References

- Arabolaza A., Rodriguez E., Altabe S., Alvarez H., Gramajo H., 2008. Multiple pathways for triacylglycerol biosynthesis in *Streptomyces coelicolor*. *Appl. Environ. Microbiol.* 74: 2573–2582.
- Behrens P. W., Kyle D. J., 1996. Microalgae as a source of fatty acids. *J. Food Lipids* 3: 259-272.
- Bogorad L., 1962. Chlorophylls., In: R. A. Lewin (ed.), *Physiology and biochemistry of algae*. Academic Press, New York, pp. 385–408.
- Brányiková I., Marsalková B., Doucha J., Brányik T., Bišová K., Zachleder V., Vítová M., 2011. Microalgae-novel highly efficient starch producers. *Biotechnol. Bioeng.*, 108: 766-776.
- Breuer G., Lamers P. P., Martens D. E., Draaisma R. B., Wijffels R. H., 2012. The impact of nitrogen starvation on the dynamics of triacylglycerol accumulation in microalgae. *Bioresour Technol*, 124: 217-226.
- Chen C.-J., Yeh K.-L., Aisyah R., Lee D.-L., Chang J.-C., 2011. Cultivation, photobioreactor design and harvesting of microalgae for biodiesel production: A critical review. *Bioresour. Technol.*, 102: 71–81.
- Dahlqvist A., Stahl U., Lenman M., Banas A., Lee M., Sandager L., Ronne H., Szymne H., 200. Phospholipid:diacylglycerol acyltransferase: An enzyme that catalyzes the acyl-CoA-independent formation of triacylglycerol in yeast and plants. *Proc. Natl. Acad. Sci. USA.* 97: 6487–6492.
- Deng X., Li Y., Fei X., 2009. Microalgae: A promising feedstock for biodiesel. *African J. Microbiol. Res.*, 3: 1008–1014.

- Douskova I., Doucha J., Livansky K., Machat J., Novak P., Umysova D., Zachleder V., Vitova M., 2009. Simultaneous flue gas bioremediation and reduction of microalgal biomass production costs. *Appl. Microbiol. Biotechnol.*, 82: 179–185.
- Dragone G., Fernandes B.D., Abreu A.P., Vicente A.A., Teixeira J.A., 2011. Nutrient limitation as a strategy for increasing starch accumulation in microalgae. *Appl. Energy* 88: 3331-3335.
- Eltgroth M. L. Watwood, R. L. Wolfe, G. V., 2005. Production and cellular localization of neutral long-chain lipids in the haprophyte algae *Isochrysis galbana* and *Emiliania huxleyi*. *J. Phycol.*, 41: 1000-1009.
- Falkowski P. G., LaRoche J., 1991. Acclimation to spectral irradiance in algae. *J Phycol*, 27, 8-14.
- Fernandes B.D., Dragone G.M., Teixeira J.A., Vicente A.A., 2010. Light regime characterization in an airlift photobioreactor for production of microalgae with high starch content. *Appl. Biochem. Biotechnol.*, 161: 218-26.
- Fernandes B., Dragone G., Abreu A. P., Geada P., Teixeira, J., Vicente A., 2012. Starch determination in *Chlorella vulgaris* — a comparison between acid and enzymatic methods. *J. Appl. Phycol.*, 24: 1203-1208.
- Hase E., 1962. Cell division. In: R. A. Lewin (ed.), *Physiology and biochemistry of algae*. Academic Press, New York, pp. 617–624
- Heredia-Arroyo T., Wei W., Hu B., 2010. Oil accumulation via heterotrophic/mixotrophic *Chlorella protothecoides*. *Appl. Biochem. Biotechnol.*, 162: 1978-1995.
- Hsieh C.-H., Wu W.-T., 2009. Cultivation of microalgae for oil production with a cultivation strategy of urea limitation. *Bioresour. Technol.*, 100: 3921–3926.
- Hu Q., Sommerfeld M., Jarvis E., Ghirardi M., Posewitz M., Seibert M., Darzins A., 2008. Microalgal triacylglycerols as feedstocks for biofuel production: perspectives and advances. *Plant Journal* 54: 621–639.
- Izumo A., Fujiwara S., Oyama Y., Satoh A., Fujita N., Nakamura Y., Tsuzuki M., 2007. Physicochemical properties of starch in *Chlorella* change depending on the CO₂ concentration during growth: Comparison of structure and properties of pyrenoid and stroma starch. *Plant Sci.*, 172: 1138-1147.
- Klok A. J., Martens D. E., Wijffels R. H., Lamers P. P., 2013. Simultaneous growth and neutral lipid accumulation in microalgae, *Bioresource Technology*, doi: <http://dx.doi.org/10.1016/j.biortech.2013.02.006>
- Krienitz L., Hegewald E. H., Hepperle D., Huss V. A. R., Rohr T., Wolf M., 2004. Phylogenetic relationship of *Chlorella* and *Parachlorella* gen. nov. (Chlorophyta, Trebouxiophyceae). *Phycologia*, 43: 529–542.
- Ledford H. K., Niyogi K. K., 2005. Singlet oxygen and photo-oxidative stress management in plants and algae. *Plant Cell Environ*, 28: 1037-1045.
- Lee D. H., 2011. Algal biodiesel economy and competition among bio-fuels. *Bioresour. Technol.*, 102: 43–49.
- Li Y., Ham D., Hu G., Sommerfeld M., Hu Q., 2010. Inhibition of starch synthesis results in overproduction of lipids in *Chlamydomonas reinhardtii*. *Biotechnol. Bioeng.* 107:258–268.

- Li Y., Han D., Sommerfeld M., Hu Q., 2011 Photosynthetic carbon partitioning and lipid production in the oleaginous microalga *Pseudochlorococcum* sp. (Chlorophyceae) under nitrogen-limited conditions. *Bioresour Technol* 102:123–129
- Li X., Přibyl P., Bišová K., Kawano S., Cepák V., Zachleder V., Čížková M., Brányiková I., Vítová M., 2013 The microalga *Parachlorella kessleri* – a novel highly-efficient lipid producer. *Biotechnol. Bioeng.*, 110: 97-107.
- Liang Y., Sarkany N., Cui Y., 2009. Biomass and lipid productivities of *Chlorella vulgaris* under autotrophic, heterotrophic and mixotrophic growth conditions. *Biotechnol.Lett.*, 31: 1043-1049.
- Liu Z. Y., Wang G. C., Zhou B. C., 2008. Effect of iron on growth and lipid accumulation in *Chlorella vulgaris*. *Bioresour. Technol.*, 99: 4717-4722.
- MacKinney G., 1941. Absorption of light by chlorophyll solutions. *J. Biol. Chem.*, 140: 315-322.
- Mandalam R. K., Palsson B. O., 1998. Elemental balancing of biomass and medium composition enhances growth capacity in high-density *Chlorella vulgaris* cultures. *Biotechnol Bioeng* 59: 605–11.
- Mizuno Y., Sato A., Watanabe K., Hirata A., Takeshita T., Ota S., Sato N., Zachleder V., Tsuzuki M., Kawano S., 2013. Sequential accumulation of starch and lipid induced by sulfur deficiency in *Chlorella* and *Parachlorella* species. *Bioresource Technology*, 129: 150-155.
- Mutlu Y. B., Isik O., Uslu L., Durmaz Y., 2011. The effects of nitrogen and phosphorus deficiencies and nitrite addition on the lipid content of *Chlorella vulgaris* (Chlorophyceae). *African J. Biotechnol.*, 10: 453-456.
- Přibyl P., Cepák V., Zachleder V., 2012. Production of lipids in 10 strains of *Chlorella* and *Parachlorella*, and enhanced lipid productivity in *Chlorella vulgaris*. *Appl. Microbiol. Biotechnol.*, 94: 549-561.
- Přibyl P., Cepák V., Zachleder V., 2013. Production of lipids and formation and mobilization of lipid bodies in *Chlorella vulgaris*. *J. Appl. Phycol.* 25(2): 545-553
- Rawsthorne S., 2002. Carbon flux and fatty acid synthesis in plants. *Prog Lipid Res* 41(2): 182–196.
- Rhiel E., Mörschel E., Wehrmeyer W., 1985. Correlation of pigment deprivation and ultrastructural organization of thylakoid membranes *Cryptomonas maculate* following nutrient deficiency. *Protoplasma*, 129: 62-73.
- Richardson B., Orcutt D. M., Schwertner H.A., Martinez C. L., Wickline H. E., 1969. Effects of Nitrogen Limitation on the Growth and Composition of Unicellular Algae in Continuous Culture. *Appl Microbiol*, 18: 245-250.
- Rodolfi L., Chini Zitelli G., Bassi N., Padovani G., Biondi N., Bonini G., Tredici M. R., 2009. Microalgae for oil: strain selection, induction of lipid synthesis and outdoor mass cultivation in a low-cost photobioreactor. *Biotechnol Bioeng* 102: 100–112
- Roessler P. G., 1990. Environmental control of glycerolipid metabolism in microalgae: Commercial implications and future research directions. *J Phycol* 26: 393–399.
- Shen Y., Yuan W., Pei Z., Mao E., 2010. Heterotrophic culture of *Chlorella protothecoides* in various nitrogen sources for lipid production. *Appl. Biochem. Biotechnol.*, 160: 1674-1684.
- Siaut M., Cuine S., Cagnon C., Fessler B., Nguyen M., Carrier P., Beyly A., Beisson F., Triantaphylides C., Li-Beisson Y., Peltier G., 2011. Oil accumulation in the model green alga *Chlamydomonas*

- reinhardtii: characterization, variability between common laboratory strains and relationship with starch reserves. *BMC Biotechnol.*, 11: 7.
- Sunda W. G., Price N. M., Morel F. M. M., 2005. Trace metal ion buffers and their use in culture studies. in: R.A. Andersen (Ed.) *Algal culturing techniques*. Elsevier, Amsterdam, pp. 35–63.
- Takagi M., Karseno Yoshida, T., 2006. Effect of salt concentration on intracellular accumulation of lipids and triacylglyceride in marine microalgae *Dunaliella* cells. *J. Biosci. Bioeng.* , 101: 223-226.
- Turpin, D. H., 1991. Effects of inorganic N availability on algal photosynthesis and carbon metabolism. *J. Phycol.*, 27: 14-20.
- Weselake R. J., Taylor D. C., Rahman M. H., Shah S., Laroche A., McVetty P. B. E., Harwood J. L., 2009. Increasing the flow of carbon into seed oil. *Biotechnol Adv* 27(6): 866–878.
- Zhu J., Zong J., Zong B., 2013. Factors in mass cultivation of microalgae for biodiesel. *Chinese Journal of Catalysis*, 34: 80-100.

CHAPTER 5

Mixotrophic cultivation of *Chlorella vulgaris* using industrial dairy waste as organic carbon source

5.1 Abstract	113
5.2 Introduction	113
5.3 Material and Methods	115
5.4 Results and discussion	118
5.5 Conclusions	124
5.6 References	124

The results presented in this chapter were adapted from:

Abreu A.P., **Fernandes B.**, Vicente A. A., Teixeira J., Dragone, G., 2012. *Mixotrophic cultivation of Chlorella vulgaris using industrial dairy waste as organic carbon source*. Bioresource Technology, 118: 61-66.

5.1 Abstract

Growth parameters and biochemical composition of the green microalga *Chlorella vulgaris* cultivated under different mixotrophic conditions were determined and compared to those obtained from a photoautotrophic control culture. Mixotrophic microalgae showed higher specific growth rate, final biomass concentration and productivities of lipids, starch and proteins than microalgae cultivated under photoautotrophic conditions. Moreover, supplementation of the inorganic culture medium with hydrolysed cheese whey powder solution led to a significant improvement in microalgal biomass production and carbohydrate utilization when compared with the culture enriched with a mixture of pure glucose and galactose, due to the presence of growth promoting nutrients in cheese whey. Mixotrophic cultivation of *C. vulgaris* using the main dairy industry by-product could be considered a feasible alternative to reduce the costs of microalgal biomass production, since it does not require the addition of expensive carbohydrates to the culture medium.

Keywords: Biofuels; cheese whey; *Chlorella vulgaris*; microalgae; mixotrophy.

5.2 Introduction

Photoautotrophic cultivation is the most common technique used for microalgae mass cultivation. However photoautotrophic cultivation presents some constrains, including low cell densities and long cultivation periods. Hence, heterotrophic and mixotrophic growth regimes have been proposed as feasible alternatives for the production of microalgal biomass (Yu *et al.*, 2009). Heterotrophic cultivation of microalgae involves the utilization of organic compounds as sole carbon source, while mixotrophic cultivation use simultaneously inorganic (for example CO₂) and organic compounds as carbon source (Dragone *et al.*, 2010). Therefore, microorganisms cultivated under mixotrophic conditions synthesize compounds characteristic of both photosynthetic and heterotrophic metabolisms at high production rates. Additionally, lower energy costs have been associated with mixotrophic cultivation in comparison with photoautotrophic cultures, due to its relatively lower requirements for light intensities (Cerón García *et al.*, 2005). Despite mixotrophic cultivation of microalgae provides higher biomass and lipid productivities than cultivation under photoautotrophic conditions, the cost of the

organic carbon substrate is estimated to be about 80% of the total cost of the cultivation medium (Bhatnagar *et al.*, 2011). As a result, less costly organic sources have to be found in order to overcome the high carbon cost resulting from mixotrophic culture conditions (Liang *et al.*, 2009). Cost reduction of growth media preparation with minimal undesired effects is crucial for a potential commercial application (Abad and Turon, 2012). In this context, crude glycerol from biodiesel production, acetate from anaerobic digestion, and carbohydrates from agricultural and industrial wastes offer great promise as inexpensive organic substrates for the cultivation of microalgae on mixotrophic mode (Bhatnagar *et al.*, 2011; Heredia-Arroyo *et al.*, 2011). Cheese whey (CW), the liquid by-product remaining from the cheese manufacturing process constitutes a serious environmental problem of dairy industries due to its high organic matter content (Dragone *et al.*, 2009). Among the major components of whey, the disaccharide lactose, which on hydrolysis yields glucose and galactose, is greatly responsible for its high Biochemical Oxygen Demand (BOD = 30,000 – 50,000 mg L⁻¹) and Chemical Oxygen Demand (COD = 60,000 – 80,000 mg L⁻¹). In addition to this carbohydrate, CW also contains proteins, lipids, water-soluble vitamins and minerals (González Siso, 1996). Exogenous sugars, such as glucose, galactose, mannose, fructose, sucrose and lactose have been commonly used for mixotrophic and heterotrophic cultivation of microalgae (Shi *et al.*, 1999). However, these carbohydrates are transported and assimilated by microalgae with different efficiencies (Sun *et al.*, 2008). A previous study revealed, for example, that some strains of *Chlorella* successfully utilize glucose and galactose during growth at different light intensities (Dvoráková-Hladká, 1966). Furthermore, recent reports indicate that *Chlorella vulgaris* grown on glucose medium may provide microalgal biomass for biofuel production and biorefinery (Kong *et al.*, 2012).

The objective of this work was to study the mixotrophic growth of *C. vulgaris*, using a hydrolysed CW solution as an alternative approach to photoautotrophic microalgal cultivation. To our knowledge, no similar study has been previously carried out using this dairy by-product for cultivation of *C. vulgaris*.

5.3 Material and Methods

5.3.1 Microalgal strain and inoculum preparation

The freshwater microalga *C. vulgaris* (strain P12) was used in all experiments. The microalgal inoculum was prepared according to the protocol described in section 3.3.1 and conducted at 30 °C under photoautotrophic conditions. The culture was aerated with CO₂-enriched air (2% v/v CO₂) at a rate of 0.4 vvm and illuminated with continuous light (70 μE m⁻² s⁻¹) as also described in section 3.3.1.

5.3.2 Media and culture conditions

Experiments consisted of four different cultivation conditions performed in duplicate (Table 5.1). The organic carbon sources used for mixotrophic cell growth were: a non-hydrolysed CW powder solution, a mixture of pure glucose and galactose and a hydrolysed CW powder solution.

Table 5.1 Different cultivation conditions of *C. vulgaris* and respective carbon sources

Growth condition	Carbon Source
Photoautotrophic	CO ₂
Mixotrophic _{nhCW}	CO ₂ + Non-hydrolyzed CW solution (10 g L ⁻¹ lactose)
Mixotrophic _{hCW}	CO ₂ + Hydrolyzed CW solution (5 g L ⁻¹ glucose + 5 g L ⁻¹ galactose)
Mixotrophic _{G+G}	CO ₂ + Glucose (5 g L ⁻¹) + Galactose (5 g L ⁻¹)

CW powder was supplied by Lactogal (Porto, Portugal). Its composition included (w/w): > 73% lactose, 12% proteins, 1.5% lipids and < 5% moisture. Non-hydrolysed CW powder solution (nhCW) was prepared with distilled water and deproteinised by heat treatment as described elsewhere (Dragone *et al.*, 2011_b). Hydrolysed CW solution (hCW) containing glucose and galactose was obtained by hydrolysing nhCW with β-galactosidase (> 8.0 units mg⁻¹, Sigma-Aldrich) from *Aspergillus oryzae*.

All assays were carried out at 30 °C in 0.5 L glass photobioreactors containing 400 mL of medium under a light intensity of approximately 70 μE m⁻² s⁻¹, measured by a LI-250 Light Meter with a LI-190 quantum sensor (LI-COR, USA). Agitation during

cell growth was supplied by sparging CO₂-enriched air (2% v/v CO₂) from the base of the photobioreactors at an aeration rate of 0.400 vvm. Initial cell concentration was about 0.5 g L⁻¹ for all the cultivation conditions.

After reaching the stationary growth phase, cells were collected and centrifuged (Sigma 4K15, Germany) at 8,750 g for 10 min, washed with distilled water and then freeze-dried for further biochemical characterization. The supernatant was also collected and frozen for subsequent sugar analyses.

5.3.3 Determination of microalgal cell concentration

Cell concentration of the culture in the photobioreactors was measured regularly by using an improved Neubauer hemocytometer. Biomass concentration was estimated by cell dry weight. Triplicate samples were centrifuged (8,750 g for 10 min), washed with distilled water and dried at 105 °C until constant weight.

5.3.4 Determination of carbohydrate concentration in culture media

Glucose, galactose and lactose concentrations in culture media were determined by High-Performance Liquid Chromatography (HPLC) in a Jasco chromatograph equipped with a refractive index (RI) detector (Jasco 830-RI, Japan) and a 300 × 6.5 mm Chrompack column (Chrompack, The Netherlands) at 60 °C, using 5 mM sulphuric acid as the eluent at a flow rate of 0.5 mL min⁻¹ and a sample volume of 20 µL.

5.3.5 Determination of microalgal starch

The starch content of *C. vulgaris* was assayed by enzymatic hydrolysis of the microalgal starch to glucose with α -amylase and amyloglucosidase, according to section 3.3.5.

5.3.6 Measurement of lipid and protein content in microalgae

According to the protocol described in section 3.3.5, total lipids were determined by

the classic Folch chloroform-based lipid extraction protocol (Folch *et al.*, 1957) and the protein content of microalgae was quantified according to Lowry *et al.* (1951).

5.3.7 Measurement of chlorophylls and total carotenoids concentration

Chlorophylls and carotenoids in *C. vulgaris* were extracted with methanol and spectrophotometrically determined as described by Dere *et al.* (1998).

Microalgae cells were placed in 96% methanol (50 ml for each gram) and homogenized with an Ultra Turrax (IKA T25D, Germany) at 1,000 rpm for one minute. The homogenate was filtered through two layer cheese cloths and was centrifuged (Hettich D-78532, Germany) at 2,500 rpm for 10 min. The supernatant was separated and the absorbances were read at 470, 642 and 662 nm on a Jasco V-560 (Japan) spectrophotometer. The experiments were repeated three times. The pigment content was calculated according to the formulas described by Dere *et al.* (1998): i) $C_a = 15.65 Abs_{666} - 7.340 Abs_{653}$; ii) $C_b = 27.05 Abs_{653} - 11.21 Abs_{666}$; iii) $C_{x+c} = 1000 Abs_{470} - 2.860 C_a - 129.2 C_b/245$, where C_a = chlorophyll *a*; C_b = chlorophyll *b*; C_{x+c} = total carotene. Total pigment content was obtained by summing chlorophylls and carotenoids contents.

5.3.8 Determination of specific growth rate

The specific growth rate (μ , day⁻¹) was calculated from Eq. 5.1:

$$\mu = (\ln N_2 - \ln N_1) / (t_2 - t_1) \quad \text{Eq. 5.1}$$

where N_1 and N_2 were the concentration of cells at the beginning (t_1) and at the end (t_2) of the exponential growth phase, respectively.

5.3.9 Determination of productivity of biomass, starch, lipids and proteins

Biomass productivity (P_{max} , g L⁻¹ d) during the culture period was calculated from Eq. 5.2:

$$P_{max} = \frac{(X_t - X_0)}{(t_x - t_0)} \quad \text{Eq. 5.2}$$

where X_t was the biomass concentration (g L^{-1}) at the end of the exponential growth phase (t_x) and X_0 the initial biomass concentration (g L^{-1}) at t_0 (day).

Productivity of starch, lipids and proteins at the end of cultivation were calculated from Eq. 5.3:

$$P_{\text{component}} = P_{\text{max}} \times F_{\text{component}} \quad \text{Eq. 5.3}$$

where $P_{\text{component}}$ was the productivity of starch, lipids or proteins, P_{max} was the biomass productivity and $F_{\text{component}}$ was the mass fraction (w/w) of each component.

Data were compared using one-way ANOVA followed by a Tukey's multiple comparison test with a 95% confidence level.

5.4 Results and discussion

5.4.1 Growth parameters of microalgae cultivated under photoautotrophic and mixotrophic conditions

Specific growth rate, final biomass concentration and biomass productivity of *C. vulgaris* cultivated under photoautotrophic and mixotrophic conditions were compared and summarized in Table 5.2. The highest specific growth rates of *C. vulgaris* were 0.43 and 0.47 day^{-1} when microalgae were cultivated under mixotrophic conditions using hydrolysed CW powder solution, and a mixture of glucose and galactose as organic carbon sources, respectively. These values were almost 3.5 times higher than those obtained when cells were grown in inorganic medium supplemented with non-hydrolysed CW powder solution, and under photoautotrophic mode of nutrition. Biomass concentration at the end of cultivation and biomass productivity were also significantly influenced by the nutritional conditions. It can be observed in Table 5.2 that the highest values of X_{max} (3.58 g L^{-1}) and P_{max} ($0.75 \text{ g L}^{-1} \text{ d}^{-1}$) achieved in the mixotrophic culture using hydrolysed CW powder solution resulted in 2.9- and 7.5-fold increase respectively, when compared to the values obtained in the photoautotrophic culture.

These results are in agreement with a previous study, which reported that mixotrophic *C. vulgaris* growth in glucose yielded higher biomass content and

productivity than cells grown under photoautotrophic conditions (Kong *et al.*, 2011). Mixotrophic cell cultivation utilizing both light and an organic carbon source has been considered the most efficient process for the production of microalgal biomass (Lee *et al.*, 1996).

Table 5.2 Growth parameters of *C. vulgaris* cultivated under photoautotrophic and mixotrophic conditions at 30 °C

Growth condition	Growth Parameters		
	μ_{max} (day ⁻¹)	X_{max} (g L ⁻¹)	P_{max} (g L ⁻¹ d ⁻¹)
Photoautotrophic	0.13 ± 0.01 ^a	1.22 ± 0.12 ^a	0.10 ± 0.01 ^a
Mixotrophic _{nhCW}	0.12 ± 0.00 ^a	1.98 ± 0.43 ^b	0.32 ± 0.13 ^{ab}
Mixotrophic _{hCW}	0.43 ± 0.00 ^b	3.58 ± 0.12 ^c	0.75 ± 0.01 ^c
Mixotrophic _{G+G}	0.47 ± 0.05 ^b	2.24 ± 0.34 ^b	0.46 ± 0.09 ^{bc}

Data are expressed as mean ± standard error.

Means in the same column followed by different letters represent significant differences ($p < 0.05$).

When the light energy used for CO₂ fixation is decreased in mixotrophic cultures, most of the energy is used for carbon assimilation. Therefore, since the amount of energy dissipated is minimal, mixotrophy provides higher energetic efficiency than other cultivation modes (Lalucat *et al.*, 1984). On the other hand, Shi *et al.* (1999) reported that glucose could be considered the best organic C-substrate for the growth of *Chlorella*. It is worth mentioning that the organic substrate played an important role in promoting biomass accumulation of *C. vulgaris* during microalgae cultivation. As shown in Table 5.2, supplementation of the inorganic culture medium with hydrolysed CW powder solution led to higher biomass concentration than supplementation with a mixture of glucose and galactose. The stimulatory effect of hydrolysed CW powder solution on biomass production is probably related to the presence of some nutrients in CW powder composition, such as phosphorous and calcium. Ozmihci and Kargi (2007) reported that CW powder contains approximately 0.96% total phosphorous on dry weight basis. Phosphorous is a macronutrient that plays a vital function in cellular metabolic processes by forming many structural and functional components required for normal growth and development of microalgae (Richmond, 2004). It should be stated that the mineral content in whey depends upon the processing techniques used for casein removal from liquid milk. Consequently, a higher microalgal biomass

concentration than that found in our study could have been obtained by using acid CW powder due to the higher concentrations of calcium and phosphorous presented in that type of whey (Mavropoulou and Kosikowski, 1973). The presence of nutrients might have also supported *C. vulgaris* growth when using non-hydrolysed CW powder solution, which showed a specific growth rate similar to the photoautotrophic control but with a higher final biomass concentration (Table 5.2). Due to the high content of nutrients, other valorisation pathways for CW have recently been proposed. Viitanen *et al.* (2003) showed that CW can be applied as an alternative inducer in recombinant high-cell density fermentations. According to these authors, CW can be directly used without any pre-treatment, not causing a dilution of the fermentation medium. Therefore, a potential application of hCW could be related with its use as a fermentation additive for microbial cultivation.

5.4.2 Consumption of glucose and galactose by *C. vulgaris*

The above-presented results demonstrated that the microalgal species used in this study is able to grow mixotrophically in the presence of glucose and galactose. Therefore, consumption of both carbohydrates by *C. vulgaris* cultivated under mixotrophic conditions is shown in Table 5.3.

Table 5.3 Consumption of glucose and galactose by *C. vulgaris* cultivated under mixotrophic conditions at 30 °C

Growth condition	Carbohydrate consumption (%)	
	Glucose	Galactose
Mixotrophic _{nhCW}	-	-
Mixotrophic _{hCW}	100.0	96.0
Mixotrophic _{G+G}	80.5	49.5

It was found that glucose and galactose were consumed in larger quantities during microalgal growth in the presence of the hydrolysed CW powder solution, in comparison to the culture supplemented with a mixture of pure sugars. In particular, glucose was completely consumed and only 4% of the initial galactose concentration remained in the growth medium at the end of cultivation when hydrolysed CW powder

solution was used as carbon source. On the other hand, after nearly 90 h of cultivation, initial contents of glucose and galactose dropped 80.5% and 49.5%, respectively, in the culture supplemented with both sugars. As discussed above, additional inorganic elements provided by hydrolysed CW might have been responsible for the increased consumption of glucose and galactose derived from CW by *C. vulgaris*. These observations are in good agreement with a previous study where it was demonstrated that some components of hydrolysed cheese whey enhanced carbohydrate utilization by microalgae (*e.g. Euglena gracilis*) (Freyssinet and Nigon, 1980).

Regardless of the media used, glucose was more efficiently assimilated than galactose by *C. vulgaris* cells grown under mixotrophic conditions. Higher consumption of glucose compared to galactose for mixotrophic *C. pyrenoidosa* cultures was already described by Rodríguez-López (1966). A greater contribution to maintenance metabolism could explain the lesser assimilation of galactose when compared to glucose (Samejima and Myers, 1958).

5.4.3 Influence of nutritional modes on biochemical composition of *C. vulgaris*

The lipid content and lipid productivity of *C. vulgaris* under different growth conditions were compared and depicted in Figure 5.1.

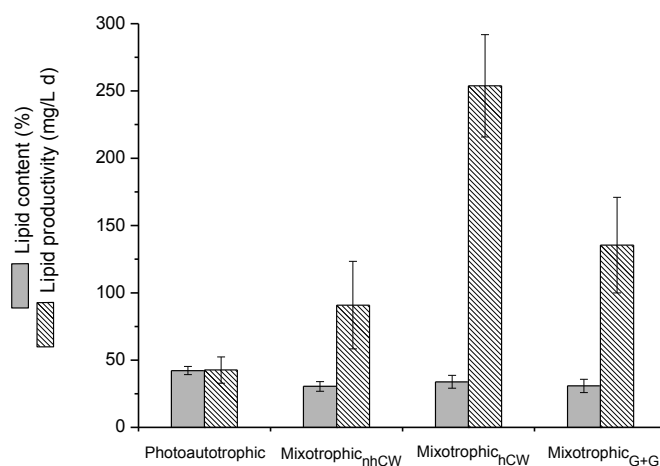


Figure 5.1 Lipid content and lipid productivity of *C. vulgaris* under different nutritional conditions.

When compared with mixotrophic cultures, higher lipid content (42%) was obtained in photoautotrophic mode at the beginning of the stationary growth phase

(approximately 190 h). Other authors (Liang *et al.*, 2009) have also shown that the amount of lipids accumulated in *C. vulgaris* under photoautotrophic growth conditions may surpass that from mixotrophic growth. On the other hand, the highest lipid productivity ($253 \text{ mg L}^{-1} \text{ d}^{-1}$) was achieved when cells were grown in culture medium supplemented with hydrolysed CW powder solution, due to the highest growth rate and cell density. Mixotrophic microalgal cultivation with hCW yielded six times higher lipid productivity than photoautotrophic culture ($42 \text{ mg L}^{-1} \text{ d}^{-1}$). These results were remarkable in comparison with values presented in previous studies (Liang *et al.*, 2009). Different nutritional conditions had also different effects on starch content and starch productivity of *C. vulgaris* (Figure 5.2). Although microalgal cells cultured photoautotrophically yielded the highest value of starch content (5.1%), maximum starch productivities were achieved mixotrophically using a mixture of pure glucose and galactose, and a hydrolysed CW powder solution, as a consequence of the highest biomass productivity obtained under mixotrophic conditions. The lower content of nutrients in the medium containing pure carbohydrates as compared to that in hydrolysed CW medium, promoted lower biomass growth and sugar consumption, and as a consequence of this stress condition, microalgal cells accumulated higher levels of starch.

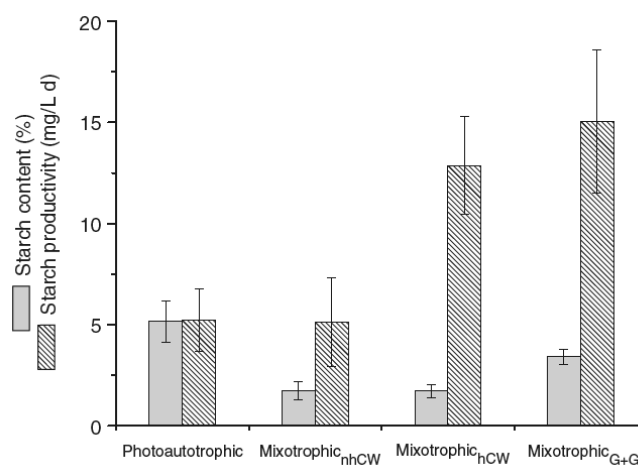


Figure 5.2 Comparison of starch content and starch productivity of *C. vulgaris* grown under photoautotrophic and mixotrophic conditions.

We have previously demonstrated (Dragone *et al.*, 2011_a) that higher starch accumulation in *C. vulgaris* P12 can be obtained under stressful growth conditions (*e.g.* by nutrient limitation). Therefore, since the starch productivity was calculated by

multiplying the biomass productivity by the starch content (w/w) in microalgae, no differences on the values of this parameter were observed for the cells cultivated under mixotrophic conditions using hydrolysed CW powder solution, and a mixture of glucose and galactose as organic carbon sources. The protein content and protein productivity of photoautotrophic and mixotrophic microalgal cells were compared in Figure 5.3. Cultivation of *C. vulgaris* P12 using hydrolysed CW powder solution as organic carbon source led to the highest protein content (63.5%) and protein productivity ($474 \text{ mg L}^{-1} \text{ d}^{-1}$). The highest protein content obtained in our study was significantly higher than that (26 %) found in *C. vulgaris* (strain 31 #) cultivated in optimized mixotrophic medium with pure glucose as carbon source (Kong *et al.*, 2012). The amount of total pigments in *C. vulgaris* cultured under photoautotrophic and mixotrophic conditions was also determined. As summarized in Table 5.4, the maximum pigment content (0.74%) was obtained in the photoautotrophic culture. It has been suggested that the formation of photosynthetic apparatus in *Chlorella* may be disturbed by the presence of organic substrates (Yang *et al.*, 2000), resulting in a decreased production of photosynthetic pigments when compared with that obtained in photoautotrophic mode.

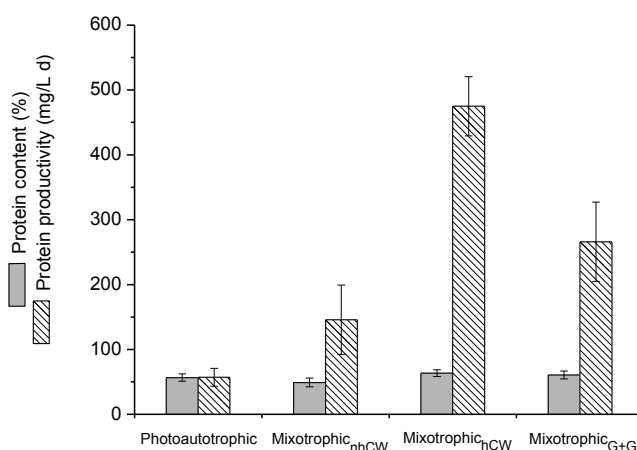


Figure 5.3 Effect of nutritional mode on protein content and protein productivity of *C. vulgaris*.

The higher content of chlorophylls obtained in the photoautotrophic culture when compared to mixotrophic cultures confirms such observation. The enhancement of chlorophyll biosynthesis by photoautotrophic *Chlorella* strains compared with that resulting from mixotrophic cells have been previously reported by several authors (Ip *et al.*, 2004; Kong *et al.*, 2011). On the other hand, Yan *et al.* (2012) reported that low chlorophyll content in mixotrophic cells decreases the dependence on light. Therefore,

reduced amount of chlorophylls in microalgae may relieve photoinhibition.

Among the different nutritional modes tested, the highest carotenoids content (0.23%) was also found in the photoautotrophic culture. This value dropped to 0.04% and 0.08% when cells were grown in inorganic medium supplemented with hydrolyzed CW powder solution, and with a mixture of pure glucose and galactose, respectively.

Table 5.4 Total pigment (chlorophylls + carotenoids) content of *C. vulgaris* cultivated under photoautotrophic and mixotrophic conditions at 30 °C

Growth condition	Pigment content (%)		
	Chlorophylls (a + b)	Carotenoids	Total pigments
Photoautotrophic	0.51 ± 0.09 ^c	0.23 ± 0.04 ^b	0.74 ± 0.09 ^c
Mixotrophic _{nhCW}	0.60 ± 0.17 ^c	0.09 ± 0.03 ^a	0.69 ± 0.17 ^c
Mixotrophic _{hCW}	0.22 ± 0.07 ^a	0.04 ± 0.02 ^a	0.26 ± 0.07 ^a
Mixotrophic _{G+G}	0.37 ± 0.05 ^b	0.08 ± 0.02 ^a	0.46 ± 0.05 ^b

Data are expressed as mean ± standard error.

Means in the same column followed by different letters represent significant differences ($p < 0.05$).

These results are consistent with those of Liu *et al.* (2009) who found lower amount of carotenoids in mixotrophic cells when compared to cells grown on photoautotrophic culture.

5.5 Conclusions

When compared with the photoautotrophic control culture, mixotrophic microalgae grew faster, providing higher productivities of biomass, lipids, starch and proteins. Furthermore, microalgal biomass production and carbohydrate consumption were enhanced by supplementing the inorganic culture medium with hydrolysed CW powder solution, than supplementing with a mixture of pure glucose and galactose, as a consequence of stimulatory effects arising from growth-promoting nutrients in CW. Mixotrophic cultivation of *C. vulgaris* using CW can be considered as a feasible strategy to reduce the costs of microalgal biomass production, while also contributing to solve the environmental problem caused by CW disposal in dairy industries.

5.6 References

Abad, S., Turon, X., 2012. Valorization of biodiesel derived glycerol as a carbon source to obtain added-value metabolites: Focus on polyunsaturated fatty acids. *Biotechnology Advances*, 30(3): 733-741

- Bhatnagar, A., Chinnasamy, S., Singh, M., Das, K.C., 2011. Renewable biomass production by mixotrophic algae in the presence of various carbon sources and wastewaters. *Applied Energy*, 88(10): 3425-3431.
- Brennan, L., Owende, P., 2010. Biofuels from microalgae - A review of technologies for production, processing, and extractions of biofuels and co-products. *Renewable and Sustainable Energy Reviews*, 14(2): 557-577.
- Cerón García, M.C., Sánchez Mirón, A., Fernández Sevilla, J.M., Molina Grima, E., García Camacho, F., 2005. Mixotrophic growth of the microalga *Phaeodactylum tricornutum*: Influence of different nitrogen and organic carbon sources on productivity and biomass composition. *Process Biochemistry*, 40(1): 297-305.
- Chen, C.-Y., Yeh, K.-L., Aisyah, R., Lee, D.-J., Chang, J.-S., 2011. Cultivation, photobioreactor design and harvesting of microalgae for biodiesel production: A critical review. *Bioresource Technology*, 102(1): 71-81.
- Das, P., Aziz, S.S., Obbard, J.P., 2011. Two phase microalgae growth in the open system for enhanced lipid productivity. *Renewable Energy*, 36(9): 2524-2528.
- Dere, Ş., Güneş, T., Sivaci, R., 1998. Spectrophotometric determination of chlorophyll - a, b and total carotenoid contents of some algae species using different solvents. *Turkish Journal of Botany* 22(1): 13-18.
- Dragone, G., Fernandes, B., Vicente, A., Teixeira, J.A., 2010. Third generation biofuels from microalgae. in: *Current Research, Technology and Education Topics in Applied Microbiology and Microbial Biotechnology*, (Ed.) A.M. Vilas, Vol. 2, Formatex Research Center. Badajoz, pp. 1355-1366
- Dragone, G., Fernandes, B.D., Abreu, A.P., Vicente, A.A., Teixeira, J.A., 2011a. Nutrient limitation as a strategy for increasing starch accumulation in microalgae. *Applied Energy*, 88(10): 3331-3335.
- Dragone, G., Mussatto, S.I., Almeida e Silva, J.B., Teixeira, J.A., 2011b. Optimal fermentation conditions for maximizing the ethanol production by *Kluyveromyces fragilis* from cheese whey powder. *Biomass and Bioenergy*, 35(5): 1977-1982.
- Dragone, G., Mussatto, S.I., Oliveira, J.M., Teixeira, J.A., 2009. Characterisation of volatile compounds in an alcoholic beverage produced by whey fermentation. *Food Chemistry*, 112(4): 929-935.
- Dvořáková-Hladká, J., 1966. Utilization of organic substrates during mixotrophic and heterotrophic cultivation of algae. *Biologia Plantarum*, 8(5): 354-361.
- Fernandes B., Dragone G., Abreu Ana P., Geada P., Teixeira J., Vicente A., 2012. Starch determination in *Chlorella vulgaris*—a comparison between acid and enzymatic methods. *Journal of Applied Phycology* 24 (5): 1203–1208.
- Fernandes, B., Dragone, G., Teixeira, J., Vicente, A., 2010. Light regime characterization in an airlift photobioreactor for production of microalgae with high starch content. *Applied Biochemistry and Biotechnology*, 161(1): 218-226.
- Folch, J., Lees, M., Sloane Stanley, G.H., 1957. A simple method for the isolation and purification of total lipides from animal tissues. *Journal of Biological Chemistry*, 226(1): 497-509.
- Freyssinet, G., Nigon, V., 1980. Growth of *Euglena gracilis* on whey. *Applied Microbiology and*

- Biotechnology, 9(4): 295-303.
- González Siso, M.I., 1996. The biotechnological utilization of cheese whey: A review. *Bioresource Technology*, 57(1): 1-11.
- Heredia-Arroyo, T., Wei, W., Ruan, R., Hu, B., 2011. Mixotrophic cultivation of *Chlorella vulgaris* and its potential application for the oil accumulation from non-sugar materials. *Biomass and Bioenergy*, 35(5): 2245-2253.
- Ip, P.-F., Wong, K.-H., Chen, F., 2004. Enhanced production of astaxanthin by the green microalga *Chlorella zofingiensis* in mixotrophic culture. *Process Biochemistry*, 39(11): 1761-1766.
- Kong, W.-B., Hua, S.-F., Cao, H., Mu, Y.-W., Yang, H., Song, H., Xia, C.-G., 2012. Optimization of mixotrophic medium components for biomass production and biochemical composition biosynthesis by *Chlorella vulgaris* using response surface methodology. *Journal of the Taiwan Institute of Chemical Engineers*, 43(3): 360-367.
- Kong, W., Song, H., Cao, Y., Yang, H., Hua, S., Xia, C., 2011. The characteristics of biomass production, lipid accumulation and chlorophyll biosynthesis of *Chlorella vulgaris* under mixotrophic cultivation. *African Journal of Biotechnology*, 10(55): 11620-11630.
- Lalucat, J., Imperial, J., Parés, R., 1984. Utilization of light for the assimilation of organic matter in *Chlorella* sp. VJ79. *Biotechnology and Bioengineering*, 26(7): 677-681.
- Lee, Y.-K., Ding, S.-Y., Hoe, C.-H., Low, C.-S., 1996. Mixotrophic growth of *Chlorella sorokiniana* in outdoor enclosed photobioreactor. *Journal of Applied Phycology*, 8(2): 163-169.
- Liang, Y., Sarkany, N., Cui, Y., 2009. Biomass and lipid productivities of *Chlorella vulgaris* under autotrophic, heterotrophic and mixotrophic growth conditions. *Biotechnology Letters*, 31(7): 1043-1049.
- Liu, X., Duan, S., Li, A., Xu, N., Cai, Z., Hu, Z., 2009. Effects of organic carbon sources on growth, photosynthesis, and respiration of *Phaeodactylum tricornutum*. *Journal of Applied Phycology*, 21(2): 239-246.
- Lowry, O.H., Rosebrough, N.J., Farr, A.L., Randall, R.J., 1951. Protein measurement with the Folin phenol reagent. *Journal of Biological Chemistry*, 193(1): 265-275.
- Ozmihci, S., Kargi, F., 2007. Kinetics of batch ethanol fermentation of cheese-whey powder (CWP) solution as function of substrate and yeast concentrations. *Bioresource Technology*, 98(16): 2978-2984.
- Richmond, A., 2004. *Handbook of microalgal culture: biotechnology and applied phycology*. 1 ed. Blackwell Science, Oxford.
- Rodríguez-López, M., 1966. Utilization of sugars by *Chlorella* under various conditions. *Journal of General Microbiology*, 43(1): 139-143.
- Samejima, H., Myers, J., 1958. On the heterotrophic growth of *Chlorella pyrenoidosa*. *Journal of General Microbiology*, 18: 107-117.
- Shi, X.-M., Liu, H.-J., Zhang, X.-W., Chen, F., 1999. Production of biomass and lutein by *Chlorella protothecoides* at various glucose concentrations in heterotrophic cultures. *Process Biochemistry*, 34(4): 341-347.

- Sun, N., Wang, Y., Li, Y.-T., Huang, J.-C., Chen, F., 2008. Sugar-based growth, astaxanthin accumulation and carotenogenic transcription of heterotrophic *Chlorella zofingiensis* (Chlorophyta). *Process Biochemistry*, 43(11): 1288-1292.
- Yan, R., Zhu, D., Zhang, Z., Zeng, Q., Chu, J., 2012. Carbon metabolism and energy conversion of *Synechococcus* sp. PCC 7942 under mixotrophic conditions: comparison with photoautotrophic condition. *Journal of Applied Phycology*, 24(4): 657-668.
- Yang, C., Hua, Q., Shimizu, K., 2000. Energetics and carbon metabolism during growth of microalgal cells under photoautotrophic, mixotrophic and cyclic light-autotrophic/dark-heterotrophic conditions. *Biochemical Engineering Journal*, 6(2): 87-102.
- Yu, H., Jia, S., Dai, Y., 2009. Growth characteristics of the cyanobacterium *Nostoc flagelliforme* in photoautotrophic, mixotrophic and heterotrophic cultivation. *Journal of Applied Phycology*, 21(1): 127-133.

CHAPTER 6

Selection of cultivation system type and geometry

6.1 Abstract	131
6.2 Cultivation system selection	132
6.3 Geometry selection based on light regime characterization	139
6.4 Split Cylinder Airlift Photobioreactor (SCAPBR) description	149
6.5 References	152

The results presented in this chapter were adapted from:

Fernandes B., Dragone G., Teixeira J., Vicente A., 2010. *Light regime characterization in an airlift photobioreactor for production of microalgae with high starch content.* Applied Biochemistry Biotechnology, 161: 218–26.

6.1 Abstract

The design of a microalgae culture system involves a series of sequential decisions. The options made (Figure 6.1) in order to develop a more cost effective and productive culture system were based mainly on literature review. For PBR geometry selection the decision was made based on experimental work in order to select the geometry that allows a more efficient light distribution inside the cultivation system.

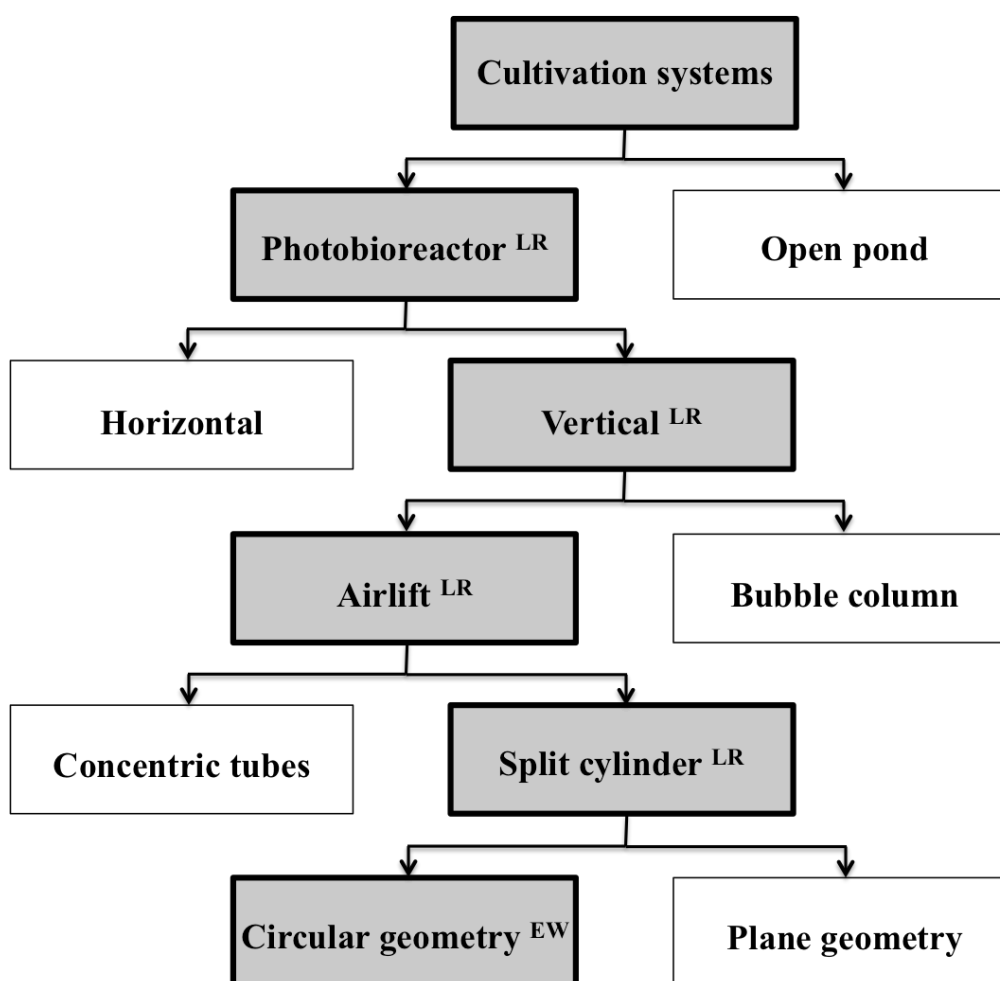


Figure 6.1 Schematic representation of sequential decisions made to select the most appropriate cultivation system for microalgae mass production (^{LR} – literature review; ^{EW} – experimental work).

After analysis of all the variables presented, the selected cultivation system was a split cylinder airlift photobioreactor (SCAPBR) with circular geometry.

Keywords: Cultivation system design; SCAPBR; light regime characterization; optical fibres.

6.2 Cultivation system selection

A variety of cultivation systems have been proposed or used for microalgae cultivation (see section 2.2.1). These cultivation systems are, in general, either too complex or too costly to be applied in large-scale production. Of the various possible culture methods, outdoor culture using sunlight appears to be the only viable option for many microalgae (Mirón *et al.*, 2003) so, indoor cultivation using artificial lighting will not be even considered in this study.

Throughout this chapter the evaluations made in the microalgae cultivation system selection, the design process and the justification for the options made will be described. The first decision that must be made is between the use of open ponds or PBRs.

6.2.1 Open pond *versus* photobioreactor

Chen (1996) and Singh and Sharma (2012) states that enclosed PBRs have the following advantages over open pond production:

1. Better control of algal culture conditions such as pH, temperature, light and CO₂ concentration;
2. Large surface-to-volume ratio;
3. Better control of gas transfer that lead to less CO₂ loss;
4. Reduction in evaporation of growth medium;
5. More uniform temperature;
6. Better protection from outside contamination allowing axenic algal cultivation of monocultures;
7. Higher algal cell densities are possible;
8. Enables the production of complex biopharmaceuticals.

Culture in PBRs becomes mandatory especially if the desired product is to be used in pharmaceutical applications or the microalgae require a culture environment that is not highly selective (Miron *et al.* 2003).

Based on the above features, PBRs seem to be the best choice for microalgae mass cultivation. However, there are a wide variety of PBRs, and the next decision that has to be taken is between the two main classes of PBRs: horizontal and vertical.

6.2.2 Horizontal versus vertical PBRs

Closed horizontal continuous-run tubular loop PBRs are usually used in commercial mass monoculture of microalgae. These horizontal PBRs are made of tubes that are typically less than 0.08 m in diameter (Tredici, 1999; Grima *et al.*, 1999; Mirón *et al.*, 1999). Although the horizontal tubular systems have notable advantages relative to conventional facilities (*e.g.*, open ponds), they also have serious limitations. These photobioreactors occupy a large land surface and are expensive to build and operate (Mirón *et al.*, 2002). They also have other serious limitations that imply additional costs, such as difficult temperature control, the need for frequent recarbonation because of the tube length, growth inhibition by dissolved oxygen, foaming and fouling. These limitations make the utilization of horizontal PBRs only justifiable for high-value products (Weissman *et al.*, 1988).

An alternative for overcoming the noted constrains of horizontal PBRs may be the vertical PBRs. Vertical PBRs can differ in their designs, possessing internal-loops, external-loops or divided column airlift systems and bubble columns (Figure 6.2). The constant agitation of the medium in vertical PBR caused by the gas bubbles also mixes the culture gently with very little shear stress (Mirón *et al.*, 2002) compared to impellers and pumps (Wang *et al.*, 2012). Consequently, very little cell damage is associated with vertical column PBRs except at extreme superficial gas velocities (Vega-Estrada *et al.*, 2005).

Various microalgae species have been tested in different pneumatically mixed PBRs by different authors (Tsavalos and Young, 1996; Lee, 1997; Csogor *et al.*, 1999; Petkov, 2000; Borja *et al.*, 2001; Lee *et al.*, 2002; Barbosa *et al.*, 2003_a; Chisti *et al.*, 2003; Walter *et al.*, 2003; Oncel and Sukan, 2008) with different results and variable degrees of success. Vertical PBR orientation has been proposed to enhance productivity by avoiding or reducing the photosaturation, as can be concluded from the work of Hu *et al.* (1996, 1998) and Cuaresma *et al.*, (2011). By placing the

photobioreactors vertical the sunlight falling on a given ground area is spread over a larger reactor surface area. As a result, more algae are exposed to lower intensities, being able to maximize their photosynthetic efficiency (Posten and Shaub, 2009).

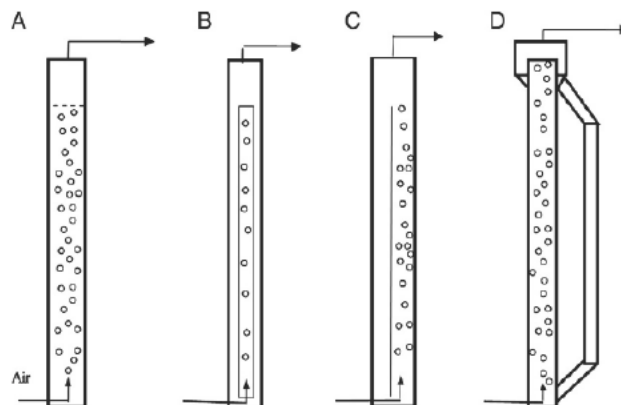


Figure 6.2 Schematic diagrams of: bubble column PBR (A); internal-loop (draft-tube) airlift PBR (B); split cylinder airlift PBR (C); external-loop airlift PBR (D) (adapted from Wang *et al.*, 2012).

Mirón *et al.* (2002) reveal that biomass in the vertical column reactors did not experience photoinhibition under conditions (photosynthetically active daily averaged irradiance value of $1,150 \mu\text{Em}^{-2} \text{s}^{-1}$) that are known to cause photoinhibition in conventional thin-tube horizontal loop reactors. Cuaresma *et al.* (2011) tested outdoor vertical and horizontal PBRs and concluded that the highest photosynthetic efficiency was found for the vertical simulation, 1.3 g of biomass produced per mol of PAR photons supplied, against 0.85 g mol^{-1} of horizontal PBR and the theoretical maximal yield (1.8 g mol^{-1}).

If, under high light intensity, vertical reactors experience less photoinhibition, under low light intensity a vertical orientation captures more reflected light (Mirón *et al.*, 1999). According to Cuaresma *et al.* (2011) these results prove that productivity per unit of ground area could be greatly enhanced by placing the photobioreactors vertically. Sánchez Mirón *et al.* (1999) concluded that vertical reactors performed better than tubular reactors because they are supposedly more suited for scale-up, require less energy for cooling because of the low surface to volume ratio, and overall outperform tubular reactors throughout the year.

Both the type of arrangement and then distance between the units has a profound influence on reactor productivity, and must be carefully planned. The closer the

reactors, the higher will be the decrease of productivity (Zittelli *et al.*, 2006). Zittelli *et al.* (2006) cultivated *Tetraselmis suecica* in outdoors annular columns placed in two different arrangements: 1) columns placed at the vertices of equilateral triangles or 2) in parallel rows. In the first experiment, the mean volumetric productivity of the full-scale column was approximately the same, and in the second experience was slightly lower than that achieved by the isolated column.

Because of their simpler construction and absence of moving, mechanical parts, bubble column and airlift photobioreactors are less vulnerable to technical malfunctions (Eriksen, 2008), a very important feature for reactors used for long-term continuous cultivation of microalgae, and are therefore a best option than horizontal PBRs for mass production of microalgae.

As mentioned above, there is an array of vertical PBRs, namely bubble columns and airlifts, among which it is necessary to make a choice.

6.2.3 Bubble column *versus* airlift PBRs

Vertical PBRs are usually cylinders with diameter of up to 0.4 m and heights of up to 4 m. These columns must have relatively small diameters to increase the surface–volume ratio. The height restriction is associated with the gas transfer limitations (can lead to CO₂ and pH gradients and O₂ accumulation) and the strength of the transparent materials used to construct the columns (Wang *et al.*, 2012). Vertical column PBRs are characterized by their high volumetric gas transfer coefficients. The bubbling of gas from the bottom of the column enables efficient CO₂ utilization and optimal O₂ removal (Wang *et al.*, 2012). Consequently algal growth is often limited by other parameters such as light efficient utilization.

It is well known that both the quantity and the quality of the light delivered to the cells are significant to the cells' growth (Fernandes *et al.*, 2010; Lou *et al.*, 2003). As described by Lambert–Beer's law, light intensity decays exponentially as it penetrates into an optically dense culture. In highly dense cultures, while the region close to PBR surface receives plenty of light, some zones in the reactor may remain in the dark due to optical absorption and self-shading of the cells, causing

photolimitation. In this region, the light intensity is too weak to maintain positive growth of the cells, and the net biomass production would be negative. Moreover, in certain periods of the day, the regions close to the surface are subject to light intensities that are greater than the saturation value of microalgae species, causing photoinhibition of cells (Wu and Merchuk, 2004).

Several strategies have been proposed in order to overcome these two opposite limitations that result in an inefficient utilization of available light and consequently, in productivities that are significantly lower than the theoretical productivity values. Increasing the volumetric surface area (reducing the culture depth) to limit the fraction of culture without sufficient light is one of the alternatives, but this strategy results in higher installation costs and does not solve the photoinhibition problem (Wu and Merchuk, 2004). The solution to this problem is to find a solution to prevent high residence time of microalgae cells under conditions of photoinhibition or photolimitation.

It is known that the conversion of light energy to biomass can be enhanced if algal cells are made to repeatedly cycle between the well-lit exterior and the dimly lit interior of the photobioreactor. Ordered mixing forces the cells to experience periodical light/dark cycles. The effect of the light/dark cycles has been studied previously (Lee and Pirt, 1981; Merchuk *et al.*, 1998; Wu and Merchuk, 2001), and it was found that periodical light/dark cycles might enhance growth (Wu and Merchuk, 2004). Random mixing does not enhance productivity as much as a regular light–dark cycle (Degen *et al.*, 2001).

According to Wang *et al.* (2012), generally, airlift PBRs can sustain better biomass production of different microalgae in comparison to other vertical column PBRs, probably due to this regular mixing, as opposed to random mixing found in bubble columns.

The only PBRs that combine the capacity to provide the cells with regular light–dark cycles and the vertical disposition are the PBRs that work under the airlift principle, making them the elected among the vertical PBRs. However, as seen in Figure 6.2, there are several types of airlift reactors.

6.2.4 Airlift PBR type selection

Although there is a wide variety of airlift reactors, they have characteristics that are common to all them. Airlift reactors are vessels with two interconnecting zones. The zone where the gas mixture is sparged is called riser whereas the other region, that does not receive the gas, is called downcomer (Figure 6.2 A, B and C). Generally airlifts exist in two main types: internal loop and external loop. In the internal loop reactor, riser and downcomer sections are separated either by a draft tube or a split-cylinder. In the external loop, riser and downcomer are separated physically by two different tubes (Singh and Sharma, 2012).

Concentric tube airlift PBRs (Figure 6.2 B) typically comprise a transparent column, an internal draft tube (riser), and an air sparger. Air or CO₂ enriched air is introduced inside the riser at the bottom; and degassing occurs in the freeboard regime, which locates on the top of the internal column. Since the gas holdup inside the riser is much larger than that in the degassed liquid outside of the internal column, an upward flow of the liquid/gas mixture will be created inside the internal column while a downward flow of degassed liquid is generated outside of it (Wang *et al.*, 2012).

In split column airlift PBRs (SCAPBR) (Figure 6.2 C), a flat plate splits the diameter of the column and separates the column into two parts: the riser and the downcomer regions. As in concentric tube airlifts, air is introduced at the bottom of the riser region to carry the liquid upwards. Liquid/gas separation occurs at the top of the column and the heavier degassed liquid falls downward. Mixing is also achieved with aeration and liquid circulation (Wang *et al.*, 2012).

In external loop airlift PBRs (Figure 6.2 D) degassing occurs in a gas/liquid separation region on the top of the column and circulation of degassed liquid is achieved through an external circulation column (Wang *et al.*, 2012).

Regardless the type of airlift PBR, it is clear that the largest advantage of an airlift PBR is the excellent and non-chaotic mixing it offers, which allows good and regular exposure of cells to light radiation even with a relatively large diameter of column and high cell density. However, airlift bioreactors have other several advantages such

as well-defined fluid flow patterns, (Fernandes *et al.*, 2010) simplicity of design and construction, lower power inputs, low shear-stress field (respectful of the microorganisms' cellular integrity), high gas-liquid mass transfer coefficients (supply of CO₂ and degassing of oxygen produced by photosynthesis), low capital and operating costs (Loubière *et al.*, 2011). Because of good gas-liquid mass transfer, the dissolved oxygen concentration in the reactors at peak photosynthesis remained < 120% of air saturation; thus, oxygen inhibition of photosynthesis and photo-oxidation of the biomass did not occur (Mirón *et al.*, 2002). The mixing efficiency of swirling flows ensures a good homogenization of nutrients inside the culture, but also promotes the microalgae displacement and renewal along the light gradient. In addition, the high shear stresses generated at walls are interesting for limiting the biofilm formation at the optical surfaces (Pruvost *et al.*, 2002, 2004; Loubière *et al.*, 2009).

The concentric tube airlift is the most commonly used airlift for microalgae cultivation (Camacho *et al.*, 1999; Barbosa *et al.*, 2003_b; Krichnavaruk *et al.*, 2005; Vunjak-Novakovic *et al.*, 2005; Ranjbar *et al.*, 2008; Oncel and Sukan, 2008), however it has some limitations, such as difficult temperature control and large fraction of dark zones inside the PBR, mainly due to the presence of the internal column which limits light penetration.

The only PBR that seems to have the potential to overcome the limitations of the concentric tube airlift, maintaining all the benefits inherent to an airlift PBR utilization, is the Split Column Airlift PBR (SCAPBR).

However, to achieve the maximization of SCAPBR potential it is necessary to select the wall geometry (circular or planar) that maximizes the light distribution inside the SCAPBR. The selection of the best geometry was based on the measurement of light distribution along different points of the PBR.

6.3 Geometry selection based on light regime characterization

6.3.1 Abstract

The slow development of microalgal biotechnology is due to the failure in the design of large-scale photobioreactors (PBRs) where light energy is efficiently utilized. In this work, both the quality and the amount of light reaching a given point of the PBR were determined and correlated with cell density, light path length, and PBR geometry. This was made for two different geometries of PBRs (circular and planar) using optical fibre technology that allows obtaining information about quantitative and qualitative aspects of light patterns. This is important since the ability of microalgae to use the energy of photons is different, depending on the wavelength of the radiation.

The results show that the circular geometry allows a more efficient light penetration, especially in the locations with a higher radial coordinate (r) when compared to the planar geometry; these observations were confirmed by the occurrence of a higher fraction of illuminated volume of the PBR for this geometry. An equation is proposed to correlate the relative light intensity with the penetration distance for both geometries and different microalgae cell concentrations. It was shown that the attenuation of light intensity is dependent on its wavelength, cell concentration, geometry of PBR, and the penetration distance of light.

6.3.2 Introduction

Due to the light gradient inside the PBR and depending on the mixing properties, microalgae cells are subjected to light/dark cycles where the light period is characterized by a light gradient. These light/dark cycles will determine productivity and biomass yield on light energy. Productivity is determined by the growth rate, which, for fixed fluid dynamics and temperature, is a function of the light profile within the reactor and the light regime to which the cells are subject to. In dense microalgal cultures, light penetration is impeded by self-shading and light absorption (Rabe and Benoit, 1962; Frohlich *et al.*, 1983; Erickson and Lee, 1986). These

effects affect the radiation profile inside the culture (Grima *et al.*, 1999). Airlift bioreactors have been indicated as attractive alternatives for cell cultivation (Gordon and Polle, 2007). This might be due to several main advantages such as good mixing, well-defined fluid flow patterns, relatively high gas–liquid mass transfer rate, and low capital and operating costs. If the volumes enclosed by annulus and draft tube can be regarded as illuminated and dark regions, respectively, this flow pattern gives defined light/dark cycles for photosynthetic cells culture. However, because of the nature of the decay in illuminance mentioned above, the description of the annulus as an “illuminated region” is in most cases an oversimplification. Local differences in photon flux density (PFD) will appear as one departs from the illuminated surface. Hence, identification of cell trajectories in the light and dark zones is required in order to describe properly the light history of a photosynthetic cell (Wu and Merchuk, 2004). In order to develop a mathematical model predicting microalgal photosynthesis or growth in a photobioreactor (PBR), it is a prerequisite to quantitatively and qualitatively describe light penetration through the microalgal suspension (Wu and Merchuk, 2004). To relate the light supply with the culture growth, light attenuation in the biological turbid medium must be accurately described. This determination is not trivial and is highly correlated to the PBR geometry (Cornet *et al.*, 1998; Pruvost *et al.*, 2006).

The utilization of optical fibre technology allows obtaining information about quantitative (photosynthetic photon flux density) and qualitative (spectral intensity distribution) aspects of light patterns, which is important since the ability of microalgae to use the energy of photons is different, depending on the wavelength of the radiation. This technology was used in the present work aiming to determine both the quality and the amount of light at different points of two alternative geometries of an airlift PBR as a function of the microalgae cell concentration and of the light penetration distance. The final goal is to characterize the light regime of the airlift PBR in view of its future utilization for the production of microalgae.

6.3.3 Material and methods

Microorganism and growth medium

The microalgae *Chlorella vulgaris* P12 was grown in 1 L Schott flasks with 400 ml of medium, using the composition described by Douskova *et al.* (2008). The original growth medium based on the elementary composition of algal biomass had the following initial composition (mg L^{-1}): 1,100 $(\text{NH}_2)_2\text{CO}$, 237 KH_2PO_4 , 204 $\text{MgSO}_4 \cdot 7\text{H}_2\text{O}$, 40 $\text{C}_{10}\text{H}_{12}\text{O}_8\text{N}_2\text{NaFe}$, 88 CaCl_2 , 0.83 H_3BO_3 , 0.95 $\text{CuSO}_4 \cdot 5\text{H}_2\text{O}$, 3.3 $\text{MnCl}_2 \cdot 4\text{H}_2\text{O}$, 0.17 $(\text{NH}_4)_6\text{Mo}_7\text{O}_{24} \cdot 4\text{H}_2\text{O}$, 2.7 $\text{ZnSO}_4 \cdot 7\text{H}_2\text{O}$, 0.6 $\text{CoSO}_4 \cdot 7\text{H}_2\text{O}$, 0.014 $(\text{NH}_4)\text{VO}_3$ in distilled water; the initial pH was adjusted to 7.0 by 0.1 M NaOH.

Photobioreactor

The culture was transferred into a set of acrylic PBRs (Figure 6.3) that represent the cross section of two different geometries (circular (PBR_C) and planar (PBR_P)) of an airlift PBR.

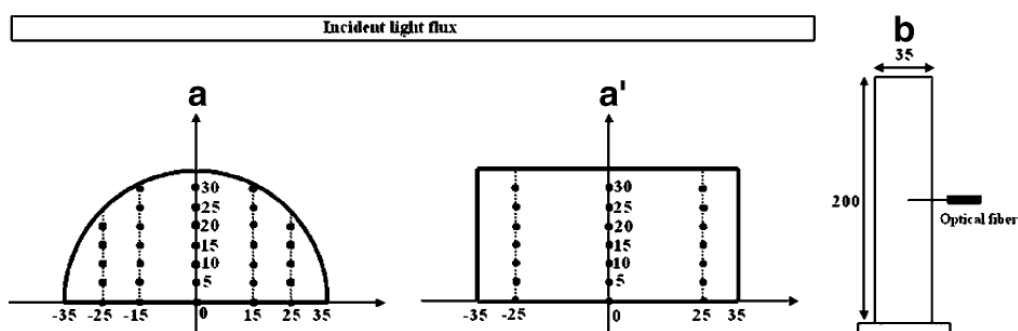


Figure 6.3 Top view of a PBR: *a* PBR_C , *a'* PBR_P , and *b* lateral view of a PBR section with an optical fibre attached; the position of the measuring points is indicated by circles. All dimensions are in mm.

The PBRs were illuminated by a set of four fluorescent lamps (Sylvania Standard F18W) placed horizontally and uniformly distributed around the reactor walls at ca. 15 cm from its surface with an incident light intensity or photosynthetic photon flux density (PPFD) of $70 \mu\text{E m}^{-2} \text{s}^{-1}$. The PPFD was determined, in the absence of the microalgal culture, behind the front surface of the reactor, by averaging the values of light intensities measured with a LI-COR Quantum/Radiometer/Photometer Model LI-250 Light Meter (San Diego, CA, USA). This value was taken as the reference value when calculating the relative light intensity (*RLI*) (see below) (Ranjbar *et al.*,

2008).

The quantitative and qualitative characterization of light regime was performed using a fibre optic spectrometer AvaSpec-2048-4-DT (2048 pixel, 200 – 1,100 nm) coupled with a standard transmission probe, model T300-RT-VIS/NIR, controlled by AvaSoft 6.0 software. Data were acquired between 200 and 1,100 nm, but only the range between 400 and 700 nm (Photosynthetically Active Radiation - PAR) was used for calculations, for two reactor configurations (circular and planar) at 14 cell concentrations (ranging from 0.18 to 2.29 kg m⁻³), three different radial positions for the circular geometry bioreactor, two different radial positions for the plane geometry bioreactor, and six or seven light penetration distances, depending on the probe radial position and the reactor configuration.

The quantification of the light penetrating in the algal culture was made through the calculation of the relative light intensity (*RLI*), which is expressed as the ratio of the light intensity (*LI*) measured at a given point and the reference light intensity (*LI_R* = 70 μE m⁻²s⁻¹), measured at the inside wall of the vessel filled with medium in the absence of algae (Eq. 6.1).

$$RLI = \frac{LI}{LI_R} \times 100 \quad \text{Eq. 6.1}$$

The concentration of suspended algal biomass was determined both by optical density measurement (700 nm) and oven drying at 60 °C for 24 h (Jacob-Lopes *et al.*, 2009). All measurements were made in triplicate, and in all experiments, the standard deviation was always below 5%.

6.3.4 Results and discussion

Overall Characterization of Light Intensity

Light intensity distribution within the culture vessel (Figure 6.4) shows cross-sectional distributions of *RLI* within the two different geometries filled with the algal suspension at different cell concentrations (0.95 and 2.67 kg m⁻³). It can be observed in Figure 6.4 that for both evaluated cell densities, the irradiance within the two different geometries varied as a function of position. Cells nearer the light-receiving surface experienced a higher irradiance than cells elsewhere in the vessel. Cells

closer to the light source shade those further away; hence, productivity varies with position and time (Laws, 1980; Ree and Gotham, 1981). Figure 6.4 also shows that for both PBR geometries, the relative light intensity at the same distance from the light-receiving surface decreased as the cell density was increased. Such behaviour was also observed for cell densities lower than 0.95 kg m^{-3} (Figure 6.5). Figure 6.4 *b*, *b'* clearly shows that the planar geometry leads to a more uniform light distribution (this is more evident for higher cell concentrations - Figure 6.4 *b'*); the circular geometry allows a more efficient light penetration, especially in the locations with a higher radial coordinate (r). For low cell concentrations (Figure 6.4 *a*, *b*), the differences between the geometries are negligible, possibly due to the low intensity of the scattering phenomena; in this case, those small differences might be attributed, mainly, to the light incidence angle at the reactor surface.

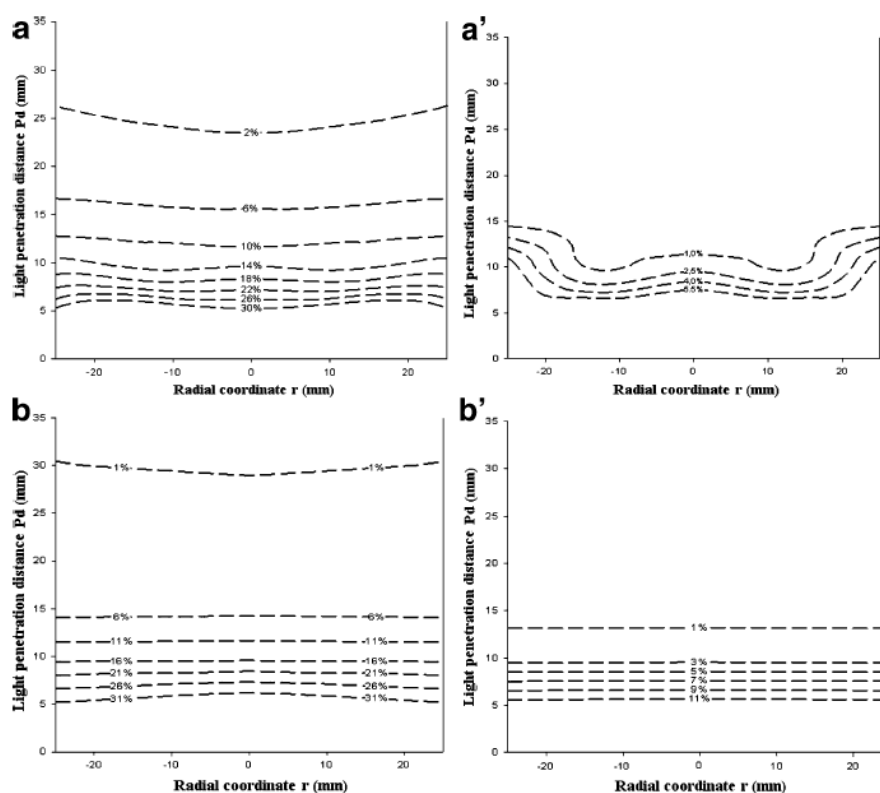


Figure 6.4 Cross-sectional distribution of light intensity within the airlift downcomer filled with algal cell suspension as a function of the light penetration distance (Pd) and radial coordinate (r), where $r = 0$ corresponds to the axis of the reactor, where: *a* PBR_C with 0.95 kg m^{-3} ; *a'* PBR_C with 2.67 kg m^{-3} ; *b* PBR_P with 0.95 kg m^{-3} and; *b'* PBR_P with 2.76 kg m^{-3} .

However, for higher cell concentrations (Figure 6.4 *a'*, *b'*), the effect of the geometry becomes more evident, and a clear difference can be observed in the *RLI*

that reaches zones of the reactor with the same light penetration distance (Pd) but with different axial coordinates (r). The fact that this difference is almost inexistent for the points at $r = 0$ and increases for increasing values of $|r|$ is a clear indication that the influence of the curved surface of the circular reactor in the availability of the light inside the vessel is a positive one, when compared to the planar geometry. Such differences are the result of both the effect of the curved surface of the circular reactor and of the higher intensity of the scattering phenomena due to the higher concentration of cells present in the reactor. For the planar geometry, all the points at a given distance from the light source will have the same light penetration distance (independently of their radial coordinate) and therefore, will be essentially under the same RLI (Figure 6.4 b').

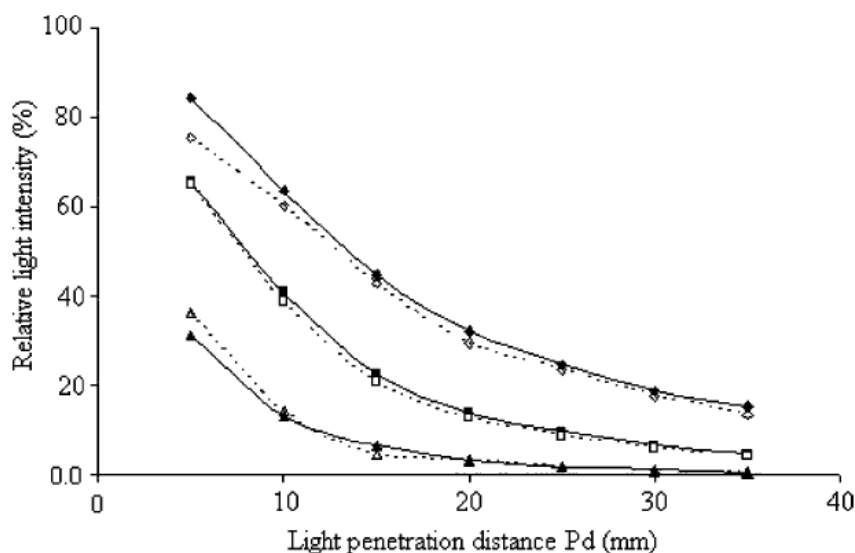


Figure 6.5 Relative light intensity distribution (in percent) in the two airlift downcomer geometries (closed symbols circular geometry and open symbols planar geometry) filled with algal cell suspension (\blacklozenge, \diamond 0.35 kg m^{-3} , \blacksquare, \square 0.50 kg m^{-3} and; $\blacktriangle, \triangle$ 0.95 kg m^{-3}) as a function of the light penetration distance (Pd). These data points correspond to measurements made for $r = 0 \text{ mm}$.

On the contrary, for the circular geometry, to the same distance from the light source, there will be different light penetration distances depending on the radial coordinate; this will have obvious consequences on the value of RLI (Figure 6.4 a') once the points at the same distance from the light source will have improved RLI values for increasing values of the modulus of the radial coordinate. As mentioned before, this effect is much more evident at higher cell concentrations due to the light

scattering effects provoked by the cells: In a limiting case, if no cells are present and if no light refraction occurs at the acrylic reactor wall, virtually no differences would be observed between the two geometries (Figure 6.4 *a, b*).

Figure 6.5 shows the attenuation of the light intensity as a function of the penetration distance for different microalgae concentrations and for the two reactor geometries under consideration, along the central radial coordinate ($r = 0$). These results confirm the analysis made from the data of Figure 6.4, but they also allow establishing correlations Eq. 6.2 and Table 6.1 between the *RLI* and the penetration distance (*Pd*) for both geometries.

$$RLI = y_0 + \left(\frac{a}{Pd}\right) + \left(\frac{b}{Pd^2}\right) + \left(\frac{c}{Pd^3}\right) \quad \text{Eq. 6.2}$$

where *RLI* is in %, *Pd* is in mm, and y_0 , *a*, *b*, and *c* are the regression coefficients, the values of which are presented in Table 6.1.

Table 6.1 Coefficients from Equation 2 for the circular and planar geometries and for different microalgae cell concentrations, with the respective value of R^2

PBR	[Cell] (kg.m ⁻³)	Coefficient (x10 ⁻²)				R ²
		y_0	<i>a</i>	<i>b</i>	<i>c</i>	
Circular	0.35	-0.1147	9.9044	-22.023	-17.7474	0.999
	0.50	-0.0221	1.0641	53.426	-209.136	0.999
	0.95	-0.0154	0.01973	18.3721	-56.1530	0.999
Planar	0.35	-0.1284	9.9721	-25.1507	-13.2912	0.999
	0.50	-0.0207	0.9085	50.9146	-193.400	1.00
	0.95	0.0356	-2.1538	44.9657	-130.148	0.999

This equation is a third-order inverted polynomial, which was chosen among six other possible models available in SigmaPlot (trial version, Systat software, Inc; Germany). These correlations will be useful when establishing the final design of the airlift bioreactor and, later on, during scaling up procedures.

It is generally accepted that a culture can be considered under darkness conditions when the light intensity is below a certain limit (between 0 and 15 $\mu\text{E m}^{-2}\text{s}^{-1}$, according to Suh and Lee (2003), in the present work, an intermediate value of 7.0 $\mu\text{E m}^{-2}\text{s}^{-1}$ was used, which corresponds to 10% of the light intensity used as reference). The volume fraction of the reactor above the limit of darkness was, thus,

calculated based on the axial relative light intensity distribution represented in Figure 6.4. This volume fraction was calculated for both reactor geometries and is compared in Figure 6.6.

For instance, at a cell concentration of 0.5 kg m^{-3} , the volume which receives a light intensity above $7.0 \mu\text{E m}^{-2}\text{s}^{-1}$ corresponds to 94% and 71% of the total volume of the PBR_C and PBR_P, respectively, while those values are reduced to 43% and 23%, respectively, at a cell concentration of 1.5 kg m^{-3} .

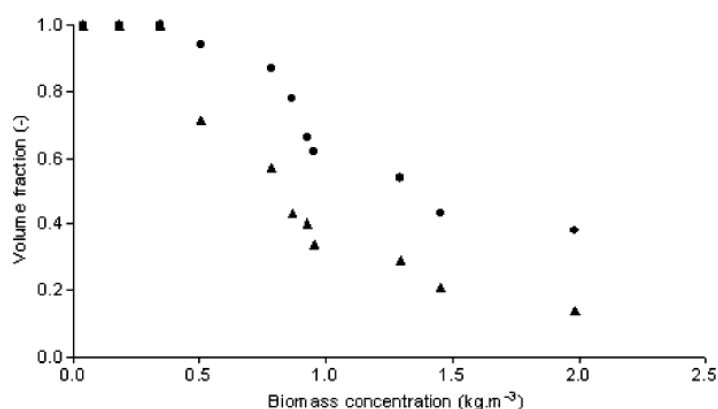


Figure 6.6 Volume fraction of the PBR (referred to the total culture volume) where the *RLI* is higher than 10% of the reference intensity ($70 \mu\text{E m}^{-2}\text{s}^{-1}$); ● PBR_C, ▲ PBR_P

The results in Figure 6.6, thus, show that the circular geometry allows a better light penetration for similar microalgae cell concentrations than the planar geometry, which means that a higher volume fraction of the reactor will be receiving sufficient amounts of light to avoid darkness conditions. Based on Figure 6.6 and considering all the other constant variables, the volumetric productivity is expected to be higher in a PBR with a circular geometry.

Qualitative characterization of light

Microalgal pigments change with algal variety, and therefore, the influences of different light qualities upon the physiological properties of different algae, such as growth, photosynthesis, and cellular metabolism, are diverse. Figure 6.7 shows the changes in the quality of the light reaching different depths inside the PBR. The depletion of light at certain wavelengths is obvious and, *e.g.*, for a cell concentration of 0.95 kg m^{-3} , almost all the radiation in the range of 400 – 450 and 650 – 680 nm is absorbed/scattered in the first 5 mm of cell suspension. The attenuation of light was

higher for the blue (400 – 500 nm) and red (650 – 700 nm) regions of the spectrum than for the green region (500 – 650 nm), which was more obvious at a higher cell concentration. This is because blue and red lights are mostly consumed by the microalgae, while the green light could penetrate further into the algal suspension (Yun and Park, 2001).

These results are due to the fact that the main pigments present in the cells of *C. vulgaris* (carotenoids and chlorophylls) absorb preferentially in the “blue” region and in the “red” region in the case of chlorophyll. *C. vulgaris* is known to be deficient in pigments absorbing light around 550 nm (green light) (Janssen *et al.*, 2003).

Apparently, only when preferred wavelengths are “consumed” will the system start to use other less-preferred wavelengths. This hypothesis is supported by Figure 6.8, where it is shown that while the relative intensity in the blue and red regions is still considerable (above 20%), the less-preferred wavelengths remain with very high intensities (close to 100%).

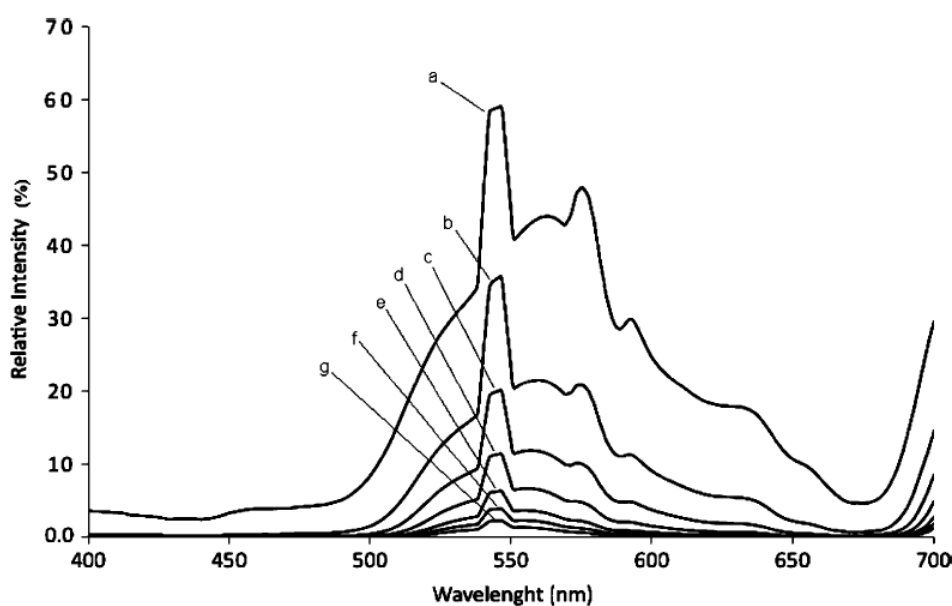


Figure 6.7 Relative light intensity spectra for different light penetration distances within the PBR_c (cell concentration=0.95 kg m⁻³); *a* 5 mm, *b* 10 mm, *c* 15 mm, *d* 20 mm, *e* 25 mm, *f* 30 mm, and *g* 35 mm.

However, when the blue and red regions are almost totally absorbed, the system seems to effectively start absorbing in the green region of the spectrum. Regardless of the wavelength of the light, the *RLI* declined with increasing cell concentration and eventually, reached zero when the cell concentration was higher (Yun and Park,

2001). Since photons are particles, the light is not only absorbed but also scattered randomly in the medium. Light scattering, thus, justifies that despite not being absorbed by the microalgae cells, green light was considerably attenuated in the algal suspension.

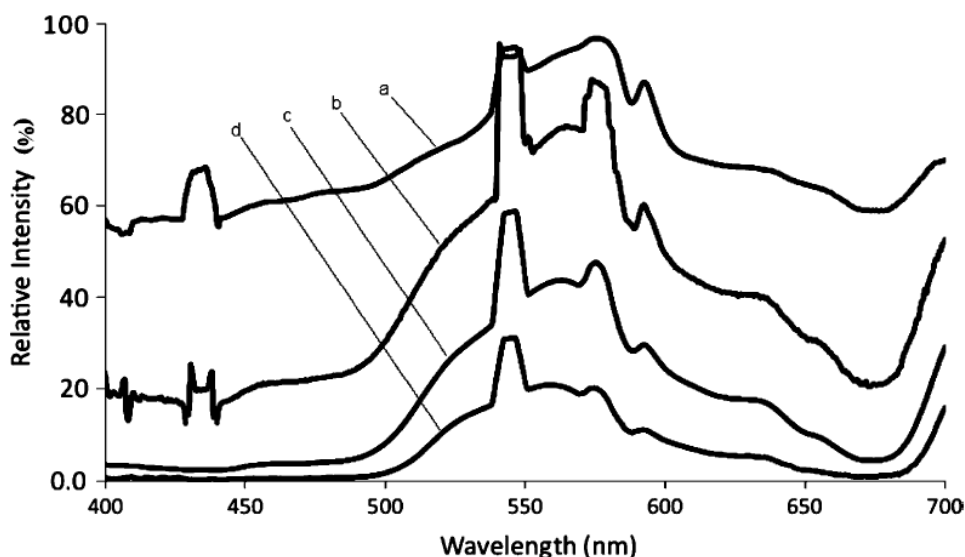


Figure 6.8 Relative light intensity spectra for different cell concentrations within PBR_c (light penetration distance=5 mm); a 0.18 kg m⁻³, b 0.50 kg m⁻³, c 0.95 kg m⁻³, and d 1.99 kg m⁻³.

6.3.5 Conclusions

Optical fibre technology was used as a new methodology for the characterization of light regime in a PBR, thus allowing the quantitative and qualitative characterization of light in two different geometries of a PBR. It was concluded that when compared with the planar geometry, the circular geometry allows a more efficient light penetration and a higher fraction of illuminated volume inside the PBR. It was shown that the attenuation of light intensity is dependent on its wavelength, cell concentration, geometry of PBR, and the penetration distance of light. An equation to correlate the *RLI* with the penetration distance (*Pd*) for both geometries, and different microalgae cell concentrations is now available. These results and methodologies presented here will be determinant to improve the design of the PBR towards a more efficient utilization of light energy with expected improvements of biomass yield.

6.4 Split Cylinder Airlift Photobioreactor (SCAPBR) description

After reviewing all the elements presented (subchapters 6.1 – 6.3), it was concluded that the split column airlift PBR (SCAPBR) with circular geometry is the most suitable cultivation system for mass production of microalgae.

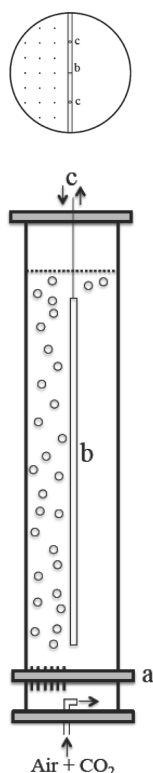


Figure 6.9 The geometry of SCAPBR and air sparger (frontal and top view). Sparger (*a*); baffle (*b*); heat exchanger inlet and outlet (*c*).

In the proposed SCAPBR (Figure 6.9), a flat plate splits the diameter of the column and separates the column into two parts (the riser and the downcomer regions), acting also as a heat exchanger and an internal light guide, as will be explained below. The SCAPBR selection and the options made in the project design had as objective to overcome some of the main limitations of existing microalgae cultivation systems.

The first, and probably the most important project consideration, is the issue of light distribution inside the PBR and its efficient utilization by the microalgae cells. The fact that this PBR operates using the airlift principle ensures that the cells will experience regular cycles of light and dark due to their regular movement pattern inside the PBR. As previously mentioned, these regular cycles of light/dark reduce

effects of photolimitation and photoinhibition, causing an increase of biomass productivity. Additionally, the fact that it is a SCAPBR instead of a concentric tube airlift decreases the volume of PBR subjected to total darkness.

Secondly, since the flat plate that splits the column into the riser and the downcomer regions is made of a transparent material and fully filled with water, it also acts as a light conductor and distributor inside the SCAPBR (Figure 6.10), thereby significantly increasing the PBR illuminated surface.

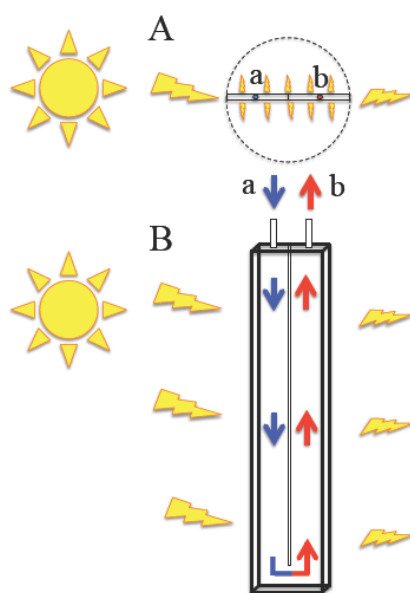


Figure 6.10 Schematic representation of top view (A) and front view (B) of SCAPBRs baffle, acting as heat exchanger and light guide. Cold water inlet (*a*); warm water outlet (*b*).

Thus, the central area of the PBR which normally would be completely devoid of light (specially for higher cell concentrations) will have a continuous supply of light. The presence of this central baffle also allows using diameters in the SCAPBR scale-up which would be otherwise impossible due to a substantial increase of dark zones within the PBR. This idea of supplying light via conducting structures inside the reactor volume is not new. A long list of authors have been using fibre optics as light guides and fibre optics light concentration systems (Feuermann and Gordon, 1999; An and Kim, 2000; Gordon, 2002; Ono and Cuello, 2004; Chen *et al.*, 2006, 2008) in order to deliver light inside the PBR. Also Zijffers *et al.* (2008_a, 2008_b) present some solutions to deliver light inside the PBR such as vertical plastic light guides and Fresnel lens. However these solutions are too expensive, difficult to implement or

have some influence in PBR hydrodynamics. The proposed design for this SCAPBR, in turn, does not require the use of expensive technologies/materials or the introduction of elements that disturb the normal PBR hydrodynamics and can be used easily without compromising the cultivation sterility.

Thirdly, besides allowing the existence of an airlift principle (by dividing the riser from the downcomer) and a larger illuminated reactor surface, the central wall of the PBR also functions as heat exchanger (Figure 6.10), thus ensuring an efficient cooling of the medium without the need of a large technical apparatus nor the use of large amounts of water.

Typical cooling mechanisms are submersion of the entire culture in a water pool, spraying with water, shading, or incorporating a heat exchanger within the PBR for cooling (Mehlitz, 2009). These methods, however, are often expensive, inefficient and with high spending of water. The proposed incorporated cooling system (Figure 6.10) is of major importance because it is known that, during outdoor cultivation with sun as the light source, biomass productivity is strongly affected by temperature. The temperature of microalgal culture broths in photobioreactors can increase to about 40 - 50 °C by irradiation of sunlight. The microalgal growth would be highly inhibited at such temperatures if the cultivation is not provided with an efficient cooling system (Ong *et al.*, 2010).

To ensure an efficient mass transfer inside the SCAPBR an aeration system was developed (Figures 6.11 and 7.1). The sparger was built with a set of needles (0.25 mm of internal diameter) with the objective of guaranteeing high mass transfer coefficients, while ensuring that the O₂ concentration within the PBR does not reach levels that may cause cell growth inhibition.

More detailed technical information about SCAPBR, the aeration system and its dimensions are given in Chapter 7. Considering all the characteristics presented (subchapters 6.2 – 6.3), SCAPBR have the potential to provide conditions for an ideal microalgae cultivation: proper exposition to light energy, good mass exchange between the gas and the liquid, flow mixing, low shear stress over the cells and a proper temperature control. In order to provide the best conditions for microalgae in SCAPBR, it is of interest to determine and optimize all the parameters that

characterize SCAPBR operation.

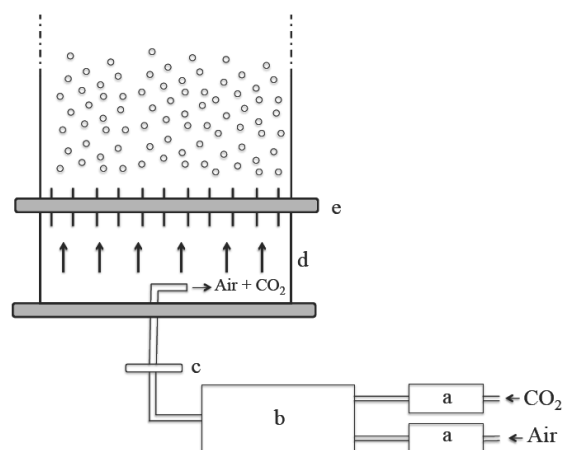


Figure 6.11 Schematic representation of the aeration system used in the tested PBRs. Mass flow controller (a); gas mixing chamber (b); air filter (c); pressure chamber (d); needle sparger (e).

In Chapter 7 an extensive characterization of gas and liquid phases, as well as mass transfer, light distribution profile and flow pattern characterization will be made in order to evaluate SCAPBR performance and to correlate these parameters with the obtained productivity in each of the tested operation conditions.

6.5 References

- An J-Y, Kim B-W., 2000. Biological desulfurization in an optical-fiber photobioreactor using an automatic sunlight collection system. *J Biotechnol.*, 80: 35-44.
- Barbosa M. J., Hoogakker J., Wijffels R. H., 2003_a. Optimisation of cultivation parameters in photobioreactors for microalgae cultivation using the A-stat technique. *Biomolecular Engineering*, 1-9.
- Barbosa M. J., Janssen M., Ham N., Tramper J., Wijffels R. H., 2003_b. Microalgae cultivation in air-lift reactors: Modelling biomass yield and growth rate as a function of mixing frequency. *Biotechnol Bioeng* 82:170-179
- Borja R., Travieso L., Hall D. O., Rao K. K., Benitez F., Sanchez E., 2001. A helical tubular photobioreactor producing *Spirulina* in a semicontinuous mode. *International Biodeterioration & Biodegradation* 47: 51-155.
- Camacho F. G., Gomez A. C., Fernandez F. G. A., Sevilla J. F., Grima E. M., 1999. Use of concentric tube airlift photobioreactors for microalgal outdoor mass cultures. *Enzyme Microb Technol*, 24: 164-72.
- Chen F., 1996. High cell density culture of microalgae in heterotrophic growth. *Trends in Biotechnology*, 14: 421-426.
- Chen C-Y., Lee C-M., Chang J-S., 2006. Feasibility study on bioreactor strategies for enhanced

- photohydrogen production from *Rhodospseudomonas palustris* WP3-5 using optical-fiberassisted illumination systems. *Int J Hydrogen Energy*, 31: 2345-2355.
- Chen C-Y., Saratale G. D., Lee C-M., Chen P-C., Chang J-S., 2008. Phototrophic hydrogen production in photobioreactors coupled with solar-energy-excited optical fibers. *Int J Hydrogen Energy*, 33: 6886-6895.
- Chisti Y., Grima E. M., Belarbia E. H., Fernandez F. G. A., Medina, A. R., 2003. Recovery of microalgal biomass and metabolites: process options and economics. *Biotechnology Advances* 20: 491–515.
- Csogor Z., Herrenbauer M., Perner I., Schmidt K., Posten C., 1999. Design of a photo-bioreactor for modeling purposes, *Chem. Eng. Process.*, 38: 517–523.
- Cuaresma M., Janssen M., Vilchez C., Wijffels R. H., 2011. Horizontal or vertical photobioreactors? How to improve microalgae photosynthetic efficiency. *Bioresour Technol.*, 102: 5129–1537.
- Degen J.; Uebele A.; Retze A.; Schmid-Staiger U.; Trosch W., 2001. A novel airlift photobioreactor with baffles for improved light utilization through the flashing light effect. *J. Biotechnol.* 92: 89-94.
- Douskova I., Doucha J., Machat J., Novak P., Umysova D., Vitova M., Zachleder V., 2008. Microalgae as a means for converting flue gas CO₂ into biomass with a high content of starch, *Bioenergy: Challenges and Opportunities. International Conference and Exhibition on Bioenergy*, April 6th – 9th 2008, Universidade do Minho, Guimaraes, Portugal.
- Erickson L. E., Lee H. Y., 1986. Process analysis and design of algal growth systems. In: Barclay, W., McIntosh, R.P. (Eds.), *Algal Biomass Technologies: An Interdisciplinary Perspective*. Nova Hedwigia, Berlin, pag 197.
- Eriksen N. T., 2008. The technology of microalgal culturing. *Biotechnology Letters*, 30: 1525–1536.
- Fernandes B., Dragone G., Teixeira J., Vicente A., 2010. Light regime characterization in an airlift photobioreactor for production of microalgae with high starch content. *Appl. Biochem. Biotechnol.* 161: 218–26.
- Feuermann D, Gordon J. M., 1999. Solar fiber-optic mini-dishes: a new approach to the efficient collection of sunlight. *Solar Energy*, 65: 159-170.
- Frohlich B. T., Webster I. A., Ataa M. M., Shuler M.L., 1983. Photobioreactors: models for interaction of light intensity, reactor design and algal physiology. *Biotechnol. Bioeng. Symp.* 13: 331–350.
- Gordon J. M., 2002. Tailoring optical systems to optimized photobioreactors. *Int J Hydrogen Energy*, 27: 1175-1184.
- Gordon J. M., Polle J. E. W., 2007. Ultrahigh bioproductivity from algae. *Applied Microbiology and Biotechnology*, 76: 969–975.
- Grima E. M., Fernández F. G. A., Camacho F. G., Chisti Y., 1999. Photobioreactors: light regime, mass transfer, and scaleup. *J Biotechnol*, 70: 231–47.
- Hu Q., Guterman H., Richmond A., 1996. A flat inclined modular photobioreactor for outdoor mass

- cultivation of photoautotrophs. *Biotechnol. Bioeng.* 51: 51–60.
- Hu Q., Faiman D., Richmond A., 1998. Optimal tilt angles of enclosed reactors for growing photoautotrophic microorganisms outdoors. *J. Ferment. Bioeng.*, 85(2): 230–236.
- Jacob-Lopes E., Scoparo C. H. G., Lacerda L. M. C. F., Franco T. T., 2009. Biotransformations of carbon dioxide in photobioreactors. *Chemical Engineering and Processing*, 48(1): 306–310.
- Janssen M., Tramper J., Mur L. R., Wijffels R. H., 2003. Enclosed outdoor photobioreactors: Light regime, photosynthetic efficiency, scale-up, and future prospects. *Biotechnology and Bioengineering* 81: 193-210.
- Krichnavaruk S., Loataweesup W., Powtongsook S., Pavasant P., 2005. Optimal growth conditions and the cultivation of *Chaetoceros calcitrans* in airlift photobioreactor. *J. Chem. Eng.*, 105: 91–98.
- Laws E. A., 1980. Nutrient and light limited growth of *Thalassiosira fluviatilis* in continuous culture with implications for phytoplankton growth in the ocean. *Limnol. Oceanogr.*, 25: 455–473.
- Lee Y. K., Pirt S. J., 1981. Energetics of photosynthetic algal growth: influence of intermittent illumination in short (40 s) cycles. *Journal of General Microbiology* 124: 43–52.
- Lee Y. K., 1997. Commercial production of microalgae in the Asia–Pacific rim, *J. Appl. Phycol.*, 9: 403–411.
- Lee C. G., Jong K. N., Suh I. S., Hur B. K., 2002. Simple monodimensional model for linear growth rate of photosynthetic microorganisms in flat–plate photobioreactors. *Journal Microbiology Biotechnology*, 12: 962–971.
- Lou H-P., Kemoun A., Al-Dahhan M. H., Sevilla J. M. F., Sánchez J. L. G., Camacho F. G., Molina Grima E., 2003. Analysis of photobioreactors for culturing high-value microalgae and cyanobacteria via an advanced diagnostic technique: CARPT. *Chem Eng Sci.*, 58: 1519–1527
- Loubière K., Olivo E., Bougaran G., Pruvost J., Robert R., Legrand J., 2009, A new photobioreactor for continuous microalgal production in hatcheries based in external-loop airlift and swirling flow, *Bioeng. Biotech.*, 102 (1): 132-147
- Loubière K., Pruvost J., Aloui F., Legrand J., 2011. Investigations in an external-loop airlift photobioreactor with annular light chambers and swirling flow. *Chem. Eng. Res. Des.*, 89: 164–171.
- Mehlitz, 2009. Temperature influence and heat management requirements of microalgae cultivation in PBRs. San Luis Obispo: California Polytechnic State University;
- Merchuk J.C., Ronen M., Giris S., Arad (Malis) S., 1998. Light/dark cycles in the growth of the red microalga *Porphyridium* sp. *Biotechnology and Bioengineering* 59: 705–713.
- Merchuk J. C., Garcia-Camacho F., Molina-Grima E., 2007. *Chemical and Biochemical Engineering Q*, 21(4): 345–355.
- Mirón A., Contreras Gómez A, García Camacho F, Molina Grima E, Chisti Y., 1999. Comparative evaluation of compact photobioreactors for large-scale monoculture of microalgae. *Journal of Biotechnology* 70: 249-270.
- Mirón A., Garcia M-C. C., Camacho F. G., Grima E. M., Chisti Y., 2002. Growth and biochemical characterization of microalgal biomass produced in bubble column and airlift photobioreactors:

- studies in fed-batch culture, *Enzyme and Microbial Technology*, 31(7): 1015-1023.
- Mirón A. S., García M-C, Gómez A. C., Camacho F. G., Grima E. G., Chisti Y., 2003. Shear stress tolerance and biochemical characterization of *Phaeodactylum tricornutum* in quasi steady-state continuous culture in outdoor photobioreactors. *Biochem Eng J.*, 16: 287–97.
- Oncel S., Sukan F. V., 2008. Comparison of two different pneumatically mixed column photobioreactors for the cultivation of *Arthrospira platensis* (*Spirulina platensis*). *Bioresour Technol.*, 99: 4755–4760.
- Ong S. C., Kao C. Y., Chiu S. Y., Tsai M. T., Lin C. S., 2010. Characterization of the thermal-tolerant mutants of *Chlorella* sp. with high growth rate and application in outdoor photobioreactor cultivation. *Bioresour. Technol.* 101: 2880–2883.
- Ono E., Cuello J. L., 2004. Design parameters of solar concentrating systems for CO₂-mitigating algal photobioreactors. *Energy*, 29: 1651-1657.
- Petkov G. D., 2000. Absorber tower as a photobioreactor for microalgae. *Russian Journal of Plant Physiology* 47(6): 786–788.
- Posten C., Schaub G., 2009. Microalgae and terrestrial biomass as source for fuels –a process view. *J. Biotechnol.*, 142: 64–69
- Pruvost J., Legrand J., Legentilhomme P., Muller-Feuga A., 2002, Simulation of microalgae growth in limiting light conditions, *AIChE J.*, 48 (5): 110-1120.
- Pruvost J., Legrand J., Legentilhomme P., Muller-Feuga A., 2004, Effect of inlet type on shear stress and mixing in an annular photobioreactor involving a swirling decaying flow, *The Canadian Journal of Chemical Engineering*, 82: 1-9
- Pruvost J., Pottier L., Legrand, J., 2006. Numerical investigation of hydrodynamic and mixing conditions in a torus photobioreactor. *Chemical Engineering Science*, 61: 4476 – 4489.
- Rabe A. E., Benoit A., 1962. Mean light intensity. A useful concept in correlating growth rates of dense cultures of microalgae. *Biotechnol. Bioeng.*, 4: 337–390.
- Ranjbar R., Inoue R., Katsuda T., Yamaji H., Katoh, S., 2008. High Efficiency Production of Astaxanthin in an Airlift Photobioreactor. *Journal of Bioscience and Bioengineering*, 106(2): 204–207.
- Ree G.Y., Gotham I. J., 1981. The effect of environmental factors on phytoplankton growth: Light and interaction of light with nitrate limitation. *Limnol. Oceanogr.*, 26: 649–659.
- Singh R. N., Sharma S., 2012. Development of suitable photobioreactor for algae production – A review, *Renewable and Sustainable Energy Reviews*, 16 (4): 2347-2353.
- Suh I. S., Lee C.-G., 2003. Photobioreactor engineering: design and performance. *Biotechnol. Bioprocess Eng.*, 8: 313-321.
- Tredici M. R., 1999. Bioreactors, photo. In: Flickinger MC, Drew SW, eds. *Encyclopedia of Bioprocess Technology: Fermentation, Biocatalysis, and Bioseparation*. New York, NY: John Wiley & Sons, 395-419.
- Tsavalos M. H. A. J., Young A., 1996. Autotrophic growth and carotenoid production of *Haematococcus pluvialis* in a 30 liter air-lift photobioreactor. *Journal of Fermentation and*

- Bioengineering, 82: 113–118.
- Vega-Estrada J., Montes-Horcasitas M. C., Domínguez-Bocanegra A. R., Cañizares- Villanueva R. O., 2005. Haematococcus pluvialis cultivation in split-cylinder internal-loop airlift photobioreactor under aeration conditions avoiding cell damage. *Appl Microbiol Biotechnol*, 68: 31–35.
- Velarde R. R., Urbina E. C, Melchor D. J. H, Thalasso F., Villanueva R. O. C., 2010. Hydrodynamic and mass transfer characterization of a flat-panel airlift photobioreactor with high light path. *Chem Eng Process Process Intens.*, 49(1): 97–103.
- Vunjak-Novakovic G., Kim Y., Wu X., Berzin I., Merchuk J. C., 2005. Air-lift bioreactors for algal growth on flue gas: mathematical modeling and pilot-plant studies. *Ind Eng Chem Res.*, 44: 6154–63.
- Walter C., Steinau T., Gerbsch N., Buchholz R., 2003. Monoseptic cultivation of phototrophic microorganisms/development and scale-up of a photobioreactor system with thermal sterilization. *Biomolecular Engineering*, 1–11.
- Wang B., Lan C. Q., Horsman M., 2012. Closed photobioreactors for production of microalgal biomasses, *Biotechnology Advances*, 30 (4): 904-912.
- Weissman J. C., Goebel R. P., and Benemann J. R., 1988. Photobioreactor design: Mixing, carbon utilization, and oxygen accumulation. *Biotechnol. Bioeng.*, 31: 336–344
- Wu X., Merchuk J. C., 2001. A model integrating fluid dynamics in the photosynthesis and photoinhibition process. *Chemical Engineering Science* 56: 3527–3538.
- Wu X., Merchuk J. C., 2004. Simulation of Algae Growth in a Bench Scale internal Loop Airlift Reactor. *Chem Eng. Sci.*, 59: 2899-2912.
- Yun Y-S, Park J. M., 2001. Attenuation of monochromatic and polychromatic lights in *Chlorella vulgaris* suspensions. *Appl Microbiol Biotechnol* 55: 765–770.
- Zijffers J-W. F., Janssen M., Tramper J., Wijffels R. H., 2008_a. Design process of an area-efficient photobioreactor. *Mar Biotechnol*, 10: 404-415.
- Zijffers J-W. F., Janssen M., Tramper J., Wijffels R. H., 2008_b. Capturing sunlight into a photobioreactor: ray tracing simulations of the propagation of light from capture to distribution into the reactor. *Chem Eng J.*, 145: 316-327.
- Zittelli G. C., Rodolfi L., Biondi N., Tredici M. R., 2006. Productivity and photosynthetic efficiency of outdoor cultures of *Tetraselmis suecica* in annular columns. *Aquaculture*, 261:932–943.

CHAPTER 7

Characterization and performance evaluation of SCAPBR as microalgae cultivation system

7.1 Abstract	159
7.2 Introduction	159
7.3 Methodology	161
7.4 Results and discussion	167
7.5 Conclusions	189
7.6 References	189

The results presented in this chapter were adapted from:

Bruno D. Fernandes, André Mota, António Ferreira, Giuliano Dragone, José A. Teixeira, António A. Vicente. *Characterization of a low cost split cylinder airlift for efficient microalgae production. – Submitted to Chemical Engineering Journal.*

Bruno D. Fernandes, André Mota, João L. Oliveira, Giuliano Dragone, José A. Teixeira, António A. Vicente. *Influence of light distribution profile and microalgae cells flow pattern on biomass productivity for different column photobioreactors – Submitted to Bioresource Technology.*

7.1 Abstract

An extensive characterization of PBRs must be made in order to optimize their operational conditions, operate design improvements and perform scale-up. It was performed a hydrodynamic characterization of liquid and gas phases, as well as the determination of mass transfer coefficient, light distribution profile and flow pattern of three different PBRs (bubble column (BC), and two SCAPBRs: SCAPBR 75 and SCAPBR 50). The effect of these parameters on biomass productivity was evaluated.

The developed SCAPBRs proved to be extremely suitable for microalgae cultivation. The design of the PBR, particularly the designed gas sparger, allowed meeting the needs of microalgae in terms of mixing and mass transfer (efficient supply and removal of CO₂ and O₂, respectively). SCAPBR 50 (at $U_{Gr} = 0.0044 \text{ m s}^{-1}$) showed, among the tested PBRs, the highest value of biomass volumetric productivity ($0.75 \text{ g L}^{-1} \text{ d}^{-1}$). This result is due to higher efficiency of light distribution inside the PBR and to a regular and defined flow pattern, which allows exposing cells to regular light - dark periods.

Keywords: SCAPBR; bubble column; hydrodynamic; cells' light history; biomass productivity.

7.2 Introduction

Unlike other biological systems in which, usually, there is a factor that is clearly predominant compared to all the others (*e.g.* efficient mass transfer or medium composition), in microalgae cultivation the balance between different factors (*e.g.* light supply, fluid dynamics and mass transfer) must be achieved in order to optimize the system productivity. If the PBR operation conditions are optimized to maximize mass transfer this will conduct to an efficient CO₂ supply to the cells and an effective O₂ removal, reducing, by this way, the potential stress and theoretically increasing the productivity. However, if this increase in mass transfer coefficient was achieved at the expense of a modification in the pattern of cells exposure to light, this might cause a decrease in the system productivity. This occurs because light availability in vertical PBRs is influenced by several factors such as aeration

rate, gas holdup, and liquid velocity (mixing and turbulence) (Miron et al., 2000).

In Chapter 6 a novel split cylinder airlift photobioreactor (SCAPBR) was proposed as a very promising microalgae cultivation system, due to a number of characteristics: vertical arrangement; a regular cells pattern movement; integrated temperature control system and transport of light to the centre of PBR. At this stage it is necessary to prove some of the assumptions on which its design was based.

Several authors like Lee and Pirt (1981), Merchuk *et al.* (1998), Wu and Merchuk (2001) refer to the regular and defined pattern flow offered by airlift PBRs as a very important factor for increasing productivity, however to our knowledge none of them fully proved this statement. Increased productivity caused by a regular and defined pattern flow of cells within the airlifts can only be confirmed by firstly ensuring that all the requirements in terms of mixing efficiency and mass transfer (mainly CO₂ supply and O₂ removal) are met and that none of these elements is a limiting factor to growth. After these requisites are assured, it is necessary to analyse the flow patterns of the airlift PBR in order to check the pattern of movements to which the cells are subjected within the PBR. Subsequently the cells flow pattern within the PBR will be correlated with light regime inside the PBR and with the obtained productivity, in order to be able to assess if the flow pattern is actually a key factor to increase microalgal productivity in SCAPBRs.

This kind of study requires a deep knowledge of the cultivation system fluid dynamics and light distribution (Fernandes *et al.*, 2010). Hydrodynamics and mass transfer characteristics that are applicable include: the mass transfer coefficient (K_La), mixing time, liquid velocity, gas bubble velocity and gas holdup. The nutritional and light requirements of photosynthetic microorganisms may be covered in PBRs with larger light paths, if hydrodynamic and mass transfer conditions are optimized in these PBRs (Velarde *et al.*, 2010). Knowledge on fluid trajectories in the PBR is required in order to describe properly the light history of a photosynthetic cell (Fernandes *et al.*, 2010). Only taking into account this point will allow to predict correctly the effects of scale-up on the performance of the SCAPBR. In this chapter a full characterization of two different SCAPBRs

(SCAPBR 50 and SCAPBR 75) and a bubble column (BC) (used as a control PBR) will be carried out.

7.3 Material and methods

7.3.1 Description of tested photobioreactors

Three different PBRs were used: a bubble column (BC) and two different SCAPBRs, as shown schematically in Figure 7.1.

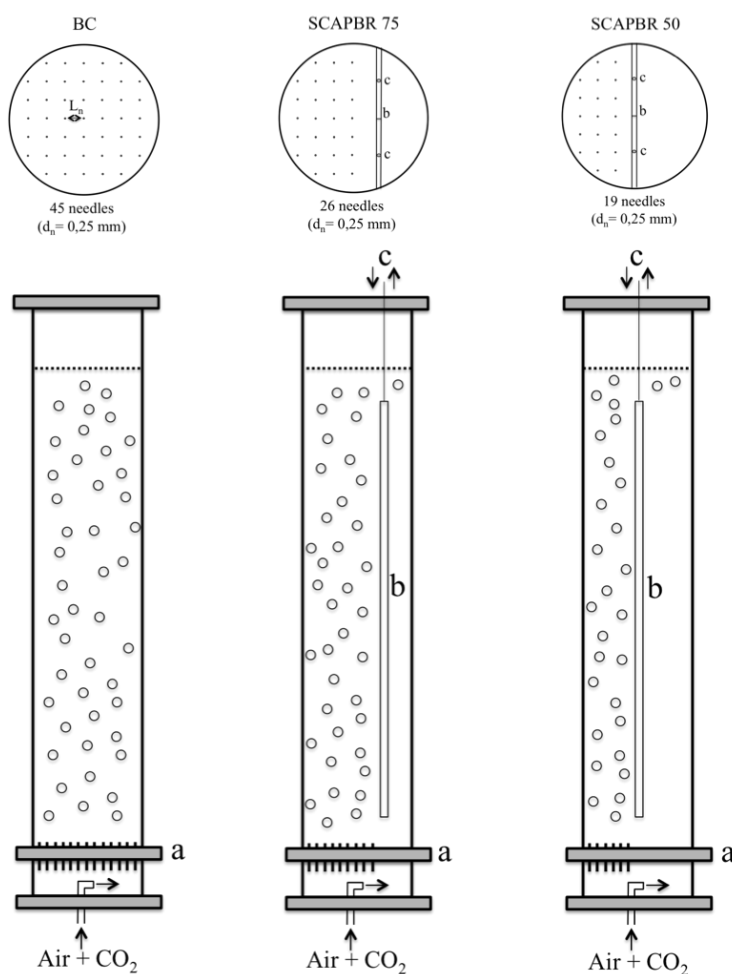


Figure 7.1 The geometry of photobioreactors and air spargers (frontal and top view). Sparger (*a*); baffle (*b*); heat exchanger inlet and outlet (*c*).

All vessels were made of 3.8 mm thick, transparent poly(methyl methacrylate) with 90 mm of internal diameter. The liquid height was 600 mm, for a working volume of 3.7 L. All the three PBRs have a total height of 700 mm. The riser-to-downcomer cross sectional area ratio was 1.0 for the SCAPBR 50 and 3.0 for the

SCAPBR 75. The baffles, with 4.0 mm of thickness, were located 50 mm from the bottom of the PBRs and 50 mm below the liquid level and were also made of transparent poly(methyl methacrylate) to allow light penetration.

7.3.1.1 Description of aeration system

The fluid was mixed by sparging with CO₂-enriched air (2% v/v CO₂) through a sparger composed by 45, 26 and 19 uniformly spaced needles (with an inner diameter (d_n) of 0.25 mm) in the BC, SCAPBR 75 and SCAPBR 50, respectively. In all the spargers, needles were placed with a spacing (L_n) of 5.0 mm between them (Figure 7.1). The shape and size of the needles ensure the formation of small and well-defined bubbles. Needles' disposal enables a uniform bubble distribution along the PBRs, which enhances the suspension of low-density solids.

The aeration system consists of two mass flow controllers that determine the CO₂ and air flow rates; these gases are subsequently mixed in a gas mixing chamber and filter before being delivered into the PBR by the sparger. Between the filter and the gas sparger there is a pressure chamber, which allows a homogeneous gas distribution through all needles even at low flow rates (Figure 6.11).

7.3.2 Hydrodynamic and mass transfer characterization of PBRs

All the hydrodynamic and mass transfer tests were performed at different superficial gas velocities (U_{Gr}) (0.001 – 0.01 m s⁻¹) based on the riser cross-section of the reactors. The superficial gas velocity U_{Gr} is easily derived from the air flow rate by dividing this last one by the cross-sectional area of the aerated zone.

All the measurements were made at 25 °C with tap water and microalgae growth medium. The viscosities of growth medium and tap water were approximately the same (0.998 x 10⁻³ Pa s). The viscosities were measured at 25 °C using a Cannon–Fenske viscometer. The surface tension of the fluids was also approximately the same (72.3 x 10⁻³ N m⁻¹). The surface tension was measured at 25 °C using a tensiometer (Kruss K6 GmBH, Germany). The conductivity (Conductivity Meter LF 538, WTW, Germany) of water and growth medium was 2.07 and 516.67 μS

cm⁻¹, respectively.

7.3.2.1 *Liquid phase characterization*

Mixing and circulation time

For determination of mixing time and circulation time, 1 mL of saturated NaCl aqueous solution was injected as a pulse near the bottom of the riser in the central region through a 1 mm stainless steel capillary by means of a syringe. The tracer influence in the system was measured by a conductivity probe (Conductivity Meter LF 538, WTW, Germany) placed near the top of the riser (Baten *et al.*, 2003). For each operating condition, experiments were run five times. The liquid phase was changed after each three runs.

Mixing time was defined as the time needed to reach 95% of complete mixing. The circulation time was computed by averaging the time spans between maximum consecutive peaks in the conductivity probe response curve (Freitas *et al.*, 2000).

Liquid circulation velocity

The mean liquid circulation velocity in the riser was obtained using a thermal tracer method, which gives the fastest response time among the various tracer methods available. The thermal tracer method involves injecting a pulse of 5 cm³ of hot water into the flowing liquid and plotting the time-temperature profile at two given points in the riser by means of two thermocouples connected to a computer. The liquid linear velocity in the riser was then obtained by the ratio of the distance between the two thermocouples and the differences in response times between the two sensors as described by Garcia-Calvo *et al.* (1999).

7.3.2.2 *Gas phase characterization*

Gas holdup

Riser gas holdup in the PBRs was determined by the use of monofibre optical probe technology described by Mena *et al.* (2008). Briefly, the optical probe is used to locally detect the presence of the gas phase in a multiphase system. A monochromatic light is transmitted through an optical fibre to the tip of the probe.

When the tip is dipped into a gas phase, the light is mainly reflected, travels back to the detector through a Y junction and is converted into an electrical signal (high level signal). This signal is converted to a digital signal which is then interpreted by the So2_4 software (Mena *et al.*, 2008), which finally provides the values of gas holdup. In order to obtain values with a statistical meaning, about 2000 bubbles were analysed for each experimental condition.

Bubble characterization

In order to obtain the bubble size distribution (Sauter mean diameter (d_{32})), bubble elongation (F_{max}/F_{min}) and bubble complexity degree (B_{CD}), a chamber with a flat straight section, filled with water was coupled to the PBRs. The chamber was designed in order to minimize the problems related with the effect of bubble position in the column on bubble size measurement using image analysis techniques. In this way, it was possible to reduce the error associated to this effect. Sets of images, obtained at 200 mm from the gas sparger, were grabbed with a black and white high speed digital video camera (frame rate of 250 images s^{-1}) connected to a PC, and used to study the bubble shape and size distribution. After the acquisition a set of images (about 5 images s^{-1}), these were automatically treated and the bubbles were identified and classified. For that, the image analysis technique and the discriminant factorial analysis were combined as described by Ferreira *et al.* (2012). In order to obtain values with a statistical meaning, about 600 bubbles were analysed for each experimental condition, this number is in accordance with the values presented by Ferreira *et al.* (2012).

Bubble gas velocity in the BC and in the SCAPBRs riser were also measured by means of the optic probe technique, previously described by Mena *et al.* (2008) and used for gas holdup determination. In order to obtain values with a statistical meaning, about 2000 bubbles were analysed for each experimental condition.

7.3.2.3 Mass transfer coefficient (K_{La}) of carbon dioxide

In microalgae cultivation, gas-liquid mass transfer of CO_2 is of major importance, because CO_2 is the main carbon source. Therefore, it is necessary to determine the volumetric mass transfer coefficient K_{La} (CO_2) that allows

characterizing the CO₂ transfer rate between gas and liquid phases.

According to the literature (Nielsen and Villadsen, 1994; Baquerisse *et al.*, 1999), volumetric mass transfer coefficients depend on the physical properties of the liquid, on the liquid flow and on system and gas injector geometries. Thus, the calculation of K_La of CO₂ has been done according to Eq. 7.1 from the determination of the K_La of O₂ :

$$K_La(CO_2) = \sqrt{\frac{D_{O_2}}{D_{CO_2}}} \cdot K_La(O_2) \quad \text{Eq. 7.1}$$

Oxygen mass transfer experiments were performed in a two-phase system at different superficial aeration velocities (U_{Gr}) (0.001 – 0.008 m s⁻¹) and liquids (water and mineral growth medium). Air was used as gas phase. The liquid height was $h_0 = 600$ mm for all experiments (no liquid throughput). Initially the liquid was deoxygenated by bubbling nitrogen. When the dissolved oxygen concentration was practically zero, humidified air is fed into the column. Dissolved oxygen concentration values were measured online using an O₂ electrode (CellOx 325, WTW, Germany), located 200 mm from the gas sparger and 30 mm from the wall, and recorded directly in a PC, through a data acquisition board. In this way, dissolved oxygen concentration data *versus* time, t , were obtained, and K_La was calculated according to Ferreira *et al.* (2012).

7.3.3 Evaluation of PBRs biomass productivity

Chlorella vulgaris (P12) obtained from the Culture Collection of Algal Laboratory (CCALA, Czech Republic), was used for cultivation. The inoculum for the photobioreactors was grown under artificial light (250 μE.m⁻² s⁻¹ light flux at the vessel's surface) in a 1 L bubble column aerated at 0.5 vvm. The preculture medium was identical to that used in the final reactor cultivation. The carbon source and agitation during cultivation of microalgae were supplied by bubbling CO₂-enriched air (2% v/v CO₂) through a needle sparger (Figure 6.11 and 7.1).

The three tested PBRs were placed in a fully closed compartment with controlled temperature, in order to maintain cultures at 30 °C. Illumination was provided by 8 fluorescent lamps (Sylvania Standard 36 FW) on one side of the

photobioreactors, at an irradiance level of $250 \mu\text{E}\cdot\text{m}^{-2} \text{ s}^{-1}$, measured using a LICOR Quantum/Radiometer/Photometer Model LI-250 Light Meter (San Diego, CA, USA).

The growth medium based on chemical components present in the microalgal biomass (Douskova *et al.*, 2009) had the following composition (mM): 18.32 $(\text{NH}_2)_2\text{CO}$, 1.74 KH_2PO_4 , 0.83 $\text{MgSO}_4\cdot 7\text{H}_2\text{O}$, 0.79 CaCl_2 , 0.11 $\text{FeNa}\cdot\text{C}_{10}\text{H}_{12}\text{O}_8\text{N}_2$, 0.017 $\text{MnCl}_2\cdot 4\text{H}_2\text{O}$, 0.013 H_3BO_3 , 0.009 $\text{ZnSO}_4\cdot 7\text{H}_2\text{O}$, 0.004 $\text{CuSO}_4\cdot 5\text{H}_2\text{O}$, 0.002 $\text{CoSO}_4\cdot 7\text{H}_2\text{O}$, 0.0001 $(\text{NH}_4)_6\text{Mo}_7\text{O}_{24}\cdot 4\text{H}_2\text{O}$ and 0.0001 $(\text{NH}_4)\text{VO}_3$ in distilled water. The medium was inoculated using inoculum in the late exponential growth phase after cell synchronization. Biomass concentration in the freshly inoculated PBRs was about $0.05 \text{ kg}\cdot\text{m}^{-3}$.

In order to determine how the hydrodynamic and mass transfer parameters affect the system productivity, microalgae cultivations were made at 3 different conditions ($U_{Gr} = 0.0011$; 0.0044 and; 0.0077 m s^{-1}) in each of the 3 different tested PBRs.

Biomass concentration was estimated by cell dry weight after centrifugation of the sample (8,750 g for 10 min), washing with distilled water and drying at $105 \text{ }^\circ\text{C}$ until constant weight.

Biomass productivity (P_{max} , $\text{g L}^{-1} \text{ d}^{-1}$) during the culture period was calculated from Eq. 7.2, where X_t is biomass concentration (g L^{-1}) at the end of the exponential growth phase (t_x) and X_0 is the initial biomass concentration (g L^{-1}) at t_0 (day).

$$P_{max} = (X_t - X_0)/(t_x - t_0) \quad \text{Eq. 7.2}$$

7.3.4 Determination of cells' light history

In order to know the cells' light history inside the PBRs, light regime characterization inside the PBRs and particle tracking movement were performed.

7.3.4.1 Light regime characterization

Light regime characterization was performed in the three different PBRs at three different cell concentrations (0.25 ; 0.50 and, 1.0 g L^{-1}) using the previously

described methodology (section 6.3.3).

7.3.4.2 *Flow visualisation by particle tracking*

For flow pattern visualization, particle tracking of one alginate (0.5% w/v) sphere having mean size of 4.0 mm with riboflavin (R4500, Sigma-Aldrich) incorporated (0.001% w/v) was used. This particle had a relative density of 0.998 (using water at 25 °C as reference). The particle was placed in the liquid phase and illuminated at 90 degrees to the camera by two fluorescent black lights (F20T9/BLB) in order to make the incorporated riboflavin glow.

In order to visualize particle flow, sets of images were grabbed with a Canon EOS 600D camera (frame rate of 50 images/s) connected to a PC. A sequence of at least 12,000 image snapshots was taken at 3 different values of U_{Gr} in the 3 different PBRs. The frames were then processed through a number of image processing steps in order to obtain a clear image of the trajectory made by the particle inside the PBR, by overlapping consecutive frames. This image processing steps were carried out using Adobe Photoshop CS5.

These films allowed determining the particle's circulation time in the SCAPBRs for each of the tested conditions. Particle circulation time was obtained by the average of ten circulations in the SCAPBRs.

7.4 Results and Discussion

7.4.1 Liquid phase characterization

The liquid phase characterization was performed for all the PBRs at different values of superficial gas velocity in the riser (U_{Gr}) using tap water and growth medium. No significant differences in liquid phase characterization parameters were found between water and growth medium suggesting that changes in ionic strength above a certain minimal value did not significantly affect mixing behaviour. This is in agreement with the results obtained by Mirón *et al.* (2004). Thus, the results presented in this section (7.4.1) refer only to results obtained with growth medium.

7.4.1.1 Liquid circulation velocity

The liquid circulation velocity is an important factor for assessing SCAPBR mixing efficiency, since the mixing time in an airlift reactor is expected to be affected by the relative velocity between the gas and the liquid phases. This happens because gas bubbles rising in a liquid stream produce axial mixing by transporting liquid elements in their wakes (Molina *et al.*, 1999). The liquid circulation velocity determines the partial gas holdups in the cultivation medium (and therefore the mass-and heat-transfer rates), the extent of mixing, the shear-stress field, and the flow regimes of gas and solid phases (Guieysse *et al.*, 2011). The liquid circulation velocity is a meaningless parameter in bubble columns, thus it was only determined for the SCAPBRs (Figure 7.2).

In both SCAPBRs the increase of U_{Gr} causes a pronounced increase in liquid circulation velocity for $U_{Gr} < 0.005 \text{ m s}^{-1}$, meaning by this that liquid circulation velocity is very dependent on U_{Gr} . However, for higher values of U_{Gr} , liquid circulation velocity appears to be nearly independent of U_{Gr} .

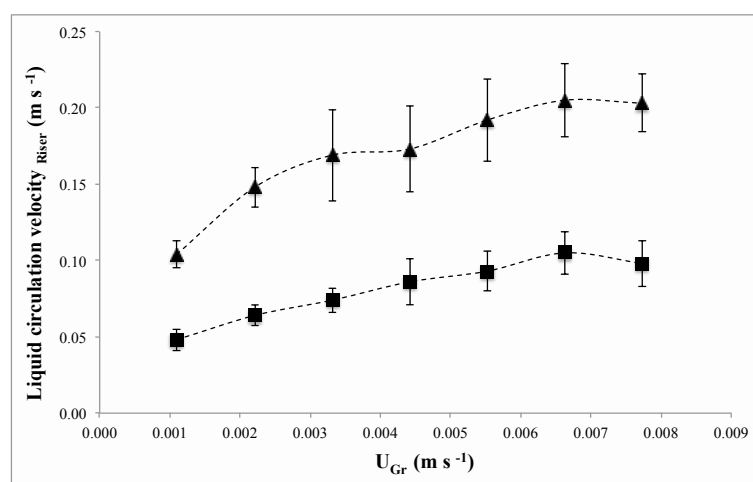


Figure 7.2 Liquid velocity for SCAPBR 50 (▲) and SCAPBR 75 (■), at different values of U_{Gr} .

Comparing the SCAPBRs it is clear that SCAPBR 50 shows higher liquid circulation velocity than SCAPBR 75 for all U_{Gr} , which is most probably explained by differences in the PBRs geometry, namely the different riser:downcomer ratios.

7.4.1.2 Mixing and circulation time

Several authors claim that the level of mixing in a reactor strongly contributes to

the growth of microalgae (Suh and Lee, 2003; Lou and Al-Dahhan, 2004). Mixing improves productivity by increasing the frequency of cell exposure to light and dark volumes of the reactor and by increasing mass transfer between nutrients and cells, maintaining uniform pH and eliminating thermal stratification. Mixing is also necessary to prevent algae sedimentation at the same time avoiding cell attachment to the reactor walls. Poor mixing will permit clumping of cells into aggregates of varying sizes, hence leading to the development of a three- phase system (solid–liquid–gas) inside the reactor that is prone to decreased mass transfer (Panda *et al.*, 1989).

Mixing times vs U_{Gr} data for the three PBRs are shown in Figure 7.3

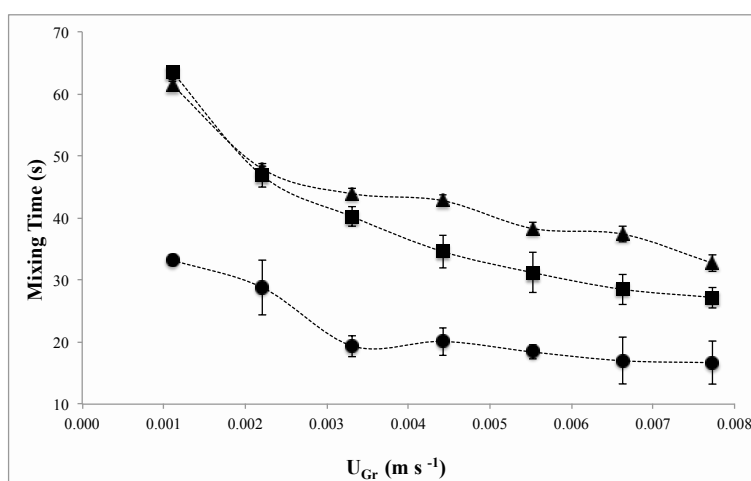


Figure 7.3 Mixing time for SCAPBR 50 (▲), SCAPBR 75 (■) and BC (●), at different values of U_{Gr} .

For a given U_{Gr} , the BC always has a lower mixing time compared with the SCAPBRs. These results are in agreement with Guieysse *et al.* (2011) who reported that analysis of mixing in bubble columns showed that they have shorter mixing times than airlift reactors. In fact, compared with the chaotic flow in the bubble column, the organized cyclic flow in the airlift reactors inhibits bulk mixing (Mirón *et al.*, 2004). In the three tested PBRs, the general tendency was a decline of mixing time with increasing U_{Gr} . At low aeration flow rates, the mixing time in the SCAPBRs was much more sensitive to aeration rate than the mixing time in the bubble column (Figure 7.3).

Comparing the two SCAPBRs it is clear that, for $U_{Gr} < 0.002$ m s⁻¹ mixing times

are almost the same, whereas for $U_{Gr} > 0.002 \text{ m s}^{-1}$ SCAPBR 75 requires less time to achieve complete mixture. This result allows assuming that, in general, SCAPBR 75 could guarantee a more efficient transport of nutrients for the cells than SCAPBR 50 at high U_{Gr} . The reason for the fact that SCAPBR 75 shows lower mixing times than SCAPBR 50 can be its higher riser:downcomer ratio, that allows a more chaotic flow in SCAPBR 75 riser, promoting bulk mixing and, consequently, reducing mixing time.

The dependence of circulation time on U_{Gr} in SCAPBRs (Figure 7.4) was quite similar to mixing time profiles in the same reactors (Figure 7.3). Circulating time is defined as the average time needed for particles to circulate one cycle in the bioreactor; it can be also used to evaluate mixing performance of bioreactors (Nagata, 1975). Circulation time is a meaningless parameter in bubble columns, thus it was only determined for SCAPBRs (Figure 7.4).

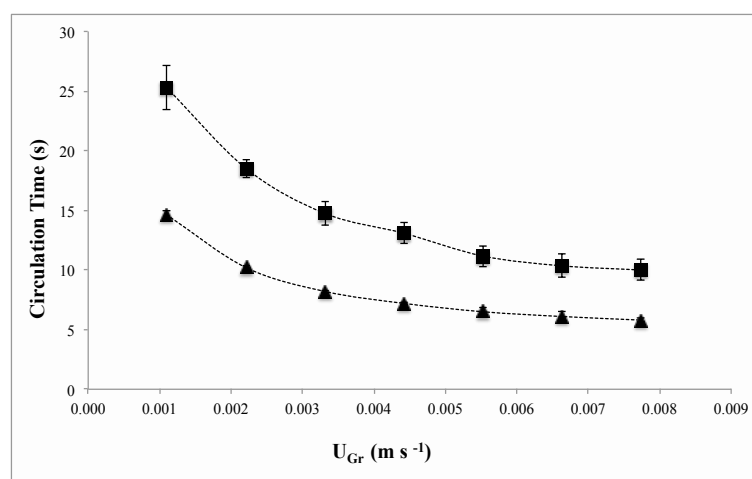


Figure 7.4 Circulation time for SCAPBR 50 (▲) and SCAPBR 75 (■), at different values of U_{Gr} .

At low gas flow rates, the circulation time decreased sharply with increasing U_{Gr} . However, at $U_{Gr} > 0.005 \text{ m s}^{-1}$ circulation time dependence on U_{Gr} becomes very small. This observation is common to both SCAPBRs and is quite typical of airlift reactors (Mirón *et al.*, 2004). This phenomenon is associated with micronization of gas bubbles because of increasing turbulence and a consequent build up of these smaller bubbles in the downcomer zone. The consequently reduced difference between gas holdup values in the riser and downcomer reduces the driving force for liquid circulation (Chisti, 1989; Mirón *et al.*, 2004). Although

the shape of the curves circulation time *versus* U_{Gr} is similar in both SCAPBRs, circulation time values differ considerably, since SCAPBR 50 shows lower circulation times for all values of U_{Gr} tested. However, it is clear that the difference between the circulation time of these two SCAPBRs decreases with increasing U_{Gr} .

A comparison between Figure 7.3 and 7.4 suggests that, in each SCAPBR, mixing time improves when circulation time is reduced. This is because rapid cycling causes the fluid to pass more frequently through the relatively well-mixed head zone of the reactor (*i.e.* the zone above the upper edge of the baffle) (Chisti, 1989; Mirón *et al.*, 2004). However, comparing the two SCAPBRs it is clear that this relationship between the mixing time and circulation time is not valid between these two different PBRs. SCAPBR 50, despite having a lower circulation time (Figure 7.4), shows a higher mixing time (Figure 7.3) than SCAPBR 75. Again, the explanation may lie in the fact that SCAPBR 75 allows bulk mixing in a greater extent due to its larger riser, which behaves somehow as a bubble column. Although it reduces mixing time when compared to SCAPBR 50, this bulk mixing in the riser of SCAPBR 75 increases the residence time in the riser and consequently increases the circulation time. This relation between circulation and mixing time will be analysed and explained by the results of flow pattern visualization (section 7.4.5.2).

It is known that mixing time depends primarily on reactor geometry and circulation time is also sensitive to geometric variables (Chisti *et al.*, 1988; Chisti and Moo-Young, 1993), which explain the observed differences in mixing and circulation times, between the three tested PBRs.

7.4.2 Gas phase characterization

As in liquid phase characterization, gas phase characterization was performed for all PBRs at different values of superficial gas velocity in the riser (U_{Gr}) using tap water and growth medium. Also in this case, no significant differences in liquid phase characterization parameters were found between water and growth medium suggesting that changes in ionic strength above a certain minimal value did not significantly affect gas phase behaviour. These conclusions are in close agreement

with similar observations about the effects of ionic strength on gas holdup made by Chisti (1989, 1998) and Sánchez Mirón *et al.* (1999). Thus, the results presented in this sub-chapter (7.4.2) refer only to results obtained with growth medium.

7.4.2.1 Gas holdup

Gas holdup (ε) is one of the most important parameters characterizing PBRs hydrodynamics since the difference between gas holdup in the riser and in the downcomer is responsible for the circulation in the reactor. In this work, gas holdup was measured in the riser, for different U_{Gr} (Figure 7.5).

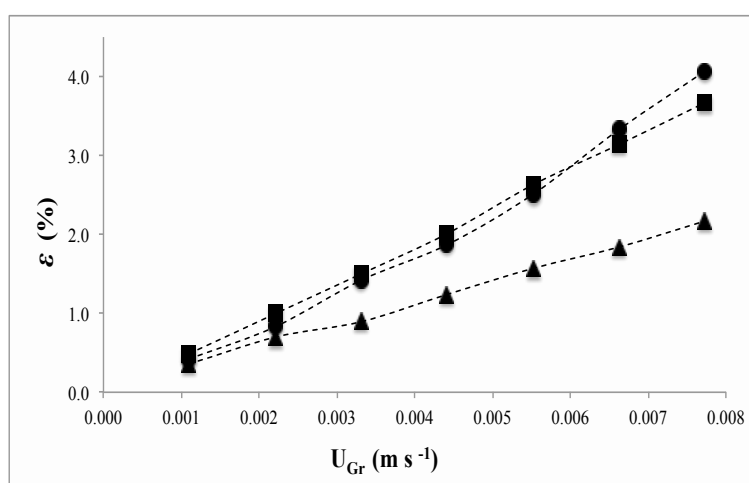


Figure 7.5 Riser gas holdup for SCAPBR 50 (▲), SCAPBR 75 (■) and BC (●), at different values of U_{Gr} .

In all the three tested PBRs riser gas holdup increased almost linearly with the increase of U_{Gr} . Probably due to its large riser fraction, SCAPBR 75 shows very similar ε values to BC. SCAPBR 50 displays considerable lower ε values. Xu *et al.* (2002) claims that in airlift reactors, holdup is influenced by the induced liquid circulation rate that depends on the geometry of the flow path, the gas-liquid separating ability of the head zone of the reactor (Chisti and Moo-Young, 1993), and also the height of the airlift column (Chisti 1989).

7.4.2.2 Bubble characterization

In combination with gas holdup, bubble size and shape influence the gas-liquid interfacial area available and consequently the mass transfer coefficient (Chisti,

1989). Interfacial area may be enhanced either by increasing gas holdup or by decreasing the prevailing bubble size. However there are limits for bubble size decrease since it is known that small bubbles induce more shear stress to cells than larger bubbles.

Sauter mean diameter (d_{32})

Bubble size is a crucial factor to minimize shear damage to cells and optimize mass transfer. Rocha *et al.* (2003) grew *Nannochloropsis gaditana* using small vs. large bubbles and they found better microalgal growth with larger bubbles and as air flow rate was increased the cells suffered more shear with smaller than with larger bubbles. Since, in practice, a diameter distribution of bubble sizes exists in the PBR, the Sauter mean bubble diameter (d_{32}) is used as a bubble size quantification parameter. The Sauter mean diameter refers to the diameter of a sphere with the same volume-to-surface ratio as the gas bubble (Chisti, 1989).

For all tested PBRs, bubbles' Sauter mean diameter (d_{32}), in general, increases with U_{Gr} (Figure 7.6).

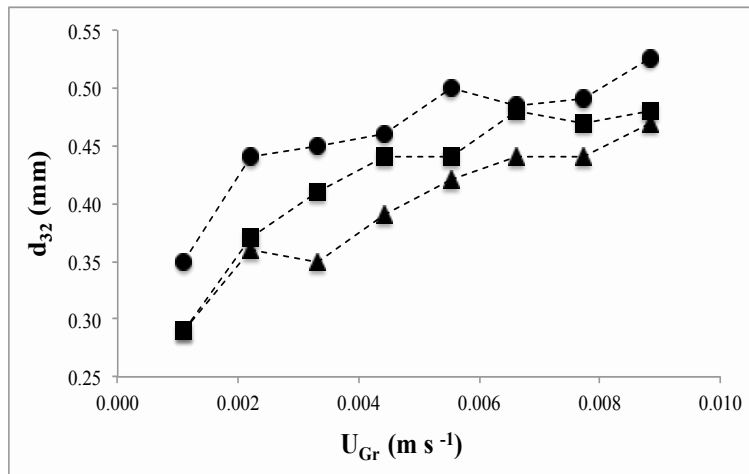


Figure 7.6 Bubble Sauter mean diameter (d_{32}) for SCAPBR 50 (\blacktriangle), SCAPBR 75 (\blacksquare) and BC (\bullet), at different values of U_{Gr} .

The dependence of d_{32} to U_{Gr} is lower for higher values of U_{Gr} . Although the difference is not very defined, it is possible to conclude that the largest bubbles are observed in BC and the smallest in SCAPBR 50 for all tested values of U_{Gr} .

Elongation (F_{max}/F_{min})

Maximum (F_{max}) and minimum (F_{min}) Feret diameters were obtained (the Feret diameter is the smallest distance between two parallel tangents to the object, the tangent position being defined by the angle between them and the horizontal axis) in order to calculate the elongation (F_{max}/F_{min}) of bubbles (Ferreira *et al.*, 2001).

It is known that the shape of bubbles is influenced by superficial gas velocity. Depending on U_{Gr} , bubbles can be more or less elongated. Figure 7.7 shows the F_{max}/F_{min} ratio (*i.e.* elongation), which gives the bubble shape for different U_{Gr} in the three tested PBRs.

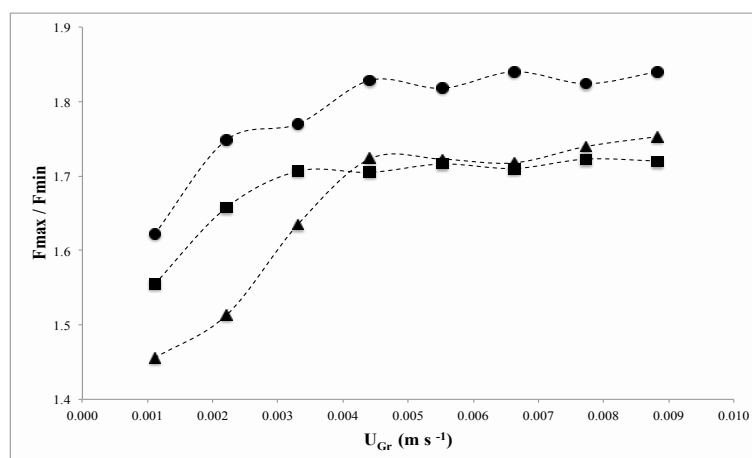


Figure 7.7 Bubbles elongation for SCAPBR 50 (\blacktriangle), SCAPBR 75 (\blacksquare) and BC (\bullet), at different values of U_{Gr} .

In the three tested PBRs, it was found that for $U_{Gr} < 0.005$ m s⁻¹ bubble shape (in terms of F_{max}/F_{min} ratio) is strongly dependent on the U_{Gr} value. However, for $U_{Gr} > 0.005$ m s⁻¹ bubble shape becomes constant. In BC, bubbles have a slightly higher elongation than in both SCAPBRs, which have very similar results in this parameter. According to F_{max}/F_{min} values and using the classification described by Mena *et al.* (2005), the bubbles present in all tested PBRs are classified as flattened spheroids. Flattened spheroids are known to have higher oscillation amplitudes that influence mass transfer. Montes *et al.* (1999) show that oscillating bubbles improve mass transfer due to the variation of contact times and concentration profiles surrounding the bubbles.

Bubble complexity degree (B_{CD})

The complexity of the bubble system can be determined through a parameter

called “bubble complexity degree” (B_{CD}). The higher the value of B_{CD} , the higher the tendency of bubbles to flow in groups (Ferreira *et al.*, 2012) which typically, above B_{CD} certain levels, means that mass transfer is reduced (Deckwer, 1992).

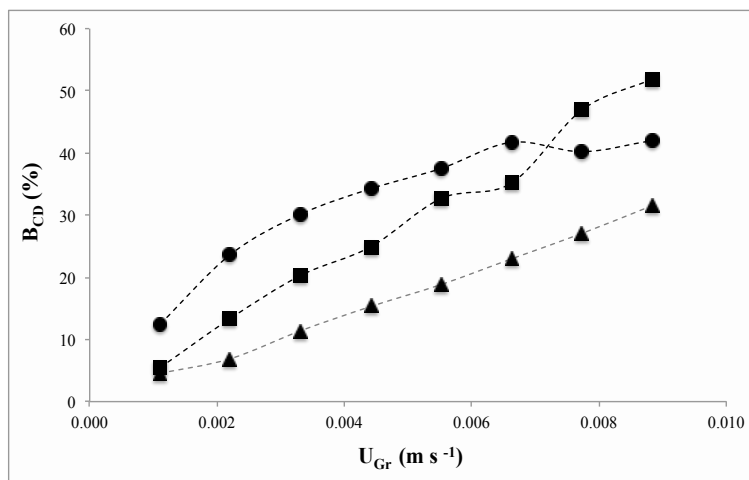


Figure 7.8 Bubbles mean complexity degree (B_{CD}) for SCAPBR 50 (\blacktriangle), SCAPBR 75 (\blacksquare) and BC (\bullet), at different values of U_{Gr} .

The values of B_{CD} of the three tested PBRs (Figure 7.8) increased almost linearly with the increase of U_{Gr} , with the exception of BC at higher values of U_{Gr} . The SCAPBR 50 shows for all U_{Gr} a lower value of B_{CD} , whereas the BC has, for $U_{Gr} < 0.07$ m s⁻¹ higher B_{CD} values than those obtained in SCAPBRs. For $U_{Gr} > 0.07$ m s⁻¹ SCAPBR 75 shows the higher bubble complexity degree.

Gas bubble velocity

Gas bubble velocity determination (Figure 7.9) shows that in SCAPBR, this parameter is almost independent of U_{Gr} since it remains almost constant over the different values of U_{Gr} . In the BC, bubble velocity decreases with the increase of U_{Gr} (probably due to an increase of turbulence), keeping constant from $U_{Gr} > 0.03$ m s⁻¹ onwards. These results are not in agreement with what would be expected by the analysis of Figure 7.6. Typically, larger bubbles tend to have higher rising velocities, which was not observed in this case. Possibly the fact that bubbles in BC have a more flattened geometry (as shown in Figure 7.7) has a major influence in the calculation of their size: they are actually sized as being bigger than they effectively are. When comparing bubbles' velocity in the different PBRs, it is expected that the BC shows the best mass transfer performance followed by

SCAPBR 75 and SCAPBR 50.

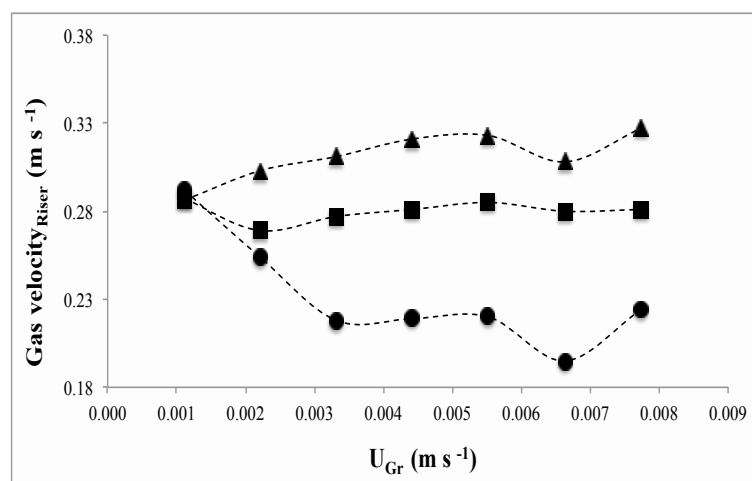


Figure 7.9 Gas velocity_{Riser} for SCAPBR 50 (▲), SCAPBR 75 (■) and BC (●), at different values of U_{Gr} .

This happens because the lower bubbles' velocity means a higher residence time in the PBR and, consequently, a better mass transfer. These differences between BC and SCAPBR are in agreement with those reported by Contreras *et al.* (1998).

7.4.3 Mass transfer of CO₂

As in liquid and gas phase characterization, in volumetric mass transfer coefficient determination (K_{La}) no statistically significant differences were obtained between the tests performed with water and mineral growth medium. Microalgae cultivation systems, especially at a large scale, are limited by the transfer of CO₂ from the gas to the liquid phase. Mass transfer can be evaluated by means of the volumetric mass-transfer coefficient (K_{La}). The results shown in Figure 7.10 are in close agreement with results obtained for mixing time (Figure 7.3), gas holdup (Figure 7.5) and gas bubble velocity (Figure 7.9). All of these previous results indicated that the BC would probably have the best mass-transfer capability followed by SCAPBR 75 and SCAPBR 50, respectively.

Among these factors, gas holdup seems to be the one that most influences K_{La} , since as for gas holdup (Figure 7.5), also K_{La} increases almost linearly with U_{Gr} . The increase verified in Sauter mean diameter (Figure 7.6) (perhaps because it was not a very marked increase) does not appear to have had a negative effect on K_{La} .

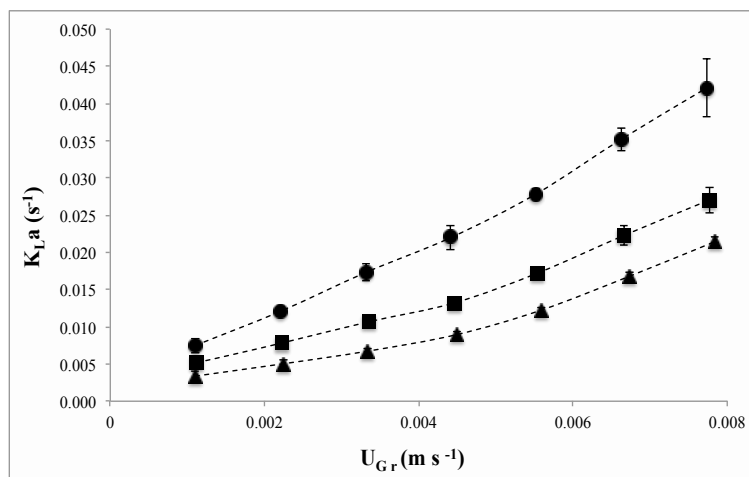


Figure 7.10 K_{La} for SCAPBR 50 (\blacktriangle), SCAPBR 75 (\blacksquare) and BC (\bullet), at different values of U_{Gr} .

The very high K_{La} values obtained for all PBRs must be highlighted. K_{La} values ranged between 0.007 – 0.04 s⁻¹ in BC; 0.005 – 0.03 s⁻¹ in SCAPBR 75 and; 0.003 – 0.02 s⁻¹ in SCAPBR 50. Through literature review (Table 7.1) it was not possible to find such high values of K_{La} in microalgae cultivation systems. The key to these K_{La} values seems to lie in the aeration system developed (Figure 6.11 and 7.1) more than in PBRs design, since comparing K_{La} values obtained in the BC with the results obtained by Merchuk *et al.* (2000) (also with a bubble column) there is a one order of magnitude difference in the values.

Table 7.1 K_{La} values obtained in different cultivation systems (adapted from Ugwu *et al.*, 2003)

PBR	U_G (m s ⁻¹)	K_{La} (s ⁻¹)	Reference
Concentric tube airlift	0.055	0.02	Contreras <i>et al.</i> , 1998
Stirred tank	0.009	0.02	Ogbonna <i>et al.</i> , 1998
Inclined tubular	0.02	0.003	Ugwu <i>et al.</i> , 2002
Bubble-column	0.008	0.005	Merchuk <i>et al.</i> , 2000
Flat plate	0.009	0.002	Zhang <i>et al.</i> , 2002
Split cylinder airlift	0.024	0.009	Vega-Estrada <i>et al.</i> , 2005
Airlift tubular horizontal	0.16	0.014	Camacho Rubio <i>et al.</i> , 1999
External-loop airlift tubular	0.25	0.006	Ación Fernández <i>et al.</i> , 2001

This excellent mass transfer capability of all the three PBRs will contribute to an efficient CO₂ delivery to cells, and an effective removal of O₂ from the culture.

7.4.4 Biomass productivity

Although extremely important for characterization, optimization and scale-up of PBRs, none of the previously analysed parameters allows concluding which is the most productive PBR. To make that evaluation, *C. vulgaris* was grown in the three PBRs (BC, SCAPBR 75 and SCAPBR 50) at three different values of U_{Gr} (0.0011, 0.0044 and, 0.0077 m s⁻¹).

The maximum biomass productivities (P_{max}) obtained in each of the conditions are reported in Figure 7.11. Contrary to what the results of liquid and gaseous phase characterization as well as mass transfer suggested (Figures 7.2 – 7.10), SCAPBR 50 presents itself as the PBR with best volumetric productivity (0.60 – 0.72 g L⁻¹ d⁻¹), exceeding BC's volumetric productivity in 15 – 36% and SCAPBR 75's volumetric productivity in 5 – 22%, depending on the U_{Gr} . Additionally it was found that in all the PBRs the highest value of P_{max} was achieved at $U_{Gr} = 0.0044$ m s⁻¹, and the lowest at $U_{Gr} = 0.0077$ m s⁻¹. In all the situations the maximum cell concentration was around 6 g L⁻¹ (data not shown).

More important than comparing the P_{max} values obtained in this study with those obtained in other studies, it is relevant to compare the relationship established between the P_{max} of BC and SCAPBRs with the relation found by other authors when comparing bubble columns with airlifts as PBRs. The comparison between P_{max} obtained in this study with those obtained in other studies using different PBRs (or even similar) would not provide any relevant information in terms of PBRs performance comparison for several reasons: *i*) the strain used was not the same in most of the studies; *ii*) the culture conditions (culture medium, CO₂ concentration, aeration flow rates, temperature, intensity and frequency of light supply) are very diverse; *iii*) cultivation systems used have a wide range of dimensions (from millilitres to hundreds of litres); *iv*) the productivity determination is not always performed in the same way (mean productivity, maximum productivity, areal productivity, volumetric productivity). For the above-mentioned reasons, it only makes sense checking in earlier studies which PBRs register the best performance (when used in the same conditions) and from there trying to establish a parallel with the results obtained in this study. Published literature shows no unanimous

conclusions when it comes to comparing the performance of airlift and bubble column PBRs. In a review by Janssen *et al.* (2003) the authors concluded that bubble column and air-lift reactors, in general, appear to have similar productivities, however bubble column reactors perform better at $U_{Gr} > 0.05 \text{ m s}^{-1}$.

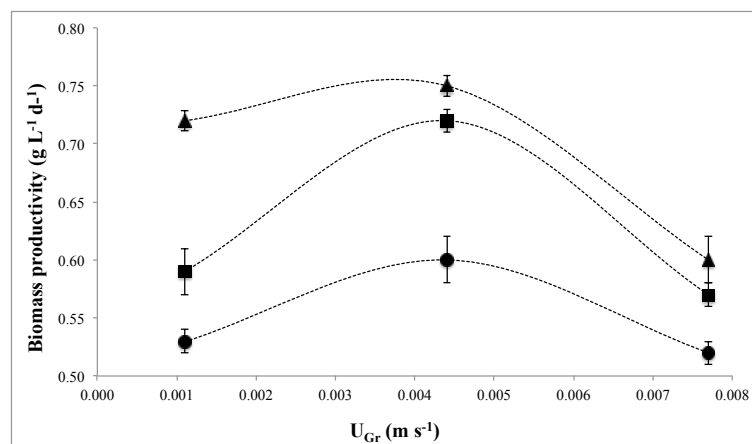


Figure 7.11 Biomass productivity for SCAPBR 50 (▲), SCAPBR 75 (■) and BC (●), at three different values of U_{Gr} .

Mirón *et al.* (2002) used pilot scale (0.19 m column diameter, 2 m tall, 0.06 m³ working volume) outdoor bubble column and airlift bioreactors (a split-cylinder and a draft-tube airlift device) for *Phaeodactylum tricornerutum* cultivation. The three PBRs produced similar biomass *versus* time profiles and final biomass concentration (~4 g L⁻¹). In a different study (Mirón *et al.*, 2003), using the same PBRs and the same microalgae but with different growth conditions, the volumetric productivity of the three PBRs was approximately 0.30 d L⁻¹ d⁻¹ with $U_{Gr} = 0.01 \text{ m s}^{-1}$. Krichnavaruk *et al.* (2007) examined the cultivation of *Chaetoceros calcitrans* in airlift and bubble column PBRs and biomass productivity was about the double in an airlift device than in a bubble column. These differences in the conclusions of different studies show that it is not possible to establish one particular type of PBR as being the most suitable for microalgae cultivation. PBR performance depends on factors such as PBR geometry, aeration system and operational conditions (*e.g.* U_{Gr} or light supply).

The results shown in Figure 7.11 seem to indicate that none of the previously discussed parameters (Figures 7.2 - 7.10) appear to be the limiting factor to PBR productivity, since SCAPBR 50 showed the least favourable values for all

parameters, while apparently being the one with the best results in terms of P_{max} . The only factor that has remained unchanged was the fact that the SCAPBR 75 is invariably displayed as the intermediate element between the two “extremes” in terms of design (SCAPBR 50 and BC). This leads to the conclusion that the fact that SCAPBR 75 has a large ratio riser:downcomer puts it in a position where, invariably, it shows characteristics that are between those of an airlift and a bubble column.

The fact that the highest value of P_{max} occurs for all PBRs at $U_{Gr} = 0.0044 \text{ m s}^{-1}$ followed by a sharp decrease in productivity for $U_{Gr} = 0.0077 \text{ m s}^{-1}$ does not seem to find an explanation in the parameters previously discussed, since higher values of U_{Gr} and K_{La} usually lead to higher productivities (Barbosa *et al.*, 2003; Zhang *et al.*, 2002). None of the parameters analyzed before (Figures 7.2 - 7.10) showed an inversion of behaviour at $U_{Gr} = 0.0044 \text{ m s}^{-1}$ (or indeed at any value of U_{Gr}).

One of the possible explanations for the decline in productivity at $U_{Gr} = 0.0077 \text{ m s}^{-1}$ is the shear stress caused by a higher flow rate, but for various reasons this does not seem plausible: *i*) the tested values of U_{Gr} are below the values reported in the literature as being capable of causing stress in microalgae (Mirón *et al.* (2007) reported that *Phaeodactylum tricornutum* were susceptible to aeration-associated hydrodynamic stress only when U_{Gr} exceeds 0.01 m s^{-1} ; also, Camacho *et al.* (2001) claimed cell damage in *Phaeodactylum tricornutum* cells at $0.01 < U_{Gr} < 0.05 \text{ m s}^{-1}$ (much higher than the U_{Gr} values used in this study)); *ii*) Sánchez Mirón *et al.* (1999) claimed that cell damage occurs when the turbulence is so intense that the fluid microeddy size approaches cellular dimension. However, in this study the bubbles present average sizes of $0.28 < d_{32} < 0.52 \text{ mm}$. Additionally, bubble size increases slightly with U_{Gr} and not the contrary (Figure 7.6); *iii*) *C. vulgaris* is described as a very robust and resistant to shear stress. Thus, the hydrodynamic stress may be discarded as a factor that led to a decrease in biomass productivity in all the PBRs.

From the results it is clear that mass transfer was not a limiting factor in the present work, since SCAPBR 50 is the PBR with lower values of K_{La} while the BC shows the highest values for this parameter (Figure 7.10). Additionally, there is a

decrease in productivity between $U_{Gr} = 0.0044$ and 0.0077 m s^{-1} , which is in opposite direction to $K_L a$ variation in all PBRs (Figure 7.10). Thus, it seems reasonable to conclude that none of the parameters discussed earlier (Figures 7.2 – 7.10) is by itself a limiting factor for the tested PBR productivities. It is also plausible to conclude that provided conditions (mainly in terms of mixing, mass transfer and hydrodynamic stress) are very suitable, in all three PBRs, and cannot be considered as limiting factors as a whole to obtain higher productivities in these PBRs.

The only parameters that have not been studied yet and, therefore, were not taken into account when evaluating the PBRs productive performance are light distribution inside PBRs and microalgal cells light history (frequency and pattern). It is known that these factors may be of great importance to define PBRs' productivity.

7.4.5 Determination of cells' light history

In photobioreactors, turbulent flow conditions and light gradients frequently occur. Thus, algal cells cultivated in such reactors experience fluctuations in light intensity that can change in extent and frequency, depending on hydrodynamic conditions and PBR geometry. It has been previously shown that light patterns influence microalgal growth and product formation (Lee and Pirt, 1981; Laws *et al.*, 1983; Terry, 1986; Merchuk *et al.*, 1998; Janssen *et al.*, 1999). Light intensity and duration of light-dark (LD) intervals are also very relevant parameters (Richmond *et al.*, 2003).

The following part of the work presents a method to visualize how cells are subject to these light-dark patterns. The research is focused on temporal and spatial aspects of light patterns, which may affect the photosynthetic reaction. The method combines light regime characterization inside the PBR (using fibre optic technology) with particle tracking (using image analysis). These determinations were performed using growth medium.

7.4.5.1 Light regime characterization

It is known that for *C. vulgaris* cells the light compensation point (*i.e.* the irradiance below which there is no net photosynthesis) is between 5 and 10 $\mu\text{E m}^{-2} \text{s}^{-1}$ and the light saturation intensity is about 250 $\mu\text{E m}^{-2} \text{s}^{-1}$ (Degen *et al.*, 2001). For that reason, cell growth experiments were performed at an incident light intensity of 250 $\mu\text{E m}^{-2} \text{s}^{-1}$, in order to avoid introducing more stress elements to the cells.

Figure 7.12 only shows light intensity (*L.I.*) variation profiles at three different concentrations, once above 1.0 g L^{-1} no changes in light profile were observed (data not shown) because the light does not penetrate more than the first 5 mm.

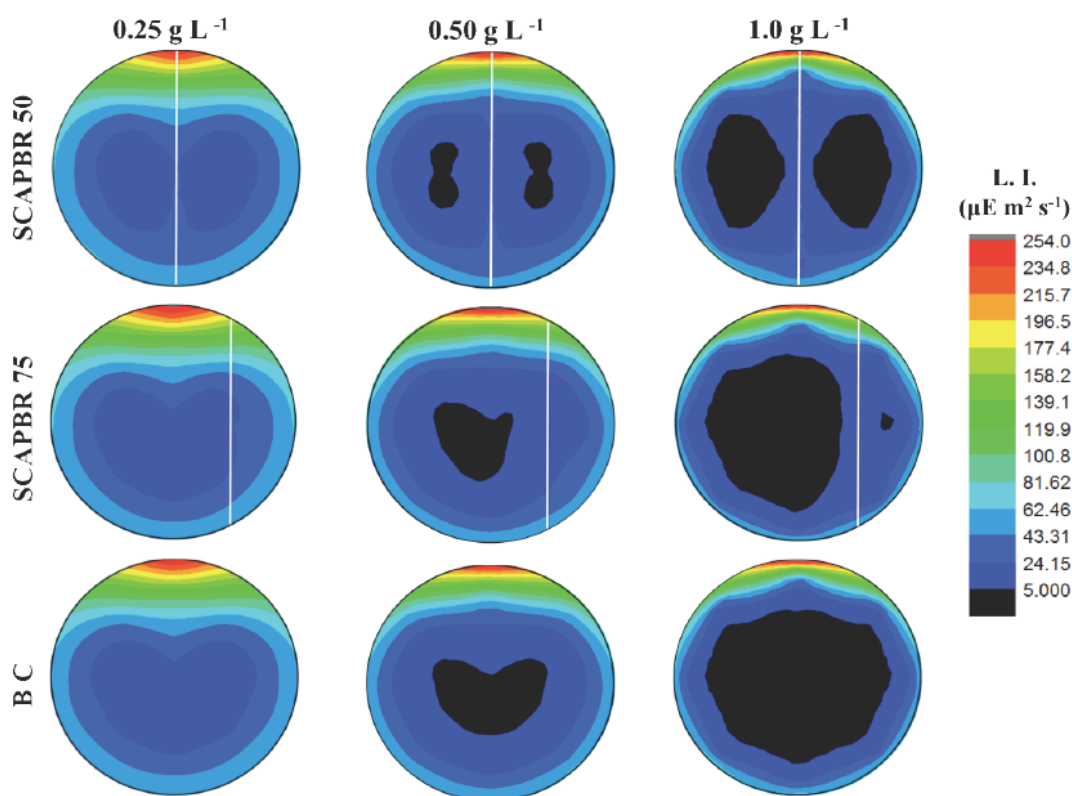


Figure 7.12 Light intensity (*L.I.*) profiles inside the PBRs (SCAPBR 50, SCAPBR 75 and BC) at different *C. vulgaris* cell concentrations (0.25, 0.50 and, 1.0 g L^{-1}).

This observation is in line with those reported by Degen *et al.* (2001). These authors claimed that, in *Chlorella* cultures with 1.8 g L^{-1} , with 980 $\mu\text{E m}^{-2} \text{s}^{-1}$ illumination, less than 1% of the light remained at a culture depth of 3 mm. Figure 7.12 shows that, compared to BC, SCAPBRs allow (due to their central wall) the

existence of a larger illuminated volume fraction for all tested concentrations. Comparing the two SCAPBRs it is possible to verify that, for low cell concentrations (0.25 and 0.50 g L⁻¹), there is no clear advantage for any SCAPBR. However, at 1.0 g L⁻¹, SCAPBR 50 enables delivery of light to a region of the PBR (central region) that in the other PBRs is in complete darkness.

Table 7.2 Continuously illuminated PBRs surface area

PBR	Illuminated surface area (m ²)
SCAPBR 50	0.290
SCAPBR 75	0.265
BC	0.190

At cell concentrations higher than 1.0 g L⁻¹, the cells only have access to light when they circulate along the PBRs walls (in all the PBRs) and along both sides of the central wall (in SCAPBRs only). Therefore, the surface area that is continuously illuminated in the BC is 0.190 m², while in SCAPBR 75 the illuminated surface is 39% higher (0.265 m²). The SCAPBR 50 has the largest illuminated surface area (0.290 m²) which is 53 and 9% higher than those presented by BC and SCAPBR 75, respectively (Table 7.2).

This information about light intensity profiles inside the PBRs provides very useful information, however it is not possible to use the full potential of this information while not knowing the cells' flow pattern.

7.4.5.2 Flow pattern visualization

Lou *et al.*, (2003) claimed that moving the cells in and out of illuminated zones at suitable frequencies can improve biomass productivity. Thus, a flow examination is required for a better understanding and optimization of PBR productivity. Flow visualization studies such as those shown in Figure 7.13 and 7.14 provide a useful insight into PBRs circulation patterns, identification of dead zones and regions of intense turbulence.

Figures 7.13 and 7.14 show the alginate particle flow pattern inside the three tested PBRs at three different values of U_{Gr} (0.0011, 0.0044 and, 0.0077 m s⁻¹), the same used in *C. vulgaris* growth tests. Figure 7.13 was obtained in a plane parallel

to the light source (used for growth), *i.e.* a plane perpendicular to the central wall of SCAPBRs (riser is on the left side and downcomer on the right side of each individual SCAPBR image). Figure 7.14 was obtained in a plane perpendicular to the illumination, *i.e.* a plane parallel to the central wall of SCAPBRs (riser is on the foreground and downcomer on the background of each individual SCAPBR image).

In both Figures 7.13 and 7.14 three representative assays (represented by different colours) are shown in each individual image. Though more assays were performed, only three are shown for each tested condition to allow an easy interpretation of the figures.

The results related to flow patterns inside the PBRs (Figures 7.13 and 7.14) allow understanding many of the results obtained previously in terms of gas and liquid phase characterization as well as mass transfer characterization.

Thus, the analysis of flow pattern results allows understanding why the SCAPBR 75, despite having a higher circulation time (Figure 7.2) shows better results in terms of mixing time (Figure 7.3). The existence of a higher turbulence induced by radial movement in the riser of SCAPBR 75 improves mixing time, but causes a higher circulation time. This conclusion is further supported by the results listed in Table 7.3, representing the mean time that the particle takes to complete a circulation (average of 10 measurements). K_La increase seen in Figure 7.10 is also supported by increased turbulence (Figures 7.13 and 7.14) and consequent radial mixing that follows exactly the same trend according to the U_{Gr} and type of PBR used. Matching the results obtained in the characterization of light distribution profile (Figure 7.12) with the flow pattern inside the PBRs (Figures 7.13 and 7.14), allows understanding and (at least partially) explaining the productivity obtained in each of PBRs (Figure 7.11).

Figure 7.11 shows that the highest P_{max} obtained for BC ($U_{Gr} = 0.0044 \text{ m s}^{-1}$) is still lower than any of the P_{max} values obtained for the SCAPBRs in the different tested conditions. Observing the particle tracking images concerning the BC (Figure 7.13), it is clear that in all tested conditions there is a chaotic movement of the particle. Mostly at $U_{Gr} = 0.0011 \text{ m s}^{-1}$ the particle tends to circulate only in a very specific zone of this PBR.

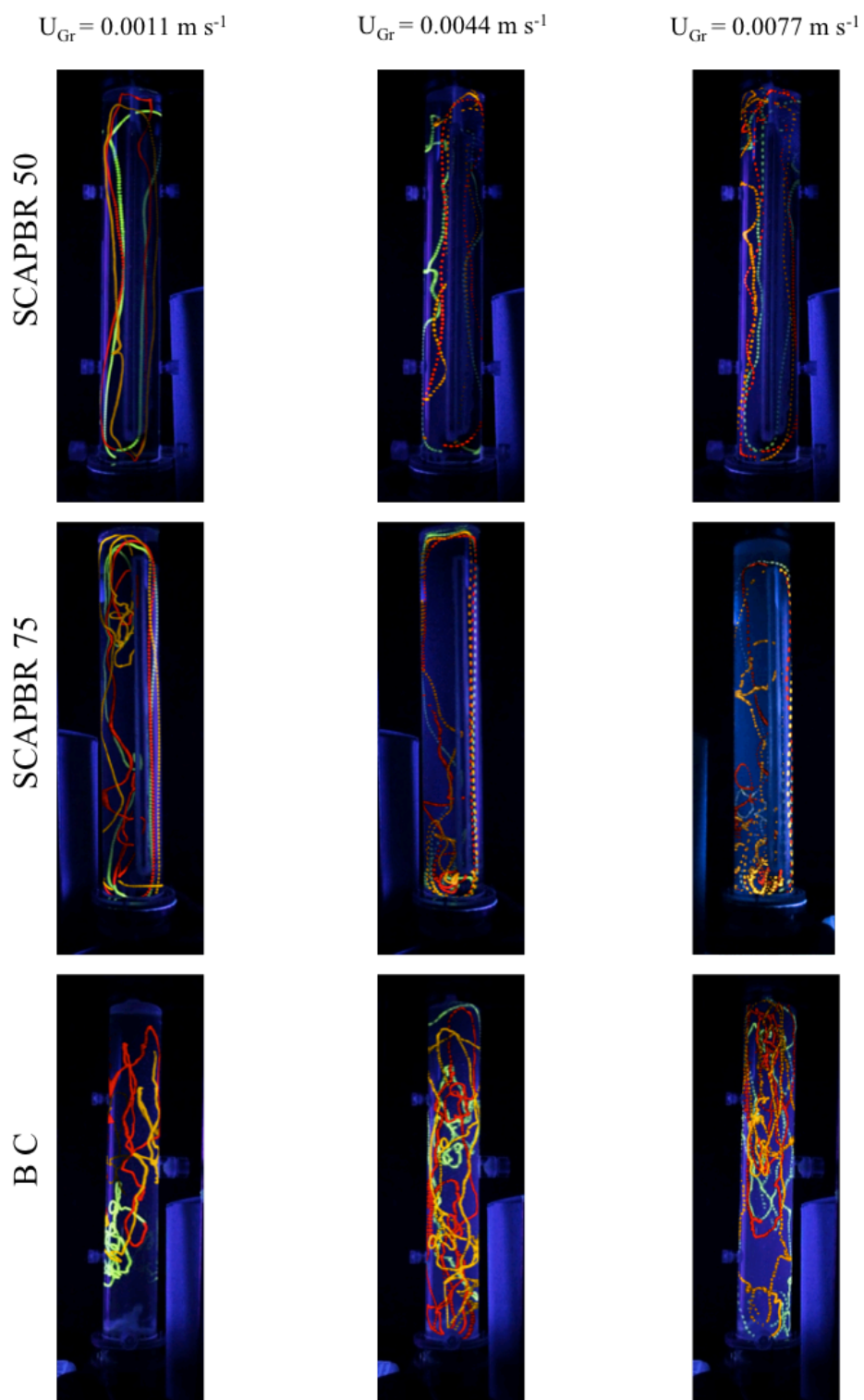


Figure 7.13 Particle tracking inside the three different PBRs at three different values of U_{Gr} (riser is on the left side and downcomer on the right side of each individual SCAPBR image, as represented in Figure 7.1).

This type of flow pattern is typical in bubble columns and is likely to cause unequal cell density along the length of the reactor, which may induce cell sedimentation, algal starvation and death (Fan et al., 2007), which in turn can lead to a productivity reduction. Considering the regions near the walls of the BC as *light* areas and the innermost region as *dark* area, it is clear that in the BC the light-dark movement was mostly chaotic and did not have a well-defined frequency. Additionally, results show that cells may reside in high or in low light intensity regions for a long time without circulation. The flow patterns found in association with the profile of light distribution within the BC justify why this PBR, although presenting the best results in terms of mixing and mass transfer, has lower productivities than those determined for SCAPBRs.

The flow patterns in SCAPBRs is relatively simpler than those in the BC. The particle flows in a defined circulation pattern through the channels defined by SCAPBRs' geometry, being driven to pass the riser and the downcomer successively.

In agreement with the observed in previous results (Figures 7.2 - 7.11), also in relation to the flow pattern inside the PBRs, SCAPBR 75 presents a behaviour that is somewhat halfway between those shown by the BC and SCAPBR 50. The SCAPBR 75, despite showing a typical airlift circulation pattern (the particle passes successively between riser and downcomer) shows also, in the riser, a typical bubble column chaotic movement with radial mixing. At $U_{Gr} = 0.0011 \text{ m s}^{-1}$ the SCAPBR 75 riser shows a flow pattern (7.13 and 7.14) that has some similarities with the typical BC flow pattern, mainly in the upper region of the riser. That kind of motion is reflected in the mean particle circulation time (Table 7.3), which is the highest among the three PBRs tested ($12.72 \pm 4.57 \text{ s}$). At $U_{Gr} = 0.0044$ and 0.0077 m s^{-1} that kind of near-chaotic movement is displaced to the bottom of SCAPBR 75, greatly increasing the turbulence in this region. Under all conditions tested, the particle has a linear movement in the SCAPBR 75 downcomer with virtually no radial motion. Increasing the value of U_{Gr} had hardly any effect on downcomer radial mixing. Considering the walls of SCAPBR 75 and both sides of the central

wall surface as *light* regions and the innermost area of riser and downcomer as *dark* region, it was observed that: *i*) in SCAPBR 75 riser occurs, albeit in a lesser extent than in BC, a near chaotic light-dark movement with a not well-defined frequency; *ii*) in SCAPBR 75 downcomer, the linear movement of the particle means that it can make the entire downcomer path only in light or dark areas without any light intensity fluctuation.

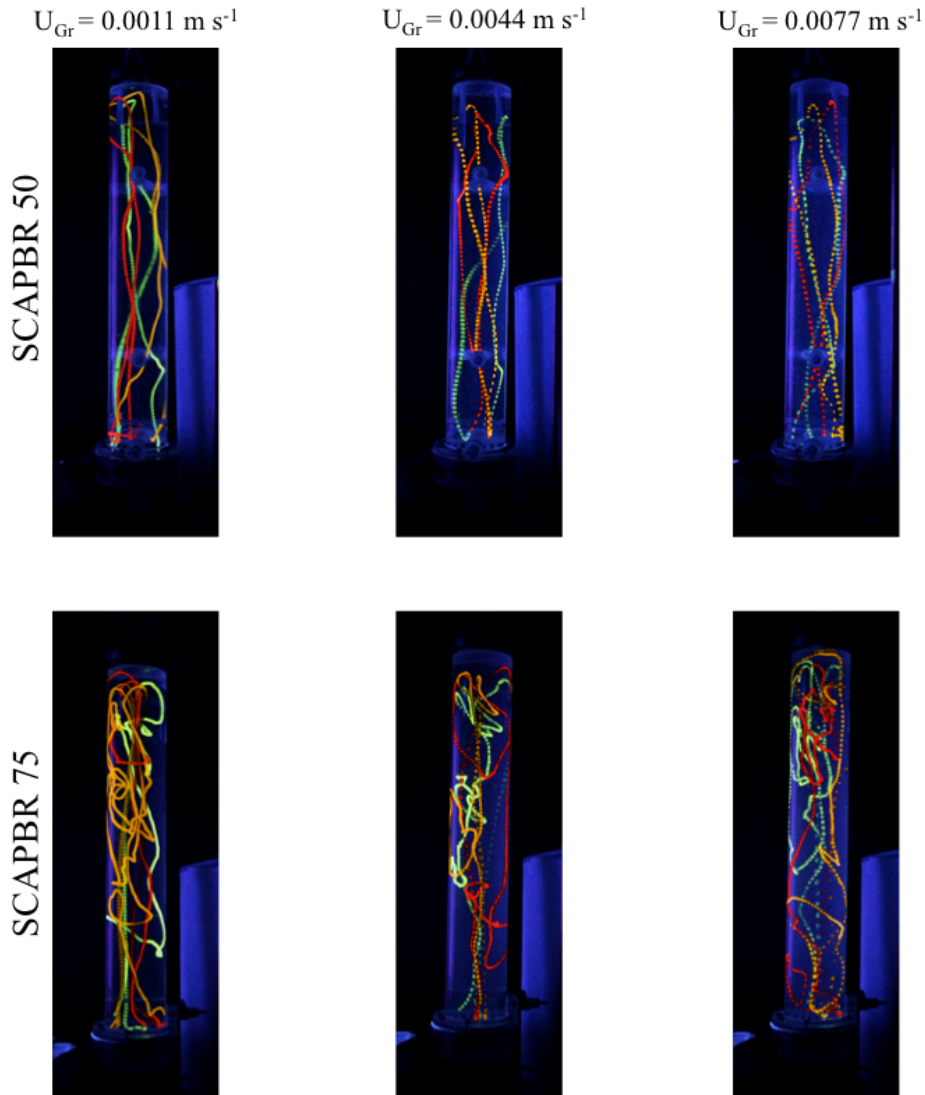


Figure 7.14 Particle tracking inside the two different SCAPBRs at three different U_{Gr} (riser is on the foreground and the downcomer on the background of each individual SCAPBR image, perpendicular perspective of Figure 7.13).

Comparing to BC, in SCAPBR 75 cells typically remain more uniformly

suspended in the medium, thus reducing the chances of occurrence of cell sedimentation or unequal cell density along the length of the reactor. Due to its more clearly defined flow pattern and higher illuminated surface area (Table 7.2), cells are subjected to a more regular frequency of exposure to light and dark conditions in the SCAPBR 75. Although the frequency at which such light-dark fluctuations occur is much greater than that seen in the BC, this frequency is not regular (due to the chaotic motion observed in the riser).

Table 7.3 Particle mean circulation time inside SCAPBRs

U_{Gr} (m s ⁻¹)	Circulation time (s)	
	SCAPBR 50	SCAPBR 75
0.0011	8.08 ± 0.69	12.72 ± 4.57
0.0044	3.63 ± 0.77	6.98 ± 2.42
0.0077	3.64 ± 0.56	8.83 ± 1.71

The SCAPBR 50, in contrast, presents a much more regular and defined flow pattern than the other two tested PBRs. At $U_{Gr} = 0.0011$ m s⁻¹ there is a well-defined particle movement without any kind of chaotic motion. The existence of a regular alternation between *light* regions (outer wall and central wall of SCAPBR 50) and *dark* regions (the innermost region of riser and downcomer) can be identified both in the riser and in the downcomer (Figure 7.13). When $U_{Gr} = 0.0044$ m s⁻¹ these regular alternating movements remain and they take place at a higher spatial (i.e., the walls are hit by the cells more often while travelling through the riser – Figure 7.13) and temporal (i.e. the cells hit the walls more times per second due to their higher velocity – Table 7.3) frequencies. At $U_{Gr} = 0.0077$ m s⁻¹ the basic features of flow patterns remain present, however a phenomenon of increased turbulence arises at the upper section of SCAPBR 50 which, due to the absence of central wall, displays a larger dark fraction than most of SCAPBR 50 volume. This turbulence verified at $U_{Gr} = 0.0077$ m s⁻¹ may be the explanation for a reduction in SCAPBR 50 productivity at this U_{Gr} . The defined mixing pattern in SCAPBR 50 effectively simulated a regular flashing-light effect (i.e. light-dark cycles). These regular light-dark cycles in addition to the reduction of exposure time to a continuous dark period are known to enhance the photosynthetic efficiency of algal cells and, consequently, biomass productivity (Grima *et al.*, 2001; Janssen *et al.*,

2001).

Through the analysis of all the results obtained in Chapter 7 it is clear that the maximum biomass productivity displayed by SCAPBR 50 at $U_{Gr} = 0.0044 \text{ m s}^{-1}$ in comparison with the other PBRs at different U_{Gr} , appears to be the result of two main characteristics: *i*) efficient light distribution inside SCAPBR 50, which results in a higher illuminated surface area, higher illuminated volume fraction and higher mean light intensity (Figure 7.12 and Table 7.2); *ii*) regular and defined flow patterns which result into the absence of chaotic movement and the existence of a regular frequency of exposure to light and dark areas.

Because the flow patterns in the three PBRs are obviously different, a bigger difference between P_{max} values would possibly be expected. However, as Mirón *et al.* (2002) reported, fairly different hydrodynamic regimes can lead to cells receiving more approximate values of cumulative average irradiance over a given period, which can result in productivities that are not as different as the differences in flow patterns would suggest.

7.5 Conclusions

The developed SCAPBRs proved to be extremely suitable for microalgae cultivation. The design of PBRs, particularly the design of the gas sparger, allowed meeting the needs of microalgae in terms of efficient mixing and good mass transfer coefficients (efficient supply and removal of CO_2 and O_2 , respectively). SCAPBR 50 (at $U_{Gr} = 0.0044 \text{ m s}^{-1}$) showed, among the tested PBRs, the highest value of biomass volumetric productivity ($0.75 \text{ g L}^{-1} \text{ d}^{-1}$). This result is due to a more effective light distribution inside the PBR and to a regular and defined flow pattern, which allows exposing cells to regular light and dark periods.

The statistical analysis of productivity results (data not shown) suggests that SCAPBR productivity can be improved by decreasing the riser:downcomer ratio.

7.6 References

- Acién Fernández, F. G., Fernández Sevilla, J. M., Sánchez Pérez, J. A., Molina Grima E., Chisti Y., 2001. Airlift-driven external loop tubular photobioreactors for outdoor production of microalgae: assessment of design and performance. *Chem. Eng. Sci.* 56: 2721–2732.

- Baquerisse D., Nouals S., Isambert A., dos Santos P. F., Durand G., 1999. Modelling of a continuous pilot photobioreactor for microalgae production. *J. Biotechnol.* 70: 335–342.
- Barbosa M. J., Albrecht M., Wijffels R. H., 2003. Hydrodynamic stress and lethal events in sparged microalgal cultures. *Biotechnol. Bioeng.*, 83: 112–120.
- Baten J. M., Ellenberger J., Krishna R., 2003. Hydrodynamics of internal air-lift reactors: experiments versus CFD simulations. *Chemical Engineering and Processing* 42: 733–742.
- Camacho Rubio F., Ación Fernández, F. G., Sánchez Pérez, J. A., García Camacho F., Molina Grima E., 1999. Prediction of dissolved oxygen and carbon dioxide concentration profiles in tubular photobioreactors for microalgal culture. *Biotechnol. Bioeng.* 62: 71–86.
- Camacho F. G., Grima E. M., Mirón A. S., Pascual V. G., Chisti Y., 2001. Carboxymethyl cellulose protects algal cells against hydrodynamic stress. *Enzyme Microb Technol.*, 29: 602–10.
- Chisti Y., Halard B., Moo-Young M., 1988. Liquid circulation in airlift reactors, *Chem Eng Sci.*, 43: 451–457.
- Chisti Y., 1989, *Airlift Bioreactors* (Elsevier, New York), p 355.
- Chisti Y., Moo-Young M., 1993. Improve the performance of airlift reactors, *Chem Eng Prog.* 89(6): 38–45.
- Chisti Y., 1998. Pneumatically agitated bioreactors in industrial and environmental bioprocessing: hydrodynamics, hydraulics and transport phenomena, *Appl Mech Rev.*, 51: 33–112.
- Contreras A., García F., Molina Grima E., Merchuk J.C., 1998. Interaction between CO₂-mass transfer, light availability and hydrodynamic stress in the growth of *Phaeodactylum tricornutum* in a concentric tube airlift photobioreactor. *Biotechnol. Bioeng.* 60: 318–325.
- Deckwer W.D., 1992. *Bubble Column Reactors*, J. Wiley, Chichester.
- Degen J.; Uebele A.; Retze A.; Schmid-Staiger U.; Trosch W., 2001. A novel airlift photobioreactor with baffles for improved light utilization through the flashing light effect. *J. Biotechnol.* 92: 89–94.
- Douskova I., Doucha J., Livansky K., Machat J., Novak P., Umysova D., Zachleder V., Vitova M., 2009. Simultaneous flue gas bioremediation and reduction of microalgal biomass production costs. *Appl. Microbiol. Biotechnol.* 82: 179–185.
- Fan L., Zhang Y., Cheng L., Zhang L., Tang D., Chen H., 2007. Optimization of carbon dioxide fixation by *Chlorella vulgaris* cultivated in membrane-photobioreactor. *Chemical Engineering Technology* 30 (8); 1094–1099.
- Ferreira A., Pereira G., Teixeira J.A., Rocha F., 2012. Statistical tool combined with image analysis to characterize hydrodynamics and mass transfer in a bubble column. *Chemical Engineering Journal*, 180(15): 216–228.
- Freitas C., Fialová M., Zahradnik J., Teixeira J. A., 2000. Hydrodynamics of a three-phase external-loop airlift bioreactor, *Chemical Engineering Science*, 55(21): 4961–4972
- Galíndez-Mayer J., Sánchez-Teja O., Cristiani-Urbina E., Ruiz-Ordaz N., 2001. A novel splay-cylinder airlift reactor for fed-batch cultures. Effect of the liquid height on the hydrodynamic characteristics and the volumetric oxygen transfer coefficient of the reactor, *Bioprocess Biosyst.*

- Eng., 24: 171–177.
- García-Calvo E., Rodríguez A., Prados A.; Klein J., 1999. A Fluid Dynamic Model for Three-Phase Airlift Reactors. *Chem. Eng. Sci.*, 54 (13-14): 2359-2370.
- Grima E. M., Pérez J. A., Camacho F. G, Medina A. R., 1993. Gas–liquid transfer of atmospheric CO₂ in microalgal cultures. *J. Chem. Tech. Biotechnol.* 56: 329–337.
- Grima E. M., Fernández J., Ación F. G., Chisti Y., 2001. Tubular photobioreactor design for algal cultures, *J. Biotechnol.*, 92: 113–131.
- Guieysse B., Quijano R., Munoz R., 2001. Airlift Bioreactor. In Murray Moo-Young (Ed) 2nd edition of “Comprehensive Biotechnology”, Elsevier. ISBN: 978-0-444-53352-4.
- Jannsen M., Kuijpers T., Veldhoen B., Ternbach M., Tramper J., Mur L., Wijffels R., 1999. Specific growth rate of *Chlamydomonas reinhardtii* and *Chlorella sorokiniana* under medium duration light/dark cycles: 13–87 s. *J. Biotechnol.* 70: 323–333.
- Janssen M., Slenders P., Tramper J., Mur L.R., Wijffels R., 2001. Photosynthetic efficiency of *Dunaliella tertiolecta* under short light/dark cycles. *Enzyme and Microbial Technology* 29: 298-305.
- Janssen M., Tramper J., Mur L. R., Wijffels R. H., 2003. Enclosed outdoor photobioreactors: Light regime, photosynthetic efficiency, scale-up, and future prospects. *Biotechnology and Bioengineering* 81: 193-210.
- Krichnavaruk S., Powtongsook S., Pavasant P., 2007. Enhanced productivity of *Chaetoceros calcitrans* in airlift photobioreactors, *Bioresour. Technol.*, 98: 2123–2130.
- Laws E. A., Terry K. L., Wickman J., Chalup M. S., 1983. A simple algal production system designed to utilize the flashing light effect. *Biotechnol. Bioeng.* 25: 2319–2335.
- Lee Y. K., Pirt J., 1981. Energetics of photosynthetic alga growth: influence of intermittent illumination in short (40 S) cycles. *J. Gen. Microbiol.* 124: 43–52.
- Lou H-P., Kemoun A., Al-Dahhan M. H., Sevilla J. M. F., Sánchez J. L. G., Camacho F. G., Molina Grima E., 2003. Analysis of photobioreactors for culturing high-value microalgae and cyanobacteria via an advanced diagnostic technique: CARPT. *Chem Eng Sci.*, 58: 2519–1527
- Lou H. P., Al-Dahhan M. H., 2004. Analyzing and modeling of photobioreactors by combining first principles of physiology and hydrodynamics. *Biotechnology and Bioengineering* 85: 4.
- Mena P.C., Pons M.C., Teixeira J.A., Rocha F.A., 2005. Using image analysis in the study of multiphase gas absorption, *Chem. Eng. Sci.*, 60: 5144–5150.
- Mena P. C., Rocha F. A., Teixeira J. A., Sechet P., Cartellier A., 2008. Measurement of gas phase characteristics using a monofibre optical probe in a three-phase flow. *Chemical Engineering Science* 63: 4100 – 4115.
- Merchuk J. C., Ronen M., Giris S., Arad S., 1998. Light/dark cycles in the growth of the red Microalga *Porphyridium* sp. *Biotechnol. Bioeng.* 59: 706–713.
- Merchuk J. C., Gluz M., Mukmenev I., 2000. Comparison of photobioreactors for cultivation of the microalga *Porphyridium* sp.. *J. Chem. Technol. Biotechnol.* 75: 1119–1126.
- Mirón S. A., Camacho G. F., Gomez C. A., Grima E. M., Chisti Y., 2000. Bubble-column and airlift

- photobioreactors for algal culture. *AIChE Journal* 46 (9).
- Mirón A. S., Cerón García M.-C. C., Camacho F. G., Grima E. M., Chisti Y., 2002. Growth and biochemical characterization of microalgal biomass produced in bubble column and airlift photobioreactors: studies in fed-batch culture, *Enzyme Microb. Technol.*, 31: 1015–1023.
- Mirón A. S., García M.-C., Gómez A. C., Camacho F. G., Grima E. G., Chisti Y., 2003. Shear stress tolerance and biochemical characterization of *Phaeodactylum tricornutum* in quasi steady-state continuous culture in outdoor photobioreactors. *Biochem Eng J.*, 16: 287–97.
- Mirón S. A., García M. C., Camacho G. F., Molina G. E., Chisti Y., 2004. Mixing in bubble column and airlift reactors. *Chemical Engineering Research and Design* 82 (A10): 1367–1374.
- Molina E., Contreras A., Chisti Y., 1999. Gas Holdup, Liquid Circulation and Mixing Behaviour of Viscous Newtonian Media in a Split-Cylinder Airlift Bioreactor, *Food and Bioprocess Processing*, 77(1): 27-32.
- Montes F., Galan M., Cerro R., 1999. Mass transfer from oscillating bubbles in bioreactors, *Chem. Eng. Sci.* 54 (15–16): 3127–3136.
- Nagata S., 1975. *Mixing: Principles and Applications*. Tokyo: Kodansha.
- Nielsen J., Villadsen J., 1994. Mass transfer. In: *Bioreaction and Engineering Principles*. Plenum, New York, 296–313.
- Ogbonna J. C., Soejima T., Tanaka H., 1998. Development of efficient large scale photobioreactors. In: Zaborosky, O.R. (Ed.), *Biohydrogen*. Plenum Press, New York, pp. 329–343.
- Oncel S., Sukan F. V., 2008. Comparison of two different pneumatically mixed column photobioreactors for the cultivation of *Arthrospira platensis* (*Spirulina platensis*). *Bioresour Technol*, 99: 4755–4760.
- Panda A. K., Mishra S., Bisaria V. S., Bhojwani S. S., 1989. Plant cell reactors - a perspective. *Enzyme Microbiology Technology* 11: 386–397.
- Richmond A., Cheng-Wu Z., Zarmi Y., 2003. Efficient use of strong light for high photosynthetic productivity: interrelationships between the optical path, the optimal population density and cell-growth inhibition. *Biomol. Eng.* 20: 229–236.
- Rocha J. M. S., Garcia J. E. C., Henriques M. H. F., 2003. Growth aspects of the marine microalga *Nannochloropsis gaditana*. *Biomolecular Engineer.*, 20: 237–242.
- Sánchez Mirón A., Contreras Gómez A., García Camacho F., Molina Grima, E., Chisti Y., 1999. Comparative evaluation of compact photobioreactors for large-scale monoculture of microalgae, *J Biotechnol*, 70: 249–270.
- Suh I. S., Lee C. G., 2003. Photobioreactor engineering: Design and performance. *Biotechnol. Bioprocess Eng.*, 8 (6): 313–321.
- Talbot P., Gortares M. P., Lencki R. W., De la Noue J., 1991. Absorption of CO₂ in algal mass culture systems: a different characterization approach. *Biotechnol. Bioeng.* 37: 834–842.
- Terry K., 1986. Photosynthesis in modulated light: quantitative dependence of photosynthetic enhancement on flashing rate. *Biotechnol. Bioeng.* 28: 988–995.
- Ugwu C. U., Ogbonna J. C., Tanaka H., 2002. Improvement of mass transfer characteristics and

- productivities of inclined tubular photobioreactors by installation of internal static mixers. *Appl. Microbiol. Biotechnol.* 58: 600–607.
- Ugwu C.U., Aoyagi H., Uchiyama H., 2008. Photobioreactors for mass cultivation of algae. *Bioresource Technology* 99(10): 4021–4028.
- Vega-Estrada J., Montes-Horcasitas M. C., Domínguez-Bocanegra A. R., Cañizares-Villanueva R. O., 2005. *Haematococcus pluvialis* cultivation in split-cylinder internal-loop airlift photobioreactor under aeration conditions avoiding cell damage. *Appl. Microbiol. Biotechnol.* 68: 31–35.
- Velarde R. R., Urbina E. C, Melchor D. J. H, Thalasso F., Villanueva R. O. C., 2010. Hydrodynamic and mass transfer characterization of a flat-panel airlift photobioreactor with high light path. *Chem Eng Process Process Intens.*, 49(1): 97–103.
- Wu X., Merchuk J. C., 2004. Simulation of Algae Growth in a Bench Scale internal Loop Airlift Reactor. *Chem Eng. Sci.*, 59: 2899-2912.
- Xu Z., Baicheng Z., Yiping Z., Zhaoling C., Wei C., Fan O., 2002. A Simple and Low&Cost Airlift Photobioreactor for Microalgal Mass Culture. *Biotechnology Letters*, 24 : 1767–1771.
- Zhang K., Kurano N., Miyachi S., 2002. Optimized aeration by carbon dioxide gas for microalgal production and mass transfer characterization in a vertical-plate photobioreactor. *Bioprocess Biosyst. Eng.*, 25: 97–101.

CHAPTER 8

General conclusions and suggestions for future work

8.1 General conclusions	197
8.2 Suggestions for future work	198

8.1 General conclusions

Three different strategies were adopted in order to make the microalgae mass cultivation an economically and environmentally sustainable process: i) maximize productivity through optimization of culture conditions, ii) maximize productivity and decrease costs by the use of agro-industrial waste as a cultivation medium; iii) development of a new, low cost and highly productive microalgae cultivation system.

Growth parameters and CO₂ uptake by *C. vulgaris* P12 were significantly affected by CO₂ concentration in air stream (ranging from 2% to 10%) and aeration rate (ranging from 0.1 vvm to 0.7 vvm). The highest rate of CO₂ fixation by microalgae (2.22 g L⁻¹ d⁻¹) was obtained under 6.5% CO₂ and 0.5 vvm. These results are an important step in the development of strategies to mitigate CO₂ in an environmentally sustainable manner by using a biological approach.

Starch content of *C. vulgaris* strain P12 reached up to 41.0% of dry cell weight, which was 8-fold higher than the control (central points of the experimental design). This result was achieved simply by altering the initial concentrations of urea and FeNa-EDTA in the culture medium. Since accumulation of starch occurred at nitrogen depletion conditions under which the cell growth was much slower than that observed during nitrogen supplemented cultivations, compromising between increasing starch content and cell growth will be necessary in order to attain high values of both biomass concentration and starch productivity.

Parachlorella kessleri uses starch as a primary carbon and energy storage source under the first days of cultivation, but the stress caused by decreased concentrations of nutrients make the microalgae to shift the fixed carbon into reserve lipids as a secondary storage product. The cells recovered growth shortly after repleting medium and grew synchronously into large mother cells with high concentration of chlorophyll. These findings indicate that nutritional limitation can be used in *P. kessleri* cultivation as a very effective strategy to increase lipid productivity, e.g. for biofuel production.

When compared with the photoautotrophic control culture, mixotrophically cultivated microalgae grew faster, providing higher productivities of biomass, lipids, starch and proteins. Furthermore, microalgal biomass production and carbohydrate

consumption were enhanced by supplementing the inorganic culture medium with hydrolysed CW powder solution, than supplementing with a mixture of pure glucose and galactose, as a consequence of stimulatory effects arising from growth-promoting nutrients in CW. Mixotrophic cultivation of *C. vulgaris* using CW can be considered as a feasible strategy to reduce the costs of microalgal biomass production, while also contributing to solve the environmental problem caused by CW disposal in dairy industries.

The developed SCAPBRs proved to be extremely suitable for microalgae cultivation. The design of PBRs, particularly the design of the gas sparger, allowed meeting the needs of microalgae in terms of efficient mixing and good mass transfer coefficients (efficient supply and removal of CO₂ and O₂, respectively). SCAPBR 50 (at $U_{Gr} = 0.0044 \text{ m s}^{-1}$) showed, among the tested PBRs, the highest value of biomass volumetric productivity ($0.75 \text{ g L}^{-1} \text{ d}^{-1}$). This result is due to a more effective light distribution inside the PBR and to a regular and defined flow pattern, which allows exposing cells to regular light and dark periods. The statistical analysis of productivity results suggests that SCAPBR productivity can be improved by decreasing the riser:downcomer ratio.

8.2 Suggestions for future work

The results obtained during this PhD show that SCAPBRs are systems with enormous potential for large-scale cultivation of microalgae. There is a clear need to explore the potentialities of SCAPBRs, namely by decreasing the riser:downcomer ratio to obtain a flow pattern which allows a further increase in biomass productivity.

It is suggested to carry out SCAPBR scale-up to a pilot scale (up to 4 m high and 0.20 m in diameter) to operate under *real conditions*, *i.e.*, outdoor cultivation with natural illumination. This process is imperative to validate SCAPBR design. Such up-scale should include the construction of SCAPBR with a low cost, transparent material (*e.g.* polyethylene or PVC). Due to SCAPBR characteristics it would be also very interesting to carry out tests of microalgae cultivation in continuous regime.

All the techniques optimized during this PhD (*e.g.* nutrient limitation, two-step cultivation strategy or mixotrophic cultivation) should be tested in this SCAPBR.